Universidad de Valladolid

Escuela de Doctorado Universidad de Valladolid

PROGRAMA DE DOCTORADO EN INGENIERÍA QUÍMICA Y AMBIENTAL

TESIS DOCTORAL:

Methane abatement biotechnologies: Targeting process microbiology, improvement of process performance and revalorisation

Presentada por Juan Carlos López Neila para optar al grado de
Doctor por la Universidad de Valladolid

Dirigida por:
Raúl Muñoz Torre
Guillermo Quijano Govantes

Universidad de Valladolid

Escuela de Doctorado Universidad de Valladolid

PROGRAMA DE DOCTORADO EN INGENIERÍA QUÍMICA Y AMBIENTAL

TESIS DOCTORAL:

Biotecnologías de eliminación de metano: Explorando la microbiología del proceso, posibles mejoras del rendimiento y la revalorización

Presentada por Juan Carlos López Neila para optar al grado de
Doctor por la Universidad de Valladolid

Dirigida por:
Raúl Muñoz Torre
Guillermo Quijano Govantes

Universidad de Valladolid

Escuela de Doctorado Universidad de Valladolid

Memoria para optar al grado de Doctor,

con **Mención Doctor Internacional**,

presentada por el Biotecnológo:

Juan Carlos López Neila

Siendo los tutores en la **Universidad de Valladolid**:

Raúl Muñoz Torre

Guillermo Quijano Govantes

Y en el **Microbial Communities Lab – National University of Ireland, Galway** (Ireland):

Prof. Gavin Collins

Valladolid, _____ de_____ de 2017

Universidad de Valladolid

Escuela de Doctorado Universidad de Valladolid

UNIVERSIDAD DE VALLADOLID

ESCUELA DE INGENIERÍAS INDUSTRIALES

Secretaría

La presente tesis doctoral queda registrada en el folio Nº _____

del correspondiente Libro de Registro con el Nº _____

Valladolid, a _____de_____ de 2017

Fdo. El encargado del Registro

Universidad de Valladolid

Escuela de Doctorado Universidad de Valladolid

Raúl Muñoz Torre

Profesor Contratado Doctor Permanente

Departamento de Ingeniería Química y Tecnología del Medio Ambiente

Universidad de Valladolid

y

Guillermo Quijano Govantes

Investigador Catedrático CONACYT

Laboratorio de Investigación en Procesos Avanzados de Tratamiento de Aguas, Instituto de Ingeniería

Universidad Nacional Autónoma de México

Certifican que:

JUAN CARLOS LÓPEZ NEILA ha realizado bajo su dirección el trabajo "*Methane abatement biotechnologies: Targeting process microbiology, improvement of process performance and revalorisation*", en el Departamento de Ingeniería Química y Tecnología del Medio Ambiente de la Escuela de Ingenierías Industriales de la Universidad de Valladolid. Considerando que dicho trabajo reúne los requisitos para ser presentado como Tesis Doctoral expresan su conformidad con dicha presentación.

Valladolid, a _____de_____ de 2017

Fdo. Raúl Muñoz Torre Fdo. Guillermo Quijano Govantes

Universidad de Valladolid

Escuela de Doctorado Universidad de Valladolid

Reunido el tribunal que ha juzgado la tesis doctoral "*Methane abatement biotechnologies: Targeting process microbiology, improvement of process performance and revalorisation*" presentada por Juan Carlos López Neila y en cumplimiento con lo establecido por el Real Decreto 99/2011 de 28 de enero de 2011 acuerda conceder por _____ la calificación de _____.

Valladolid, a _____de_____ de 2017

PRESIDENTE SECRETARIO

1er Vocal 2do Vocal 3er Vocal

Índice de contenidos

Table of contents

Resumen

El cambio climático asociado al calentamiento global representa hoy en día uno de los mayores desafíos medioambientales a nivel mundial. El calentamiento global se ha atribuido inequívocamente a la cada vez más alta concentración atmosférica de gases de efecto invernadero (GEIs), que ha ido incrementándose ya desde la época preindustrial hasta nuestros días. Se estima que la situación se agrave en el presente siglo en base al aumento de la población mundial previsto y, por tanto, de la actividad industrial y de gestión de residuos asociada. Por ello, es necesario no sólo un mayor grado de concienciación medioambiental por parte de la población, sino también el desarrollo de nuevos avances tecnológicos que prevengan y reduzcan activamente dichas emisiones, para cumplir con una legislación cada vez más estricta y dirigida a limitar el aumento de la temperatura del planeta a 2 ºC por encima de los niveles registrados en la época preindustrial.

Dentro del inventario mundial de GEIs, el metano (CH_4) es considerado un agente climático de acción a corto plazo con una alta prevalencia en la atmósfera, siendo su vida útil de 12.4 años. Las emisiones de este GEI son las segundas más abundantes después de las del CO_2 a nivel mundial. El CH_4 se produce de forma natural por descomposición anaerobia de materia orgánica, aunque más de la mitad de sus emisiones son antropogénicas, y se originan generalmente en instalaciones de tratamiento de residuos, ganaderas y de minería del carbón. Tecnologías de final de proceso tanto físico-químicas como biológicas se encuentran disponibles comercialmente para el tratamiento de emisiones de CH_4, estando determinada la selección de la tecnología más apropiada para el tratamiento por la concentración y el flujo de la emisión de CH_4 a tratar.

Las biotecnologías de tratamiento del CH_4, basadas en la actividad biocatalítica de las bacterias oxidantes del CH_4, se han posicionado en las últimas décadas como una alternativa viable a las tecnologías físico-químicas, dado que son respetuosas con el medio ambiente, rentables y tienen potencial para crear valor añadido a través de la eliminación del CH_4 mediante la producción de bioproductos (p. e. polihidroxialcanoatos, PHAs) o para favorecer otros procesos de tratamiento de la contaminación. Sin embargo, estas biotecnologías aún presentan ciertas limitaciones operacionales que limitan su implementación a gran escala. Por ello, se hace necesario ahondar en su investigación (tanto a nivel micro- como macroscópico) y superar las actuales limitaciones de las biotecnologías de tratamiento de CH_4 con el fin de potenciar el escalado a nivel industrial de procesos biológicos de eliminación de CH_4 mediante un concepto de biorrefinería.

De este modo, en esta tesis se exploraron las biotecnologías de eliminación de CH_4 con el objeto de i) mejorar el rendimiento del proceso a largo plazo, ii) determinar el efecto de múltiples parámetros ambientales y operacionales sobre la estructura y las características de las comunidades metanotróficas y iii) crear valor añadido a partir de la degradación de CH_4 con miras al desarrollo de una bioeconomía sostenible.

La biofiltración es una de las biotecnologías más aplicadas para el tratamiento de CH_4 a nivel mundial. Sin embargo, los tiempos de residencia del gas (GRTs) requeridos para garantizar eficacias de eliminación de contaminantes con baja solubilidad en agua como el CH_4 son a día de hoy altos, incrementando así significativamente los costes de inversión. En este sentido, el uso de biopelículas fúngicas ha sido propuesto recientemente como alternativa al uso de biopelículas bacterianas como una vía más eficiente para el tratamiento de contaminantes hidrofóbicos, aunque su capacidad para degradar CH_4 como única fuente de carbono y energía no ha sido aún comprobada experimentalmente. En el primer estudio, se investigó la capacidad y el papel de los

hongos en la eliminación de CH_4 en experimentos en botellas y en un biofiltro empacado con compost y tratando en continuo emisiones de CH_4 diluidas. La cepa fúngica *Graphium* sp. fue capaz de degradar co-metabólicamente CH_4 cuando se añadió metanol al cultivo como agente de poder reductor. El biofiltro mixto fúngico-bacteriano empleado durante el estudio alcanzó eficacias de eliminación altas y estables (hasta del 90 %) con caídas de presión mínimas, aplicando una frecuencia óptima de irrigación y a un GRT de 20 minutos, que es significativamente más bajo que los empleados en trabajos previos de eliminación de CH_4 en biofiltros bacterianos.

Otra limitación operacional encontrada frecuentemente durante la biofiltración de gases es el excesivo crecimiento de biomasa en el lecho. Éste puede llegar a limitar el rendimiento de biodegradación del contaminante y aumentar la caída de presión en el sistema, como resultado de los fenómenos de canalización preferencial y colmatación, respectivamente. La estrategia basada en alternar fases de alimentación-hambruna fue propuesta en el segundo trabajo de la presente tesis como estrategia de bajo coste para el control de biomasa, permitiendo así solventar la limitación anteriormente citada en una operación a largo plazo. Así, el rendimiento de dos biofiltros alternos bajo esta estrategia operacional fue evaluado comparativamente con un biofiltro control sometido a alimentación continua, y utilizándose CH_4 como contaminante gaseoso modelo a concentraciones diluidas. La estrategia operacional aquí evaluada permitió alcanzar capacidades de eliminación significativamente mayores en los biofiltros alternos que las registradas en el biofiltro control, especialmente durante las primeras etapas de operación. Los biofiltros sometidos a periodos alternos de alimentación-hambruna sufrieron caídas de presión inferiores como consecuencia de las menores concentraciones de biomasa presentes en estos lechos, lo que supondría en última instancia un aumento de la vida útil del material de relleno y una reducción de los costes de operación del proceso de biofiltración a escala industrial. Además, se evaluó la robustez de las comunidades microbianas enriquecidas frente al aumento de los

periodos de hambruna (3:3 días → 5:5 días), la reducción de la frecuencia de irrigación o la privación de aire durante la operación bajo esta estrategia. Los resultados obtenidos mostraron claramente que la actividad máxima de eliminación de CH_4 fue alcanzada progresivamente en periodos de tiempo cada vez menores (de 72 a 1.5 h). Las comunidades metanotróficas involucradas en el proceso se vieron significativamente afectadas por el procedimiento operacional desarrollado, presentando las comunidades de las unidades alternas una mayor diversidad y un predominio de metanótrofos tipo I, con mayor afinidad por el CH_4.

El enriquecimiento de comunidades metanotróficas con alta afinidad y altas tasas específicas de biodegradación de CH_4 durante estos procesos biológicos de tratamiento es deseable para garantizar cortos periodos de arranque y un rendimiento global efectivo. En este sentido, en esta tesis se evaluó la influencia de la concentración de CH_4 sobre los parámetros cinéticos y la estructura de la población durante un proceso de enriquecimiento a largo plazo en reactores de tanque agitado. Además, los diferentes cultivos mixtos fueron sometidos durante el experimento a limitaciones secuenciales de nitrógeno con el fin de evaluar su capacidad para sintetizar PHAs. La concentración de CH_4 influyó significativamente en la estructura de la población y el tipo de metanótrofos enriquecidos, que predominantemente fueron de tipo I. Las tasas de biodegradación específica de CH_4 más altas fueron registradas en las primeras etapas del enriquecimiento para los consorcios expuestos a concentraciones de CH_4 media y alta (2 and 20 g m^{-3}, respectivamente), mientras que las mayores afinidades por CH_4 fueron obtenidas para los consorcios a baja y alta concentración de CH_4 (0.2 y 20 g m^{-3}, respectivamente). Las máximas acumulaciones de PHAs (13 %) obtenidas en continuo fueron alcanzadas por el consorcio enriquecido a la concentración media de CH_4, y fueron atribuidas a la presencia de metanótrofos tipo II pertenecientes al género *Methylocystis*.

El biogás procedente de la digestión anaerobia de lodos en plantas de tratamiento de agua residual (EDARs) ha sido propuesto recientemente como una materia prima renovable para la acumulación metanotrófica de PHAs, con potencial para reducir los costes de producción de biopolímero y sustentar una bioeconomía basada en la mitigación de GEIs. En este aspecto, el cuarto capítulo de la presente tesis se centró en investigar la viabilidad del biogás mediante ensayos en botellas, con o sin H_2S, para el crecimiento y la acumulación de PHAs en la cepa *Methylocystis hirsuta*, un metanótrofo tipo II. El efecto de la adición individual de ácidos grasos volátiles (AGVs), fácilmente disponibles durante el proceso de digestión anaerobia vía hidrólisis, fue también evaluado en términos de crecimiento y generación de PHAs de diferente composición. El experimento llevado a cabo reveló que ambos tipos de biogás, con y sin H_2S, eran fuentes de CH_4 aptas tanto para sustentar el crecimiento de la cepa bajo condiciones sin limitación de nutrientes, como para acumular PHAs en la forma de poli-3-hidroxibutirato (PHB) hasta valores del 45 % bajo condiciones de limitación de nitrógeno. La cepa además mostró capacidad para crecer en ácido acético, propiónico, butírico y valérico hasta concentraciones en torno a los 200 mg L^{-1}, con o sin biogás. El uso combinado de biogás como sustrato principal y AGVs como cosustratos (representando un 10 % de carbono extra respecto al aportado por el CH_4 del biogás) bajo condiciones de limitación de nitrógeno condujo a incrementos del 10-30 % del rendimiento máximo y del contenido de PHA sobre los valores basales obtenidos sólo con biogás. Finalmente, la adición de ácido valérico en estos ensayos promovió la obtención de fracciones de hidroxivalerato en el biopolímero sintetizado hasta del 25 %, lo que conlleva la obtención de un bioplástico con propiedades físico-químicas significativamente mejoradas. Los prometedores resultados aquí obtenidos representan un paso más al frente en el desarrollo de una nueva generación de biorrefinerías basadas en procesos de digestión anaerobia, pudiendo ser este estudio considerado como una prueba de concepto de una tecnología a implementar en reactores en continuo.

Finalmente, se investigó el potencial del biogás como sustrato viable para la creación de valor añadido mediante la combinación de la oxidación anaerobia de CH_4 con un proceso de desnitrificación (DAMO). Con este fin, se seleccionó un biofiltro percolador como mejor configuración de biorreactor para retener eficazmente la biomasa en el seno del lecho y asegurar un contacto efectivo entre el biogás y la biopelícula. Las emisiones de óxido nitroso correspondientes a una desnitrificación incompleta del nitrato se relacionaron con la concentración de nitrato aplicada en el sistema y se minimizaron sin comprometer la actividad de la comunidad DAMO, que representó en torno a un 60 % de la población tras sólo 4.5 meses de enriquecimiento. La adición de H_2S como co-donador de electrones para la desnitrificación en la corriente de biogás alimentada al biofiltro percolador condujo a la formación de un consorcio microbiano mixto formado por la ya existente comunidad DAMO (13 %) y las bacterias reductoras de nitrato y oxidantes de sulfhídrico (NR-SOB) recientemente enriquecidas. El co-enriquecimiento con este último grupo de bacterias permitió un aumento significativo de las tasas de reducción de nitrato sin comprometer la biodegradación de CH_4 y una desnitrificación completa, lo cual se confirmó posteriormente mediante análisis de qPCR de los genes de desnitrificación *narG*, *nirK* y *nosZ*. Estos hallazgos podrían incentivar el escalado a nivel industrial de biofiltros percoladores con comunidades mixtas DAMO/NR-SOB como plataforma para la eliminación de N a bajo coste en EDARs.

Abstract

Climate change mediated by global warming represents nowadays one of the greatest environmental challenges all over the world. Global warming has been unequivocally attributed to the gradual increase in the atmospheric concentration of heat-trapping greenhouse gases (GHGs) from the preindustrial era to date, and is expected to increase in the current century based on the forthcoming scenario of increasing human population and, therefore, industrial and waste management activities. Thus, this scenario demands not only the assumption of a higher degree of environmental responsibility in our daily life, but also the implementation of new technological approaches in order to prevent or actively reduce GHGs emissions and comply with the currently enforced regulations devoted to limit the increase of temperature of the planet to 2 ºC above preindustrial levels.

Methane (CH_4) is considered a near-term climate forcer with a high prevalence in the atmosphere (lifespan of 12.4 years). The emissions of this GHG are the second most abundant after CO_2 on a worlwide basis. CH_4 is naturally produced by anaerobic decomposition of organic matter, although more than half of its emissions are anthropogenic. Indeed, anthropogenic CH_4 emissions originate from waste management, livestock farming or coal mining facilities. Both physical/chemical and biological technologies are commercially available end-of-the-pipe systems for the treatment of CH_4 emissions. The selection of the most appropriate technology for CH_4 abatement is often function of the concentration and the flowrate of the CH_4 emission.

Biotechnologies for CH_4 abatement, which are mainly based on the biocatalytic activity of methane-oxidizing bacteria (MOB), have emerged in the past decades as a viable alternative to physical/chemical technologies due to their environmentally-friendly nature, cost-efectiveness and potential to create additional value out of CH_4 mitigation

through the production of high-added value bioproducts (e. g. polyhydroxyalkanoates, PHAs) or to support to other pollution treatment processes. However, these technologies still present severe operational limitations that hinder their implementation at full-scale. Hence, further research (both at micro- and macroscopic levels) is required to overcome the current constraints of CH_4 abatement biotechnologies in order to boost their widespread implementation for CH_4 mitigation and the development of CH_4-based biorefineries.

In the current thesis, CH_4 abatement biotechnologies were investigated in order to i) improve their long-term process performance, ii) elucidate the effects of multiple environmental and operational parameters on methanotrophic communities structure and characteristics and iii) create added value out of CH_4 mitigation towards the creation of a sustainable bioeconomy.

Biofilters are so far the most applied biotechnology for the abatement of CH_4 worldwide. However, high empty bed residence times (EBRTs) are to date required to ensure moderate-high removal efficiencies (REs) of pollutants with a low aqueous solubility such as CH_4, which significantly increases the footprint of the process. In this context, fungal biofilms have been claimed to be more efficient coping with hydrophobic pollutants compared to bacterial biofilms, though their capability to degrade CH_4 as the sole carbon and energy source remains unclear. In the first study, the capability and role of fungi on CH_4 abatement were investigated batchwise and in a compost biofilter treating diluted CH_4 emissions, respectively. The fungal strain *Graphium* sp. proved to be able to co-metabolically degrade CH_4 when methanol was added as a reductive power source. The mixed fungal-bacterial biofilter exhibited stable and high CH_4 REs (90 %) with negligible pressure drops under an optimized irrigation frecuency at an EBRT of 20 min, which is by far lower than the EBRT previously used in CH_4 abatement bacterial biofilters.

Another operational limitation typically encountered during gas biofiltration is biomass overgrowth within the packed bed, which usually ends up in a reduced pollutant biodegradation performance and a higher pressure drop as a result of channelling and clogging phenomena, respectively. Alternate feast-famine strategies were proposed in the second work of this thesis as a low-cost biomass control strategy to overcome this limitation under long-term operation. Thus, the performance of two alternate biofilters under this operational strategy was comparatively evaluated against a standard biofilter under continuous operation using CH_4 as a model gas pollutant at diluted concentrations. The operational strategy here evaluated supported significantly higher elimination capacities (ECs) than those recorded in the standard biofilter, especially during the early stages of operation. Feast-famine biofilters exhibited lower pressure drops as a result of the lower biomass concentrations within the units, which might ultimately increase the packing material lifespan and reduce the operating costs during full-scale biofiltration. In addition, the robustness of the microbial community enriched during feast-famine operation was challenged with increasing feast-famine periods (3:3 days → 5:5 days), the reduction of the irrigation frecuency or the deprivation of air supply. The results clearly showed that the maximum CH_4 abatement activity was progressively achieved at shorter periods of time (from 72 to 1.5 h). The methanotrophic communities involved in the process were significantly affected by the operational strategy here implemented, and resulted in more diversed type I-dominated communities with higher affinities for CH_4.

The enrichment of specific MOB communities with a high affinity for CH_4 and high specific CH_4 biodegration rates during CH_4 abatement is desirable to guarantee a reduced start-up period in biotechnologies and an effective overall performance. In this context, the influence of CH_4 concentration during long-term culture enrichment in stirred tank reactors on the biodegradation kinetics and population structure was studied. At the end of the experiment, the culture enrichments were also subjected to sequential nitrogen

limitations in order to assess their potential for PHAs synthesis. CH_4 concentration greatly influenced population structure and the type of methanotrophic bacteria enriched, which were predominantly type I methanotrophs. High specific biodegradation rates were recorded in the early stages of enrichment in the consortia exposed to moderate-high CH_4 concentrations (2 and 20 g m^{-3}, respectively), whereas the highest affinity for CH_4 was exhibited by the consortia enriched at low and high CH_4 concentrations (0.2 and 20 g m^{-3}, respectively). The highest PHA accumulation (~13 %) obtained under continuous operation was observed in the consortium enriched at moderate CH_4 concentrations, and was attributed to the presence of type II methanotrophs belonging to the genus *Methylocystis*.

Biogas from anaerobic sludge digestion at wastewater treatment plants (WWTPs) has been recently proposed as a renewable feedstock for methanotrophic PHA accumulation, with potential to reduce biopolymer production costs and sustain a new GHG-based bioeconomy. In this sense, the fourth chapter of this thesis was devoted to investigate in batch experiments the feasibility of biogas, with and without H_2S, to support the growth and PHA accumulation in *Methylocystis hirsuta*, a type II methanotroph. The effect of the individual addition of volatile fatty acids (VFAs), readily available on-site during anaerobic sludge digestion via hydrolysis, was also assessed in terms of methanotrophic growth and synthesis of tailor-made PHAs. The experiments here conducted revealed that both types of biogas (with and without biogas) are feasible CH_4 substrates to sustain *M. hirsuta* growth under nutrient-sufficient conditions and the accumulation of PHAs in the form of poly-3-hydroxybutyrate (PHB) up to 45 % under nitrogen-limited conditions. The strain was also able to grow on acetic, butyric, propionic and valeric acids up to concentrations of 200 mg L^{-1}, with and without biogas. The use of biogas as the main substrate, and individual VFAs as cosubstrates (10 % extra C regarding the CH_4 input), under nitrogen-limited conditions led to an increase in the maximum PHA yields and contents by 10-30 % over the basal values obtained only with

biogas. Finally, valeric acid supplementation supported a hydroxyvalerate fraction of up to 25 % within the biopolymer, which can significantly enhance the physical/chemical properties of the biocomposite produced. The promising results here obtained represent a step further in the development of a new generation of anaerobic digestion biorefineries and can be considered as a solid proof of concept study of a technology to be implemented under continuous operation.

Finally, the potential of biogas from anaerobic sludge digestion at WWTPs as a feasible substrate for the creation of additional value out of CH_4 mitigation when combined with denitrifying anaerobic methane oxidation (DAMO) was investigated. For this purpose, a biotrickling filter was selected as bioreactor configuration to both effectively retain the biomass and promote an effective gas-biofilm contact. Nitrous oxide emissions from incomplete nitrate denitrification were correlated with the concentration of nitrate applied to the system and were minimized without compromising the activity of the DAMO community, which accounted for up to 60 % of the population after only 4.5 months of enrichment. The presence of H_2S in the biogas fed to the biotrickling filter, which represented a co-electron donor for denitrification, resulted in a combined microbial consortium composed by the DAMO community (13 %) and the newly enriched nitrate-reducing and sulphide-oxidising bacteria (NR-SOB). The co-enrichment of NR-SOB significantly enhanced nitrate reduction without compromising CH_4 biodegradation and led to a complete denitrification, which was further supported by qPCR analysis targeting *narG*, *nirK* and *nosZ* denitrifying genes. These findings could trigger the full-scale implementation of DAMO/ NR-SOB-based biotrickling filters as a novel low-cost nitrogen removal platform in WWTPs.

List of publications

The publications cited below are presented as part of the current thesis. Three of them have been published in international journals indexed in the ISI Web of Knowledge (Manuscripts I to III). Manuscripts IV and V have been also submitted for publication in two different international journals.

Manuscript I. López, J.C., Quijano, G., Pérez, R., Muñoz, R., 2014. Assessing the influence of CH_4 concentration during culture enrichment on the biodegradation kinetics and population structure. Journal of Environmental Management 146, 116-123. DOI: 10.1016/j.jenvman.2014.06.026.

Manuscript II. Lebrero, R., López, J.C., Lehtinen, I., Pérez, R., Quijano, G., Muñoz, R., 2016. Exploring the potential of fungi for methane abatement: Performance evaluation of a fungal-bacterial biofilter. Chemosphere 144, 97-106. DOI: 10.1016/j.chemosphere.2015.08.017.

Manuscript III. López, J.C., Porca, E., Collins, G., Pérez, R., Rodríguez-Alija, A., Muñoz, R., Quijano, G., 2017. Biogas-based denitrification in a biotrickling filter: Influence of nitrate concentration and hydrogen sulfide. Biotechnology and Bioengineering 114(3), 665-673. DOI: 10.1002/bit.26092.

Manuscript IV. López, J.C., Merchán, L., Lebrero, R., Muñoz, R., 2017. Feast-famine biofilter operation as a more robust strategy towards cost-effective methane mitigation. Journal of Cleaner Production (accepted).

Manuscript V. López, J.C., Arnáiz, E., Merchán, L., Lebrero, R., Muñoz, R., 2017. Biogas-based polyhydroxyalkanoates production by *Methylocystis hirsuta*: a step further

in anaerobic digestion biorefineries. Chemical Engineering Journal (submitted for publication).

Contribution to the manuscripts included in the thesis

Manuscript I. In this work, I was responsible for the design, start-up and operation of the experimental set-up, and results evaluation, under the supervision of Dr. Guillermo Quijano and Dr. Raúl Muñoz. Dr. Rebeca Pérez was responsible of the molecular biology analysis, where I actively collaborated. I prepared the manuscript under the supervision of both Dr. Guillermo Quijano and Dr. Raúl Muñoz.

Manuscript II. During the execution of this work, I was responsible for the operation of the experimental set-up, and results evaluation, under the supervision of Dr. Raquel Lebrero, Dr. Guillermo Quijano and Dr. Raúl Muñoz. Dr. Rebeca Pérez was responsible of the molecular biology analysis, where I actively collaborated. I collaborated with Dr. Raquel Lebrero in the preparation of the manuscript, where she was the main responsible, under the supervision of Dr. Raúl Muñoz.

Manuscript III. In this research, I was in charge of the design, start-up and operation of the experimental set-up, and results evaluation, under the supervision of Dr. Guillermo Quijano. Dr. Rebeca Pérez was responsible for the FISH analysis, where I actively collaborated. I carried out qPCR analyses in collaboration with Dr. Estefanía Porca at the Department of Microbiology of the National University of Ireland Galway (Ireland), under the supervision of Dr. Gavin Collins. I prepared the manuscript under the supervision of Dr. Guillermo Quijano, Dr. Gavin Collins and Dr. Raúl Muñoz.

Manuscript IV. In this work, I was responsible for the design, start-up and operation of the experimental set-up, and results evaluation, with the collaboration of Miss Laura Merchán. This experimental study was supervised by Dr. Raquel Lebrero and Dr. Raúl Muñoz. Following the external MiSeq Illumina sequencing analysis of the biological samples, I was responsible for the data handling and bioinformatics analyses. I prepared the manuscript under the supervision of both Dr. Raquel Lebrero and Dr. Raúl Muñoz.

Manuscript V. In this research, I was in charge of the design, start-up and operation of the experimental set-up, and results evaluation, with the collaboration of Miss Laura Merchán and Dr. Esther Arnáiz. This work was supervised by Dr. Raquel Lebrero and Dr. Raúl Muñoz. I prepared the manuscript under the supervision of both Dr. Raquel Lebrero and Dr. Raúl Muñoz.

Chapter 1

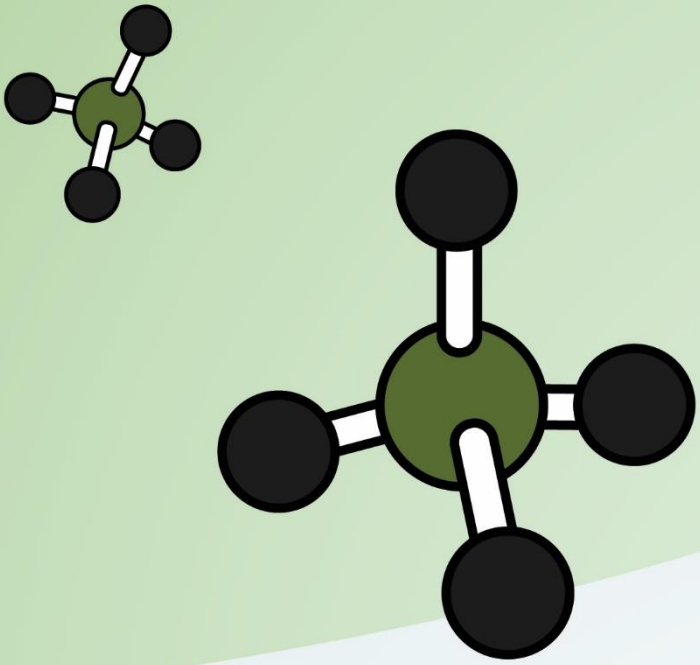

Introduction

1.1 Key figures and implications of GHG emissions on climate change

Over the past two centuries, the combustion of fossil fuels such as coal, natural gas and oil, deforestation, land-use changes and other anthropogenic activities have supported a significant increase in the atmospheric concentration of heat-trapping greenhouse gases (GHGs) such as carbon dioxide (CO_2), methane (CH_4) and nitrous oxide (N_2O) (Fig. 1.1A).[1] These gases absorb part of the energy irradiated from the Earth's surface and return it to the planet to maintain Earth's average temperature around 16 ºC. The emissions of these GHGs represent nowadays approximately 98 % of the total GHG inventory worldwide, and their share is expected to increase in this twenty-first century based on their industrial and organic-based nature and the forthcoming scenario of increasing human population.[2] In this context, the total anthropogenic GHGs emissions increased at 2.2 % year^{-1} in the period 2000-2010 compared to the rates recorded in the period 1970-2000 (1.3 % year^{-1}). Thus, despite the increasing number of climate change mitigation policies implemented worldwide, the total GHG emissions peaked at 49 $GtCO_2$-eq year^{-1} in 2010 (Fig. 1.1B).[1]

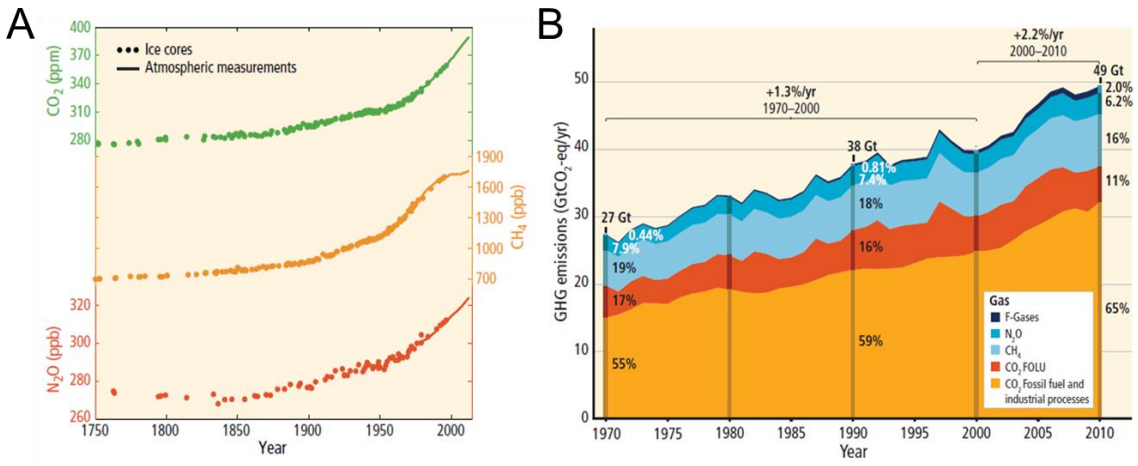

Fig. 1.1 Time course of A) the atmospheric CO_2 (green), CH_4 (orange) and N_2O (red) concentrations the past 250 years, and B) total annual anthropogenic emissions of the main GHGs in the period 1970-2010. Source: Intergovernmental Panel on Climate Change.[1]

As a result of this increase in GHG emissions, the average temperature of the Earth has gradually increased at rates never reported in the past 50 years. Indeed, the average

global temperature across land and ocean surface areas for 2016 was 0.94º C above the twentieth century average.[3] GHG's emissions are promoting a disruption in the Earth's energy budget, which has resulted in recent changes in the rainfall patterns, snow and ice cover area or in the level and acidification of oceans.[1,4] For instance, satellite inspections have recently revealed that the Greenland and West Antarctic ice covers are shedding about 125 billion tons of ice $year^{-1}$ (equivalent to 0.35 mm $year^{-1}$), which will directly mediate a rise of the sea level between 0.27 and 0.6 m by the end of 2099 as warming sea water expands.[1] More importantly, global warming is boosting the migration of hundreds of both marine and land-based plants and animals to cope with the extreme temperatures encountered in the past decades in many parts of the globe.[4]

1.2 CH_4 emissions – nature and future trends

CH_4 is the second most prevalent GHG within the global GHG inventory. This GHG contributes to approximately 14 % of the worldwide annual emissions (on a 100-year horizon) and its atmospheric concentration has increased by ~160% in the past 250 years.[1,4] CH_4 possesses a global warming potential (GWP) 25 times higher than that of CO_2 (on a 100-year horizon) due to its high chemical stability, which results in a lifespan in the atmosphere of 12.4 years.[4] However, the analysis of current GHG emissions (1-year pulse emission) shows that near-term climate forcers, such as CH_4, can exhibit contributions in terms of GWP or global temperature change potential (GTP) comparable to that of CO_2 for short time horizons, their impacts becoming progressively lower for longer time horizons (Fig. 1.2A).[5] This fact is attributed to the higher values of GWP for CH_4 estimated on 10- and 20-year horizons, which account for 90 and 72, respectively (Fig. 1.2B).[6]

A

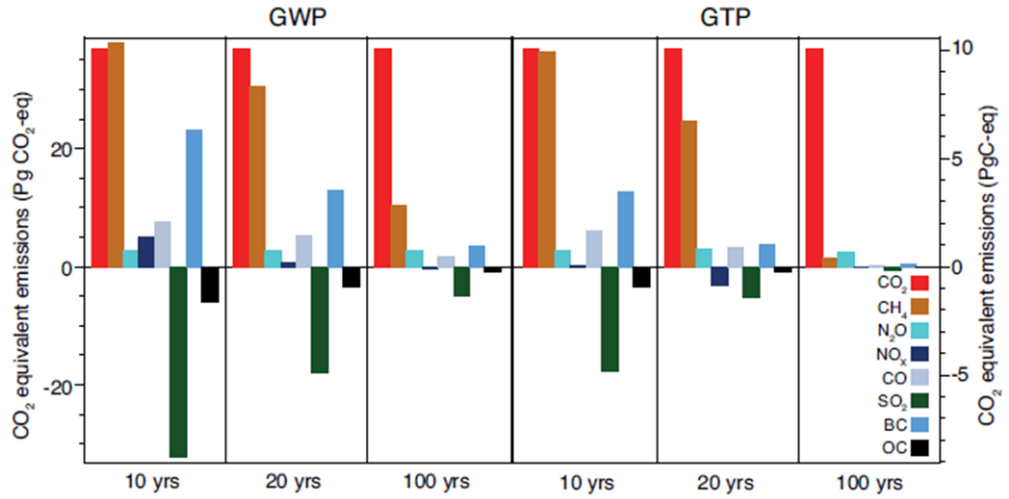

B

Time horizon (year)	1	5	10	15	20	25	30	40	50	100	500
GWP	103	101	90	80	72	64	58	49	42	25	7.6

Fig. 1.2 A) Present-day global anthropogenic emissions weighted by the GWP and the GTP for the given time horizons and considering year 2008 emissions as the single-year pulse (Source: Intergovernmental Panel on Climate Change[5]), and B) GWP estimations for CH_4 (pulse emission) at different time horizons (adapted from Dessus et al.[6]).

In nature, most CH_4 fluxes to the atmosphere originate from the anaerobic decomposition of organic matter in ecosystems such as wetlands or oceans, though more than 60% of the CH_4 emissions worldwide are anthropogenic.[2] Anthropogenic CH_4 emissions by 2015 accounted for 464 and 650 Mt CO_2-eq in the EU-28 and US, respectively, with livestock farming (45 %), anaerobic waste treatment (18 %), coal mining (6 %), natural gas operation (5 %) and wastewater treatment and discharge (4 %) as the main contributors.[2,4] The concentration of CH_4 in these emissions greatly varies from 0-0.2 g m^{-3} (compost piles, animal farming) to 20-100 g m^{-3} (old landfills) or even up to 250-450 g m^{-3} (biogas from wastewater treatment plants, WWTPs). Diluted CH_4 emissions (< 30 % (*v/v*) CH_4 content), which are not suitable for energy recovery or incineration, are commonly released to the atmosphere without prior treatment.[7,8] In this context, more than 55 % of the anthropogenic CH_4 emissions possess concentrations below the lower explosive limit of CH_4-air mixtures (5% *v/v*).[9] In addition, despite the potential for heat and electricity generation of the biogas (40-70 % (*v/v*) CH_4) produced from anaerobic

sludge digestion at WWTPs, the share of biogas used for this purpose has been estimated to be less than 1 % in the U.S., which is typically burned or vented to the atmosphere without any treatment.[10,11] This fact has been attributed to i) the presence of undesirable compounds (e.g., siloxanes, H_2S, halocarbons) within biogas, ii) the high investment costs needed for energy recovery on-site or iii) the high costs associated to biomethane production (1.08 € m^{-3} in the EU market compared to 0.30-0.67 € m^{-3} for natural gas).[11-13]

Climate change represents nowadays one of the greatest environmental concerns all over the world, and therefore governments are gradually implementing policies in order to limit the impacts of their GHG emissions. In this context, in view of the foreseeable increase of the global average temperature from 1.4 to 5.8 ºC by 2100, most members of the United Nations have commited to reduce their GHG emissions by at least 18 % below 1990 levels in the eight-year period from 2013 to 2020.[14] Thus, adaptation policies have been implemented across all levels of European governance, with some adaptation planning integrated into coastal and water management, into environmental protection and land planning and into disaster risk management. Likewise, governments of US and Canada are engaging in incremental adaptation assessment and planning (particularly at a municipal level), together with some proactive adaptation devoted to protect longer-term investments in energy and public infrastructure.[1] In this context, an active abatement of GHG emissions is mandatory and expected to become a general trend worldwide in the next decades in order to comply with the Paris Climate Agreement.

1.3 End-of-the-pipe technologies for CH_4 mitigation

End-of-the-pipe technologies for waste gas treatment are often based on the initial pollutant mass transfer from the target gas emission to a solid or a liquid phase – via

adsorption or absorption, respectively – and a further chemical/biological oxidation.[15] In the particular case of technologies such as incineration or ozonation, the gas pollutants are directly oxidized in the gas phase. Confination and gas extraction allow an effective end-of-the-pipe treatment of GHGs in animal farms, industry and waste management facilities. Technologies devoted to CH_4 mitigation are commonly classified into two main categories, physical/chemical and biological technologies, depending on the mechanism underlying CH_4 destruction.[16] The most representative physical/chemical and biological CH_4 abatement technologies are presented in the following sections.

1.3.1 Physical/chemical technologies

Physical/chemical technologies such as incineration, catalytic oxidation, condensation or activated carbon adsorption have been extensively applied in the past century for the abatement of industrial waste gases (e. g. volatile organic compounds, VOCs) or biogas upgrading. In the particular case of CH_4 abatement, thermal and in a lesser extent catalytic oxidation, have been the most applied technologies.

1.3.1.1 Thermal oxidation (fume incineration)

Thermal oxidation, also known as incineration, is based on the complete oxidation of the gas pollutants at high temperatures in the presence of air/O_2, with CO_2 and H_2O as the main byproducts from pollutant oxidation. Incineration is a common technology for the control of CH_4 emissions derived from landfills and WWTPs. The 3 T's of combustion – time, temperature and turbulence – must be properly optimized to achieve an effective emission control. The appropriate selection of the incinerator configuration, which is strongly influenced by the emission flowrate and the targeted CH_4 concentration, allows CH_4 removal efficiencies (REs) ≥ 96.0 %.[17] In this sense, three main configurations of incinerators can be distinguished:

- Direct fired thermal oxidizers (flares/burners). Flares are devised as the most simple incinerator configuration and can be used either as emergency control systems or as the main CH_4 abatement unit. Direct fired thermal oxidizers are currently used in the petroleum, petrochemical and other industries that require the treatment of waste gases containing high pollutant concentrations on both a continuous or intermittent basis. In these systems, the waste gas is often premixed with air in a controlled venturi prior to the burner to ensure a more uniform combustion, a higher temperature and a potentially more complete combustion. Flares are typically divided into open and enclosed flares based on the absence or presence of an insulated enclosure for the flame, respectively, which surrounds a series of one or more clusters of gas burners (the array of gas inlet jets located just above the base of the flare) (Fig. 1.3A).[18] Open flares operate at smaller flow rates, temperatures and CH_4 concentrations – 10-2500 m^3 h^{-1}, 350-950 ºC and >20 % (*v/v*), respectively – though they exhibit lower combustion efficiencies, a lack of performance monitoring and higher emissions of VOCs/particles.[19] According to the US Environmental Protection Agency (US-EPA), flares must be enclosed and operated at a minimum temperature of 1000 ºC and 0.3 s of gas retention time to ensure an effective CH_4 destruction.[20] Conventional flares not meeting these flaring criteria, which typically occurs during the treatment of emissions with CH_4 concentrations below 30 % *v/v*, can be modified (e. g. at burner level) or supplemented with an additional fuel supply to treat CH_4-laden emissions at flow rates of 40-2500+ m^3 h^{-1} and CH_4 contents from 10 to 50 % (*v/v*).[19]

- Recuperative thermal oxidizers. These incinerators are forced draft systems currently used in many industrial processes including natural gas processing, chemical manufacturing, animal feed production and oil-gas refining. Briefly, the polluted air stream is drawn into the system fan and discharged into the inlet of the recuperative thermal oxidizer, where it is typically preheated in the tube side of a shell-and-tube style heat exchanger. The CH_4-laden air (preferentially with CH_4 concentrations below 30%

v/v) then passes through the burner, which supports the exothermic reaction. Typical temperatures, residence times and flow rates range from 900 to 1200 ºC, from 0.5 to 2 s and from 100 to 50000 m^3 h^{-1}, respectively (Fig. 1.3B). Finally, the hot purified air circulates again through the shell side of the heat exchanger, where the energy released by the reaction is used to preheat the incoming air. This configuration ensures up to 50-70 % heat recovery efficiencies and minimizes the overall fuel consumption of the recuperative thermal oxidizer.[17]

- Regenerative thermal oxidizers (RTO). RTO are based on the same principle as recuperative thermal oxidizers and can be used to treat CH_4 concentrations ranging from 0.2 to 27 % at high flow rates (up to 250000 m^3 h^{-1}) in off-gases from coal mines and spray painting in the automotive industry.[19,21] The operation of a RTO requires the initial preheating of the heat exchanger to the desired temperature (900-1200 ºC). The heat exchanger (consisting of two ceramic porous heat transfer beds) operates in a flow-reversal mode to transfer the heat of combustion of CH_4 to the incoming air via a solid heat storage medium (Fig. 1.3C). The use of diverter valves in RTO allows the flow direction switch, thus keeping the reactor core at ignition temperatures and enabling autothermal operation even when working with cold lean feeds (energy saving efficiencies around 95 %), which significantly lower the operating costs of this technology.[21,22] Despite the high CH_4 REs achieved by both recuperative and regenerative thermal oxidizers, the high investment and operating costs, together with the increased likelihood of explosion at operation temperatures in the region of 1000 ºC (above the CH_4 auto-ignition temperature of 617 ºC), still hinder their widespread implementation at full-scale.[23]

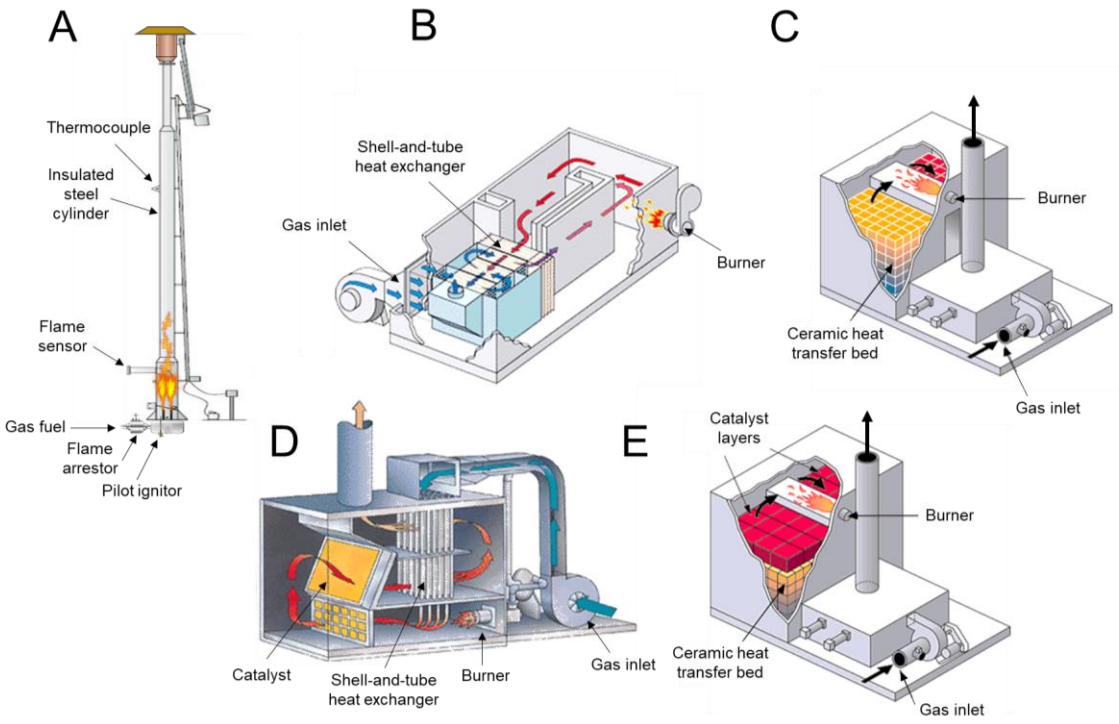

Fig. 1.3 Physical/chemical technologies reported to date for CH_4 mitigation (adapted from Anguil[17]). A) Enclosed direct fired thermal oxidizer, B) recuperative thermal oxidizer, C) regenerative thermal oxidizer (RTO), D) recuperative catalytic oxidizer (CATOX) and E) regenerative catalytic oxidizer (CTO).

1.3.1.2 Catalytic oxidation

Catalytic oxidation represents an alternative to conventional incinerators to abate CH_4 at concentrations of 0.1-30 %, whose effectiveness has been proven in the abatement of malodorous emissions from WWTPs and biogas production plants at flow rates ranging from 10 to 5000 $m^3 h^{-1}$.[24] Both recuperative (CATOX) and regenerative catalytic oxidizers (RCO) are commercially available at industrial scale, and differ from their thermal counterparts in the use of a layer of catalyst to conduct CH_4 oxidation (Fig. 1.3D, E). State-of-the-art active catalytic formulations for an efficient CH_4 abatement include Pd/PdPt/PdO. Unfortunately, the presence of sulfur compounds or particles in the off-gas, or the formation of water vapor along the process, may reduce the performance of the combustion reactions due to inhibition or adsorption of these compounds to the active sites of the catalyst, respectively.[23,24] The catalyst operation temperature is usually set

at 350-750 ºC for CH_4 combustion, which supports REs > 99.0 % and fuel savings of up to 40-60 % compared to their thermal counterparts.[17,23,24]

1.3.2 Biological technologies

Biotechnologies for CH_4 abatement are based on the enzymatic oxidation of this GHG catalysed by the methane monooxygenase (MMO) enzyme present in all methane-oxidizing bacteria (MOB). This oxidation occurs at ambient temperature and pressure, does not require an external supply of chemicals (apart from water and nutrients) and takes place in the aqueous phase (or inside the biofilm) following CH_4 mass transport from the gas emission (Fig. 1.4A).[25] The absence of extreme operating conditions and hazardous chemicals constitutes an additional advantage from a safety viewpoint for on-site staff and operators. The use of biological methods for CH_4 abatement has gradually increased based on their proven high robustness and efficiency (especially in a wide range of flowrates and at CH_4 concentrations below its lower explosive limit of 5 %), and on their lower operating costs when compared to their physical/chemical counterparts (lower energy requirements and no chemicals requirements). In addition, CH_4 abatement biotechniques typically show lower environmental impacts as a result of their lower CO_2 footprint and generation of innocuous or less-contaminating degradation products (CO_2, H_2O and new biomass).[15,16] Biotechnologies require: i) the presence of an aqueous phase to support the metabolic reactions underlying CH_4 biodegradation and ii) the availability of macronutrients (N, P, K, S) and micronutrients (usually heavy metals such as Cu, Fe, Zn or Mn needed for the synthesis and functioning of enzymes) to support microbial activity.[26] In the particular case of CH_4 abatement biotechnologies, their cost-efficient application is often constrained by the poor mass transport of this GHG from the gas emission to the aqueous phase due to its low aqueous solubility (dimensionless Henry's law constant, $H = C_G/C_L$, of 29.1 at 25º C and 1 atm). This low H results in low concentration gradients, and thus, in a reduced CH_4 biodegradation performance (Fig. 1.4B).[8,27] Therefore, the development of innovative compact bioreactor configurations

with a high mass transfer potential at reduced energy requirements constitutes a key research niche to boost the widespread implementation of GHG abatement biotechnologies. On the other hand, biotechnologies can create additional value out of CH_4 mitigation when coupled to the production of high-added value bioproducts from CH_4 bioconversion or when combined with other pollution treatment processes on-site that can eventually use CH_4 as a substrate. This will promote the development of a sustainable GHG bioeconomy and indirectly mitigate climate change.[28] In the following sections, the available bioreactor configurations for CH_4 abatement along with the microbiology underlying CH_4 biodegradation are discussed in detailed in order to provide a comprehensive background to understand Chapters 3 to 7.

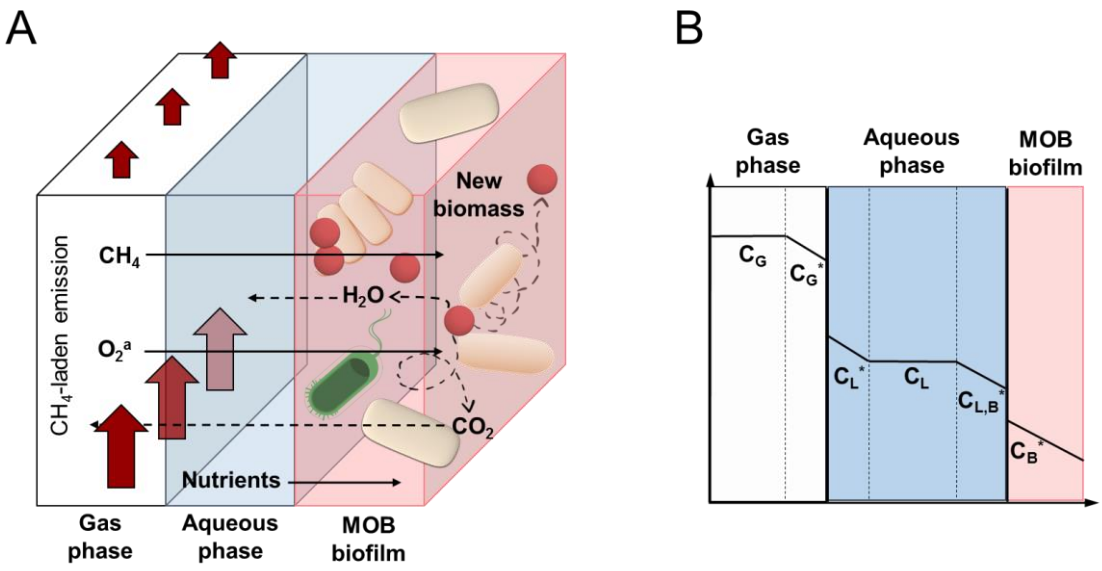

Fig. 1.4 A) Schematic of CH_4 mass transport and biodegradation mechanisms in bioreactors (adapted from Estrada et al.[16]), and B) CH_4 concentration profile representing the mass transfer processes occurring within an off-gas treatment biofilm bioreactor. C_G = Bulk concentration of CH_4 in the gas phase, C_G* = Gas phase concentration of CH_4 at the gas–liquid interphase, C_L* = Liquid phase concentration of CH_4 in equilibrium with the gas phase, C_L = Bulk concentration of CH_4 in the liquid phase, $C_{L,B}$* = Liquid phase concentration of CH_4 at the liquid–biofilm interphase, C_B* = Biofilm concentration of CH_4 in equilibrium with the liquid phase (adapted from Estrada et al.[27]). $^aO_2$: only required in aerobic methane abatement technologies.

1.3.2.1 Bioreactors for biological CH_4 oxidation

Biotechnologies for CH_4 mitigation have been implemented in the past 20 years either as actively vented bioreactors, where the CH_4-laden emission (containing O_2) is supplied

by forced ventilation in an upflow or downflow mode, or as passively vented bioreactors, where the CH_4-laden emission flows upwards from the bottom of the system whereas atmospheric O_2 diffuses from the top.[8,29] CH_4 abatement bioreactors are also classified into packed bed systems (biofilters, biotrickling filters or horizontal flow biofilm reactors) and suspended growth systems (stirred tank bioreactors, airlift bioreactors, bubble column bioreactors, membrane biofilm reactors and Taylor flow bioreactors) as a function of the presence or absence of a support media for biomass attachment, respectively.[28] A detailed description of the functioning, and typical design and operational parameters of the aforementioned bioreactors, is provided below:

- Biofilters (BFs). Methanotrophs-based BFs are likely the most widespread bioreactor configuration employed worldwide (both at laboratory and field scale) for the treatment of CH_4 emissions from landfills, coal mines or livestock farms.[30] The off-gas emission in these laminar contactors gets humidified before passing through a packed bed supporting the biofilm responsible of pollutant biodegradation, while a nutrient aqueous solution or water is irrigated intermittently (the latter if nutrients are uptaken from the support) (Fig. 1.5A). Two types of BFs are distinguished – actively and passively vented – depending on whether the flow of the CH_4 laden emission occurs forcibly or naturally upwards, respectively.[29] The intensive research conducted in the field of biofiltration and material science in the past years has resulted in important advances in packing material. Packing material is a key design parameter determining both water activity (and therefore microbial activity) and the specific surface available for biofilm formation and gas-biofilm mass transfer.[8,28] Thus, inorganic and organic beds from simple materials such as compost, gravel, coal, stone, clay or pine bark to more sophisticated structured packings such as autoclaved aerated concrete, polymeric rings and foams have been used (readers are referred to Table 2 in López et al.[8] for further details).[32,33] BFs are designed with empty bed residence times (EBRTs) sufficiently high to support an effective CH_4 mass transfer from the gas phase to the biofilm. BFs exhibit

large gas-biofilm interfacial areas, a rapid start-up and low operating costs (annual cost of ~2 € m^{-3} h^{-1}). On the contrary, they present a limited height in order to maintain low pressures drops (<10 cm H_2O) and a large footprint due to the high EBRTs needed for an efficient CH_4 removal (20-70 min and 1-14 h for removal efficiencies of 60-90 % in actively and passively vented BFs, respectively).[8,34-36] In this regard, the use of fungi in biofiltration, either standalone or in combination with bacteria, has been proposed as a microbiological platform to achieve higher removal efficiencies at lower EBRTs than those supported by bacterial BFs due to the larger surface areas and lower *H* of these microbes.[37] However, and to the best of our knowledge, the potential of fungi for CH_4 oxidation remains still unclear and no systematic studies have investigated the performance of CH_4 bacterial-fungal BFs. Another potential drawback that must be addressed during CH_4 biofiltration is biomass overgrowth, which can compromise the abatement performance and increase the pressure drop in biofilters under long-term operation, thus leading to higher operating costs.[38] In this context, several low-cost biomass control strategies such as protozoa and mite predation, continuous ozone addition, step feed biofiltration or famine periods have been recently proposed. Among them, feast-famine strategies can reduce the overall biomass accumulated per volume unit of the biofilter without significant down-time during implementation, complex reactor designs or additional operating costs.[39-42] Nonetheless, this innovative strategy has not been hitherto systematically evaluated under long-term operation for any gas pollutant, which hinders its applicability at full-scale biofiltration.

- Biotrickling filters (BTFs). BTFs are also laminar contactors where the polluted gas emission passes through a biofilm immobilised onto a packed bed continuously irrigated with an aqueous nutrient solution at rates typically ranging from 5 to 30 L m^{-3}_{bed} min^{-1} (Fig. 1.5B). The CH_4 initially absorbed in the trickling aqueous solution is subsequently degraded in the fixed biofilm using the nutrients contained in the trickling solution to support biomass growth. The investment costs of this bioreactor configuration

(10-41 € m^{-3} h^{-1}) are scale-dependent and can be up to 2-times higher than those of BFs. In contrast, the operating costs of BTFs are lower (annual costs of 1.2 € m^{-3} h^{-1}) than those of BFs as a result of their lower pressure drops.[36] This biotechnology supports a more efficient control of pH, temperature, water activity and nutrient supply compared to BFs. However, the presence of a continuous water layer over the biofilm entails a limited abatement performance for hydrophobic gas pollutants such as CH_4 due to their poor gas-liquid mass transport, thus resulting in REs ≤ 30 % at EBRT of 4-5 min.[8,27] In this context, recent studies have been focused on the addition of a non-aqueous phase (NAP) such as Brij 35 or silicone oil with a high affinity for CH_4 to boost CH_4 absorption, and subsequently, achieve higher CH_4 removals.[43-45]

- Horizontal flow biofilm reactors (HFBRs). This novel trickled technology comprises a stack of multiple horizontal plastic sheets, positioned vertically one above the other, with integrated frustums to sustain biofilm growth (Fig. 1.5C). Compared to other packed bed technologies, this configuration enables easier access to the different reactor parts, hence allowing for i) the examination of the pollutant biodegradation profile and microbial structure, and ii) biomass harvesting during the co-production of high added-value products. Both the liquid and gas phases flow horizontally across the sheets before moving to the sheet below, which ensures a good contact with the biofilm attached to the sheets and alleviates conventional biofiltration' drawbacks such as clogging, channelling or compaction.[46] Average CH_4 REs of 50 % at EBRTs of 45-50 min and negligible pressure drops (<10 mm H_2O) have been recorded in this bioreactor configuration under long-term operation (>1 year).[46,47] The addition of one or two NAPs to the tricking aqueous phase can also significantly enhance CH_4 REs in HFBRs up to 65-78 % at the aforementioned EBRTs.[47]

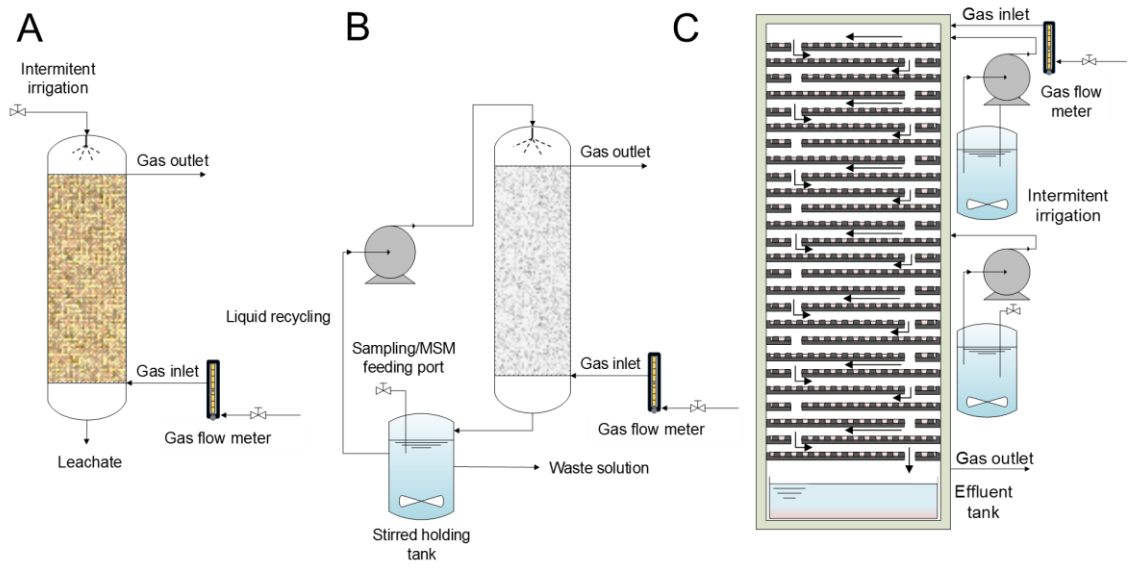

Fig. 1.5 Packed bed biotechnologies available to date for CH_4 mitigation (adapted from Muñoz et al.[34] and Kenelly et al.[47]). A) Biofilter (BF), B) Biotrickling filter (BTF) and C) horizontal flow biofilm reactor (HFBR).

- Stirred tank bioreactors (STRs). STRs are turbulent contactors where the continuous agitation, often mechanical, ensures perfect mixing and biomass suspension (Fig. 1.6A). The energy input for mixing is used to break down the bubbles of the polluted gas emission supplied at the bottom of the reactor (which increases the gas-liquid interfacial area) and to reduce the liquid film (thus increasing the overall volumetric mass transfer coefficient of the pollutant from the gas to the liquid phase).[48] Hence, REs of 50-60 % have been achieved in STRs devoted to CH_4 abatement at relatively low EBRTs (4-10 min).[44,49] The addition of a NAP in this type of bioreactor has been also recently assessed with enhanced CH_4 REs of up to 70 % at an EBRT of 4.8 min. However, despite the promising results obtained in STRs, their higher power consumption (by 1-2 orders of magnitude) compared to packed bed systems has resulted in the preferential implementation of BFs or BTFs in full-scale applications.[48,50]

- Bubble column bioreactors (BCB) and airlift reactors (ALR). These suspended growth configurations differ from the STRs on the fact that no mechanical agitation is provided. Thus, adecuate mixing and effective pollutant mass transfer to the microorganisms is typically achieved either using micropore diffusers in BCBs, or

installing a concentric draft-tube (riser) to create a density gradient within the culture broth in order to enhance the turbulence in ALRs (Fig. 1.6B, C).[8] Similarly to the STRs, these suspended growth bioreactors are ideal for both biomass harvesting during the co-production of bioproducts from CH_4 and community structure monitoring. In addition, their lower power requirements, as a result of the lack of mechanical agitation, guarantee a higher cost-efectiveness of BCBs and ALRs compared to STRs. However, either the addition of NAPs or the implementation of gas-recycling strategies is hitherto mandatory to boost CH_4 biodegradation over the basal REs of 20-30 % typically recorded in ALRs and BCBs.[51,52]

- Membrane biofilm reactors (MBfRs). MBfRs are based on the passive or active diffusion of the gas pollutant across the pores of a membrane into the liquid-biofilm located on the other side, which is driven by a concentration or a pressure gradient (Fig. 1.6D). This bioreactor configuration can overcome the CH_4 mass transfer limitations aforementioned due to the high permeability and affinity of some membrane materials for hydrophobic pollutants such as CH_4. Thus, both the membrane material and membrane configuration must be properly selected to ensure an optimum pollutant abatement performance.[53] The few studies reported on CH_4 abatement with MBfRs have employed micro- (polyvinylidene difluoride, 0.40 μm pore size) and ultrafiltration (Zenon and acrylonitrile, < 0.1 μm pore size) hollow fiber membranes, the later supporting the highest gas-liquid interfacial areas for mass transfer. However, little attention was paid to the CH_4 REs in these studies, which were focused on the use of CH_4 as electron donor for denitrification, either coupling aerobic methane oxidation to denitrification or denitrifying anoxic methane oxidation (DAMO) to anammox.[54-57] In this context, MBfRs represent a promising technology to support the growth of DAMO microorganisms due to their higher capacity for biomass retention (see section *1.3.2.4* for further discussion on this issue). However, it must be stressed that their high construction costs and the

lack of pilot-scale studies demonstrating their long-term operational stability still limit the widespread implementation of MBfRs for gas treatment applications.[53]

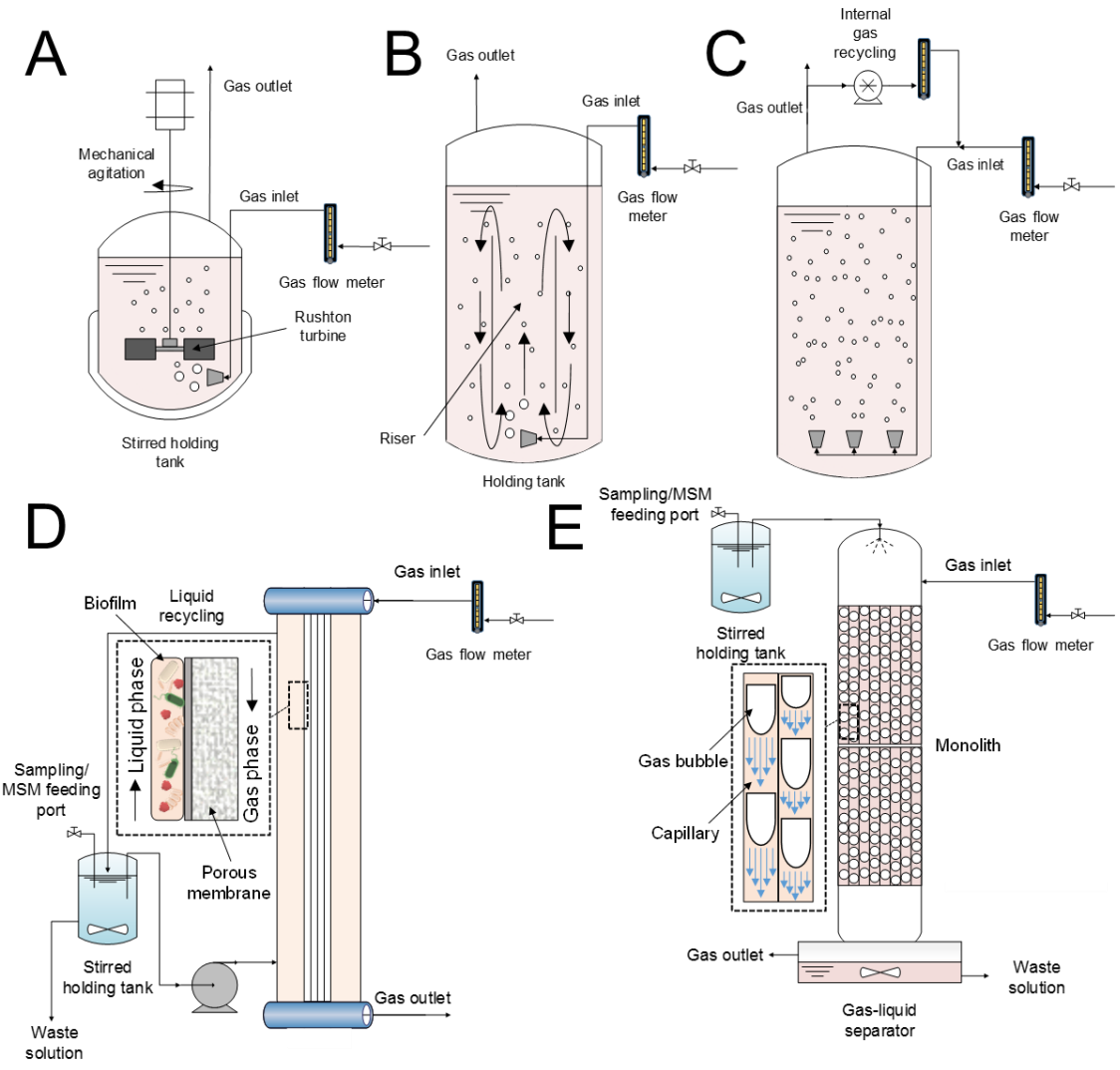

Fig. 1.6 Suspended growth bioreactors reported to date for CH_4 mitigation (adapted from Muñoz et al.[34], Cai et al.[57] and Rocha-Rios et al.[58]). A) Stirred tank bioreactor (STR), B) airlift bioreactor (ALR), C) bubble column bioreactor (BCB) with internal gas recycling, D) membrane biofilm reactor (MBfR) and E) Taylor flow bioreactor (TFB).

- Taylor flow bioreactors (TFBs). These innovative bioreactors are composed of parallel straight microcapillaries (Ø of 1-5 mm) separated by a thin wall (Fig. 1.6E). The preferred flow pattern, the so-called segmented or Taylor flow, is a bubble train of alternate liquid slugs and small gas bubbles, with both gas and liquid flowing upwards or downwards. Taylor flow in capillaries enables CH_4 mass transfer coefficients equivalent to those in STRs at around one order of magnitude lower power consumptions.[48] In this

regard, the only work published to date on CH_4 abatement capillary bioreactors reported 50 % higher CH_4 removals at significant lower reactor sizes and pressure drops compared to STRs supplemented with a NAP.[50,58] However, since monolith multichannel bioreactors with Taylor flow have not been yet designed and validated at lab-scale, this CH_4 abatement biotechnology remains in an embryonic stage and still requires further research.

1.3.2.2 Aerobic methanotrophy: Taxonomy, metabolic pathways and ecophysiology

Aerobic methanotrophs are methylotrophic microorganisms with the ability to oxidize CH_4 in the presence of O_2 and use it as their main carbon and energy source. Despite most aerobic methanotrophs are bacteria, several yeasts, fungi and green microalgae have been also tentatively identified as methane oxidizers.[59-63] MOB are widely distributed in environments such as wetlands, peat bogs, forests, rice paddies, groundwater, landfill cover soils, sewage sludge or marine sediments, preferentially in the interface between aerobic and anaerobic zones with significant CH_4 fluxes.[63,64] Traditionally, MOB have been classified into three different groups according to their physiological and morphological characteristics: type I, type II and type X (also known as Ib) methanotrophs. Type I includes MOB that i) present intracytoplasmatic membranes as bundles of vesicular discs, ii) use the ribulose monophosphate (RuMP) pathway for carbon assimilation and iii) contain phospholipid fatty acids of 14 and 16 carbons length. Type II MOB are characterized by i) an intracytoplasmatic membrane aligned along the peripheral part of the cell, ii) the use of the serine pathway for carbon assimilation and iii) phospholipid fatty acids of 18 carbons length. On the other hand, type X share characteristics of both type I and II, including the RuMP pathway to assimilate formaldehyde and the synthesis of the enzyme ribulose biphosphate carboxylase from the serine pathway to fix CO_2.[8,65] The current classification of known aerobic MOB based on 16S rRNA encloses a wide phylogenetic distribution within two different phyla: *Proteobacteria* (subdivisions *α*- and *γ-Proteobacteria*) and *Verrucomicrobia*. The most

representative genera within the *α-Proteobacteria* phylum are *Methylocystis*, *Methylosinus* (clustered within *Methylocystaceae* family), *Methylocella* and *Methylocapsa* (clustered within *Beijerinckiaceae*). Methanotrophs within *γ-Proteobacteria* (e. g. *Methylomonas*, *Methylobacter*, *Methylosarcina* or *Methylococcus* genera) belong to the *Methylococcaceae* family. Finally, methanotrophs from *Verrucomicrobia* phylum are essentially affiliated within the *Methylacidiphilacecae* family, and more specifically to the *Methylacidiphilum* and *Methylacidimicrobium* genera.[63,65] Based on their different ecophysiology and taxonomical affiliation, MOB from *Verrucromicrobia* have been recently referred as type III methanotrophs.[66] Furthermore, the phylogenetic relationships between methanotrophs are usually examined as a function of the enzyme MMO, which catalyses the conversion of methane to methanol. Thus, the particulate methane monooxygenase (pMMO) is found in most MOB and is located in the cytoplasmatic membrane, while the soluble methane monooxygenase (sMMO) is present in the cytoplasm and can be expressed either as the sole form of MMO or together with pMMO. The enzyme sMMO has been traditionally associated with type II methanotrophs, though few genera of type I methanotrophs with the capability to synthesize sMMO have been recently identified.[65-67]

Methane biodegradation comprises a multistage process with methanol, formaldehyde and formic acid as sequential metabolic intermediates, finally ending up with the production of CO_2 (Fig. 1.7).[8] Part of the carbon contained in the formaldehyde may be either converted to formic acid or incorporated as bacterial cell material through the RuMP (type I/X methanotrophs) or the serine pathways (type II methanotrophs).[63] The stoichiometric equations summarizing the oxygen and nitrogen demands of both the RuMP and serine pathways are shown in Equations 1 and 2, respectively, where $C_4H_8O_2N$ represents microbial biomass:[68]

$$CH_4 + 1.50O_2 + 0.12NH_4^+ \rightarrow 0.12(C_4H_8O_2N) + 0.53CO_2 + 1.71H_2O + 0.12H^+ \quad \text{(Eq. 1)}$$

$$CH_4 + 1.57O_2 + 0.10NH_4^+ \rightarrow 0.10(C_4H_8O_2N) + 0.59CO_2 + 1.75H_2O + 0.10H^+ \quad \text{(Eq. 2)}$$

Type I methanotrophs exhibit a higher CH_4 conversion efficiency and require only 1 ATP molecule to form 3 formaldehyde molecules during CH_4 oxidation. In contrast, type II methanotrophs are superior in terms of CH_4 storage as phospholipid fatty acids and polyhydroxyalkanoates (PHAs), though they require 3 ATP and 2 NADH molecules to fix 2 formaldehyde and one CO_2 molecules.[69] Consequently, type I methanotrophs tend to outcompete their type II counterparts, unless cultivation conditions provides a competitive advantage for the later. A 100 % conversion of CH_4 to microbial biomass is not possible since assimilatory pathways result in a net production of at least 12 % CO_2 according to previous studies.[70]

Both Monod and Michaelis-Menten models are often used to describe microbial CH_4 oxidation. However, the different experimental setups and models used for the estimation of the kinetic parameters usually hinder the direct comparison of the data available in literature (readers are referred to Table 1 in López et al.[8] for further details). Among the kinetic parameters, the Monod constant (K_S) characterizes the affinity of microorganisms for the substrates, and in the particular case of CH_4, K_S typically ranges from 1×10^{-6} to 4.7×10^{-4} M. pMMO-bearing bacteria have been reported to exhibit a higher affinity for CH_4 (lower K_S values) than those bearing sMMO.[71] Moreover, the maximum specific biodegradation rates (q_{max}) for CH_4 typically range from 4.16×10^{-5} to 1.3×10^{-4} $gCH_4\ g_X^{-1}\ h^{-1}$. In this context, microorganisms with a high q_{max} and a high affinity for CH_4 (low K_S) are desirable to guarantee an efficient biocatalytic activity and to reduce the start-up period of bioreactors devoted to CH_4 mitigation. However, it must be stressed that most CH_4 biodegradation kinetic studies reported to date were carried out at high biomass concentrations, which did not ensure the absence of mass transport limitations and, therefore, the validity of the kinetic parameters obtained.[8]

The rates of CH_4 oxidation, and thus methanotrophic growth, greatly depend on cultivation parameters such as O_2 and CH_4 concentrations, temperature, pH, the concentration and type of nitrogen source and copper levels. According to the above stoichiometry, molar O_2:CH_4 ratios should be maintained ≥ 1.5:1 to ensure a proper CH_4 oxidation.[70] In this context, low O_2:CH_4 ratios stimulate the growth of type II methanotrophs, while high O_2:CH_4 ratios promote the growth of type I methanotrophs.[72] These findings support the hypothesis that the enzyme sMMO (predominantly found in type II methanotrophs) is often expressed at high CH_4 concentrations and pMMO at low CH_4 concentrations.[73] Methanotrophs typically exhibit maximum oxidation rates under mesophilic conditions (25-30 ºC), though thermotolerant and thermophilic *Methylotermus*, *Methylocaldum*, *Methylococcus* or several *Verrucomicrobia* strains have been isolated from active silts, hot springs and aquifers and volcanic soils, with and optimal growth in the range of 42-65 ºC.[65,74-78] Similarly, psychrophilic strains of *Methylobacter*, *Methylosphaera*, and *Methylomonas* have been isolated from tundra soils, Antarctic meromictic lakes, and deep igneous groundwater, exhibiting an optimal growth range of 3.5-15 °C.[77,78] On the other hand, most methanotrophs preferentially grow and oxidize CH_4 at pHs of 7-7.6, though type II seem to be more tolerant than type I methanotrophs to low pHs (4-5).[79] In this sense, acidophilic species from the *Methylocella* and *Methylocapsa* genera, and more especially from the *Verrucomicrobia* phylum, have been found in acidic environments optimally growing under pH values lower than 2.5.[78] In contrast, the CH_4 biodegradation ability of the halophilic *Methylomicrobium alcaliphilum* strain 20Z is enhanced at pH as high as 9.0.[80] Despite type II methanotrophs are able to fix N_2 at low O_2 levels, nitrate and ammonium are the preferred N sources over nitrite for both type I and II methanotrophs.[81] Type I methanotrophs are dominant in environments with low CH_4 concentrations and high inorganic nitrogen levels, whereas type II methanotroph predominate under high CH_4/N conditions and outcompete type I under nutrient (e. g. N) limitations.[71,79] Microbial stimulation or inhibition mediated by inorganic nitrogen sources such as ammonium or

nitrate greatly depend on the nitrogen concentration, the pH and the type of methanotroph. Hence, optimal growth and CH_4 oxidation rates were recorded at ammonium concentrations of 12–61 mM for some methanotrophic communities, while other studies revealed that NH_4^+ concentrations of 4–10 mM could already reduce CH_4 oxidation by 30 %.[74] Some *in-situ* investigations suggested that high ammonium concentrations could inhibit CH_4 oxidation either by toxicity or enzymatic competition, although such detrimental effects could be also due to a nitrite accumulation from ammonium oxidation.[71] Among micronutrients, copper positively regulates the activity of the enzymes pMMO and sMMO, and controls the expression of their genes. However, copper concentration in the cultivation broth must be adjusted in order to maintain copper homeostasis and prevent metal toxicity. Most methanotrophs grow optimally at copper concentrations lower than 4.3 mM, though previous enzymatic assays have demonstrated that sMMO in type II methanotrophs is properly synthesized at low Cu^{2+} concentrations (below 0.8 mM).[74,82,83] In contrast, the expression of the *pmoA* gene (encoding a subunit of pMMO) occurred at significant levels regardless of the Cu^{2+} concentration, the transcript numbers increasing concomitantly with copper concentrations.[84] Finally, some aerobic methanotrophs under copper-limiting scenarios can excrete a molecule called methanobactin, which is able to bind copper from the extracellular medium and actively transport it into the cell to maintain copper homeostasis.[85]

1.3.2.3 CH_4-driven PHA production as a case-scenario of GHG-based biorefineries

PHAs such as poly-3-hydroxybutyrate (PHB) or poly-3-hydroxyvalerate (PHV) are linear polyesters completely synthesized by microorganisms intracellularly under nutrient-limiting conditions (usually N, P or Mg). These high-added value products have recently gained commercial interest worldwide due to their biodegradable nature and the forthcoming shortage of the fossil fuels used to produce conventional plastics such as polyethylene and polypropylene. PHAs are easily moldable and soft (high tensile

strength – 40 MPa), sticky, easy to blend with other polymers, highly elastic (Young's Modulus – 3500 MPa) and heat tolerant (crystalline melting point at 175 ºC), which makes them suitable substitutes of petroleum-based polymers.[86] Their market price currently ranges from 4-20 € kg_{PHA}^{-1}, which depends on the type of biopolymer, carbon source, microbial strain and product purity.[28] Despite the price of PHAs has significantly decreased in the past years, their competitiveness is still hindered by the costs associated to their downstream processing and, in a major extent, to the cost associated to the acquisition of the raw materials used, which accounts for 30-40% of the total costs.[87] In this regard, CH_4 has recently emerged as a promising feedstock for PHA accumulation that might i) significantly decrease PHA production costs and ii) be a realistic approach for carbon sequestration and GHGs emission reduction.[68]

Type II methanotrophs (such as *Methylocystis*, *Methylosinus* and *Methylocella* genera) have shown to be the only methanotrophs with the metabolic capability to produce PHAs through the serine pathway, where acetyl-CoA is converted into the corresponding hydroxyacyl (HA) coenzyme A thioester, which is finally transformed into the HA monomer.[82] When CH_4 is used as the sole C and energy source, PHB of high molecular weight is the sole PHA synthesized within the first 48-72 h after culture exposure to nutrient-limiting conditions (Fig. 1.7).[88,89] The overall equation for PHB accumulation in methanotrophs using the serine pathway is given below:

$$8CH_4 + 12O_2 + FP \rightarrow C_4H_6O_2 + 4CO_2 + 12ATP + FPH_2 \quad \text{(Eq. 3)}$$

where FP is the oxidised succinate dehydrogenase (involved in the tricarboxylic acid cycle, TCA), FPH_2 the reduced succinate dehydrogenase and $C_4H_6O_2$ the empirical formula of the PHA monomer. According to Eq. 3, the theoretical yield for bioconversion of CH_4 into PHA (Y_{PHA}) can be estimated to 67 %. However, the fact that part of the CH_4 and O_2 consumed has to be converted to CO_2 to generate $NADP^+$ for the acetoacetyl-CoA reductase in the PHB biosynthetic pathway, results in a decrease of the theoretical

Y_{PHA} to 54 %.[90] The adjustment of the experimental Y_{PHA} values to the theoretical ones depends not only on the purity and the type of the strain, but also on the cultivation conditions. Previous studies with mixed bacterial cultures typically reported lower PHA accumulations (up to 35-45 % wt) than those obtained with pures strains.[91,92] Several nutrient limitations have been assessed to promote PHB production, N-limitation often resulting in the highest PHA contents (up to 50 % wt).[88,91] Rostkowski et al.[93] demonstrated that the oxygen concentration and the nitrogen source employed for methanotrophic growth influence PHB synthesis, nitrogen gas mediating a PHA content of 45 % and ammonium of 50-60 % in *Methylosinus trichosporium* OB3b and *Methylocystis parvus* OBBP, respectively, at oxygen partial pressures of 0.10-0.30 atm. Furthermore, previous studies also optimized macro- and micronutrient concentrations in the culture broth to maximize PHB accumulation in *M. parvus* OBBP, copper and calcium representing the most critical elements to be adjusted.[89] It must be highlighted that most works on PHA production by obligate methanotrophs have been carried out batchwise, which challenges its implementation in bioreactors under continuous operation. In addition, mosts studies were conducted using pure CH_4 (readers are referred to Table 3 in Cantera et al.[28] for detailed information on previous works), the feasibility of biogas as a viable feedstock requiring further experimental assessment. Recent studies have evaluated the production of new PHAs – PHV and copolymers such as poly(3-hydroxybutyrate-*co*-3-hydroxyvalerate) (PHBV) or poly(3-hydroxybutyrate-*co*-4-hydroxybutyrate) (P3HB4HB)) – through the addition of ω-hydroxyalkanoates, organic acids or alcohols as co-substrates for methanotrophs.[94-96] This innovative approach might enhance not only the PHA yields and contents, but also the mechanical properties of the tailor-made biocomposite compared to PHB. However, future research should focus on the evaluation of the influence of new cosubstrates on methanotrophic growth and PHA production, aiming at cointegrating this innovative approach within a biorefinery concept.

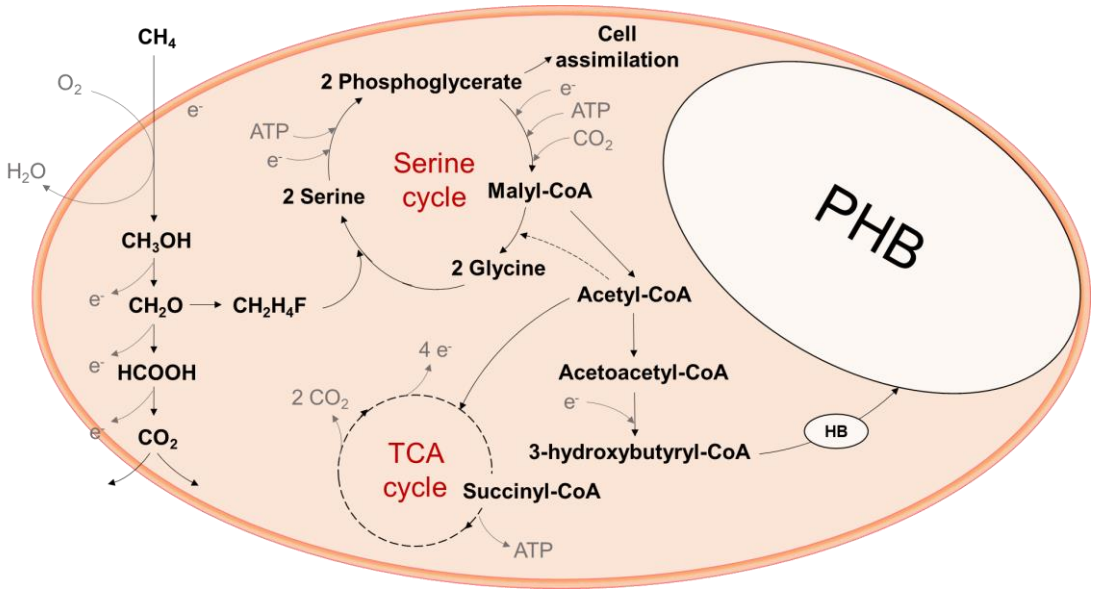

Figure 1.7 PHB production pathway in obligate type II methanotrophs. Dotted arrows indicate the existence of not-mentioned intermediates (adapted from Pieja et al.[97]).

1.3.2.4 Denitrifying anaerobic CH_4 oxidation: A promising microbial nitrogen removal process in WWTPs

Approximately 300 Tg of CH_4 are produced annually through methanogenesis, of which 90% is anoxically oxidized by specialized groups of microorganisms before diffusion into oxic environments.[98] Anaerobic oxidation of methane (AOM) was first discovered in the 1970s in marine sediments, where the process occurred coupled to sulfate reduction (S-DAMO, sulfate-dependent anaerobic methane oxidation) (Fig. 1.8A).[99] However, the archaea and bacteria responsible of this process were actually identified 20 years later.[100] In the past decade, new AOM processes coupled to nitrate, nitrite (N-DAMO, nitrate- and nitrite-dependent anaerobic methane oxidation), manganese and iron (M-DAMO, metal ion (Mn^{4+} and Fe^{3+})-dependent anaerobic methane oxidation) reduction were discovered (Fig. 1.8B, C).[101,102]

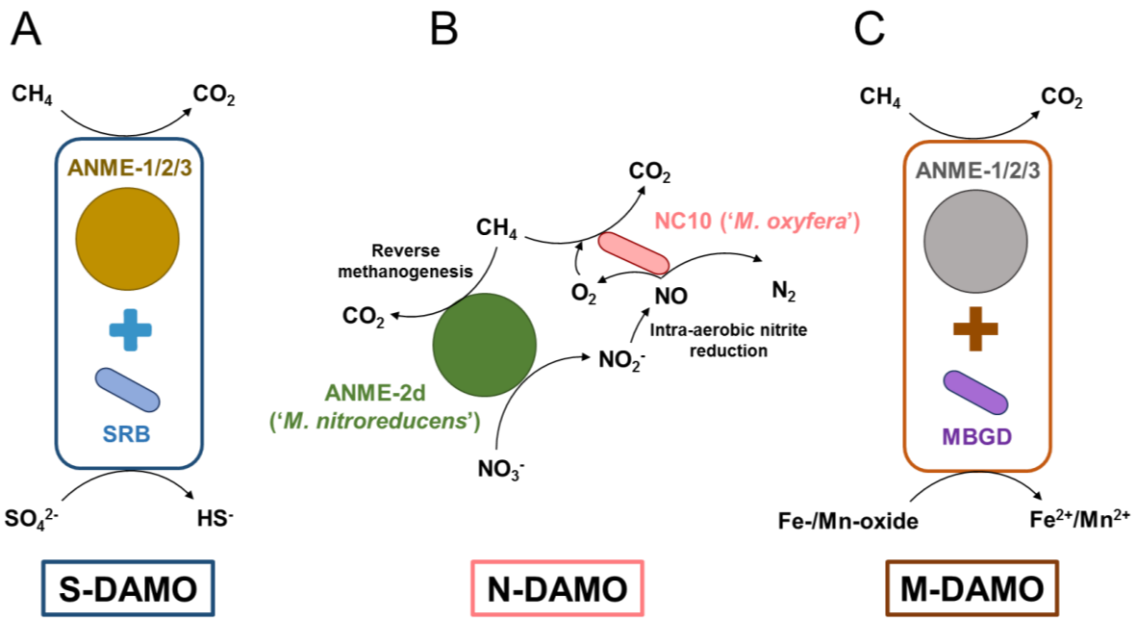

Fig. 1.8 AOM processes described to date as a function of the electron acceptors (adapted from Cui et al.[103]). A) Sulfate-dependent anaerobic methane oxidation (S-DAMO), B) nitrate- and nitrite-dependent anaerobic methane oxidation (N-DAMO) and C) metal ion (Mn^{4+} and Fe^{3+})-dependent anaerobic methane oxidation (M-DAMO). ANME = anaerobic methanotrophic archaea; SRB = sulfate-reducing bacteria; *M. oxyfera* = *Candidatus 'Methylomirabilis oxyfera'*; *M. nitroreducens* = *Candidatus 'Methanoperedens nitroreducens'*; MBGD = marine benthic group D.

Among AOM processes, N-DAMO (namely for clarity purposes DAMO, denitrifying anaerobic methane oxidation) represents an important link between the nitrogen and the carbon cycles, and might be of interest in WWTPs for a combined global warming mitigation and N removal through denitrification (since it would avoid the use of expensive electron donors such as acetate, methanol, ethanol, etc).[104] The microorganisms reported to date as the main responsible of DAMO have been identified within the archaeal lineage ANME-2d (*Candidatus 'Methanoperedens nitroreducens'*) and the bacterial phylum NC10 (*Candidatus 'Methylomirabilis oxyfera'*) in both natural habitats and engineered systems. Both DAMO microorganisms are often found together in microbial clusters. Indeed, while the archaeal partner reduces nitrate to nitrite using electrons derived from CH_4, the bacterial partner reduces nitrite to NO and further to N_2 and O_2 via the inter-aerobic denitrification pathway (Fig. 1.8B).[105,106] This O_2 is mainly used for aerobic CH_4 oxidation, while the remaining is consumed by terminal respiratory

oxidases.[107] Equations 4 and 5 show the overall reactions of the DAMO process with nitrate or nitrite as the electron acceptor, respectively:[108]

$$CH_4 + 4NO_3^- \rightarrow CO_2 + 4NO_2^- + 2H_2O \ (\Delta G^o = -503 \text{ kJ mol}^{-1} \text{ CH}_4) \quad \text{(Eq. 4)}$$

$$3CH_4 + 8NO_2^- + 8H^+ \rightarrow 3CO_2 + 4N_2 + 10H_2O \ (\Delta G^o = -928 \text{ kJ mol}^{-1} \text{ CH}_4) \quad \text{(Eq. 5)}$$

The control of the cultivation conditions such as substrate concentrations and environmental parameters is crucial in order to ensure a proper DAMO performance. In this context, despite *M. oxyfera* can be acclimated at 20º C, the maximum DAMO activity was recorded at 25-30 ºC.[109] Previous studies also confirmed that nitrite might result in a toxic effect at loadings higher than 1.4 mmol $N\text{-}NO_2^-$ L^{-1} d^{-1}, though the effect of nitrate concentration/loading was not investigated.[110] Similarly, O_2 headspace concentrations over 2 % (*v/v*) (corresponding to aqueous concentrations of 0.8 mgO_2 L^{-1}) induced a ~3-fold decrease in CH_4 and nitrite consumption rates by *M. oxyfera* due to oxidative stress.[111] However, it must be highlighted that DAMO studies reported to date are restricted to the use of pure CH_4 as electron donor. Since the biogas produced from sludge digestion in WWTPs also contains CO_2 and H_2S, the impact of these components on DAMO performance remains unclear. At this point it must be stressed that DAMO microbes have been successfully enriched in bioreactors fed with effluent discharged from WWTPs, which indicates that DAMO could be applied in wastewater treatment.[56,112] However, the slow growth rate of these microorganisms often jeopardise the implementation of DAMO at full-scale. Thus, DAMO strictly demands i) reactor configurations with an effective biomass retention and ii) an efficient gas-liquid mass transfer of CH_4 to trigger biofilm formation (12-24 months to ensure > 50 % DAMO in the whole community) and enhanced bioreaction rates.[113] In this context, recent studies have proposed the co-cultivation of DAMO and anammox microbial communities in MBfRs in order to achieve higher N removals and an effective CH_4 mitigation, though the time required to enrich these consortia (12-15 months) still hinders its implementation at full-

scale.[57,114] Further research should then be focused on the implementation of high-mass transfer bioreactors and on exploring alternative microbial partners to increase both CH_4 and N removals.

1.4 References

(1) Intergovernmental Panel on Climate Change. *Fifth assessment report: Climate change 2014, Synthesis Report*, 2014; https://www.ipcc.ch/report/ar5/syr/. Accessed 7 June 2017.

(2) European Environment Agency. *Annual European Union Greenhouse Gas Inventory 1990 - 2015 and Inventory Report 2017*, 2017. http://www.eea.europa.eu//publications/european-union-greenhouse-gas-inventory-2017. Accessed 7 June 2017.

(3) National Oceanic and Atmospheric Administration, National Centers for Environmental Information, State of the Climate: *Global Climate Report for Annual 2016*, 2017. https://www.ncdc.noaa.gov/sotc/global/201613. Accessed 8 June 2017.

(4) Environmental Protection Agency. *Inventory of US Greenhouse Gas Emissions and Sinks: 1990 – 2015*, 2017. http://epa.gov/climatechange/ghgemissions/usinventoryreport.html. Accessed 7 June 2017.

(5) Intergovernmental Panel on Climate Change. *Climate Change 2013, the physical science basis. Working group I contribution to the fifth assessment report of the Intergovernmental Panel on Climate Change*, 2013; http://www.ipcc.ch/report/ar5/wg1/. Accessed 23 August 2017.

(6) Dessus, B.; Laponche, B.; Le Treut, H. The importance of a methane reduction policy for the 21st century, 2009; http://www.global-chance.org/IMG/pdf/BDBLHT5Methane.pdf. Accessed 23 August 2017.

(7) Girard, M.; Nikiema, J.; Brzezinski, R.; Buelna, G.; Heitz, M. A review of the environmental pollution originating from the piggery industry and of the available mitigation technologies: towards the simultaneous biofiltration of swine slurry and methane. *Can. J. Civ. Eng.* **2009**, *36*, 1946–1957; DOI 10.1139/L09-141.

(8) López, J. C.; Quijano, G.; Souza, T. S. O.; Estrada, J. M; Lebrero, R.; Muñoz, R. Biotechnologies for greenhouse gases (CH_4, N_2O, and CO_2) abatement: State of the art and challenges. *Appl. Microbiol. Biotechnol.* **2013** *97*(6), 2277–2303; DOI 10.1007/s00253-013-4734-z.

(9) Avalos-Ramirez, A.; Jones, J. P.; Heitz, M. Methane treatment in biotrickling filters packed with inert materials in presence of a non-ionic surfactant. *J. Chem. Technol. Biot.* **2012**, 87, 848–853; DOI 10.1002/jctb.3811.

(10) McCarty, P. L.; Bae, J.; Kim, J. Domestic wastewater treatment as a net energy producer–can this be achieved? *Environ. Sci. Technol.* **2011**, *45*, 7100–7106; DOI 10.1021/es2014264.

(11) Muñoz, R.; Souza, T. S. O.; Glittmann, L.; Pérez, R.; Quijano, G. Biological anoxic treatment of O2-free VOC emissions from the petrochemical industry: A proof of concept study. *J. Hazard. Mater.* **2013**, *260*, 442–450; DOI 10.1016/j.jhazmat.2013.05.051.

(12) Vestman, J.; Liljemark, S.; Svensson, M. *Cost benmarking of the production and distribution of biomethane/CNG in Sweden*, 2014. http://www.sgc.se/ckfinder/userfiles/files/SGC296_v2.pdf. Accessed 8 June 2017.

(13) Eurostat Statistics Explained. *Natural gas price statistics*, 2016. http://ec.europa.eu/eurostat/statistics-explained/index.php/Natural_gas_price_statistics. Accessed 8 June 2017.

(14) United Nations Framework Convention on Climate Change. *Report of the Conference of the Parties serving as the meeting of the Parties to the Kyoto Protocol on its eighth session, held in Doha from 26 November to 8 December 2012*, 2013. http://unfccc.int/bodies/body/6409/php/view. Accessed 10 June 2017.

(15) Kennes, C.; Thalasso, F. Waste gas biotreatment technology. *J. Chem. Technol. Biotechnol.* **1998**, *72*, 303–319; DOI 10.1002/(SICI)1097-4660(199808)72:4<303::AID-JCTB903>3.0.CO;2-Y.

(16) Estrada, J. M; et al. Strategies for Odour Control. In *Odour Impact Assessment Handbook*; Belgiorno, V.; Naddeo, V.; Zarra, T., Eds.; John Wiley & Sons, Inc., 2012; pp. 85–124.

(17) Anguil, G. H. Emission control technology – Thermal oxidation. In *Odor and VOC control Handbook*; Rafson, H. J., Ed.; 1st edn. McGraw-Hill Handbooks, New York, U.S., 1998.

(18) Noyola, A.; Morgan-Sagastume, J. M.; López-Hernández, J. E. Treatment of biogas produced in anaerobic reactors for domestic wastewater: odor control and energy/resource recovery. *Rev. Environ. Sci. Bio.* **2006**, *5*, 93–114; DOI 10.1007/s11157-005-2754-6.

(19) Environmental Protection Agency. *Management of low levels of landfill gas*, 2011. http://www.epa.ie/pubs/advice/waste/waste.html. Accessed 12 August 2017.

(20) Environmental Protection Agency. *Landfill manual – Site design*, 2000. https://www.epa.ie/pubs/advice/licensee. Accessed 12 August 2017.

(21) Qi, X.; Liu, Y.; Xu, H.; Liu, Z., Liu, R. Modeling thermal oxidation of coal mine methane in a non-catalytic reverse-flow reactor. *J. Mech. Eng.* **2014**, *60*(7-8), 495–505; DOI 10.5545/sv-jme.2013.1393.

(22) Su, S.; Beath, A.; Guo, H.; Mallett, C. An assessment of mine methane mitigation and utilisation technologies. *Prog. Energ. Combust.* **2005**, *31*, 123–170; DOI 10.1016/j.pecs.2004.11.001.

(23) Hinde, P.; Mitchell, I.; Riddell, M. COMET^{TM} – A new ventilation air methane (VAM) abatement technology. *Johnson Matthey Technol. Rev*., **2016**, *60*(3), 211–221; DOI 10.1595/205651316X692059.

(24) Hargitai, T.; Silversand, F. A.; Gunnarsson, L. *Evaluation of catalytic abatement technology for elimination of methane and odor emissions from biogas production plants, SGC Rapport 287*, 2013. https://www.sgc.se/ckfinder/userfiles/files. Accessed 12 August 2017.

(25) Ménard, C.; Avalos-Ramirez, A.; Nikiema, J.; Heitz, M. Biofiltration of methane and trace gases from landfills: A review. *Environ. Rev.* **2012**, *20*, 40–53; DOI 10.1139/A11-022.

(26) Deshusses, M. A. Biological waste air treatment in biofilters. *Curr. Opin. Biotechnol.* **1997**, *8*, 335–339; DOI 10.1016/S0958-1669(97)80013-4.

(27) Estrada, J. M.: Lebrero, R.; Quijano, G.; Pérez, R.; Figueroa-González, I.; García-Encina, P. A.; Muñoz, R. Methane abatement in a gas-recycling biotrickling filter: Evaluating innovative operational strategies to overcome mass transfer limitations. *Chem. Eng. J.* **2014**, *253*, 385–393; DOI 10.1016/j.cej.2014.05.053.

(28) Cantera, S.; et al. Technologies for the bio-conversion of GHGs into high added value products: Current state and future prospects. In *Carbon Footprint and the Industrial Life Cycle, From Urban Planning to Recycling*; Álvarez-Fernández, R.; Zubelzu, S.;

Martínez R., Eds.; Springer International Publishing, 2017; pp. 359–388; DOI 10.1007/978-3-319-54984-2.

(29) Gebert, J.; Gröngröft, A. Performance of a passively vented field-scale biofilter for the microbial oxidation of landfill methane. *Waste Manage.* **2006**, *26*(3), 245–251; DOI 10.1016/j.wasman.2005.01.022.

(30) Nikiema, J.; Brzezinski, R.; Heitz, M. Elimination of methane generated from landfills by biofiltration: a review. *Rev. Environ. Sci. Bio.* **2007**, *6*(4), 261–284; DOI 10.1007/s11157-006-9114-z.

(31) Ménard, C.; Ramirez, A. A.; Nikiema, J.; Heitz, M. Effect of trace gases, toluene and chlorobenzene, on methane biofiltration: An experimental study. *Chem. Eng. J.* **2012**, *204–206*, 8–15; DOI 10.1016/j.cej.2012.07.070.

(32) Ganendra, G.; Mercado-Garcia, D.; Hernandez-Sanabria, E.; Boeckx, P.; Ho, A.; Boon, N. Methane biofiltration using autoclaved aerated concrete as the carrier material. *Appl. Microbiol. Biotechnol.* **2015**, *99*(17), 7307–7320; DOI 10.1007/s00253-015-6646-6.

(33) Limbri, H.; Gunawan, C.; Thomas, T.; Smith, A.; Scott, J.; Rosche, B. Coal-packed methane biofilter for mitigation of green house gas emissions from coal mine ventilation air. *PLOS One* **2014**, *9*(4), e94641; DOI 10.1371/journal.pone.0094641.

(34) Muñoz, R.; Malhautier, L.; Fanlo, J. L.; Quijano, G. Biological technologies for the treatment of atmospheric pollutants. *Int. J. Environ. An. Ch.* **2015**, *95*(10), 950–967; DOI 10.1080/03067319.2015.1055471.

(35) Estrada, J. M.; Kraakman, N. J. R. B.; Lebrero, R.; Muñoz, R. A sensitivity analysis of process design parameters, commodity prices and robustness on the economics of odour abatement technologies. *Biotechnol. Adv.* **2012**, *30*(6), 1354–1363; DOI 10.1016/j.biotechadv.2012.02.010.

(36) Estrada, J. M.; Kraakman, N. J. R. B.; Muñoz, R.; Lebrero, R. A comparative analysis odour treatment technologies in wastewater treatment plants. *Environ. Sci. Technol.* **2011**, *45*(3), 1100–1106; DOI 10.1021/es103478j.

(37) Vergara-Fernandez, A.; Hernandez, S.; Revah, S. Phenomenological model of fungal biofilters for the abatement of hydrophobic VOCs. *Biotechnol. Bioeng.* **2008**, *101*(6), 1182–1192; DOI 10.1002/bit.21989.

(38) Morgan-Sagastume, F.; Sleep, B. E.; Allen, D. G. Effects of biomass growth ongas pressure drop in biofilters. *J. Environ. Eng.* **2001**, *127*(5); DOI:10.1061/(ASCE)0733-9372(2001)127:5(388).

(39) Covarrubias-García, I.; Aizpuru, A.; Arriaga, S. Effect of the continuous addition of ozone on biomass clogging control in a biofilter treating ethyl acetate vapors. *Sci. Total Environ.* **2017**, *584-585*, 469–475; DOI: 10.1016/j.scitotenv.2017.01.031.

(40) Dorado, A. D.; Baeza, J. A.; Lafuente, J.; Gabriel, D.; Gamisans, X. Biomass accumulation in a biofilter treating toluene at high loads – Part 1: Experimental performance from inoculation to clogging. *Chem. Eng. J.* **2012**, *209*, 661–669; DOI 10.1016/j.cej.2012.08.018.

(41) Cox, H. H. J.; Deshusses, M. A. Biomass control in waste air biotrickling filters by protozoan predation. *Biotechnol. Bioeng.* **1999**, *62*, 216–224; DOI: 10.1002/(SICI)1097-0290(19990120)62:2b216::AID-BIT12N3.0.CO;2-4.

(42) Estrada, J. M.; Quijano, G.; Lebrero, R.; Muñoz, R. Step-feed biofiltration: A low-cost alternative configuration for off-gas treatment. *Water Res.* **2013**, *47*(13), 4312–4321. DOI: 10.1016/j.watres.2013.05.007.

(43) Avalos-Ramirez, A.; Jones, J. P.; Heitz, M. Methane treatment in biotrickling filters packed with inert materials in presence of a non-ionic surfactant. *J. Chem. Technol. Biot.* **2012**, *87*(6), 848–853; DOI 10.1002/jctb.3811.

(44) Rocha-Rios, J.; Bordel, S.; Hernández, S.; Revah, S. Methane degradation in two-phase partition bioreactors. *Chem. Eng. J.* **2009**, *152*, 289–292; DOI 10.1016/j.cej.2009.04.028.

(45) Lebrero, R.; Hernández, L.; Pérez, R.; Estrada, J. M.; Muñoz, R. Two-liquid phase partitioning biotrickling filters for methane abatement: Exploring the potential of hydrophobic methanotrophs. *J. Environ. Manage.* **2015**, *151*, 124–131; DOI 10.1016/j.jenvman.2014.12.016.

(46) Kennelly, C.; Clifford, E.; Gerrity, S.; Walsh, R.; Rodgers, M.; Collins, G. A horizontal flow biofilm reactor (HFBR) technology for the removal of methane and hydrogen sulphide at low temperatures. *Water Sci. Technol.* **2012**, *66*(9), 1997–2006; DOI 10.2166/Wst.2012.411.

(47) Kennelly, C.; Gerrity, S.; Collins, G.; Clifford, E. Liquid phase optimisation in a horizontal flow biofilm reactor (HFBR) technology for the removal of methane at low temperatures. *Chem. Eng. J.* **2014**, *242*, 144–154; DOI 10.1016/j.cej.2013.12.071.

(48) Kraakman, N. J. R.; Rocha-Rios, J.; van Loosdrecht, M. C. M. Review of mass transfer aspects for biological gas treatment. *Appl. Microbiol. Biotechnol.* **2011**, *91*, 873–886; DOI 10.1007/s00253-011-3365-5.

(49) Cantera, S.; Estrada, J. M.; Lebrero, R.; García-Encina, P. A.; Muñoz, R. Comparative performance evaluation of conventional and two-phase hydrophobic stirred tank reactors for methane abatement: Mass transfer and biological considerations. *Biotechnol. Bioeng.* **2016**, *113*(6), 1203–1212; DOI 10.1002/bit.25897.

(50) Rocha-Rios, J.; Muñoz, R.; Revah, S. Effect of silicone oil fraction and stirring rate on methane degradation in a stirred tank reactor. *J. Chem. Technol. Biot.* **2010**, *85*, 314–319; DOI: 10.1002/jctb.2339.

(51) Rocha-Rios, J.; Quijano, G.; Thalasso, F.; Revah, S.; Muñoz, R. Methane biodegradation in a two-phase partition internal loop airlift reactor with gas recirculation. *J. Chem. Technol. Biot.* **2011**, *86*, 353–360; DOI 10.1002/jctb.2523.

(52) Rahnama, F.; Vasheghani-Farahani, E.; Yazdian, F.; Shojaosadati, S. A. PHB production by *Methylocystis hirsuta* from natural gas in a bubble column and a vertical loop bioreactor. *Biochem. Eng. J.* **2012**, *65*, 51–56; DOI 10.1016/j.bej.2012.03.014.

(53) Kumar, A.; Dewulf, J.; van Langenhove, H. Membrane-based biological waste gas treatment. *Chem. Eng. J.* **2008**, *136*(2-3), 82–91; DOI 10.1016/j.cej.2007.06.006.

(54) Sun, F. Y.; Dong, W. Y.; Shao, M. F.; Lv, X. M.; Li, J.; Peng, L. Y.; Wang, H. J. Aerobic methane oxidation coupled to denitrification in a membrane biofilm reactor: Treatment performance and the effect of oxygen ventilation. *Biores. Technol.* **2013**, *145*, 2–9; DOI 10.1016/j.biortech.2013.03.115.

(55) Sánchez, A.; Rodríguez-Hernández, L.; Buntner, D.; Esteban-García, A. L.; Tejero, I.; Garrido, J. M. Denitrification coupled with methane oxidation in a membrane bioreactor after methanogenic pre-treatment of wastewater. *J. Chem. Technol. Biot.* **2016**, *91*(12), 2950–2958; DOI 10.1002/jctb.4913.

(56) Shi, Y.; Hu, S.; Lou, J.; Lu, P.; Keller, J.; Yuan, Z. Nitrogen removal from wastewater by coupling anammox and methane-dependent denitrification in a membrane biofilm reactor. *Environ. Sci. Technol.* **2013**, *47*(20), 11577–11583; DOI 10.1021/es402775z.

(57) Cai, C.; Hu S.; Guo, J.; Shi, Y.; Xie, G-J.; Yuan, Z. Nitrate reduction by denitrifying anaerobic methane oxidizing microorganisms can reach a practically useful rate. *Water Res.* **2015**, *87*, 211–217; DOI 10.1016/j.watres.2015.09.026.

(58) Rocha-Rios, J.; Kraakman, N. J. R.; Kleerebezem, R.; Revah, S.; Kreutzer, M. T.; van Loosdrecht, M. C. M. A capillary bioreactor to increase methane transfer and

oxidation through Taylor flow formation and transfer vector addition. *Chem. Eng. J.* **2013**, *217*, 91–98; DOI 10.1016/j.cej.2012.11.065.

(59) Wolf, H. J.; Hanson R. S. Isolation and characterization of methane-utilizing yeasts. *J. Gen. Microbiol.* **1979**, *114*, 187–194.

(60) Enebo, L. A methane-consuming green algae. *Acta Chem. Scand.* **1967**, *21*, 625–632.

(61) Volesky, B.; Zajic, J. E. Batch production of protein from ethane and ethane-methane mixtures. *Appl. Microbiol.* **1971**, *2*1, 614–622.

(62) Hanson, R. S.; Hanson, T. E. Methanotrophic bacteria. *Microbiol. Rev.* **1996**, *60*, 439–471.

(63) Pawlowska, M. Biological oxidation as a method for mitigation of LFG emission. In *Mitigation of landfill gas emissions*; Pawlowska, M., Ed.; 1st edn. CRC Press, Taylor & Francis Group, London, UK, 2014; pp 59–101.

(64) Semrau, J. D.; DiSpirito, A. A.; Yoon, S. Methanotrophs and cooper. *FEMS Microbiol. Rev.* **2010**, *34*, 496–531; DOI 10.1111/j.1574-6976.2010.00212.x.

(65) Knief, C. Diversity and habitat preferences of cultivated and uncultivated aerobic methanotrophic bacteria evaluated based on *pmoA* as molecular marker. *Front. Microbiol.* **2015**, *6*, 1346; DOI 10.3389/fmicb.2015.01346.

(66) Sazinsky, M. H.; Lippard, S. J. Methane monooxygenase: functionalizing methane at iron and copper. *Met. Ions Life Sci.* **2015**, *15*, 205–256; DOI 10.1007/978-3-319-12415-5_6.

(67) Hilger, H.; Humer, M. Biotic landfill cover treatments for mitigating methane emissions. *Environ. Monit. Assess.* **2003**, *84*, 71–84; DOI 10.1023/A:1022878830252.

(68) Karthikeyan, O. P.; Chidambarampadmavathy, K.; Cirés, S.; Heimann, K. Review of sustainable methane mitigation and biopolymer production. *Crit. Rev. Environ. Sci. Technol.* **2015**, *45*, 1579–1610; DOI 10.1080/10643389.2014.966422.

(69) Scheutz, C.; Kjeldsen, P.; Bogner J. E.; Visscher, A. D.; Gebert, J.; Hilger, H. A.; Huber-Humer, M.; Spokas, K. Microbial methane oxidation processes and technologies for mitigation of landfill gas emissions. *Waste Manag. Res.* **2009**, *27*, 716–723; DOI 10.1177/0734242X09339325.

(70) Bédard, C.; Knowles, R. Physiology, biochemistry and specific inhibitors of CH_4, NH_4 and CO oxidation by methanotrophs and nitrifiers. *Microbiol. Rev.* **1989**, *53*, 68–84.

(71) Amaral, J. A.; Knowles R. Growth of methanotrophs in methane and oxygen counter gradients. *FEMS Microbiol. Lett.* **1995**, *126*, 215–220; DOI 10.1016/0378-1097(95)00012-T.

(72) Henckel, T.; Roslev, P.; Conrad, R. Effects of O_2 and CH_4 on presence and activity of the indigenous methanotrophic community in rice field soil. *Environ. Microbiol.* **2000**, *2*, 666–679; DOI 10.1046/j.1462-2920.2000.00149.x.

(73) Van Teeseling, M. C.; Pol, A.; Harhangi, H. R.; van der Zwart, S.; Jetten, M. S. M.; Op den Camp, H. J.; van Niftrik, L. Expanding the verrucomicrobial methanotrophic world: description of three novel species of *Methylacidimicrobium* gen. nov. *Appl. Environ. Microbiol.* **2014**, *80*,6782–6791; DOI 10.1128/AEM.01838-14.

(74) Bender, M.; Conrad, R. Effect of CH_4 concentrations and soil conditions on the induction of CH_4 oxidation activity. *Soil Biol. Biochem.* **1995**, *27*, 1517–1527; DOI 10.1016/0038-0717(95)00104-M.

(75) Whalen, S. C.; Reeburgh, W. S.; Sandbeck, K. A. Rapid methane oxidation in a landfill cover soil. *Appl. Environ. Microbiol.* **1990**, *56*, 3405–3411.

(76) Bowman, J. P.; McCammon, S. A.; Skerratt, J. H. *Methylosphaera hansonii* gen. nov., sp. nov., a psychrophilic, group I methanotroph from Antarctic marine-salinity, meromictic lakes. *Microbiol.* **1997**, *143*, 1451–1459; DOI: 10.1099/00221287-143-4-1451.

(77) Kalyuzhnaya, M. G.; Khmelenina, V. N.; Kotelnikova, S.; Holmquist, L.; Pedersen, K.; Trotsenko, Y. A. *Methylomonas scandinavica* sp. nov., a new methanotrophic psychrotrophic bacterium isolated from deep igneous rock ground water of Sweden. *Syst. Appl. Microbiol.* **1999**, *22*, 565–572; DOI 10.1016/S0723-2020(99)80010-1.

(78) Pol, A.; Heijmans, K.; Harhangi, H. R.; Tedesco, D.; Jetten, M. S. M.; Op den Camp, H. J. M. Methanotrophy below pH 1 by a new *Verrucomicrobia* species. *Nature* **2007**, *450*, 874–878; DOI 10.1038/nature06222.

(79) Pieja, A. J.; Rostkowski, K. H.; Criddle, C. S. Distribution and selection of poly-3-hydroxybutyrate production capacity in methanotrophic proteobacteria. *Microb. Ecol.* **2011**, *62*, 564–573; DOI 10.1007/s00248-011-9873-0.

(80) Kalyuzhnaya, M. G.; Yang, S.; Rozova, O. N.; Smalley, N. E.; Clubb, J.; Lamb, A.; Nagana-Gowda, G. A.; Raftery, D.; Fu, Y.; Bringel, F.; Vuilleumier, S.; Beck, D. A. C.; Trotsenko, Y. A.; Khmelenina, V. N.; Lidstrom, M. E. Highly efficient methane biocatalysis revealed in a methanotrophic bacterium. *Nat. Commun.* **2013**, *4*, 2785; DOI 10.1038/ncomms3785.

(81) Dunfield, P.; Knowles, R. Kinetics of inhibition of methane oxidation by nitrate, nitrite, and ammonium in a humisol. *Appl. Environ. Microbiol.* **1995**, *61*(8), 3129–3135.

(82) Semrau, J. D.; Dispirito, A. A.; Yoon, S. Methanotrophs and copper. *FEMS Microbiol. Rev.* **2010**, *34*, 496e531; DOI 10.1111/j.1574-6976.2010.00212.x.

(83) Graham, D. W.; Chaudhary, J. A.; Hanson, R. S.; Arnold, R. G. Factors affecting competition between type I and type II methanotrophs in two-organism, continuous-flow reactors. *Microbial Ecol.* **1993**, *25*(1), 1–17; DOI: 10.1007/BF00182126.

(84) Murrel, J. C.; Gilbert, B.; McDonald, I. R. Molecular biology and regulation of methane monooxygenase. *Arch. Microbiol.* **2000**, *173*, 325e332; DOI 10.1007/s002030000158.

(85) DiSpirito, A. A.; Semrau, J. D.; Murrell, J. C.; Gallagher, W. H.; Dennison, C.; Vuilleumier, S. Methanobactin and the link between copper and bacterial methane oxidation. *Microbiol. Mol. Biol. Rev.* **2016**, *80*(2), 387–409; DOI 10.1128/MMBR.00058-15.

(86) Chanprateep, S. Current trends in biodegradable polyhydroxyalkanoates. *J. Biosci. Bioeng.* **2010**, *110* (6), 621–632; DOI 10.1016/j.jbiosc.2010.07.014.

(87) Bugnicourt, E.; et al. The main characteristics, properties, improvements, and market data of polyhydroxyalkanoates. In *Handbook of sustainable polymers: Processing and applications*, Thakur, V.K.; Thakur, M.K., Eds., 1st edn. Pan Stanford Publishing Pte. Ltd., Boca Ratón, 2016; pp. 899–928.

(88) Wendlandt, K. D.; Jechorek, M.; Helm, J.; Stottmeister, U. Producing poly-3-hydroxybutyrate with a high molecular mass from methane. *J. Biotechnol.* **2001**, *86*, 127–133; DOI 10.1016/S0168-1656(00)00408-9.

(89) Sundstrom, E.; Criddle, C. S. Optimization of methanotrophic growth and production of poly(3-hydroxybutyrate) in a high-throughput microbioreactor system. *Appl. Environ. Microbiol.* **2015**, *81*(14), 4767–4773; DOI 10.1128/AEM.00025-15.

(90) Khosravi-Darani, K.; Mokhtari, Z. B.; Amai, T.; Tanaka, K. Microbial production of poly(hydroxybutyrate) from C_1 carbon sources. *Appl. Microbiol. Biotechnol.* **2013**, *97*, 1407–1424; DOI 10.1007/s00253-012-4649-0.

(91) Helm, J.; Wendlandt, K. D.; Jechorek, M.; Stottmeister, U. Potassium deficiency results in accumulation of ultra-high molecular weight poly-β-hydroxybutyrate in a methane-utilizing mixed culture. *J. Appl. Microbiol.* **2008**, *105*, 1054–1061; DOI 10.1111/j.1365-2672.2008.03831.x.

(92) Zhang, T.; Wang, X.; Zhou, J.; Zhang, Y. Enrichments of methanotrophic-heterotrophic cultures with high poly-β-hydroxybutyrate (PHB) accumulation capacities. *J. Environ. Sci.* **2017** (In Press); DOI 10.1016/j.jes.2017.03.016.

(93) Rostkowski, K. H.; Pfluger, A. R; Criddle, C. S. Stiochiometry and kinetics of the PHB-producing type II methanotrophs *Methylosinus trichosporium* OB3b and *Methylocystis parvus* OBBP. *Biores. Technol.* **2013**, *132*, 71–77; DOI 10.1016/j.biortech.2012.12.129.

(94) Zhang, Y.; Xin, J.; Chen, L.; Song, H.; Xia, C. Biosynthesis of poly-3-hydroxybutyrate with a high molecular weight by methanotroph from methane and methanol. *J. Nat. Gas Chem.* **2008**, *17*, 103–109; DOI 10.1016/S1003-9953(08)60034-1.

(95) Myung, J.; Galega, W. M.; Van Nostrand, J. D.; Yuan, T.; Zhou, J.; Criddle, C. S. Long-term cultivation of a stable *Methylocystis*-dominated methanotrophic enrichment enabling tailored production of poly(3-hydroxybutyrate-*co*-3-hydroxyvalerate). *Biores. Technol.* **2016**, *198*, 811–818; DOI 10.1016/j.biortech.2015.09.094.

(96) Myung J.; Flanagan, J. C. A.; Waymouth, R. M.; Criddle, C. S. Expanding the range of polyhydroxyalkanoates synthesized by methanotrophic bacteria through the utilization of omega-hydroxyalkanoate co-substrates. *AMB Express* **2017**, *7*, 118; DOI 10.1186/s13568-017-0417-y.

(97) Pieja, A. J.; Sundstrom, E. R.; Criddle, C. S. Poly-3-hydroxybutyrate metabolism in the type II methanotroph *Methylocystis parvus* OBBP. *Appl. Environ. Microbiol.* **2011**, *77*(17), 6012–6019; DOI 10.1128/AEM.00509-11.

(98) Reeburgh, W. S. Oceanic methane biogeochemistry. *Chem. Rev.* **2007**, *107*, 486–513; DOI 10.1021/cr050362v.

(99) Reeburgh, W. S. Methane consumption in Cariaco Trench waters and sediments. *Earth Planet. Sci. Lett.* **1976**, *28*, 337–344.

(100) Boetius, A.; Ravenschlag, K.; Schubert, C. J.; Rickert, D.; Widdel, F.; Gieseke, A.; Amann, R.; Jørgensen, B. B.; Witte, U.; Pfannkuche, O. A marine microbial consortium apparently mediating anaerobic oxidation of methane. *Nature* **2000**, *407*, 623–626; DOI 10.1038/35036572.

(101) Beal, E. J.; House, C. H.; Orphan, V. J. Manganese and iron-dependent marine methane oxidation. *Science* **2009**, *325*, 184–187; DOI 10.1126/science.1169984.

(102) Raghoebarsing, A.A.; Pol, A.; van de Pas-Schoonen, K. T.; Smolders, A.J.; Ettwig, K.F.; Rijpstra, W.I.; Schouten, S.; Damste, J.S.; Op den Camp, H.J.; Jetten, M.S.M.; Strous, M. A microbial consortium couples anaerobic methane oxidation to denitrification. *Nature* **2006**, *440*(7086), 918–921; DOI 10.1038/nature04617.

(103) Cui, M.; Ma, A.; Qi, H.; Zhuang, X.; Zhuang, G. Anaerobic oxidation of methane: an “active” microbial process. *MicrobiologyOpen* **2015**, *4*(1), 1–11; DOI 10.1002/mbo3.232.

(104) Wang, Y.; Wang, D.; Yang, Q.; Zeng, G.; Li, X. Wastewater opportunities for denitrifying anaerobic methane oxidation. *Trends Biotechnol.* **2017**, 35(9), 799–802; DOI 10.1016/j.tibtech.2017.02.010.

(105) Haroon, M.F.; Hu, S.; Shi, Y.; Imelfort, M.; Keller, J.; Hugenholtz, P.; Yuan, Z.; Tyson, G.W. Anaerobic oxidation of methane coupled to nitrate reduction in a novel archaeal lineage. *Nature* **2013**, *500*, 567–570; DOI 10.1038/nature12375.

(106) Ettwig, K.F.; Butler, M.K.; Le Paslier, D.; Pelletier, E.; Mangenot, S.; Kuypers, M.M.M.; Schreiber, F.; Dutilh, B.E.; Zedelius, J.; de Beer, D.; Gloerich, J.; Wessels, H.J.C.T.; van Alen, T.; Luesken, F.; Wu, M.L.; van de Pas-Schoonen, K.T.; Op den Camp, H.J.M.; Janssen-Megens, E.M.; Francoijs, K.J.; Stunnenberg, H.; Weissenbach, J.; Jetten, M.S.M.; Strous, M. Nitrite-driven anaerobic methane oxidation by oxygenic bacteria. *Nature* **2010**, *464*(7288), 543–548; DOI 10.1038/nature08883.

(107) Wu, M. L.; Ettwig, K. F.; Jetten, M. S.; Strous, M.; Keltjens, J. T.; van Niftrik, L. A new intra-aerobic metabolism in the nitrite-dependent anaerobic methane-oxidizing bacterium *Candidatus* 'Methylomirabilis oxyfera'. *Biochem. Soc. Trans.* **2011**, *39*(1), 243–248; DOI 10.1042/BST0390243.

(108) Caldwell, S. L.; Laidler, J. R.; Brewer, E. A.; Eberly, JO, Sandborgh, S. C.; Colwell, F.S. Anaerobic oxidation of methane: mechanisms, bioenergetics, and the ecology of associated microorganisms. *Environ. Sci. Technol.* **2008**, *42*, 6791–6799; DOI 10.1021/es800120b.

(109) Kampman, C., Piai, L., Hendrickx, T. L. G., Temmink, H., Zeeman, G., Buisman, C. J. N. Effect of temperature on denitrifying methanotrophic activity of 'Candidatus Methylomirabilis oxyfera'. *Water Sci. Technol.* **2014**, *70*(10), 1683–1689; DOI 10.2166/wst.2014.431.

(110) Hu, S.; Zeng, R. J.; Keller, J.; Lant, P. A.; Yuan Z. Effect of nitrate and nitrite on the selection of microorganisms in the denitrifying anaerobic methane oxidation process. *Env. Microbiol. Rep.* **2011**, *3*(3), 315–319; DOI 10.1111/j.1758-2229.2010.00227.x.

(111) Luesken, F. A.; Wu, M. L.; Op den Camp, H. J. M.; Keltjens, J. T.; Stunnenberg, H.; Francoijs, K. J.; Strous, M.; Jetten, M. S. M. Effect of oxygen on the anaerobic methanotroph '*Candidatus* Methylomirabilis oxyfera': kinetic and transcriptional analysis. *Environ. Microbiol.* **2012**, *14*, 1024–1034; DOI 10.1111/j.1462-2920.2011.02682.x.

(112) Kampman, C.; Temmink, H.; Hendrickx, T. L. G.; Zeeman, G.; Buisman, C. J. N. Enrichment of denitrifying methanotrophic bacteria from municipal wastewater sludge in a membrane bioreactor at 20ºC. *J. Hazard. Mater.* **2014**, *274*, 428–435; DOI 10.1016/j.jhazmat.2014.04.031.

(113) Wang, D.; Wang, Y.; Liu, Y.; Ngo, H. H.; Lian, Y.; Zhao, J.; Chen, F.; Yang, Q.; Zeng, G.; Li, X. Is denitrifying anaerobic methane oxidation-centered technologies a solution for the sustainable operation of wastewater treatment plants? *Biores. Technol.* **2017**, *234*, 456–465; DOI 10.1016/j.biortech.2017.02.059.

(114) Hu, S.; Zeng, R. J.; Haroon, M. F.; Keller, J.; Lant, P. A.; Tyson, G. W.; Yuan, Z. A laboratory investigation of interactions between denitrifying anaerobic methane oxidation (DAMO) and anammox processes in anoxic environments. *Sci. Rep.* **2015**, *5*, 8706; DOI 10.1038/srep08706.

Chapter 2

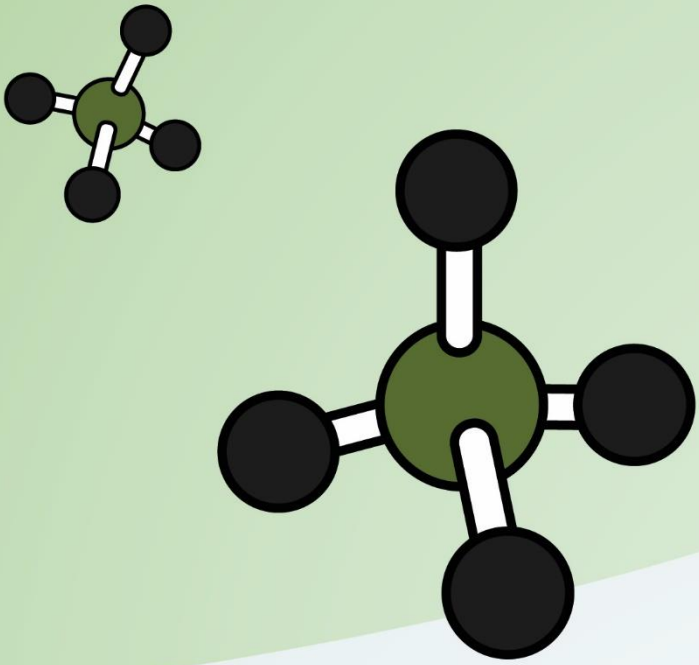

Aim and scope of the thesis

Justification of the thesis

The severe environmental impacts governing climate change have been unequivocally attributed to the increasing concentration of GHGs in the atmosphere. Since most ecosystems and forms of life in Earth are threatened in the forthcoming scenario of increasing GHGs (e. g. CH_4) emissions, there is an urgent need to develop sustainable technologies for the active abatement of CH_4 emissions. In this regard, biotechnologies can become, if properly tailored, a promising alternative to physical/chemical technologies for a cost-effective and environmentally friendly CH_4 mitigation. However, several limitations must be still addressed in order to ensure a cost-effective implementation of these technologies at full-scale. Moreover, further research is still required to optimize the creation of additional value out of biological CH_4 mitigation and convert CH_4 abatement biotechnologies into a key platform for the development of a sustainable bioeconomy.

Main objectives

The overall objective of this thesis was to overcome some of the current limitations of CH_4 abatement biotechnologies restricting their widespread implementation beyond lab-scale applications, to add new insights on the microbiology underlying CH_4 biodegradation and to create additional value out of CH_4 mitigation within a biorefinery concept. More particularly, the specific objectives addressed to achieve this overall goal are:

i. Elucidation of the fungal ability to biodegrade CH_4 and evaluation of the role of fungi in a mixed bacterial-fungal biofilter treating diluted CH_4 emissions in order to improve the mass transfer (and thus, the abatement performance) of this GHG at reduced empty bed residence times (EBRTs).

ii. Evaluation of feast-famine strategies as a novel operational approach to minimize biomass overgrowth and therefore, to reduce the pressure drops and improve the lifespan of the packing material used during the biofiltration of diluted CH_4 emissions. Evaluation of the influence of these strategies on the methanotrophic community structure through metagenomics.

iii. Assessment of the influence of CH_4 concentration during culture enrichment on the methanotrophic population structure, CH_4 biodegradation kinetics and polyhydroxyalkanoate (PHA) accumulation. This knowledge will help identifying inocula with adequate biodegradation features to facilitate the start-up of CH_4 abatement biotechnologies and ensure a proper abatement performance in the long-term bioreactor operation with a concomitant production of high-added value products.

iv. Assessment of the feasibility of biogas (with and without H_2S) as a substrate to grow type II methanotrophs and accumulate PHAs under nitrogen-limited conditions. Evaluation of the feasibility of volatile fatty acids (VFAs) as carbon and energy source to support the growth of type II methanotrophs and to produce tailor-made PHAs with and without biogas.

v. Evaluation of the potential of denitrifying anaerobic methane oxidation (DAMO) in a biotrickling filter using nitrate as a nitrogen source and electron acceptor, and CH_4 from biogas as the unique electron donor, with a special focus on minimizing nitrous oxide emissions. Assessment of the influence of H_2S (typically present in biogas) on the DAMO community and the overall denitrification performance.

Development of the thesis

In the current thesis, CH_4 abatement biotechnologies were investigated from a macro- and microscopic point of view. More specifically:

In order to fullfill the first two objectives aforementioned and overcome the mass transfer limitation and biomass overgrowth issue, the potential of fungi and feast-famine regimes during CH_4 biofiltration was evaluated in Chapters 3 and 4, respectively. Then, the characteristics of the microbial communities involved in CH_4 biodegradation were investigated during culture enrichment under different CH_4 concentrations in accordance to the third specific objective (Chapter 5). The creation of additional value out of CH_4 mitigation was further evaluated using biogas as a readily available and low-cost substrate, according to the fourth and five objectives. For this purpose, the growth and PHA accumulation potential of a type II methanotroph using biogas and/or VFAs as carbon and energy sources was addressed in Chapter 6. Finally, the potential of DAMO as a cost-effective platform for nitrogen removal using biogas (with and without H_2S) as an electron donor in a biotrickling filter configuration was investigated in Chapter 7

Chapter 3

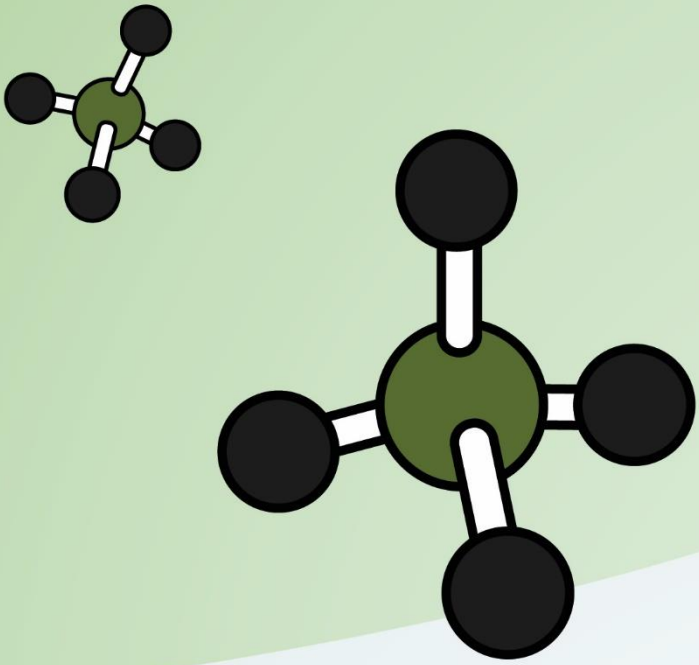

Exploring the potential of fungi for methane abatement: Performance evaluation of a fungal-bacterial biofilter

Chemosphere 144 (2016) 97–106

Contents lists available at ScienceDirect

Chemosphere

journal homepage: www.elsevier.com/locate/chemosphere

Exploring the potential of fungi for methane abatement: Performance evaluation of a fungal-bacterial biofilter

Raquel Lebrero*, Juan Carlos López, Iiro Lehtinen, Rebeca Pérez, Guillermo Quijano, Raúl Muñoz

Department of Chemical Engineering and Environmental Technology, School of Industrial Engineerings-venue Dr. Mergelina, University of Valladolid, Dr. Mergelina s/n, 47011 Valladolid, Spain

HIGHLIGHTS

- *Graphium* sp. was able to sustain CH_4 oxidation when methanol was supplemented.
- Fungal-bacterial biofilter showed REs ~90% at an EBRT of 20 min.
- Indigenous fungal community played a key role in process performance.
- Frequent irrigation prevented metabolite accumulation and supported steady removal.

GRAPHICAL ABSTRACT

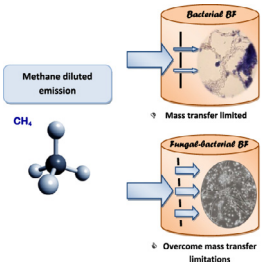

ARTICLE INFO

Article history:
Received 3 February 2015
Received in revised form 2 July 2015
Accepted 1 August 2015
Available online 5 September 2015

Handling editor: Jörg E. Drewes

Keywords:
Biofiltration
Fungal-bacterial biofilter
Graphium sp.
Greenhouse gases
Irrigation rate
Methane abatement

ABSTRACT

Despite several fungal strains have been retrieved from methane-containing environments, the actual capacity and role of fungi on methane abatement is still unclear. The batch biodegradation tests here performed demonstrated the capacity of *Graphium* sp. to co-metabolically biodegrade methane and methanol. Moreover, the performance and microbiology of a fungal-bacterial compost biofilter treating methane at concentrations of ~2% was evaluated at empty bed residence times of 40 and 20 min under different irrigation rates. The daily addition of 200 mL of mineral medium resulted in elimination capacities of 36.6 ± 0.7 g m^{-3} h^{-1} and removal efficiencies of ≈90% at the lowest residence time. The indigenous fungal community of the compost was predominant in the final microbial population and outcompeted the inoculated *Graphium* sp. during biofilter operation.

1. Introduction

Methane (CH_4), with a global warming potential 25 times higher than that of CO_2 is the second most important greenhouse gas (GHG), accounting nowadays for nearly 20% of the greenhouse impact in a 100 years horizon. The atmospheric concentration of CH_4 has increased by a factor of 2.5 over the past millennium, thus seriously compromising the maintenance of the average earth temperature in this 21st century (IPCC, 2013; EPA, 2013). CH_4 is currently emitted by natural and anthropogenic sources at an average rate of 600 Tg yr^{-1}, 55% of the anthropogenic emissions presenting CH_4 gas concentrations below 3% *v/v* (Avalos Ramírez et al., 2012).

* Corresponding author.
E-mail address: raquel.lebrero@iq.uva.es (R. Lebrero).

http://dx.doi.org/10.1016/j.chemosphere.2015.08.017
0045-6535/

In order to limit the adverse effects of CH_4 on climate change, these emissions must be prevented or properly treated using cost-effective end-of-the-pipe technologies. Despite CH_4 emissions not suitable for energy recovery (i.e. CH_4 gas concentrations below 30–40% *v/v*) can be mitigated by flaring, minimal flow rates of 15–30 m^3 h^{-1} and CH_4 concentrations preferably above 20–30% *v/v* are required to ensure its cost-effectiveness (Nikiema and Heitz, 2009). However, significantly lower CH_4 concentrations can be found in fugitive emissions from landfills (0–20%), ventilated coal mines (0.1–1%), or covered liquid manure storage tanks (0–3%) among others (Estrada et al., 2014). In this context, biological technologies represent a potential alternative approach for mitigating these low CH_4-loaded emissions. These biotechnologies entail lower operating costs and environmental impacts compared to their physical-chemical counterparts, biofiltration offering the simplest implementation and operation (Estrada et al., 2012).

Methanotrophs-based biofilters have been extensively applied during the past two decades to reduce CH_4 emissions from landfills, livestock farms or even coal mines (Girard et al., 2011; Haubrichs and Widmann, 2006). However, the low aqueous solubility of CH_4 (dimensionless Henry's law constant, $H = C_{gas}/C_{water}$, of 29.4 at 1 atm and 25 °C) limits its cost-effective biological abatement (López et al., 2013). Therefore, there is an urgent need to investigate alternative approaches to increase the mass transfer of CH_4 from the gas phase to the methanotrophic communities responsible for its bioconversion to CO_2, H_2O and new biomass. In this context, fungal biofilters exhibit a better performance than their bacterial counterparts during the abatement of hydrophobic gas pollutants due to the presence of cell surface-associated hydrophobins (which lower the overall H of the process) and to the aerial hyphae associated to the mycelial growth of fungi (which supports a larger surface area available for gas pollutant mass transfer) (Kennes and Veiga, 2004; Vergara-Fernández et al., 2008). Unfortunately, despite the potential of fungal biofiltration for the abatement of poorly water soluble gas pollutants, few studies have systematically investigated the performance of fungal-based biofilters for CH_4 abatement (either standalone or in consortium with bacteria), and to the best of our knowledge, the potential of fungi for CH_4 oxidation remains still unclear (Girard et al., 2012; Zajic et al., 1969).

This study aimed at evaluating the performance of fungal-bacterial biofiltration for the abatement of CH_4 at low concentrations. The influence of the biofilter irrigation rate on the CH_4 abatement performance was assessed. The structure and composition of the bacterial and fungal communities was also investigated. Finally, the ability of a pure strain of the fungus *Graphium* sp. to biodegrade CH_4 was evaluated.

2. Materials and methods

2.1. Chemicals and inocula preparation

The modified Bruner mineral salt medium (MSM) used for biofilter irrigation and microbial cultivation was composed of (g L^{-1}): $Na_2HPO_4{\cdot}12H_2O$ (6.15), KH_2PO_4 (1.52), $NaNO_3$ (2.44), $MgSO_4{\cdot}7H_2O$ (0.8), $CaCl_2{\cdot}2H_2O$ (0.2) and 40 mL L^{-1} of a trace elements solution prepared according to Lebrero et al. (2012). Additionally, 2.4 mL L^{-1} of a 1 g Cu^{2+} L^{-1} stock solution were added to the MSM to achieve an initial Cu^{2+} concentration of ~40 μM. The MSM was also supplemented with the antibiotic chloramphenicol (Sigma–Aldrich, USA) at 0.02 g L^{-1} to promote fungal growth over possible competing bacterial strains, and its final pH was adjusted to 4.

The biofilter was inoculated with 200 mL of a pure strain of *Graphium* sp. NRRL 3915 (ATCC 58400, USA) cultivated for 5 days under sterile conditions according to the ATCC 58400 guidelines in potato starch broth in an orbital agitator (MaxQ4000, Thermo Scientific, USA) at 150 rpm and 25 °C.

All chemicals for MSM preparation were purchased from Panreac® (Barcelona, Spain), potato starch was supplied by Fluka (Fluka Analytical 70139-500 G, Switzerland) and methane (>99.95%) was supplied by Abello-Linde (Spain).

2.2. Biofilter set-up and operation

The biofilter consisted of a jacketed PVC column with 1 m height and 0.08 m of inner diameter (Fig. 1). The BF was filled with 4 L of compost (Compos Sana® Universal, Spain) to a final height of 0.8 m. The packing material, characterized according to standard methods (TMECC, 2002), exhibited a pH of 5.25 and a moisture content of 13.9%. A CH_4 gas stream, accurately regulated with a mass flow controller (Aalborg, USA), was mixed with pre-humidified air (sparged through a 8.5 L water column) and fed to the BF in an up-flow configuration (gas rotameter, Aalborg, USA). This operation resulted in a CH_4 concentration of 13.6 ± 0.8 g m^{-3} (≈2% v/v CH_4). The temperature of the CH_4 laden air stream was maintained at 25 ± 1 °C and the humidity averaged 82 ± 1%.

The BF was operated for 2 days under abiotic conditions (prior to compost packing) in order to rule out the occurrence of non-biological CH_4 removal derived from photolysis or CH_4 adsorption in the pipeline or the reactor material. Then, the BF was inoculated with *Graphium* sp. and operated for 17 days at an inlet load (IL) of 20.0 ± 0.8 g m^{-3} h^{-1} (empty bed residence time, EBRT, of 40 min). Despite the IL was increased to 41.1 ± 1.3 g m^{-3} h^{-1} (EBRT = 20 min) from days 17–25, the initial IL value was restored due to an unexpected inhibition of the microbial community. Finally, the IL was again increased and maintained at 40.8 ± 0.7 g m^{-3} h^{-1} from day 54 onward. The irrigation frequency was adjusted throughout the experimentation: 200 mL of MSM every three days from days 7–33, 200 mL every two days from day 33–67, and 200 mL daily irrigated from day 67–97. A perforated plate was placed at the top of the bed in order to ensure uniform wetting of the packing material and to avoid the occurrence of dry zones.

2.3. Batch CH_4 degradation tests

Batch biodegradation tests were performed in order to assess the ability of *Graphium* sp. to degrade CH_4. A pure strain of *Graphium* sp. NRRL 3915 (ATCC 58400, USA) was cultivated on agar plates for 6 days until clear mycelial growth was observed. Agar plates consisted of potato starch agar gel (Sigma–Aldrich, USA) with 1 mL L^{-1} of lactic acid to suppress bacterial growth by medium acidification. A portion of fungal mycelium was re-suspended under sterile conditions in duplicate 125 mL serological bottles containing 30 mL of sterile MSM. The bottles were sealed with rubber butyl stoppers and aluminium caps, and CH_4 was supplied to the air headspace in order to achieve a final concentration of ~20% *v/v*. The bottles were incubated in an orbital shaker at 150 rpm and 25 °C for 33 days. By day 8, 1 mL of a 24 g L^{-1} potato starch solution was injected into the bottles. By days 25 and 29, 4 and 8 μL of methanol, respectively, were added into the bottles to achieve aqueous concentrations of 100 and 200 mg L^{-1}, respectively. The headspace concentration of CH_4, O_2 and CO_2 were periodically determined by GC-TCD.

2.4. Analytical procedures

CH_4, O_2 and CO_2 gas concentrations were determined in a Bruker 430 GC-TCD (Palo Alto, USA) equipped with a CP-Molsieve 5A (15 m × 0.53 μm × 15 μm) and a CP-PoraBOND Q

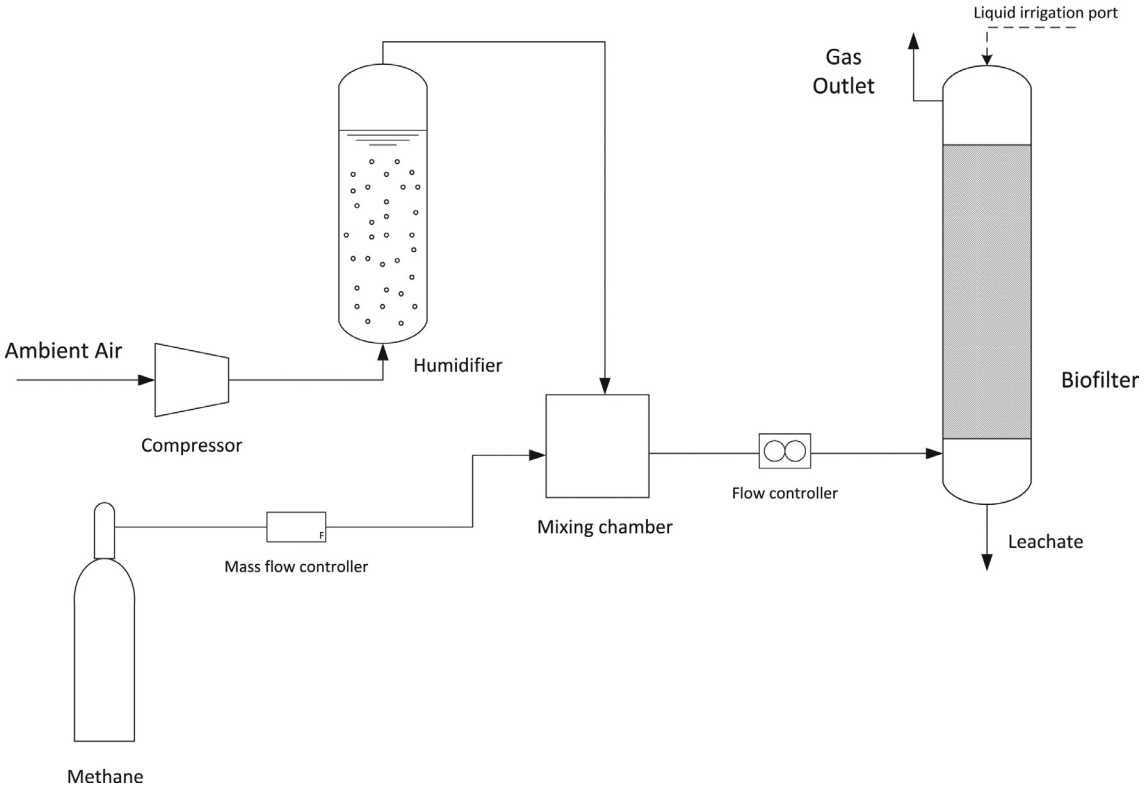

Fig. 1. Schematic of the experimental set-up.

(25 m × 0.53 μm × 10 μm) columns. The oven, injector and detector temperatures were maintained at 45 °C, 150 °C and 200 °C, respectively. Helium was used as the carrier gas at 13.7 mL min^{-1}. Samples for the determination of total organic carbon (TOC) and total nitrogen (TN) concentrations were filtered through 0.7 μm glass fiber filters (Merck Millipore, USA) prior to analysis in a TOC-VCSH analyzer (Shimadzu, Japan) coupled with a chemiluminescence detection TN module (TNM-1) (Shimadzu, Japan). The temperature and humidity of the CH_4-laden air flow were measured using a Testo 605-H1 detector (Testo AG, Germany). Pressure drop was monitored by means of a differential pressure meter using water as the manometric fluid. The pH of the leachate collected before each new irrigation was measured with a pH meter Basic 20 (Crison, Spain).

2.5. Microbiological procedures

The structure and composition of the bacterial and fungal communities in the BF were evaluated in samples of the initial compost used as BF packing material (1), and samples of compost (2) and leachate (3) at the end of the experiment. Genomic DNA was extracted using the protocol described in the Fast® DNA Spin Kit for Soil handbook (MP Biomedicals, LLC), adjusting the time of binding of DNA to the silica matrix to 1 h. The V6–V8 regions of the bacterial 16S rRNA genes were amplified by Polymerase Chain Reaction (PCR) using the universal bacterial primers 968-F-GC and 1401-R (Sigma–Aldrich, St. Louis, MO, USA) (Nübel et al., 1996). The V4–V5 regions of the universal fungal 18S rRNA genes were amplified by PCR using the primers nu-SSU-0817F and nu-SSU-1196R (Borneman and Hartin, 2000). The PCR mixture contained 2 μL of each bacterial or fungal primer (10 ng μL^{-1} each primer), 25 μL of BIOMIX ready-to-use 2 × reaction mix (Bioline, UK), PCR reaction buffer and deoxynucleotide triphosphates (dNTPs), 2 μL of the extracted DNA and Milli-Q water up to 50 μL. PCR was performed in a iCycler Thermal Cycler (Bio-Rad Laboratories, Hercules, CA) with the following thermo-cycling program for bacterial amplification: 2 min of pre-denaturation at 95 °C, 35 cycles of denaturation at 95 °C for 30 s, annealing at 56 °C for 45 s, and elongation at 72 °C for 1 min, with a final elongation at 72 °C for 5 min. The thermo-cycling program for fungal amplification was characterized by 5 min of pre-denaturation at 94 °C, 35 cycles of denaturation at 94 °C for 45 s, annealing at 50 °C for 45 s, and elongation at 72 °C for 1 min, with a final elongation at 72 °C for 5 min.

DGGE analyses of the bacterial and fungal amplicons were performed on 8% (*w*/*v*) polyacrylamide gels with urea/formamide denaturing gradients of 45–65% and 23–45%, respectively (Borneman and Hartin, 2000; Roest et al., 2005). Electrophoresis was performed with a D-Code Universal Mutation Detection System (Bio-Rad Laboratories, Hercules, CA) in 0.5 × Tris-acetate-EDTA (TAE) buffer at 60 °C and 85 V for 16 h (bacterial DNA electrophoresis) or 70 V for 18 h (fungal DNA electrophoresis). The gels were stained with GelRed Nucleic Acid Gel (1:10000 dilution) (Biotium Inc, Hayward, CA) for 1.5 h. Individual bands were excised from the DGGE gel with a sterile blade, resuspended in 50 μL of ultrapure water, and maintained at 60 °C for 1 h to allow DNA extraction from the gel. A volume of 5 μL of the supernatant was used for reamplification with the original primer sets. Before sequencing, PCR products were purified using the GenElute PCR DNA Purification Kit (Sigma–Aldrich, St. Louis, MO, USA). The taxonomic position of the bacterial sequenced DGGE bands was obtained using the RDP classifier tool (50% confidence level) (Wang et al., 2007). The closest matches to each band for both bacteria and fungi were obtained using the Standard Nucleotide BLAST search tool at the NCBI (National Centre for Biotechnology Information) (McGinnis and Madden, 2004). The nucleotide sequences were deposited in GenBank database under accession numbers KM886276 - KM886289 for bacteria and KM886290 - KM886306 for fungi. The DGGE patterns obtained were compared using the GelCompar IITM

software (Applied Maths BVBA, Sint-Martens-Latem, Belgium). The gels were normalized by using internal standards within the DGGE gels. After image normalization, bands were defined for each sample using the bands search algorithm within the program. The software carried out a density profile analysis for each lane, detected the bands and calculated their relative contribution to the total band intensity in the lane, thus allowing the estimation of the relative abundances. Similarity indexes within the bacterial populations were calculated from the densitometric curves of the scanned DGGE profiles by using the Pearson product–moment correlation coefficient (Häne et al., 1993), and were subsequently used to generate the dendrogram by using UPGMA clustering with error resampling (500 resampling experiments). Peak heights in the densitometric curves were also used to determine the diversity indexes based on the Shannon–Wiener diversity index, calculated as follows (Eq. (1)):

$$H = -\sum [P_i \ln(P_i)] \quad (1)$$

where P_i is the importance probability of the bands in a lane ($P_i = n_i/n$, n_i is the height of an individual peak and n is the sum of all peak heights in the densitometric curves).

3. Results

3.1. Biofilter operation

The BF did not show any significant CH_4 removal until the start up of irrigation by day 8, its CH_4 abatement performance rapidly increasing afterwards and stabilizing at an EC of 19.5 ± 0.9 g m^{-3} h^{-1} (corresponding to a removal efficiency, RE, of ~100%) from day 11–17 (Fig. 2A). Similarly, CO_2 production (PCO_2) increased with system irrigation and stabilized at 29.8 ± 1.7 g m^{-3} h^{-1} (corresponding to a CH_4 mineralization of 55.6 ± 4.7%) (Fig. 2B). At this point, it is important to notice that compost biodegradation could have slightly contributed to CO_2 production despite a highly stabilized compost was used as packing bed material. Thus the mineralization ratios here presented might be slightly overestimated. The increase in IL by a factor of 2 at day 18 resulted in an immediate increase of the EC to 44.6 g m^{-3} h^{-1}. However, this initial EC peak was followed by a gradual deterioration of the biofilter performance in terms of both CH_4 abatement and CO_2 production, which entailed the restoration of the initial IL by day 26. Whereas this decrease in IL prevented from a further deterioration of the EC, neither CH_4 abatement nor CO_2 production stabilized, and fluctuated from 6.7 to 17.0 g CH_4 m^{-3} h^{-1} and from 19.9 to 28.0 g CO_2 m^{-3} h^{-1}, respectively, within the following 7 days. During this period, the highest ECs were always recorded after biofilter irrigation. The irrigation frequency was thus increased to 200 mL of MSM every 2 days (100 mL day^{-1}) from day 33, which resulted in the stabilization of CH_4 abatement by day 46 at REs of 96.6 ± 1.7% and ECs of 19.3 ± 0.4 g m^{-3} h^{-1}. A steady PCO_2 of 41.6 ± 1.3 g m^{-3} h^{-1} was also recorded, corresponding to a CH_4 mineralization of 78.3 ± 1.4%.

The IL was increased again to ~41 g m^{-3} h^{-1} by day 53, and a concomitant increase in the EC to 38.5 g m^{-3} h^{-1} was recorded. The EC during this operational stage fluctuated between 27.3 and 38.5 g m^{-3} h^{-1}, the highest bed humidity corresponding to the highest ECs. A daily irrigation of the packed bed was thus implemented by day 67, resulting in the stabilization of the EC at 36.6 ± 0.7 g m^{-3} h^{-1} (REs = 88.8 ± 1.4%) between days 78 and 87 of operation. PCO_2 also increased as a result of the higher IL, stabilizing after the implementation of the new irrigation rate at 82.2 ± 2.9 g m^{-3} h^{-1} (corresponding to a CH_4 mineralization of 81.7 ± 4.1%).

In order to assess the occurrence of CH_4 mass transfer limitation in the system, a 3 times step increase in the IL was induced by day 88 (by increasing CH_4 concentration from 13.5 up to 40.5 g m^{-3}) for 2.5 h (Fig. 3). Methane and CO_2 concentrations were continuously monitored. The increase in IL resulted in an increase in the EC and CO_2 production by a factor of 2.3 and 1.6, respectively.

A low pressure drop was recorded in the BF regardless of the irrigation rate, with average and maximum values of 1.8 ± 1.0 Pa m^{-1} and 4.4 Pa m^{-1}, respectively. Finally, the pH of the collected leachate during the first and second irrigation strategies remained at 6.0 ± 0.3, while the intensification of the irrigation rate during the last operational period resulted in a progressive increase and stabilization of the pH at 7.1 ± 0.2.

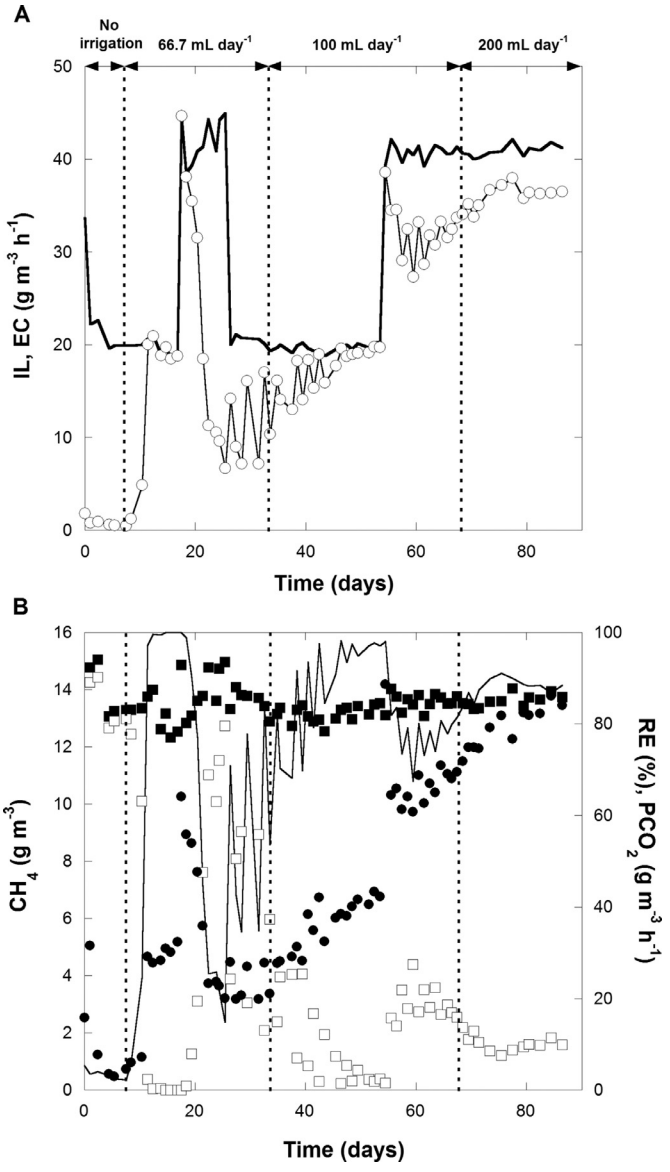

Fig. 2. (A) Time course of the inlet CH_4 load (continuous line) and EC (○, continuous line). (B) Time course of the inlet (■) and outlet (□) CH_4 concentration, CO_2 production (●) and removal efficiency (continuous line). Vertical lines represent the shifts in the irrigation frequency.

Table 1
RDP classification of the bacterial DGGE bands sequenced and corresponding matches (BLASTN) using the NCBI database with indication of the similarity percentages and sources of origin. The presence/absence of each band in each sample tested is also shown.

Taxonomic placement (50% confidence level)	Band n°	A	B	C	Closest relatives in blast name (accession number)	Similarity (%)	Source of origin
Phylum *Proteobacteria*							
Class *Gammaproteobacteria*							
Order *Methylococcales*							
Family *Methylococcaceae*							
	B1			X	*Methylomicrobium agile* (NR_116197)	94	Culture collection
	B2		X	X	Uncultured bacterium (KF957454)	92	Activated sludge from WWTP, soil from a landfill cover and sludge from an aerobic lagoon stabilizing the effluents from an anaerobic digester
	B3		X	X	*Methylomicrobium album* (NR_116196)	98	Culture collection
					Uncultured bacterium (AB504639)	96	Methane oxidizing DHS reactor
	B4		X	X	Uncultured bacterium (KF957454)	98	Activated sludge from WWTP, soil from a landfill cover and sludge from an aerobic lagoon stabilizing the effluents from an anaerobic digester
					Methylomicrobium agile (X72767)	97	Culture collection
Genus *Methylomicrobium*							
	B5			X	*Methylomicrobium agile* (NR_116197)	99	Culture collection
					Methylomicrobium album (NR_116196)	99	Culture collection
	B6	X	X	X	Uncultured bacterium (KF957454)	100	Activated sludge from WWTP, soil from a landfill cover and sludge from an aerobic lagoon stabilizing the effluents from an anaerobic digester
					Methylomicrobium agile (NR_116197)	100	Culture collection
					Methylomicrobium album (NR_116196)	100	Culture collection
Genus *Methylosarcina*							
	B7		X	X	Uncultured bacterium (KF957454)	93	Activated sludge from WWTP, soil from a landfill cover and sludge from an aerobic lagoon stabilizing the effluents from an anaerobic digestor
Order *Xanthomonadales*							
Family *Xanthomonadaceae*							
Genus *Silanimonas*							
	B8			X	Uncultured bacterium (GQ480152)	92	Activated sludge from waste water treatment plant
Genus *Dokdonella*							
	B9	X	X	X	Uncultured gamma proteobacterium (HM238179)	99	Biofilter treating waste gas
					Dokdonella soli (NR_044554)	99	Soil
					Uncultured bacterium (JQ914121)	99	Biotrickling filters (BTFs) treating butanone, toluene, alpha-pinene and hexane
					Uncultured bacterium (JQ038783)	99	Biotrickling filter (BTF) treating low concentrations of methyl mercaptan, toluene, alpha-pinene and hexane
Genus *Rhodanobacter*							
	B10	X		X	Uncultured gamma proteobacterium (JQ919699)	98	Gasoline-polluted soil
					Rhodanobacter soli (NR_116741)	98	Soil from ginseng field
					Rhodanobacter caeni (NR_108570)	97	Culture collection
Class *Alphaproteobacteria*							
Order *Rhizobiales*							
	B11	X	X	X	Uncultured *Mesorhizobium* sp. (HM492840)	94	Bioreactor simulating a low temperature oil reservoir
Family *Methylocystaceae*							
Genus *Methylosinus*	B12		X	X	*Methylosinus trichosporium* (AJ868424)	99	Soil
					Methylosinus trichosporium (KC353469)	99	Methane-rich landfill sediment
Order *Caulobacterales*							
Family *Caulobacteraceae*							
Genus *Asticcacaulis*							
	B13	X	X	X	Uncultured *Asticcacaulis* sp. (JN590648)	94	Cluster roots
Phylum *Actinobacteria*							
Class Actinobacteria							
Subclass *Actinobacteridae*							
Order *Actinomycetales*							
Suborder *Micrococcineae*							
Family *Microbacteriaceae*							
	B14	X		X	*Labedella gwakjiensis* (KF040994)	99	Culture collection
					Microbacteriaceae (AF409008)	99	
					Uncultured *Microbacteriaceae* (AM934973)	98	Pilot-scale bioremediation process of a hydrocarbon-contaminated soil

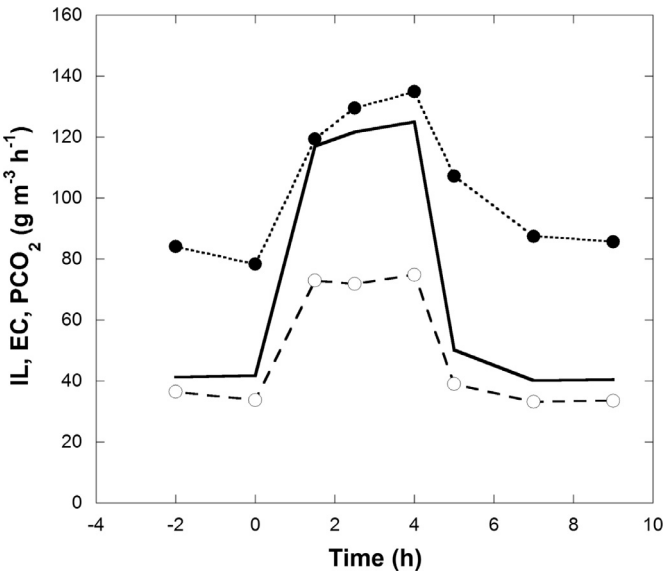

Fig. 3. Time course of the IL (continuous line), EC (○, dashed line), and CO_2 production (●, dotted line) during the mass transfer limitation test.

3.2. Internal structure and molecular composition of the microbial communities

The bacterial Shannon–Wiener diversity index, with typical values ranging from 1.5 to 3.5 (low and high species evenness and richness, respectively) (McDonald, 2003), was high in both the initial compost (3.2) and final packing material (3.5) communities, whereas the leachate community showed the lowest diversity (2.9). Similarity indexes of 34 and 28% were obtained between the initial compost and the final packing and leachate samples, respectively. An 84% similarity was obtained between the communities of both end-of-operation samples. From the bacterial DGGE gel, 14 bands were sequenced (Fig. 4A). Two different phyla were retrieved according to the RDP classifier tool (bootstrap value of 50%): *Proteobacteria* (13 bands) and *Actinobacteria* (1 band). The closest matches for each band are shown in Table 1, along with its similarity percentages and sources of origin.

The Shannon–Wiener diversity indexes calculated for the fungal communities were considerably lower compared to those of bacteria, ranging from 1.9 for the leachate to 2.2 and 2.3 for the final packing material and initial compost, respectively. The communities present in the leachate and final packing material showed a high similarity (83%), whereas Pearson similarity values as low

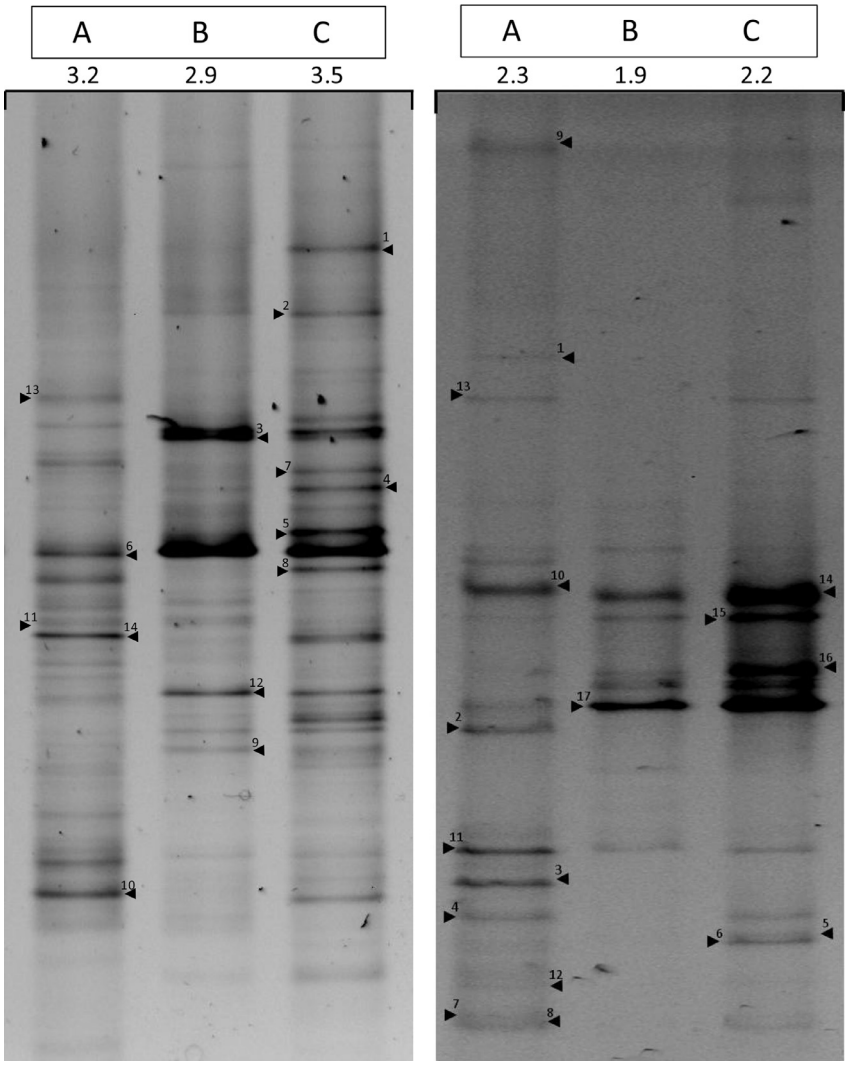

Fig. 4. Bacterial (A) and fungal (B) DGGE patterns of the initial compost (1), leachate (2) and final packing material (3) in the BF. The numbers correspond to the 14 bacterial and 17 fungal bands sequenced.

Table 2
Classification of the fungal DGGE bands sequenced and corresponding matches (BLASTN) using the NCBI database with indication of the similarity percentages and sources of origin. The presence/absence of each band in each sample tested is also shown.

Phylum	Band n°	A	B	C	Closest relatives in blast name (accession number)	Similarity (%)	Source of origin
Phylum *Ascomycota*	1	x			Unultured *Leotiomycetes* (JQ320934)	100	Soil
					Teberdinia hygrophila (JQ780655)	99	Peat
					Graphium sp. (HQ595739)	99	
	2	x			Uncultured *Leotiomycetes* (JQ320934)	100	Peanut soil
					Phialocephala sp. (EU155146)	99	
					Graphium rubrum (AB007660)	99	
					Graphium silanum (AB007661)	99	
	3	x			*Collophora rubra* (GQ154627)	99	
					Graphium sp. (HQ595739)	99	
	4	x		x	Uncultured *Sordariomycetes* (JQ321200)	99	Peanut soil
					Hypoxylon haematostroma (AF346543)	99	Soil
					Uncultured fungus (GU201204)	98	Test site free air carbon exchange enrichment elevated CO_2 ring 2
	5	x		x	*Penicillium oxalicum* (KF152942)	99	Soil
					Penicillium chrysogenum (JF718786)	99	Heavy metal contaminated soil
					Eupenicillium javanicum (JN546126)	99	Oxygen minimum zone, Arabian Sea
	6	x		x	*Thysanophora penicillioides* (AF454064)	99	
					Penicillium spinulosum (FJ717700)	99	
					Penicillium sp. (KF741226)	99	Marine sediment
	7	x			*Penicillium oxalicum* (KF152942)	99	Soil
					Penicillium sp. (KF769006)	99	
					Uncultured fungus (AB468631)	99	Methane cold seep sediment
	8	x		x	*Penicillium* sp. (HM773238)	100	
					Penicillium oxalicum (KF152942)	99	Soil
Phylum *Basidiomycota*	9	x			Uncultured fungus (AB534336)	97	Soil
					Mrakiella aquatica (AB032621)	97	
					Uncultured *Auriculariaceae* (EF023155)	97	Trembling aspen rhizosphere under ambient CO_2 conditions
					Trichosporon pullulans (AB001766)	97	
	10	x			*Mrakia frígida* (KC991038)	93	
					Uncultured fungus (AB534336)	93	Soil
	11	x	x	x	Uncultured fungus (AB534491)	99	Paddy field soil
					Uncultured *Tremellaceae* (EF023503)	99	Trembling aspen rhizosphere under ambient CO2 conditions
					Uncultured *Basidiomycota* (JQ627512)	99	Microbial biofilm on mineral composite substrate
					Uncultured *Tremellomycetes* (FM178256)	99	Malthouse waste water
	12	x			Uncultured fungus (EU726037)	98	Laboratory litter decomposition microcosom
					Uncultured fungus (EU726037)	97	Activated sludge from municipal wastewater treatment plant
					Uncultured fungus (EU708416)	97	Subsurface soil contaminated with lightweight fuel and lubrication oil
					Uncultured fungus (JN638383)	97	Activated sludge from high-sulfur antibiotic waste water
Unidentified fungi	13	x		x	Uncultured fungus (EU910609)	92	Sediment sample
	14		x	x	Uncultured fungus (EU053242)	99	Rhizosphere of plants on mine tailings
					Uncultured *Chytridiomycota* (GQ995262)	93	Soil
	15	x	x	x	Uncultured fungus (EU053242)	99	Rhizosphere of plants on mine tailings
	16		x	x	Uncultured fungus (EU053242)	99	Rhizosphere of plants on mine tailings
					Uncultured *Chytridiomycota* (GQ995261)	92	Soil
	17	x	x	x	Uncultured fungus (EU053242)	98	Rhizosphere of plants on mine tailings

as 31% between the initial compost and the leachate and 34% between the initial compost and the packing material were obtained. Among the 17 bands sequenced from the fungal DGGE gel (Fig. 4B), 8 bands were assigned to the *Ascomycota* phylum, 4 bands to the *Basidiomycota* phylum and 5 bands corresponded to unidentified fungi. The closest matches for each band are shown in Table 2, along with its similarity percentages and sources of origin.

3.3. Batch CH_4 degradation tests

No CH_4 degradation was observed during the first 8 days of experimentation, when CH_4 headspace concentrations remained constant at 136 ± 5 and 147 ± 6 g CH_4 m^{-3} in bottles 1 and 2, respectively (Fig. 5). The addition of potato starch to promote fungal growth resulted in an increase in the CO_2 headspace concentration concomitantly with a decrease in the O_2 headspace concentration, whereas no significant CH_4 uptake was recorded (CH_4 concentrations of 133 ± 4 and 147 ± 4 g CH_4 m^{-3} in bottles 1 and 2). The first addition of methanol promoted CH_4 oxidation to steady values of 115 ± 2 and 129 ± 2 g m^{-3} in bottles 1 and 2, respectively, concomitantly with an increase in CO_2 and a decrease in O_2 concentrations. By day 29, the additional supplementation of methanol significantly boosted CH_4 degradation by *Graphium* sp. to final concentrations of 30 ± 3 g m^{-3} in bottle 1 and 29 ± 4 g m^{-3} in bottle 2.

4. Discussion

Bacterial BFs for CH_4 abatement usually face mass transfer limitations as a result of the poor water solubility of this greenhouse gas pollutant. Hydrophilic storage compounds such as exopolysaccharides are produced by methanotrophs, which accumulation in the biofilm can slightly decrease CH_4 and O_2 transfer from

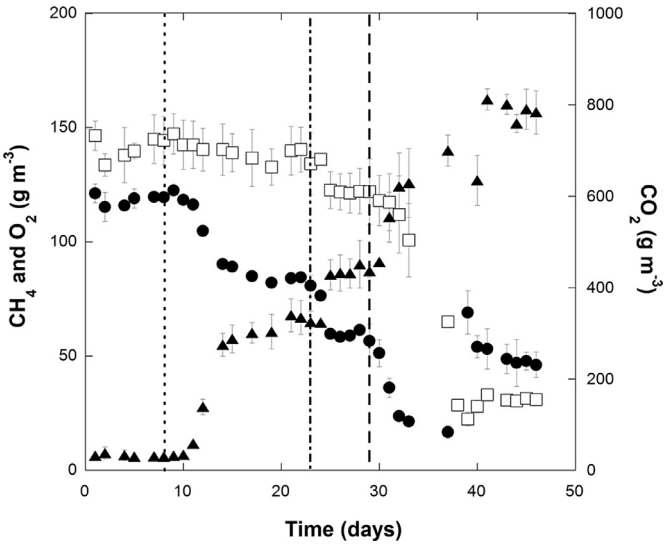

Fig. 5. Time course of CH_4 (□), CO_2 (▲) and O_2 (●) average concentrations and their corresponding standard deviation in the batch tests in bottles 1 and 2. Vertical lines represent the supplementation of a potato starch solution (dotted line), 4 μL of methanol (dotted-dashed line) and 8 μL of methanol (dashed line).

the air emission and therefore deteriorate BF performance (Avalos-Ramírez et al., 2012). On the other hand, fungal BFs have been widely employed for the abatement of hydrophobic pollutants as a result of their enhanced mass transfer due to the high hydrophobicity of the fungal cell wall and to the ability of fungi to colonize with their aerial hyphae the empty space in the BF (Arriaga and Revah, 2005). However, fungi-based BFs have been scarcely applied to CH_4 removal.

The fungal-bacterial BF achieved stable ECs of 36.6 ± 0.7 g m^{-3} h^{-1} (maximum EC = 38.5 g m^{-3} h^{-1}) and REs ~ 90% operating at an EBRT of 20 min. Despite the wide variability of data found in literature, these ECs are comparable to those previously observed in bacterial organic-based BFs treating diluted CH_4 emissions at higher EBRTs (López et al., 2013). Conversely, none of the BFs operated at lower or similar EBRTs than those implemented in this study achieved such high removal efficiencies, which are mandatory to avoid the detrimental environmental effects derived from diluted CH_4 emissions (Table 1, supporting information). For instance, Pratt et al. (2012) completely removed 0.1% v/v CH_4 in a soil-based BF working at 90 min of EBRT, whereas studies conducted at EBRTs ranging from 4 to 18 min and working at significantly lower inlet CH_4 concentrations (0.1–1% v/v) did not exceed RE of ~50% (Nikiema and Heitz, 2009; Girard et al., 2012; Ramirez et al., 2012). Similarly, the removal of CH_4 in biotrickling filters packed with inorganic materials and operated at EBRTs of ~4 min achieved maximum ECs of 21–45 g m^{-3} h^{-1} with REs as low as 11–34% (Avalos-Ramírez et al., 2012; Estrada et al., 2014; Lebrero et al., 2015). Finally, whereas the ECs here obtained did not reach the maximum ECs (106 and 51 g m^{-3} h^{-1}) recorded in stirred tank reactors and multiphase systems, respectively, at low EBRTs (~5 min), these ECs were obtained at the expenses of prohibitively high energy consumptions and low REs (57% and 39%, respectively) (Rocha-Rios et al., 2009). Nevertheless, and in spite of the promising results here obtained in the fungal-bacterial BF, mass transfer still limited CH_4 abatement as demonstrated by the mass transfer test.

This study also highlighted the relevance of the irrigation strategy on BF performance, a high irrigation frequency being essential to achieve steady ECs in the BF and to avoid performance deterioration. This frequent irrigation likely prevented metabolite accumulation in the bed, and the subsequent inhibition of the microbial community. All reported metabolites from CH_4 biodegradation possess higher water solubility than CH_4 (i.e. methanol Henry law's constant is 5 orders of magnitude higher than that of CH_4, Sander, 1999), and therefore any potentially inhibitory metabolite would be preferentially present in the aqueous phase and washed out with the trickling irrigation. The increase in the leachate pH when increasing the irrigation frequency further supported this hypothesis. Moreover, while an excess of irrigation in BFs has been reported to cause packing material compaction or water accumulation (Lebrero et al., 2014), the intensification of BF irrigation here tested did not trigger any of these operational failures. Indeed, 90–95% of the irrigated MSM leached and was removed from the compost bed, probably as a result of the high hydrophobicity of fungal hyphae which might have avoided MSM retention. CH_4 mineralization also increased from ~56% up to 82% by the end of the experimentation period, which might be attributed to accumulation of biomass.

Despite the supplementation of antibiotic to the irrigated MSM and its low pH, a high bacterial diversity was found (i.e. diversity index of 3.5 in the packing material). Most of the bacteria phyla retrieved from both the leachate and the final packing material samples were previously found either in CH_4 polluted environments or in biological CH_4 treatment systems. Within the phylum *Proteobacteria*, type I methanotrophs genera such as *Methylomicrobium* and *Methylosarcina* were identified in bands 5–7. These methanotrophs have been identified as communities involved in CH_4 oxidation (Hatamoto et al., 2010; López et al., 2014). Similarly, type II methanotrophs belonging to the genus *Methylosinus* were found in samples retrieved from the BF. *Methylosinus trichosporium* (band 12) has been commonly found in soils and several studies have demonstrated its potential to oxidize CH_4 (Hatamoto et al., 2010; Limbri et al., 2014) and to co-metabolically degrade trichloroethylene and CH_4 (Kang et al., 2001; Lontoh and Semrau, 1998). Whereas type I methanotrophs are commonly predominant at low CH_4 concentration, the low pH of the MSM might explain the significant presence of type II methanotrophs in our BF (Pieja et al., 2011). López et al. (2014) also found *Xanthomonadales*-related organisms (bands 8–10) in a bioreactor treating CH_4. Similarly, bacteria from the order *Caulobacterales* have been also identified as possible degraders of methanol (Caspi et al., 2010). Finally, the family *Microbacteriaceae* (band 14), belonging to the *Actinobacteria* phylum, has been previously associated to the biodegradation of CH_4 in a coal-packed BF (Limbri et al., 2014).

On the other hand, 7 fungal species initially present in the compost, including *Graphium* sp., disappeared throughout the operation of the BF. On the contrary, other fungi belonging to the phyla *Ascomycota* and *Basidiomycota* became dominant, together with some unidentified fungi. The most abundant fungi within the *Ascomycota* phylum was *Penicillium*, which despite never associated with CH_4 biodegradation, has demonstrated the capability to degrade methanol (De Oliveira et al., 2012; Pineda et al., 2004). Within the unidentified fungi (5 bands), the most abundant according to the thickness of the bands in the DGGE gel were associated with fungi found in soil, sediment samples, or plants growing on wastelands. The high number of unidentified bands highlighted the lack of microbiological data related to fungal characterization and activity, and the need for further research in the area. The results here obtained also showed the key role of indigenous microbial communities on process performance, which likely supported methane and/or metabolites degradation.

Despite the fungus *Graphium* sp. has been retrieved from enrichment cultures using natural gas as a carbon and energy source (Curry et al., 1996; Zajic et al., 1969), to the best of our knowledge, no fungi species have been reported to degrade this GHG. The batch biodegradation tests here performed demonstrated that

Graphium sp. was not able to sustain the oxidation of CH_4 unless methanol, used as an exogenous metabolite, was supplemented to the system. In our batch tests, complete methanol mineralization should have resulted in an increase in CO_2 concentration of ~46 and 92 g m^{-3} after the first and second methanol amendments, respectively. Experimentally, a CO_2 concentration increase of 110 ± 1 and 385 ± 32 g m^{-3} was recorded after each methanol addition, which confirmed the simultaneous occurrence of CH_4 degradation in both culture bottles. This co-metabolic effect was previously documented for CH_4-oxidizing bacteria by Jesen et al. (1998), who observed an improvement in CH_4 uptake as a result of methanol supplementation likely due to a replenishment of reductive power. These promising results encourage for additional research in order to elucidate the actual role of methanol in the fungal CH_4 biodegradation process as well as to determine the optimum methane/methanol ratio to promote a co-metabolic CH_4 abatement. Moreover, the potential implementation of this finding in full scale biofiltration deserves further investigation.

In summary, this study demonstrated the ability of *Graphium* sp. to co-metabolically degrade CH_4 and methanol, which constitutes an important step in the elucidation of the potential and role of fungi in CH_4 abatement. Whereas the methanotrophic activity of *Graphium* sp. could not be proved in the organic-based biofilter, the fungal-bacterial biofilter showed a more stable and enhanced performance compared with previous bacterial biofilters operated at higher EBRTs, supporting ECs of up to 38.5 g m^{-3} h^{-1} at REs of 90%. Moreover, a proper irrigation strategy avoided microbial inhibition derived from metabolite accumulation without inducing a significant pressure drop.

Acknowledgements

This research was supported by the Spanish Ministry of Economy and Competitiveness (BES-2013-063922 grant and CTQ2012-34949 project) and the European Union through the FEDER Funding Program.

Appendix A. Supplementary data

Supplementary data related to this article can be found at http://dx.doi.org/10.1016/j.chemosphere.2015.08.017.

References

Arriaga, S., Revah, S., 2005. Removal of n-hexane by *Fusarium solani* with a gas-phase biofilter. J. Ind. Microbiol. Biotechnol. 32, 548–553. http://dx.doi.org/10.1007/s10295-005-0247-9.

Avalos-Ramírez, A., García-Aguilar, B.P., Jones, J.P., Heitz, M., 2012. Improvement of methane biofiltration by the addition of non-ionic surfactants to biofilters packed with inert materials. Process. Biochem. 47, 76–82. http://dx.doi.org/10.1016/j.procbio.2011.10.007.

Borneman, J., Hartin, J.R., 2000. PCR primers that amplify fungal rRNA genes from environmental samples. Appl. Environ. Microb. 66, 4356–4360. http://dx.doi.org/10.1128/AEM.66.10.4356-4360.2000.

Caspi, R., Altman, T., Dale, J.M., Dreher, K., Fulcher, C.A., Gilham, F., Kaipa, P., Karthikeyan, A.S., Kothari, A., Krummenacker, M., Latendresse, M., Mueller, L.A., Paley, S., Popescu, L., Pujar, A., Shearer, A.G., Zhang, P., Karp, P.D., 2010. The MetaCyt database of metabolic pathways and enzymes and the BioCyc collection of pathway/genome databases. Nucl. Acids Res. 38, D473–D479. http://dx.doi.org/10.1093/nar/gkp875.

Curry, S., Ciuffetti, L., Hyman, M., 1996. Inhibition of growth of a *Graphium* sp. on gaseous n-alkanes by gaseous n-alkynes and n-alkenes. Appl. Environ. Microb. 62, 2198–2200.

De Oliveira, B.V., Teixeira, G.S., Reis, O., Barau, J.G., Teixeira, P.J., do Rio, M.C., Domingues, R.R., Meinhardt, L.W., Paes Leme, A.F., Rincones, J., Pereira, G.A., 2012. A potential role for an extracellular methanol oxidase secreted by *Moniliophthora perniciosa* in Witches' broom disease in cacao. Fungal Genet. Biol. 49, 922–932. http://dx.doi.org/10.1016/j.fgb.2012.09.001.

Environmental Protection Agency, 2013. Inventory of US Greenhouse Gas Emissions and Sinks: 1990-2011 (April 2013) EPA 430-R-13-001. Accessed September 2014. http://epa.gov/climatechange/ghgemissions/usinventoryreport.html.

Estrada, J.M., Kraakman, N.J.R., Lebrero, R., Muñoz, R., 2012. A sensitivity analysis of process design parameters, commodity prices and robustness on the economics of odour abatement technologies. Biotechnol. Adv. 30, 1354–1363. http://dx.doi.org/10.1016/j.biotechadv.2012.02.010.

Estrada, J.M., Lebrero, R., Quijano, G., Pérez, R., Figueroa-Gonzáles, I., García-Encina, P.A., Muñoz, R., 2014. Methane abatement in a gas-recycling biotrickling filter: evaluating innovative operational strategies to overcome mass transfer limitations. Chem. Eng. J. 253, 385–393. http://dx.doi.org/10.1016/j.cej.2014.05.053.

Girard, M., Avalos-Ramirez, A., Buelna, G., Heitz, M., 2011. Biofiltration of methane at low concentrations representative of the piggery industry – influence of the methane and nitrogen concentrations. Chem. Eng. J. 168, 151–158. http://dx.doi.org/10.1016/j.cej.2010.12.054.

Girard, M., Viens, P., Avalos-Ramirez, A., Brzezinski, R., Buelna, G., Heitz, M., 2012. Simultaneous treatment of methane and swine slurry by biofiltration. J. Chem. Technol. Biot. 87, 697–704. http://dx.doi.org/10.1002/jctb.3692.

Häne, B.G., Jäger, K., Drexler, H.G., 1993. The Pearson product-moment correlation coefficient is better suited for identification of DNA fingerprint profiles than band matching algorithms. Electrophoresis 14, 967–972. http://dx.doi.org/10.1002/elps.11501401154.

Hatamoto, M., Yamamoto, H., Kindaichi, T., Ozaki, N., Ohashi, A., 2010. Biological oxidation of dissolved methane in effluents from anaerobic reactors using a down-flow hanging sponge reactor. Water Res. 44, 1409–1418. http://dx.doi.org/10.1016/j.watres.2009.11.021.

Haubrichs, R., Widmann, R., 2006. Evaluation of aerated biofilter systems for microbial methane oxidation of poor landfill gas. Waste Manage. 26, 408–416. http://dx.doi.org/10.1016/j.wasman.2010.11.020.

Intergovernmental Panel on Climate Change, 2013. Fifth Assessment Report: Climate Change 2013, the Physical Science Basis http://www.climatechange2013.org accessed January 2014.

Jesen, S., Priemé, A., Bakken, L., 1998. Methanol improves methane uptake in starved methanotrophic microorganisms. Appl. Environ. Microbiol. 64, 1143–1146.

Kang, J., Lee, E.Y., Park, S., 2001. Co-metabolic biodegradation of trichloroethylene by *Methylosinus trichosporium* is stimulated by low concentrations methane or methanol. Biotechnol. Lett. 23, 1877–1882. http://dx.doi.org/10.1023/A:1012758803576.

Kennes, C., Veiga, M.C., 2004. Fungal biocatalysts in the biofiltration of VOC-polluted air. J. Biotechnol. 113, 305–319. http://dx.doi.org/10.1016/j.jbiotec.2004.04.037.

Lebrero, R., Rodríguez, E., Estrada, J.M., García-Encina, P.A., Muñoz, R., 2012. Odor abatement in biotrickling filters: effect of the EBRT on methyl mercaptan and hydrophobic VOCs removal. Bioresour. Technol. 109, 38–45. http://dx.doi.org/10.1016/j.biortech.2012.01.052.

Lebrero, R., Hernández, M., Quijano, G., Muñoz, R., 2014. Hexane biodegradation in two-liquid phase biofilters operated with hydrophobic biomass: effect of the organic phase-packing media ratio and the irrigation rate. Chem. Eng. J. 237, 162–168. http://dx.doi.org/10.1016/j.bej.2012.09.009.

Lebrero, R., Hernández, L., Pérez, R., Estrada, J.M., Muñoz, R., 2015. Two-phase partitioning biotrickling filters for methane abatement: exploring the potential of hydrophobic methanotrophs. J. Environ. Manage. 151, 124–131. http://dx.doi.org/10.1016/j.jenvman.2014.12.016.

Limbri, H., Gunawan, C., Thomas, T., Smith, A., Scott, J., Rosche, B., 2014. Coal-packed methane biofilter for mitigation of green house gas emissions from coal mine ventilation air. Plos One 9 (4), e94641. http://dx.doi.org/10.1371/journal.pone.0094641.

Lontoh, S., Semrau, J.D., 1998. Methane and trichloroethylene degradation by *Methylosinus trichosporium* OB3b expressing particulate methane monooxygenase. Appl. Environ. Microbiol. 64, 1106–1114.

López, J.C., Quijano, G., Souza, T.S.O., Estrada, J.M., Lebrero, R., Muñoz, R., 2013. Biotechnologies for greenhouse gases (CH_4, N_2O and CO_2) abatement: state of the art and challenges. App. Microbiol. Biot. 97, 2277–2303. http://dx.doi.org/10.1007/s00253-013-4734-z.

López, J.C., Quijano, G., Pérez, R., Muñoz, R., 2014. Assessing the influence of CH_4 concentration during culture enrichment on the biodegradation kinetics and population structure. J. Environ. Manage. 146, 116–123. http://dx.doi.org/10.1016/j.jenvman.2014.06.026.

McDonald, G., 2003. Biogeography: Space, Time and Life. John Wiley & Sons, New York, p. 409.

McGinnis, S., Madden, T.L., 2004. BLAST: at the core of a powerful and diverse set of sequence analysis tools. Nucleic Acids Res. 32, W20–W25. http://dx.doi.org/10.1093/nar/gkh435.

Nikiema, J., Heitz, M., 2009. The influence of the gas flow rate during methane biofiltration on an inorganic packing material. Can. J. Chem. Eng. 87, 136–142. http://dx.doi.org/10.1002/cjce.20131.

Nübel, U., Engelen, B., Felske, A., Snaidr, J., Wieshuber, A., Amann, R.I., Ludwig, W., Backhaus, H., 1996. Sequence heterogeneities of genes encoding 16S rRNAs in *Paenibacillus polymyxa* detected by temperature gradient gel electrophoresis. J. Bacteriol. 178, 5636–5643.

Pieja, A.J., Rostkowski, K.H., Criddle, C.S., 2011. Distribution and selection of poly-3-hydroxybutyrate production capacity in methanotrophic proteobacteria. Microb. Ecol. 62, 564–573. http://dx.doi.org/10.1007/s00248-011-9873-0.

Pineda, R., Alba, J., Thalasso, F., Ponce-Noyola, T., 2004. Microbial characterization of organic carrier colonization during a model biofiltration experiment. Lett. Appl. Microbiol. 38, 522–526. http://dx.doi.org/10.1111/j.1472-765X.2004.01530.x.

Pratt, C., Walcroft, A.S., Tate, K.R., Ross, D.J., Roy, R., Reid, M.H., Veiga, P.W., 2012. In vitro methane removal by volcanic pumice soil biofilter columns over one year. J. Environ. Qual. 41, 80–87. http://dx.doi.org/10.2134/jeq2011.0179.

Ramirez, A.A., Garcia-Aguilar, B.P., Jones, J.P., Heitz, M., 2012. Improvement of methane biofiltration by the addition of non-ionic surfactants to biofilters packed with inert materials. Process Biochem. 47, 76–82. http://dx.doi.org/10.1016/j.procbio.2011.10.007.

Rocha-Rios, J., Bordel, S., Hernández, S., Revah, S., 2009. Methane degradation in two-phase partition bioreactors. Chem. Eng. J. 152, 289–292. http://dx.doi.org/10.1016/j.cej.2009.04.028.

Roest, K., Heilig, H.G.H.J., Smidt, H., de Vos, W.M., Stams, A.J.M., Akkermans, A.D.L., 2005. Community analysis of a full-scale anaerobic bioreactor treating paper mill waste water. Syst. Appl. Microbiol. 28, 175–185. http://dx.doi.org/10.1099/mic.0.036715-0.

Sander, R., 1999. Compilation of Henry's Law Constants for Inorganic and Organic Species of Potential Importance in Environmental Chemistry http://www.rolf-sander.net/henry/ accessed October 2014.

TMECC. Test Methods for the Examination of Composting and Compost, June 2002. The US Composting Council Research and Education Foundation, and the US Department of Agriculture.

Vergara-Fernández, A., Hernández, S., Revah, S., 2008. Phenomenological model of fungal biofilters for the abatement of hydrophobic VOCs. Biotechnol. Bioeng. 101, 1182–1192. http://dx.doi.org/10.1002/bit.21989.

Wang, Q., Garrity, G.M., Tiedje, J.M., Cole, J.R., 2007. Naïve Bayesian classifier for rapid assignment of rRNA sequences into the new bacterial taxonomy. Appl. Environ. Microbiol. 73, 5261–5267. http://dx.doi.org/10.1128/AEM.00062-07.

Zajic, J.E., Volesky, B., Wellman, A., 1969. Growth of *Graphium* sp. on natural gas. Can. J. Microbiol. 15, 1231–1236. http://dx.doi.org/10.1139/m69-222.

Exploring the potential of fungi for methane abatement: Performance evaluation of a fungal-bacterial biofilter

*Raquel Lebrero, Juan C. López, Iiro Lehtinen, Rebeca Pérez, Guillermo Quijano, Raúl Muñoz**

Department of Chemical Engineering and Environmental Technology, University of Valladolid, Dr. Mergelina, s/n, 47011, Valladolid, Spain.
*Corresponding author: mutora@iq.uva.es, Tel. +34 983186424, Fax: +34 983423013.

Supporting Information Section

containing 3 pages, with 1 table.

Table 1 SI. Comparison of methane abatement performance in biofilters and biotrickling filters. Adapted from López et al. (2014) and Ganendra et al. (2015).

Packed bed medium	Inlet CH_4 (% v/v)	EBRT (min)	CH_4 load (g CH_4 m^{-3} h^{-1})	Maximum EC (g CH_4 m^{-3} h^{-1})	Maximum RE (%)	Reference
BIOFILTERS						
Compost	2	20-40	20-41	36.6	90	This study
Pine bark and perlite(70:30 v/v)	0.1-2.5	30-600	0.03-16	13	81	du Plessis et al. (2003)
Soil mixture	2.5	6	165	64	39	Streese and Stegmann (2003)
Compost and perlite (40:60 v/v)	0.07-0.8	43-4800	0.07-25	19	76	Melse and Van der Werf (2005)
Gravel, sand and compost layers	50	21600	1.2	1.14	95	Berger et al. (2005)
Gravel / compost	0.7	4.3	71.2 / 65.8	29.2 / 12.5	41 / 19	Nikiema et al. (2005)
Compost	6.6-10.8	102-450	5-29	27.5	95	Haubrichs and Widmann (2006)
Compost and wood chips (50:50 v/v)		120-450	5-24	21.6	90	
Gravel, clay, sand and topsoil layers	0.1	24-1200	46.4-80	80	100	Gebert and Gröngröft (2006)
Municipal solid waste	0.1	240-840	2.5-6.5	5.6	85	Einola et al. (2008)
Gravel and stone	0.15-1	3-18	13-130	65	50	Nikiema and Heitz (2009)
Soil and earthworm cast (60:40 w/w)	5-25	4.2-72	31-560	280	50	Park et al. (2009)
Gravel	0.02-0.4	4.2	5-28	14.5	52	Girard et al. (2012)
Landfill soil	0.1	90	24	24	100	Pratt et al. (2012)
Stones	0.7	4.2	61.8	33	53	Ramirez et al. (2012)
Landfill soil	1.5	20	30.4	18	59	Kim et al. (2013)
Perlite	5	180	106.5	65.1	43-88	Kim et al. (2014a)
Trombolite	5	20	96.6	32-41	33-42	Kim et al. (2014b)
Autoclaved aerated concrete	0.1	0.8	944.7	~280	~30	Ganendra et al. (2015)
BIOTRICKLING FILTERS						
Clay spheres	0.7	4.2	62	10	16	Avalos-Ramirez et al. (2012)
Polypropylene spheres				8	13	
Stones				21	34	
Polyurethane foam	2.2	4	229	30	11	Estrada et al. (2014)
Polyurethane foam (two-phase system)	2	4	410-440	45	15	Lebrero et al. (2015)

References

Avalos-Ramírez, A., García-Aguilar, B.P., Jones, J.P., Heitz, M., 2012. Improvement of methane biofiltration by the addition of non-ionic surfactants to biofilters packed with inert materials. Process. Biochem. 47, 76-82. doi: 10.1016/j.procbio.2011.10.007

Berger, J., Fornés, L.V., Ott, C., Jager, J., Wawra, B., Zanke, U., 2005. Methane oxidation in a landfill cover with capillary barrier. Waste. Manag. 25, 369–373. doi:10.1016/j.wasman.2005.02.005

Du Plessis, C.A., Strauss, J.M., Sebapalo, E.M.T., Riedel, K.H.J., 2003. Empirical model for methane oxidation using a composted pine bark biofilter. Fuel 82, 1359–1365. doi:10.1016/S0016-2361(03)00040-1

Einola, J.K.M., Karhu, A.E., Rintala, J.A., 2008. Mechanically–biologically treated municipal solid waste as a support medium for microbial methane oxidation to mitigate landfill greenhouse emissions.Waste Manag. 28, 97–111. doi:10.1016/j.wasman.2007.01.002

Estrada, J.M., Lebrero, R., Quijano, G., Pérez, R., Figueroa-González, I., García-Encina, P.A., Muñoz, R., 2014. Methane abatement in a gas-recycling biotrickling filter: Evaluating innovative operational strategies to overcome mass transfer limitations. Chem. Eng. J. 253, 385-393. doi: 10.1016/j.cej.2014.05.053

Ganendra, G., Mercado-Garcia, D., Hernandez-Sanabria, E., Boeckx, P., Ho, A., Boon, N., 2015. Methane biofiltration using autoclaved aerated concrete as the carrier material. Appl. Microbiol. Biotechnol. 99(17), 7307-7320; doi: 10.1007/s00253-015-6646-6.

Gebert. J., Gröngröft, A., 2006. Performance of a passively vented fieldscale biofilter for the microbial oxidation of landfill methane.Waste Manag. 26, 399–407. doi:10.1016/j.wasman.2005.11.007

Girard, M., Viens, P., Avalos-Ramirez, A., Brzezinski, R., Buelna, G., Heitz, M., 2012. Simultaneous treatment of methane and swine slurry by biofiltration. J. Chem. Technol. Biot. 87, 697-704. doi: 10.1002/jctb.3692

Haubrichs, R., Widmann, R., 2006. Evaluation of aerated biofilter systems for microbial methane oxidation of poor landfill gas. Waste Manag. 26, 408–416. doi:10.1016/j.wasman.2005.11.008

Kim, T.G., Lee, E-H., Cho, K-S., 2013. Effects of nonmethane volatile organic compounds on microbial community of methanotrophic biofilter. Appl. Environ. Microbiol. 97, 6549–6559. doi:10.1007/s00253-012-4443-z

Kim, T.G., Jeong, S-Y., Cho, K-S., 2014a. Characterization of tobermolite as a bed material for selective growth of methanotrophs in biofiltration. J. Biotechnol. 173, 90–97. doi:10.1016/j.jbiotec.2014.01.010

Kim, T.G., Jeong, S-Y., Cho, K-S., 2014b. Functional rigidity of a methane biofilter during the temporal microbial succession. Appl. Environ. Microbiol. 98, 3275–3286. doi:10.1007/s00253-013-5371-2

Lebrero R., Hernández L., Pérez R., Estrada J.M., Muñoz R., 2015. Two-phase partitioning biotrickling filters for methane abatement: exploring the potential of hydrophobic methanotrophs. J. Environ. Manage. 151, 124-131. doi: 10.1016/j.jenvman.2014.12.016

Melse, R.W., Van derWerf, A.W., 2005. Biofiltration for mitigation of methane emission from animal husbandry. Environ. Sci. Technol. 39, 5460–5468. doi:10.1021/es048048q

Nikiema, J., Bibeau, L., Lavoie, J., Brzezinski, R., Vigneux, J., Heitz, M., 2005. Biofiltration ofmethane: an experimental study. Chem. Eng. J. 113, 111–117. doi:10.1016/j.cej.2005.04.005

Nikiema, J., Heitz, M., 2009. The influence of the gas flow rate during methane biofiltration on an inorganic packing material. Can. J. Chem. Eng. 87, 136-142. doi: 10.1002/cjce.20131

Park, S., Lee, C-H., Ryu, C-R., Sung, K., 2009, Biofiltration for reducing methane emissions from modern sanitary landfills at the low methane generation stage. Water Air Soil Pollut. 196, 19–27. doi:10.1007/s11270-008-9754-4

Pratt, C., Walcroft, A.S., Tate, K.R., Ross, D.J., Roy, R., Reid, M.H., Veiga, P.W., 2012. In vitro methane removal by volcanic pumice soil biofilter columns over one year. J. Environ. Qual. 41, 80-87. doi:10.2134/jeq2011.0179

Ramirez, A.A., Garcia-Aguilar, B.P., Jones, J.P., Heitz, M., 2012. Improvement of methane biofiltration by the addition of non-ionic surfactants to biofilters packed with inert materials. Process Biochem. 47, 76-82. doi:10.1016/j.procbio.2011.10.007

Streese, J., Stegmann, R., 2003. Microbial oxidation of methane from old landfills in biofilters. Waste Manag. 23, 573–580. doi:10.1016/s0956-053x(03)00097-7.

Chapter 4

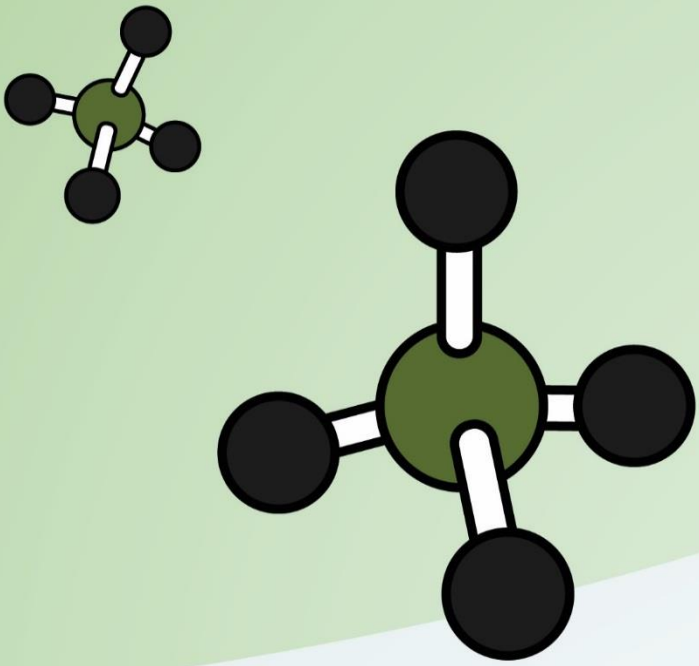

Feast-famine biofilter operation for methane mitigation

Feast-famine biofilter operation for methane mitigation

*Juan C. López, Laura Merchán, Raquel Lebrero, Raúl Muñoz**

Department of Chemical Engineering and Environmental Technology, University of Valladolid, Dr. Mergelina, s/n, 47011, Valladolid, Spain.

*Corresponding author: mutora@iq.uva.es, Tel. +34 983186424, Fax: +34 983423013.

Abstract

Packed bed clogging and channeling derived from the accumulation of biomass still represent technical challenges to be addressed in gas biofiltration in order to enable a more cost-effective performance under long-term operation. In the present study, multiple feast-famine strategies were assessed, for the first time, in two alternate biofilters and compared with a standard continuous biofilter using CH_4 as the model carbon source. The robustness of the biofilters towards increasing famine periods, the decrease of the irrigation frequency and air deprivation was evaluated. The alternate biofilters, where the lowest average pressure drops were recorded, exhibited higher CH_4 elimination capacities (by 27.2 ± 6.4 %) and mineralizations (by 18.3 ± 8.6 %) than the standard biofilter (CH_4 elimination capacities and mineralizations of 10.3 ± 3.6 g m^{-3} h^{-1} and 79.7 ± 20.8 %, respectively), along with the lowest recovery period so far reported in biofiltration after pollutant supply resumption (1.5 ± 0.0 h). Metagenomics analysis revealed a significant shift in the structure of the microbial population induced by the feast-famine regimes, which favoured the occurrence of *Planctomycetes* and *Proteobacteria* phyla. Type I/II methanotroph ratios in the alternate units were 7.5 times higher than those found in the control unit, *Methylomonas* becoming the most resilient genus under feast/famine operation. The current work represents a scaled-down study that demonstrates the feasibility of applying feast-famine strategies at full-scale to increase the performance of biofilters under long-term operation and the lifespan of the packed bed.

Keywords: Biofilter, biomass control strategy, greenhouse gas abatement, methane, methanotroph, *Methylomonas*.

1 Introduction

International greenhouse gas (GHG) inventories rank methane (CH_4) as the second most prevalent GHG, with a contribution of 10-16% to the annual GHG emissions worldwide and an atmospheric concentration increase of 150% in the past 250 years (IPCC, 2014; EPA, 2016). Despite the lower mass emissions of CH_4 compared to CO_2, its global warming potential is 25 times higher than that of CO_2 over a 100-y horizon, this factor increasing up to 72 in a 20-y horizon. Therefore, CH_4 contributes to ~30 % of the so-called "current net climate forcing" (Solomon et al., 2007). In nature, CH_4 is mainly emitted from the anaerobic decomposition of organic matter in wetlands and oceans. However, more than 60% of the CH_4 emissions worldwide are anthropogenic. These anthropogenic CH_4-laden emissions are usually generated from livestock farming (199 million tons of CO_2-eq), landfilling, composting and wastewater treatment (125 million tons CO_2-eq), and coal mining (24 million tons CO_2-eq) (EEA, 2015). The concentration of CH_4 in these emissions varies from 0 – 0.2 $gCH_4\ m^{-3}$ for compost piles to 20 – 100 $gCH_4\ m^{-3}$ for old landfills. It is noteworthy that more than 55% of anthropogenic CH_4 emissions possess concentrations below the lower explosive limit of CH_4-air mixtures (5% *v/v*), which render them unsuitable for energy recovery (Estrada et al. 2014). In addition, the gradual implementation of the Kyoto protocol and the EU landfill Directive 1999/31/EC has tightened European regulations on GHGs, thus resulting in emissions with even lower CH_4 concentrations. In this context, the development of cost-efficient and sustainable technologies for the abatement of these diluted CH_4 emissions is crucial (López et al., 2013).

Biotechnologies have emerged as a cost-efficient and environmentally-friendly alternative to conventional physical-chemical technologies (Estrada et al., 2012) and showed to be promising for the abatement of methane mediated by the activity of methanotrophs (Ménard et al., 2012; Rocha-Rios et al., 2013; Estrada et al., 2014). Among biotechnologies, biofilters (BFs) have been extensively employed in the past decades for industrial off-gas control and represent the most cost-effective option for the mitigation of diffuse CH_4 emissions at full-scale, ensuring that the optimum packed bed selection, nutrient requirements and operational conditions are implemented (Gómez-Cuervo et al. 2017). However, despite the significant advances carried out in the past years in the field of biological CH_4 abatement, biotechnologies are still limited by the low aqueous solubility of CH_4 (dimensionless Henry's law constant of 29.5 at 25 ^oC and 1 atm) and the

unresolved problems of conventional biofiltration such as bed clogging and channeling as a result of biomass overgrowth. In this regard, previous studies have consistently demonstrated that an excess of biomass in BFs ultimately reduces the stability and abatement performance of the target pollutant, with an associated increase in operating costs derived from bed conditioning and energy consumption for air circulation (Morgan-Sagastume et al., 2001; Devinny and Ramesh, 2005). Design and operational strategies to control biomass growth in BFs such as back- or chemical washing and mechanical bed stirring or continuous ozone addition often entail a significant down-time after treatment, complex reactor design and additional operating costs, which has limited their widespread use in off-gas biofiltration (Smith et al., 1996; Wübker et al. 1997; Covarrubias-García et al. 2017). In this context, the implementation of innovative low-cost biomass control strategies such as protozoa and mite predation (Woertz et al., 2002), reverse gas flow operation (Rojo et al. 2012), step-feed operation (Estrada et al. 2013) and the implementation of famine regimes (Dorado et al., 2012) have resulted in an efficient long-term performance in biotechnologies devoted to the treatment of VOCs, the later strategy significantly reducing the overall biomass accumulated per volume unit of the biofilter at the expenses of an additional abatement unit. To date, few studies have systematically compared the performance of alternate units operated under feast-famine regimes with that of a continuous control unit. Indeed, the recovery of CH_4 abatement performance following the suppression of pollutant supply during feast-famine regimes (microbial activity robustness) has been poorly explored in biotechnologies devoted to GHG treatment (Ferdowsi et al., 2016). In addition, to the best of our knowledge, the influence of these feast-famine regimes on the diversity and structure of the active methane-oxidizing populations has not been previously assessed.

The main aim of this work was to develop an innovative operational strategy in order to minimize biomass accumulation and sustain long-term CH_4 mitigation. Thus, a systematic evaluation of the feasibility of feast-famine strategies as a promising alternative to conventional biomass control approaches during CH_4 biofiltration, with a special focus on the influence of the extent of feast-famine periods, the frequency of irrigation and air deprivation on the recovery of pollutant abatement performance was carried out. Next-generation sequencing was used to assess the influence of feast-famine strategies on the structure

and diversity of the active methanotrophic populations.

2 Materials and methods

2.1 Chemicals and nutrient solution

Methane was purchased from Abelló Linde S.A. (Barcelona, Spain) with a purity of at least 99.5%. All reagents and chemicals were purchased from Panreac® (Barcelona, Spain) with a purity of at least 99%.

Centrate wastewater from the centrifugation of anaerobically digested mixed sludge of wastewater treatment plants (WWTPs) was selected as low-cost nutrient medium for the enrichment of methanotrophs and the irrigation of the inorganic biofilters. Centrate, which is characterized by a low biodegradable fraction of organic matter and high nutrient concentrations, was monthly obtained from Valladolid WWTP (Valladolid, Spain) and stored at 4ºC prior to use. According to preliminary batch tests conducted in our lab, a 3-fold dilution was applied to centrate for the irrigation of the BFs in order to avoid inhibition of methanotrophs due to its high $N\text{-}NH_4^+$ concentrations. Additionally, this diluted centrate was supplemented with SO_4^{2-} (using $MgSO_4 \cdot 7H_2O$) to a final concentration of 150 mg L^{-1} (~50 mgS L^{-1}) in order to prevent any biological limitation due to the absence of $S\text{-}SO_4^{2-}$ in the nutrient medium. $S\text{-}SO_4^{2-}$ was not detected through HPLC-IC measurements (lower detection limit of 5 ppm SO_4^{2-}) in the raw centrate used in the present study. Based on elemental composition analyses (CHONS) carried out for methanotrophic biomass samples in our laboratory, a S content ranging from 0.5 to 1 % is typically found, which highlighted the need of $S\text{-}SO_4^{2-}$ supplementation in the diluted centrate used for biofilter irrigation. The adjusted sulfate concentration was selected according to the concentrations used in previous studies on CH_4 biodegradation (30-130 mgS L^{-1}, Whittenbury et al., 1970; López et al., 2014). The final composition of the diluted centrate is shown in Table S1 (Supporting Information).

2.2 Methanotrophic enrichment

A 10-L laboratory scale stirred tank reactor (STR) was set-up for the enrichment of methanotrophs under continuous feeding of a CH_4-laden air stream for 30 days. Fresh aerobic activated sludge from Valladolid WWTP was used as inoculum. The operational conditions of the STR were described in the Supporting Information.

2.3 Experimental set-up, inoculation, operation mode and biomass sampling

Three lab-scale BFs consisting of cylindrical PVC columns (height = 0.45

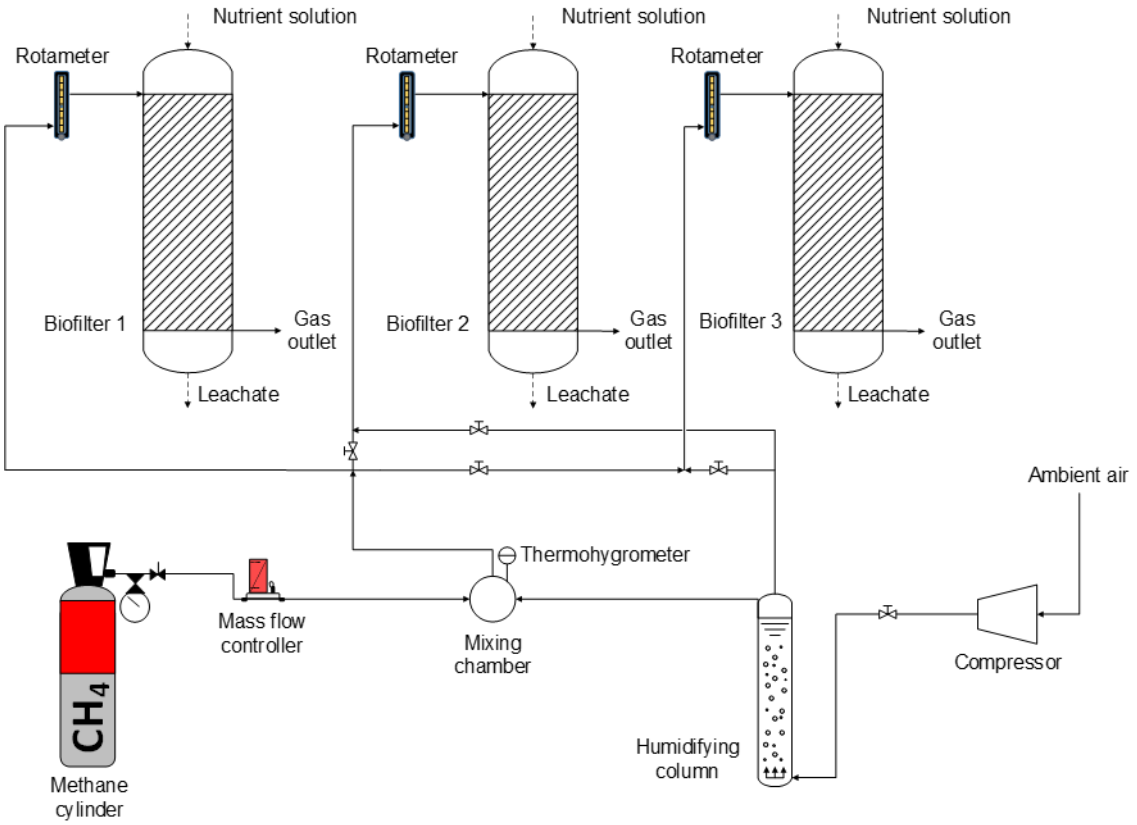

Figure 1. Schematic representation of the experimental set-up.

m; inner diameter = 0.08 m) were set-up (Fig. 1). Each BF was packed with 2.3 L of the impregnated Kaldnes rings used during methanotrophic enrichment and further irrigated with 150 mL of the concentrated methanotrophic biomass suspension. The BFs were maintained at a temperature of 24.7 ± 1.0 ºC in a temperature-controlled room. A pure CH_4 gas stream, regulated with a mass flow controller (Aalborg™, USA), was mixed with pre-humidified air in a mixing chamber and the resulting stream was continuously fed at 8.4 L h^{-1} to the control BF (BF 1) and the BF operated under feast conditions (either BF 2 or BF 3). This operation resulted in a gas stream with an inlet CH_4 concentration of 31.0 ± 1.3 g m^{-3} (4.7 ± 0.2% *v/v*), a humidity of 96.8 ± 3.2% and an empty bed residence time (EBRT) of 17.1 min. Thus, a CH_4 inlet load (IL) of 108.7 ± 4.5 g m^{-3} h^{-1} was applied to the units under CH_4 supply. The concentrations here applied can be typically found in old landfills, coal mines and WWTPs, and remained under the lower explosive limit (< 5 % (*v/v*)). Since the treatment of CH_4 emissions via incineration or energy recovery are only applicable for CH_4 concentrations above 30 % (*v/v*), biotechnologies such as BFs represent an environmentally-friendly platform for the treatment of these off-gases. The use of such relatively high CH_4 concentration might mediate a faster biomass accumulation, which allows evaluating the impact of feast-famine

strategies on biofilter performance. On the other hand, the BF unit under famine conditions (either BF 3 or BF 2) was either fed with CH_4 free-air at 8.4 L h^{-1} or enclosed to prevent air circulation through the BF, depending on the operational stage evaluated. The succession of each feast-famine cycle occurred through alternate shifts in gas feeding between BFs 2 and 3 from CH_4-deprived (famine regime) to CH_4-supplemented (feast regime) conditions and *vice versa*. Before each change, the gas phase of the unit under famine was purged with air at 30 L h^{-1} for 0.5 h to avoid an overestimation of the CO_2 production during the first hours of the feast periods.

The BFs were initially operated for 3 days under abiotic conditions prior to inoculation in order to rule out the occurrence of CH_4 photolysis or adsorption in the experimental set-up. After inoculation, the leachates containing unadhered microbes from the inoculum were recycled for the first two weeks at least twice per day through the packed bed of the BFs to ensure a proper biomass attachment.

Four operational conditions, corresponding to Stages A, B, C and D, were tested in order to evaluate the performance and robustness of feast-famine strategies during CH_4 biofiltration. During Stage A (days 0 – 30), all BFs were fed continuously with the CH_4-air stream and irrigated with diluted centrate at a rate of 130.4 mL L^{-1} of packed bed d^{-1}. In Stage B (days 31 – 103), BFs 2 and 3 were alternately subjected to 3d:3d CH_4 feast-famine cycles maintaining the same irrigation rate as in Stage A for all units. A mass transfer test according to Lebrero et al. (2016) was carried out on days 104-108 in order to confirm the occurrence of mass transfer limitations during the operation of the BFs. Afterwards, the CH_4 feast-famine cycles in BFs 2 and 3 were increased to 5d:5d, while the irrigation rate was reduced to 78.3 mL L^{-1} of packed bed d^{-1} in all units (Stage C, days 109 – 173). During Stage D (days 174 – 243), the CH_4 feast-famine cycles and irrigation rates were maintained as in Stage C, though neither air nor irrigation were supplied to the alternate unit under starvation (Table 1).

Gas samples were drawn periodically from the sampling ports located at the inlet and outlet of the BFs to monitor the CH_4, O_2 and CO_2 concentrations by GC-TCD. Liquid samples from the leachate of the BFs and the diluted centrate used for irrigation were also drawn once a week to monitor the concentrations of total nitrogen (TN), NH_4^+, NO_2^-, NO_3^-, PO_3^{4-}, SO_4^{2-} and pH. The pressure drop across the packed bed was periodically measured by means of a U-tube manometer connected to the gas inlet

Table 1. Operational conditions evaluated in the three BFs.

Stage	Duration (days)	Gas feeding regime	Gas feeding applied to the famine unit	Duration of the feast-famine cycles (days)	Irrigation rate (mL L^{-1} of packed bed d^{-1})
A	0-30	Continuous	-	-	130
B	31-103	Feast/famine (alternately BF 2/3) Continuous (BF 1)	Air	3:3	130
C	109-173	Feast/famine (alternately BF 2/3) Continuous (BF 1)	Air	5:5	78
D	174-243	Feast/famine (alternately BF 2/3) Continuous (BF 1)	None	5:5	78 (working units only)

and outlet of the BFs using water as the manometric fluid. The total amount of biomass in each BF at the end of the experiment was retrieved and measured as TSS and VSS concentrations. The pressure drop caused by the packing material was determined before BFs inoculation. Finally, biomass samples from the inoculum (sample I) and from the packed bed of BFs 1, 2 and 3 at the end of operation (samples 1, 2 and 3, respectively) were collected and immediately stored at -80º C for further microbiological analysis.

2.4 Analytical procedures

CH_4, O_2 and CO_2 gas concentrations were determined by GC-TCD according to López et al. (2014). NO_3^-, NO_2^-, SO_4^{2-} and PO_4^{3-} concentrations in the biofilter leachates and nutrient solution were quantified by HPLC-IC according to López et al. (2017) after sample filtration through 0.20 µm nylon filters. NH_4^+ concentration was also determined after filtration with an ammonium specific electrode Orion Dual Star (Thermo Scientific, The Netherlands). TN concentrations were measured in a Shimadzu TOC-VCSH analyzer (Japan) equipped with a TNM-1 chemiluminescence module according to López et al. (2014). The determination of TSS and VSS concentrations was performed according to standard methods (APHA, 2005). The humidity of the inlet stream was on-line measured

by a thermohygrometer (Testo 605-H1, Testo AG, Germany).

2.5 cDNA generation, Illumina library preparation and sequencing

RNA was extracted from biomass samples I, 1, 2 and 3 using both the RNeasy Plus Mini Kit together with the protection buffer RNAprotect Bacteria Reagent (Qiagen, Hilden, Germany) according to the manufacturer in order to identify active microbial populations (Blazewicz et al., 2013). The integrity of the extracted rRNA was checked by electrophoresis on a 1% (*w/v*) agarose gel. RNA purity was tested using a nanodrop spectrophotometer (NanoDrop Technologies, Wilmington, USA) by measuring the absorbance ratio at 260/280 nm, which was consistently found to be 1.9 – 2. Then, cDNA was synthesized through reverse transcription in a total volume of 20 µL using the iScript cDNA Synthesis Kit (Bio-Rad Laboratories, Hercules, CA) and was sent for further Illumina MiSeq sequencing to the laboratories of the Foundation for the Promotion of Health and Biomedical Research of Valencia Region (FISABIO, Valencia, Spain).

Amplicon sequencing was carried out targeting the 16S V3 and V4 regions (464bp, *Escherichia coli* based coordinates) with the bacterial primers S-D-Bact-0341-b-S-17 and S-D-Bact-0785-a-A-21, forward and reverse, respectively, which were chosen according to Klindworth et al. (2013). Illumina adapter overhang nucleotide sequences were added to the gene-specific sequences, thus resulting in the following full-length primers for the analysis: 5' TCGTCGGCAGCGTCAGATGTGTATAAGAGACAGCCTACGGGNGGCWGCAG (16S amplicon PCR forward primer), and 5' GTCTCGTGGGCTCGGAGATGTGTATAAGAGACAGGACTACHVGGGTATCTAATCC (16S amplicon PCR reverse primer). Indexed paired-end libraries were generated using the Nextera XT DNA Sample Preparation Kit (Illumina, San Diego, CA), with a reduced number of PCR cycles (25) using 55º C as annealing temperature. Libraries were then normalized and pooled prior to sequencing. Non-indexed PhiX library (Illumina, San Diego, CA) was used as performance control. Samples containing indexed amplicons were loaded onto the MiSeq reagent cartridge and onto the instrument along with the flow cell for automated cluster generation and paired-end sequencing with dual indexes (2×300bp run, MiSeq Reagent Kit v3) (Illumina, San Diego, CA).

2.6 Quality filtering and 16S rDNA-based taxonomic analysis

After demultiplexing, only reads that had quality value scores of ≥ 20 for more than 99 % of the sequence were extracted for further analysis. All sequences with ambiguous base calls were discarded. Quality assessment was performed by the use of prinseq-lite program (Schmieder and Edwards, 2011). After quality assessment, paired-end reads were joined together with the fastq-join program (Aronesty, 2011). Once eventual chimeras belonging to PCR artifacts among the sequences were discarded using the usearch program (Edgar, 2010), taxonomic assignments were carried out using the RDP_Classifier from the Ribosomal Database Project (Cole et al., 2005; Wang et al., 2007). Sequences were clustered by confidence thresholds of 97 % and 70 % at family and genus levels, respectively, to be further subjected to downstream analyses. Rarefaction curves were determined based on the calculated operational taxonomic units (OTUs) and were employed to standardise and compare the observed taxon richness among samples and to verify the representativeness of collected samples. Complete cluster and correlation distance methods were applied to construct cluster dendograms among samples during hierarchical cluster analyses with pvclust in R version 3.2.0 (R Core Team, 2014). Hierarchical clustering of OTUs was performed using the percentage of reads per OTU for the most abundant taxa, that is, >0.5 % population in at least one sample. Simpson and Shannon indexes, ordination plots and canonical correlation analyses (CCA) – based on the type of C feeding and the operational time – were calculated using the Vegan library version 2.3-1 (Oksanen et al., 2015). Krona tool was used to represent relative abundances and confidences within the complex hierarchies of metagenomic classifications (Ondov et al., 2011). The nucleotide sequence dataset was deposited in the European Nucleotide Archive (ENA) under the study and samples accession numbers PRJEB20207 and ERS1634195 – ERS1634198, respectively.

2.7 Calculations

Process performance was evaluated by monitoring the CH_4 elimination capacity (EC), the CH_4 removal efficiency (RE), the CO_2 production rate (PCO_2), the CH_4 mineralization (R_{CO2}), the CO_2 production yield (Y_{CO2}), the pressure drop in the biofilters, the removal efficiency (RE) of TN, N-NH_4^+ and P-PO_4^{3-} and the concentration of NO_2^- and NO_3^- in the leachate along the different operational stages. The calculation procedures for the above-referred parameters are detailed in the

Supporting Information section (Table S2).

2.8 Statistical analysis

The values reported for CO_2 and CH_4 gas concentrations at the inlet and outlet of the BFs are the mean of triplicate measurements. Error bars represent standard deviations from triplicates. The statistical data analysis was performed using OriginPro 8.5 (OriginLab Corporation, USA). The occurrence of significant differences among biofilter performance parameters was analysed by a one-way analysis of variance (ANOVA) and a Tukey test. A Levene test was also applied to study homocedasticity. Differences were considered significant at $P \leq 0.05$. Vegan and stats packages in R (R Core Team, 2014; Oksanen et al., 2015) were applied for the statistical analysis of the metagenomics data.

3 Results and Discussion

3.1 Effect of the feast-famine strategies on CH_4 abatement performance and pressure drop evolution in BFs

The performance of the three BFs – in particular that of BFs 2 and 3 – was initially characterized by unstable ECs (6.8 ± 3.2 g m^{-3} h^{-1}, corresponding to REs of 5.3 ± 2.0 %), likely due to the heterogeneous distribution and weak attachment of the inoculated biomass along the whole packed bed within Stage A (Fig. 2). This hypothesis is in accordance with the occurrence of initially high pressure drops in the BFs (Table 2). On the other hand, PCO_2 remained at 9.9 ± 3.1 g m^{-3} h^{-1} in the three units, which resulted in R_{CO2} ranging from 24.3 to 83.5 %. This corresponded to Y_{CO2} values ranging from 0.7 to 2.3 gCO_2 gCH_4^{-1} during Stage A (Fig. 2, Table 2). In this regard, these relatively low R_{CO2} and Y_{CO2} values have been previously observed during the start-up of methanotrophic biotrickling filters (BTFs) and are typically attributed to the preferential formation of biomass through anabolism (Estrada et al., 2014; Lebrero et al., 2015).

The EC and PCO_2 in the control BF steadily increased at the beginning of Stage B up to values of 11.3 ± 1.2 and 19.7 ± 2.6 g m^{-3} h^{-1}, respectively (R_{CO2} of 64.7 ± 14.6 %), later on stabilizing at 6.4 ± 2.6 and 14.3 ± 2.1 g m^{-3} h^{-1}, respectively (R_{CO2} of 76.3 ± 17.8 %), from day 82 onwards (Fig. 2A). Likewise, CH_4 biodegradation performance gradually increased in BFs 2 and 3 following the implementation of the feast-famine strategies, thus achieving a pseudo-steady state from day 75 onwards. During each feast period, steady increases in EC were consistently observed (average R_{CO2} values of 71.8 ± 12.6 %) (Fig. 2B, C;

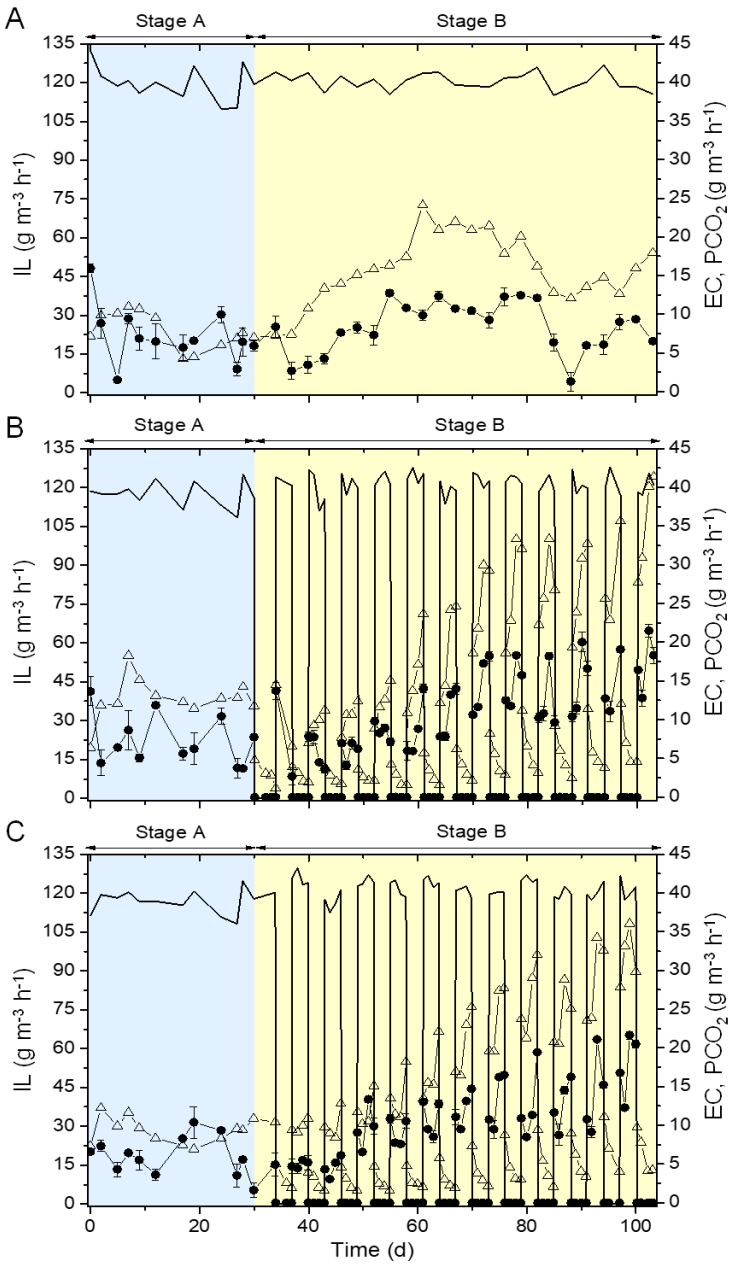

Figure 2. Time course of the IL (continuous line), EC (●) and PCO_2 (Δ) in BF 1 (A), BF 2 (B) and BF 3 (C) during operational stages A and B.

Table 2). These empirical findings demonstrate that short-term starvation periods, which could represent weekend shutdowns in many industrial facilities, could even boost the performance of CH_4-treating biofilters in the early stages of operation, as previously reported for toluene abatement biotechnologies (Wright et al., 2005; Álvarez-Hornos et al., 2008; Álvarez-Hornos et al., 2011). Despite the microbial community of BFs 2 and 3 exhibited maximum activity by the end of the feast cycles (48-72 h), it must be highlighted that these alternate units were able to recover the methane-oxidizing activity in only 1.5 h after CH_4 resumption. This was likely due to the enrichment of methanotrophic communities acclimated to sequential feast-famine scenarios (Fig. 2B, C). To

Table 2. Performance of BFs 1, 2 and 3 along the different operational stages.

Stage	Average/Maximum EC ($g\ m^{-3}\ h^{-1}$)			Average/Maximum RE (%)			Maximum R_{CO2} (%)			Maximum activity time (h)[a]		Average/Maximum pressure drop ($Pa\ m^{-1}$)		
	BF 1	BF 2	BF 3	BF 1	BF 2	BF 3	BF 1	BF 2	BF 3	BF 2	BF 3	BF 1	BF 2	BF 3
A	6.4/10.0	6.6/11.9	6.0/10.4	5.2/8.7	5.4/9.2	5.0/8.2	56.8	79.5	83.5	-	-	5.1/15.0	29.2/72.0	19.7/87.0
B	8.3/12.7	11.3/21.5	11.0/21.6	8.8/10.6	10.5/16.4	9.8/17.4	113.9	113.3	106.7	48-72	48-72	7.2/12.0	5.1/9.0	3.8/9.0
C	10.9/17.4	14.0/23.3	14.2/20.7	8.6/13.1	11.2/18.8	11.5/16.7	107.5	130.7	124.9	48	48	9.5/54.0	4.3/12.0	4.9/9.0
D	12.3/18.9	13.5/27.8	15.5/23.4	9.6/14.7	11.7/21.4	13.7/18.9	114.1	171.4	139.0	1.5-19	1.5-19	14.4/25.5	5.6/9.0	4.9/9.0

[a] Only applicable to units subjected to feast-famine cycles. Maximum activity time is referred to the time required to recover the maximum methane-oxidizing activity within each feast cycle.

the best of the authors' knowledge, this recovery period was shorter than those of previous works on CH_4 biotechnologies (Ferdowsi et al., 2016; Ferdowsi et al., 2017) and is one of the shortest recovery periods so far reported in biotechnologies subjected to starvation cycles, which confirms the high robustness of biofilters operated under feast-famine regimes (Cox and Deshusses, 2002; Álvarez-Hornos et al., 2008; Cheng et al., 2016). However, it must be highlighted that an instantaneous recovery of the microbial activity has been reported for less recalcitrant pollutants such as isopropanol (San-Valero et al., 2013). Finally, the pressure drop recorded during Stage B in the control unit remained slightly higher than those in the alternate units (Table 2).

The reduction of the irrigation rate during Stage C resulted in an improvement in the CH_4 biodegradation performance of the control unit, where EC and PCO_2 increased up to steady values of 10.9 ± 2.0 and 27.2 ± 1.1 g m^{-3} h^{-1}, respectively (R_{CO2} of 75.6 ± 11.4 %), from day 130 onwards (Fig. 3A). This enhancement could be attributed to a higher CH_4 mass transfer rate as a result of the thinner stagnant liquid phase mediated by the lower irrigation rate here applied. On the other hand, the ECs and PCO_2 recorded in the alternate units during the feast periods fluctuated within the ranges previously observed during Stage B (average R_{CO2} values of 81.8 ± 18.3 and 80.1 ± 23.1 % for BF 2 and 3, respectively) (Fig. 3B, C). It must be stressed that the maximum R_{CO2} values recorded in BFs 2 and 3 during Stage C were ~15 and 20 % higher than the maximum R_{CO2} observed in BF 1, likely due to the more active endogenous metabolism during the famine periods (Table 2). Though no significant differences in terms of EC and PCO_2 were found in the alternate units compared to the previous stage despite the higher length of the feast/famine cycles, it must be noticed that the time required to achieve maximum activity during feast conditions was significantly reduced to 48 h (Table 2). A slightly higher average pressure drop was observed in BF 1 (9.5 ± 2.9 Pa m^{-1}) compared to previous Stages A and B and to the average pressure drops in the alternate units (4.7 ± 2.9 Pa m^{-1}). In fact, the gradually different pressure drops here recorded for the control and alternate units were likely due to the increasingly higher biomass concentration in BF 1, which agreed with the visual observations of the BFs (Fig. S1).

Finally, the performance of BF 1 remained stable during Stage D, with ECs and PCO_2 of 12.3 ± 3.1 and 27.9 ± 3.7 g m^{-3} h^{-1}, respectively, which accounted for R_{CO2} values of 86.7 ± 17.7

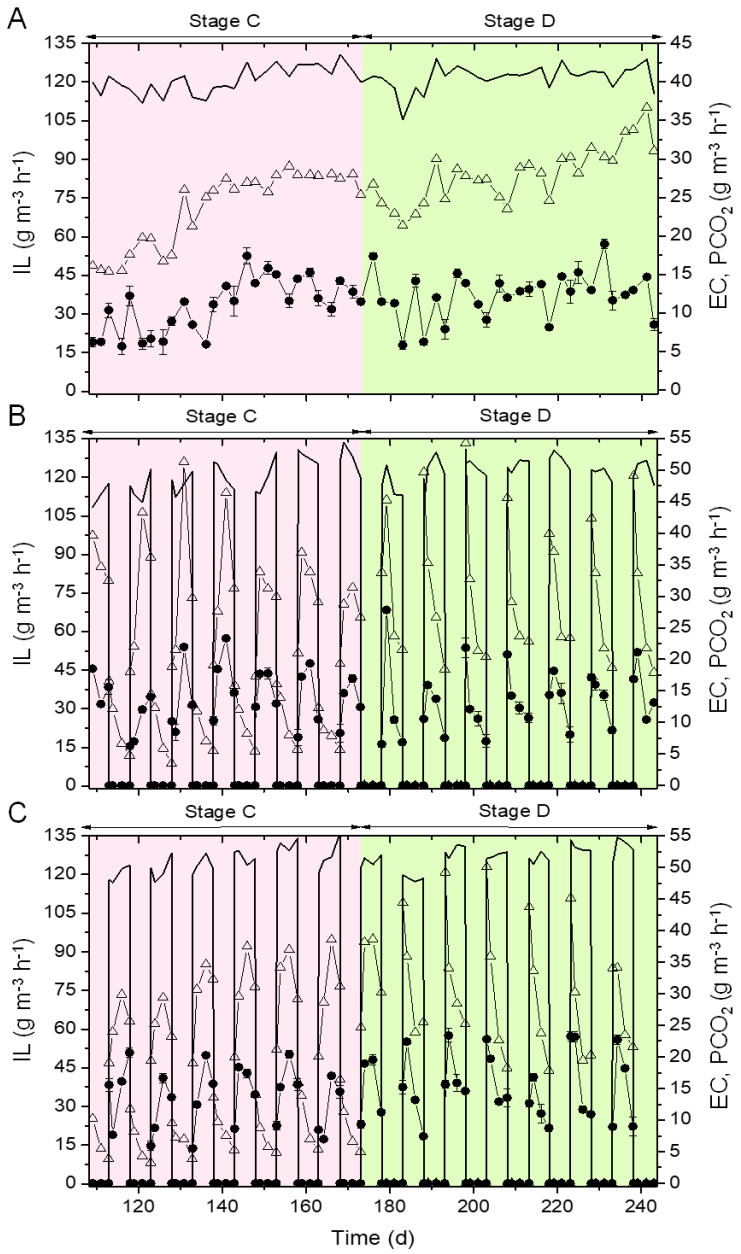

Figure 3. Time course of the IL (continuous line), EC (●) and PCO_2 (Δ) in BF 1 (A), BF 2 (B) and BF 3 (C) during operational stages C and D.

% (Y_{CO2} of 2.4 ± 0.5) (Fig. 3A, Table 2). On the other hand, despite the absence of air during the famine periods in this stage, maximum EC and PCO_2 values were recorded in BFs 2 and 3 under pseudo-steady state conditions, respectively (average R_{CO2} value of 83.8 ± 23.6 %). Process performance during feast periods was not significantly different to the one recorded in Stages B and C, since average REs remained at 13 % in both BFs (Fig. 3B, C). In addition, the time required to achieve maximum activity was sharply decreased to 1.5 h in several of the feast-famine cycles in this last operational stage, which can be attributed to the acclimated to sequential feast-famine scenarios of a community adapted to this operational strategy. In

contrast, previous works on CH_4 biofilters subjected to starvation episodes fully recovered their biodegradation performance after a minimum of 5 days (Ferdowsi et al., 2016; Ferdowsi et al., 2017). In addition, Cox and Deshusses (2002) found that at least 10 h of re-acclimation were needed to reach maximum activity in a toluene-degrading BF after a similar starvation episode (5 days of carbon, air and irrigation deprivation), possibly due to a lack of adaptation of the microbial community to those process fluctuations. In addition, it is noteworthy that the CO_2 production pattern after CH_4 resumption significantly changed compared to the one observed in earlier stages, the maximum R_{CO2} increasing by 20-50% in BFs 2 and 3 compared to that recorded in BF 1 (Fig. 3B, C; Table 2). This fact can be explained by the higher stimulation of the endogenous metabolism when neither air nor irrigation were applied, which promoted the utilization of cell lysis products, exopolysaccharides and/or by-products of CH_4 biodegradation (Cox and Deshusses, 2002; Dorado et al., 2012). Finally, the pressure drop in BFs 2 and 3 remained negligible at 5.1 ± 2.9 Pa m^{-1}, increasing up to 14.4 ± 4.4 Pa m^{-1} in BF 1 during Stage D (Table 2). The good reproducibility of the biofilters operated was confirmed by the results obtained in the alternate units (which indeed constituted a test in duplicate), not only from an engineering point of view (identical operational patterns), but also from a microbiological point of view (≥ 98% similarity between the communities, see the discussion below on Figures S6-S8).

The average pressure drops here reported in the BFs along Stages A-D were similar to those obtained in CH_4-oxidizing BTFs operated during shorter operational times, and were far below the average pressure drops typically recorded during waste gas biofiltration. Nevertheless, the average pressure drop recorded in BF 1 along the entire experiment (10.2 Pa m^{-1}) exceeded by 108 and 126 % the average pressure drops obtained in BFs 2 and 3. This fact can be attributed to the higher concentration of biomass accumulated in the control unit (8.9 g L^{-1} of packed bed) compared to the values of 5.1 and 4.0 g L^{-1} of packed bed found in BF 2 and 3, respectively (Fig. 4). At this point it must be highlighted that the 3-fold diluted centrate used in the present study exhibited average total organic carbon (TOC) concentrations of 16.3 ± 12.3 mg L^{-1} (Table S1). Despite BOD concentration was not monitored, this parameter is usually 1.5 times higher than the TOC concentration, which implies maximum BOD values < 25 mgO_2 L^{-1} in the worst-case scenario. Indeed, the total biomass accumulated in BF 1 (~21 g of biomass) matched the

total biomass accumulated in the alternate units when considered as a sole unit (11.7 + 9.2 = 20.9 g of biomass; < 1 % error), which demonstrated that the biodegradable TOC of the centrate did not entail an extra biomass formation since all BFs were irrigated at the same rate in Stages A-C. These results are in agreement with the fact that methanotrophic bacteria do not consume any additional organic carbon when CH_4 is available (López et al., 2014). In this context, the occurrence of clogging events during biofiltration, and thus the extra costs associated to compressor operation and packing material washing or replacement, is mainly determined by biofilter design. At full- scale, the increase in investment costs derived from the use of two alternate units operated under a feast-famine regime might be outbalanced by i) the higher ECs obtained, which would entail lower individual biofilter volumes, ii) the lower total operating costs mediated by the energy savings and iii) the higher lifespan of the packed bed (Estrada et al., 2012). The scaled-down study here conducted demonstrated the potential of feast-famine strategies to support a superior biofiltration performance in industrial biofilters under long term operation. However, it must be stressed that the maximum REs here obtained remained below 20 % and additional optimization of the biofiltration process is required to achieve appropriate removals of 60-90 % as previously reported during CH_4 biofiltration (Lebrero et al. 2016).

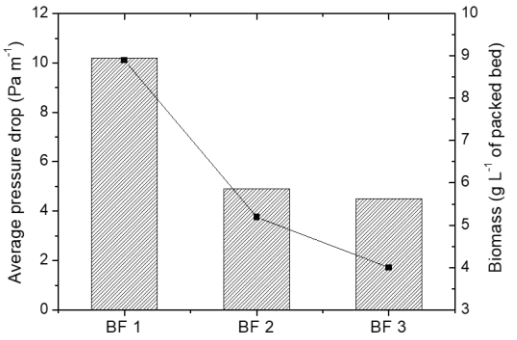

Figure 4. Average pressure drop along the entire experiment (▨) and biomass concentration at the end of the experiment (■) in BFs 1, 2 and 3.

3.2 Potential of the technology for nitrogen removal

No significant differences in nitrification activity were recorded among the BFs during Stage A, which was characterized by average NO_2^- and NO_3^- concentrations in the leachates of 38.7 ± 8.3 and 15.6 ± 4.7 mg L^{-1}, respectively, and N-NH_4^+ REs of 20.5 ± 5.5 % (Fig. 5). From Stage A onwards, NO_2^- concentrations decreased in all units to negligible values by the end of Stage D (1.2 ± 1.0 mg L^{-1}), while NO_3^- concentrations reached maximum values of ~40 mg L^{-1} in BF 1 during Stage B and ~60 mg L^{-1} in BFs 2 and 3 during Stage C. However, NO_3^- concentration unexpectedly decreased by the end of Stage D to average values of 2.0 ± 1.8 mg L^{-1} regardless of the unit evaluated (Fig. 5). These findings could be attributed to a more efficient N

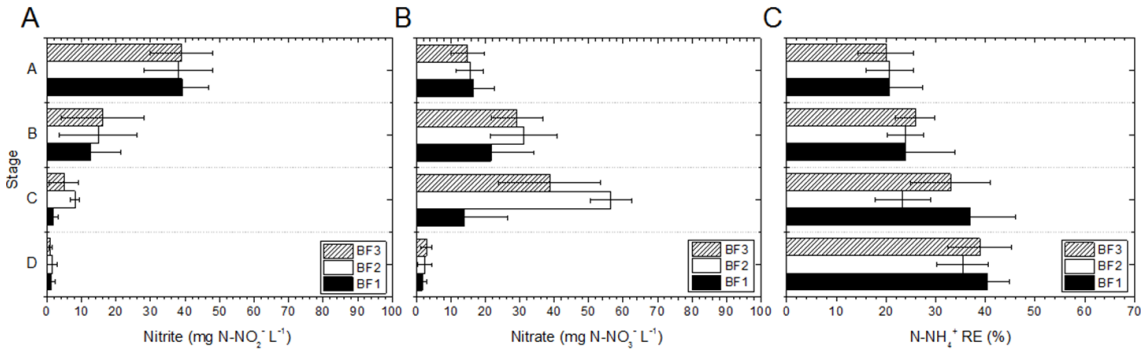

Figure 5. Nitrite (A) and nitrate (B) concentrations, and N-NH_4^+ RE (C), in BF 1 (■), BF 2 (□) and BF 3 (▨) during the four operational stages evaluated. Horizontal bars represent standard deviation from replicates during steady state.

assimilation within the biofilm due to the increasing biomass concentration over time in all units. In this context, N-NH_4^+ REs steadily increased up to 38.8 ± 5.3 % from Stage A onwards and regardless of the unit evaluated, which agreed well with the TN REs of 34.3 ± 7.8 % recorded during Stage D. N-NH_4^+ REs of ~30 % have been previously reported for CH_4-treating biofilters under similar NH_4^+ feeding rates (Veillette et al., 2011). Moreover, maximum P-PO_4^{3-} REs of 30-35 % were recorded within BFs 1-3 regardless of the unit and the stage evaluated. Therefore, the use of centrate to irrigate inorganic biofilters devoted to CH_4 abatement in WWTPs was proven to be a feasible alternative to partially mitigate the eutrophication potential of these effluents.

3.3 Richness and diversity of the active microbial communities

A total of 195796 initial bacterial 16S rRNA sequence reads were generated by the MiSeq Illumina platform, from which 146741 effective reads (12034, 45658, 50004 and 39045 for samples I, 1, 2 and 3, respectively) passed the quality and taxonomic cutoff. The rarefaction curve at a genus level for sample I suggested the occurrence of additional diversity not accounted by the MiSeq-based sequencing, since the curve did not tend toward saturation. In contrast, bacterial libraries from samples 1, 2 and 3 effectively represented the diversity of the active microbial communities based on the plateau reached by their rarefaction curves (Fig. S2). These differences were also noticeable in the diversity found among the samples, as both Simpson and Shannon indexes were significantly higher for sample I than for the rest of samples. For instance, while the Shannon index for samples 1-3 ranged from 2.77 to 3.09, it accounted for 3.84 in sample I (Table S3). This observation can be attributed to the gradual enrichment and specialization of the methanotrophic community present in the BFs, which resulted in a less diverse bacterial population by the end of

operation in the three units. A similar decrease in diversity indexes from inoculation has been reported for methanotrophic enrichments within only 5 weeks, with final Shannon indexes even lower than those here reported (Oshkin et al., 2015). Interestingly, the microbial diversity found in the control BF (2.77) was slightly lower than that recorded in the alternate units (2.92 and 3.09 in BFs 2 and 3, respectively), likely due to the enhanced cell lysis and heterotrophic growth mediated by the starvation events here applied (Table S3). In this sense, this higher richness possibly associated to methanotroph-accompanying heterotrophs could explain the superior methane oxidation recorded in the alternate units (Ho et al., 2014).

3.4 Effect of the feast-famine strategies on the structure of the active microbial communities

Effective bacterial sequences from the active communities of the samples were affiliated to a total of 38 phyla, 76 classes, 135 orders, 247 families and 752 genera. Of them, the most dominant phyla (≥ 0.5 % abundance in at least one sample) were 14: *Acidobacteria*, *Actinobacteria*, *Armatimonadetes*, *Bacteroidetes*, *Candidate division WPS-1*, *Candidatus Saccharibacteria*, *Chloroflexi*, *Firmicutes*, *Hydrogenedentes*, *Ignavibacteriae*, *Planctomycetes*, *Proteobacteria*, *Spyrochaetes*, and *Verrucomicrobia*. Dominant phyla in terms of activity in sample I were *Proteobacteria* (55.7 %), *Bacteroidetes* (28.5 %), *Firmicutes* (3.5 %), *Verrucomicrobia* (2.2 %) and *Planctomycetes* (2.0 %), which are phyla commonly found in WWTPs' activated sludge at these abundances (Zhang et al. 2012; Da Silva et al. 2015). The activity of *α*-, *β*-, *γ*-, *δ*-, and *ε*-*Proteobacteria* within the *Proteobacteria* phylum was evenly represented (Fig. S3), though the one of methanotrophs was almost negligible (0.12 %) (Table 3).

Continuous CH_4 feeding in BF 1 resulted in both a significant increase in the activity of *Verrucomicrobia* phylum (19.4 %) and a decrease of *Proteobacteria* (46.2 %) phylum by the end of operation, while the activity of *Bacteroidetes* (29.6 %) phylum remained roughly stable (Fig. S4). In BF 1, *Chitinophagaceae* was the most representative family within *Bacteroidetes*, and *Terrimonas* the most active genus (78.0 % abundance in *Bacteroidetes*). *Terrimonas* genus includes aerobic heterotrophic species involved in nitrate reduction and has been previously found in nitritation bioreactors (Zhang et al., 2015; Rodríguez-Sánchez et al., 2016). On the other hand, *Verrumicrobiaceae* was the most active family within *Verrucomicrobia*, *Prosthecobacter*

Table 3. 16S rRNA effective gene sequence reads obtained for methanotrophic genera from cDNA samples I, 1, 2 and 3.

Methanotrophic genera (type)	Number of reads (%)			
	Sample I	Sample 1	Sample 2	Sample 3
Methylomonas (type I)	0 (0.00)	92 (0.20)	17266 (34.53)	11249 (28.81)
Methylosarcina (type I)	0 (0.00)	5506 (12.06)	319 (0.64)	508 (1.30)
Methylobacter (type I)	0 (0.00)	17 (0.04)	41 (0.08)	147 (0.38)
Methylomarinum (type I)	1 (0.01)	0 (0.00)	73 (0.14)	52 (0.13)
Methylosoma (type I)	0 (0.00)	1 (<0.01)	34 (0.07)	32 (0.08)
Methylococcus (type I/X[a])	2 (0.02)	3 (0.01)	31 (0.06)	10 (0.03)
Methylomicrobium (type I)	0 (0.00)	6 (0.01)	2 (<0.01)	1 (<0.01)
Methylosphaera (type I)	1 (0.01)	0 (0.00)	1 (<0.01)	2 (0.01)
Methylovulum (type I)	0 (0.00)	1 (<0.01)	0 (0.00)	1 (<0.01)
Methylosinus (type II)	2 (0.02)	4182 (9.16)	50 (0.10)	103 (0.26)
Methylocystis (type II)	9 (0.07)	128 (0.28)	915 (1.83)	1851 (4.74)

[a]*Methylococcus*, often accommodated within the type X (subset of type I methanotrophs), was grossly considered as type I for further estimations.

genus exhibiting the highest abundance (80.4 % abundance in *Verrucomicrobia*) (Fig. 6, Fig. 7). *Prosthecobacter* are heterotrophic organisms often considered as oligotrophic bacteria due to their preference for low-nutrient environments (Wang et al. 2012). In this sense, the higher biomass concentration recorded in BF 1 could explain the faster nutrient consumption, and thus, the eventual macro- and/or micronutrients limitations supporting the enrichment of *Prosthecobacter* in the unit under continuous CH_4 supply (Fig. S5). However, the role of nutrients on members of this genus needs further research to fully understand the implications of their presence in methanotrophic cultures. Moreover, both *γ*- and *α-Proteobacteria* (where type I and II methanotrophs are taxonomically clustered, respectively) actively dominated the phylum *Proteobacteria* with similar abundances (39.9 and 37.2 %, respectively) (Fig. S4). In this context, *Methylocystaceae*, which represented 51.3 % of *α-Proteobacteria* activity, mainly included the genus *Methylosinus* (9.2 % in the

whole population), while *Methylococcaceae* accounted for 71.7 % of the activity within *γ-Proteobacteria* and was mainly composed of the genus *Methylosarcina* (12.1 % in the whole population) (Fig. 6, Fig. 7). In brief, the active community of BF 1 was composed of 21.2 % methanotrophs, with a type I/II ratio of 1.31 (Table 3). Most methanotrophic genera here identified have been previously found in CH_4-degrading bioreactors, though type I methanotrophs such as *Methylomonas*, *Methylosarcina* and *Methylobacter* were clearly the most abundant in those communities (López et al., 2014; Xing et al., 2017). In contrast, type II methanotrophs are often encountered in a minor proportion in CH_4 abatement systems, since their enrichment is typically achieved only under low-nutrient conditions, lower pH and high CH_4/O_2 ratios (Graham et al., 1993; Pieja et al., 2011). Hence, the similar activity share of type I and II methanotrophs in BF 1 reinforced the aforementioned hypothesis of an eventual occurrence of nutrient limitations and could be likely due to a limited O_2 diffusion within the thick biofilm of the control BF according to previous studies (Pfluger et al. 2011). Less active OTUs within the families *Xanthomonadaceae*, *Methylophilaceae* and *Hyphomicrobiaceae* were found in BF 1, whose role has been previously associated to both heterotrophic opportunism and methylotrophic activity (Fig. S4, Fig. 6, Fig. 7) (López et al., 2014; Rodríguez-Sánchez et al., 2016).

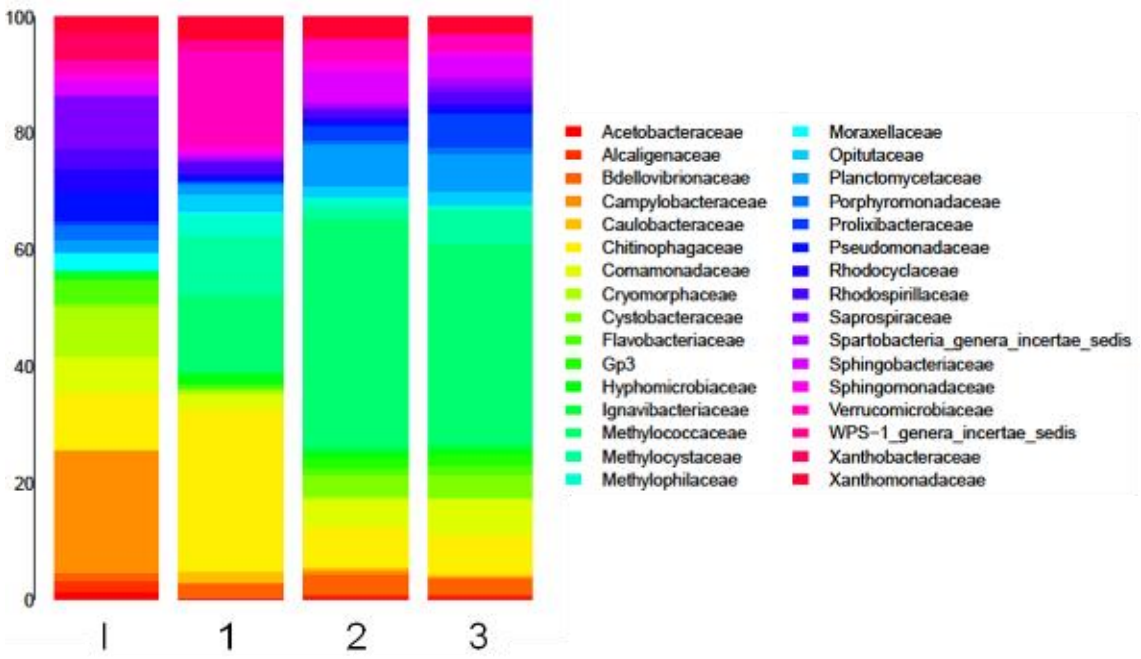

Figure 6. Community composition at a family level across samples. The abundance is presented in terms of percentage in total effective bacterial sequences in a sample, classified using RDP Classifier. Taxa represented occurred at a threshold abundance >0.5 % in at least one sample.

Interestingly, ammonia-oxidizing bacteria (AOB) and nitrite-oxidizing bacteria (NOB) within *Nitrosomonadaceae* (*Nitrosospira* and *Nitrosomonas* genera) and *Bradyrhizobiaceae* (*Nitrobacter* genus), respectively, were detected, though their abundances in terms of activity within all samples did not surpass the minimum cutoff abundance (0.5 %), probably as a result of the significantly lower NH_4^+ load compared to the CH_4 one applied, and the inherently low biomass yields of nitrifiers.

Biofilter operation under feast-famine cycles led to a shift in the active community structure of BFs 2 and 3, which behaved as proper replicates and exhibited a similarity ≥98 % through dendrogram clustering (Fig. S6). The most active phyla in samples 2 and 3 were *Proteobacteria* (62.8 ± 2.9 %), *Bacteroidetes* (18.4 ± 1.9 %), *Planctomycetes* (6.8 ± 0.3 %) and *Verrucomicrobia* (6.2 ± 0.1 %) (Fig. S7, S8). *Planctomycetaceae* was the most active family within *Planctomycetes* (88.5 ± 12.0 %) and included genera such as *Pirellula*, *Planctopirus* and *Schlesneria* (Fig. 6, Fig. 7). The phylum *Planctomycetes* has been previously found in both lab-scale nitritation/anammox reactors, some of the genera within the phylum acting merely as heterotrophic aerobes/anaerobes and others as annamox organisms (Kirkpatrick et al., 2006; Ye et al., 2011). In our particular study, the periodic shutdowns of both CH_4 and air supply in the alternate units likely promoted a higher cell lysis and eventual exposure to anoxic conditions, which might have favoured the activity of *Planctomycetes* and explain the low NO_3^- and NO_2^- concentrations by the end of stage D (Fig. S5). Moreover, the phylum *Verrucomicrobia* was mainly composed of the family *Verrucomicrobiaceae* (47.5 ± 12.0 %), which comprised the genus *Prosthecobacter* (99.0 % abundance in *Verrumicrobiaceae*). Despite the lower activity of *Bacteroidetes* in the alternate units, this phylum exhibited a higher family diversity compared to the control unit (Fig. 6). Interestingly, the phylum *Proteobacteria* was mainly dominated by *γ-Proteobacteria* (59.0 ± 4.2 %) in samples 2 and 3, *α*-, *β*- and *δ*-*Proteobacteria* thus presenting at least 4 times lower activities (Fig. S7, S8). The family *Methylococcaceae* dominated *γ-Proteobacteria* phylum and accounted for 33.1 ± 3.4 % of the whole active community of both BFs. This taxon was mainly composed by type I methanotrophs belonging to the genus *Methylomonas* (95.5 ± 2.1 %) and, in a lesser extent, to *Methylosarcina* (3.0 ± 1.7 %) (Table 3, Fig. 6, Fig. 7). In contrast, the activity of *Methylocystaceae* family was significantly lower (3.5 ± 2.2 % in the

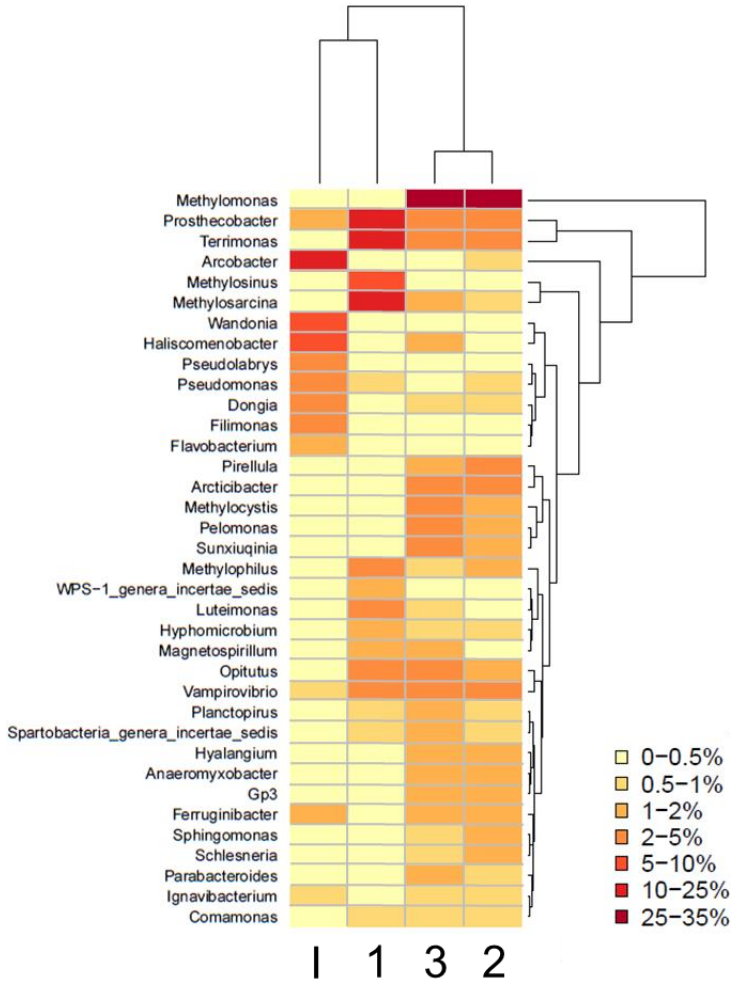

Figure 7. Heat map of major genera across samples. The represented taxa occurred at a threshold abundance >0.5 % in at least one sample. The color intensity in each panel shows the share of a genus within a sample.

whole active community) and was formed by the type II methanotrophic genera *Methylocystis* (94.3 ± 0.0 %) and *Methylosinus* (5.2 ± 0.0 %) (Table 3, Fig. 6, Fig. 7). Hence, methanotrophs in BFs 2 and 3 represented a higher proportion in the active community (35.6 ± 1.1 %) compared to the control unit, with an average type I/II ratio of 9.5, which was nearly 7.5 times higher than that recorded in BF 1. This finding could be attributed to the higher affinity for CH_4 of type I methanotrophs, which boosted their preferential growth over type II methanotrophs after CH_4 supply resumption at the low CH_4 concentrations here applied (López et al., 2014). In this regard, Cai et al. (2016) demonstrated the higher activity and preferential growth of type I methanotrophs in scenarios of intermittent CH_4 flush-feedings compared to type II methanotrophs in CH_4-amended microcosms, with the highest CH_4-oxidizing activities associated to *Methylosarcina* genus among type I, and *Methylocystis* genus among type II methanotrophs. In our

particular study, the genus *Methylomonas* and, in a lesser extent *Methylocystis*, were preferentially active under feast-famine operation (Fig 7).

4 Conclusions

Multiple feast-famine strategies were systematically evaluated in alternate CH_4-treating BFs under long-term operation by comparison with a standard continuous BF. The key conclusions are summarized below:

- BFs operated under feast-famine regimes underwent a rapid recovery (< 1.5 h) of CH_4 EC when they were subjected to C starvation periods of 3 and 5 days, under low irrigation frequencies (78 mL $L^{-1}_{packed\ bed}$ d^{-1}) and air deprivation. Unexpectedly, short-term starvations boosted CH_4 ECs during the early stages of operation, while more severe famine conditions (air deprivation and limited nutrient supply) led to the maximum CH_4 EC (27.8 g m^{-3} h^{-1}) and mineralization values (171.4 %), likely due to a higher stimulation of the endogenous metabolism of the microbial communities.
- The CH_4 ECs of the alternate units were on average 27.2 % higher than those for the continuous BF.
- The gradual acclimation of the communities to these feast-famine cycles resulted in shorter periods to reach maximum microbial activity (< 19 h at the end of the experiment).
- Feast-famine BFs exhibited a significantly lower biomass accumulation and therefore, lower average pressure drops, which would boost the implementation of CH_4 biofiltration at full-scale.
- *Bacteroidetes* and *Verrucomicrobia* families were more active under continuous CH_4 feeding, whereas *Proteobacteria* and *Planctomycetes* were under feast-famine regimes. Type I and type II methanotrophs belonging to the genera *Methylosarcina* and *Methylosinus* equally dominated the active community of the continuous BF, while the type I *Methylomonas* outcompeted the rest of microbial partners in the feast-famine BFs, likely due to its higher affinity for CH_4.

Acknowledgements

This research was supported by the Spanish Ministry of Economy and Competitiveness (CTM2015-70442-R project and BES-2013-063922 contract), the European Union through the FEDER Funding Program and the Regional Government of Castilla y León (UIC71). The authors thank Llucía Martínez, Giuseppe D'Auria and David Pérez from FISABIO for their valuable practical assistance in the laboratory and during manuscript preparation.

References

Álvarez-Hornos, F.J., Gabaldón, C., Martínez-Soria, V., Marzal, P., Penya-Roja, J.M., 2008. Biofiltration of toluene in the absence and the presence of ethyl acetate under continuous and intermittent loading. Journal of Chemical Technology and Biotechnology 83(5), 643-653. DOI: 10.1002/jctb.1843.

Álvarez-Hornos, F.J., Izquierdo, M., Martínez-Soria, V., Penya-roja, J.M., Sempere, F., Gabaldón C., 2011. Influence of ground tire rubber on the transient loading response of a peat biofilter. Journal of Environmental Management 92, 1978-1985. DOI: 10.1016/j.jenvman.2011.03.045.

APHA, 2005. Standard methods for the examination of water and wastewater, 21st ed. American Public Health Association, Whasington, D.C.

Aronesty, E., 2011. ea-utils: Command-line tools for processing biological sequencing data. https://github.com/ExpressionAnalysis/ea-utils (accessed 01.02.17).

Blazewicz, S.J., Barnard, R.L., Daly, R.A., Firestone, M.K., 2013. Evaluating rRNA as an indicator of microbial activity in environmental communities: limitations and uses. The ISME Journal 7(11), 2061-2068. DOI: 10.1038/ismej.2013.102.

Cai, Y., Zheng, Y., Bodelier, P.L.E., Conrad, R., Jia, Z., 2016. Conventional methanotrophs are responsible for atmospheric methane oxidation in paddy soils. Nature Communications 7:11728. DOI: 10.1038/ncomms11728.

Cheng, Z., Lu, L., Kennes, C., Yu, J., Chen, J., 2016. Treatment of gaseous toluene in three biofilters inoculated with fungi/bacteria: Microbial analysis, performance and starvation response. Journal of Hazardous Materials 303, 83-93. DOI: 10.1016/j.jhazmat.2015.10.017.

Cole, J.R., Chai, B., Farris, R.J., Wang, Q., Kulam, S.A., McGarrell, D.M., Garrity, G.M., Tiedje, J.M., 2005. The ribosomal database project (RDP-II): sequences and tools for high-throughput rRNA analysis. Nucleic Acids Research 33, D294-D296. DOI: 10.1093/nar/gki038.

Covarrubias-García, I., Aizpuru, A., Arriaga, S., 2017. Effect of the continuous addition of ozone on biomass clogging control in a biofilter treating ethyl acetate vapors. Science of the Total Environment 584-585, 469-475. DOI: 10.1016/j.scitotenv.2017.01.031.

Cox, H.H.J., Deshusses, M.A., 2002. Effect of starvation on the performance and re-acclimation of biotrickling filters for air pollution control. Environmental

Science and Technology 36, 3069-3073. DOI: 10.1021/es015693d.

Da Silva, M.L., Cantão, M.E., Mezzari, M.P., Ma, J., Nossa, C.W., 2015. Assessment of bacterial and archaeal community structure in swine wastewater treatment processes. Microbial Ecology 70(1), 77-87. DOI: 10.1007/s00248-014-0537-8.

Devinny, J.S., Ramesh, J., 2005. A phenomenological review of biofilter models. Chemical Engineering Journal 113(2-3), 187-196. DOI: 10.1016/j.cej.2005.03.005.

Dorado, A.D., Baeza, J.A., Lafuente, J., Gabriel, D., Gamisans, X., 2012. Biomass accumulation in a biofilter treating toluene at high loads – Part 1: Experimental performance from inoculation to clogging. Chemical Engineering Journal 209, 661-669. DOI: 10.1016/j.cej.2012.08.018.

Edgar, R.C., 2010. Search and clustering orders of magnitude faster than BLAST. Bioinformatics 26(19), 2460-2461. DOI: 10.1093/bioinformatics/btq461.

Environmental Protection Agency, 2016. Inventory of US Greenhouse Gas Emissions and Sinks: 1990 - 2014. http://epa.gov/climatechange/ghgemissions/usinventoryreport.html (accessed 12.08.16).

Estrada, J.M., Kraakman, N.J.R., Lebrero, R., Muñoz, R., 2012. A sensitivity analysis of process design parameters, commodity prices and robustness on the economics of odour abatement technologies. Biotechnology Advances 30, 1354-1363. doi:10.1016/j.biotechadv.2012.02.010.

Estrada, J.M., Quijano, G., Lebrero, R., Muñoz, R., 2013. Step-feed biofiltration: A low-cost alternative configuration for off-gas treatment. Water Research 47(13), 4312-4321. DOI: 10.1016/j.watres.2013.05.007.

Estrada, J. M., Lebrero, R., Quijano, G., Pérez, R., Figueroa-González, I., García-Encina, P. A., Muñoz, R., 2014. Methane abatement in a gas-recycling biotrickling filter: Evaluating innovative operational strategies to overcome mass transfer limitations. Chemical Engineering Journal 253, 385-393. doi:10.1016/j.cej.2014.05.053.

European Environment Agency, 2015. Annual European Union Greenhouse Gas Inventory 1990 - 2013 and Inventory Report 2015. http://www.eea.europa.eu//publications/european-union-greenhouse-gas-inventory-2015 (accessed 12.08.16).

Ferdowsi, M., Veillette, M., Avalos-Ramírez, A., Jones, J.P., Heitz, M., 2016. Performance evaluation of a methane biofilter under steady state, transient state and starvation conditions.

Water, Air, & Soil Pollution 227, 168. DOI: 10.1007/s11270-016-2838-7.

Ferdowsi, M., Avalos-Ramirez, A., Jones, J.P., Heitz, M., 2017. Methane biofiltration in the presence of ethanol vapor under steady and transient state conditions: an experimental study. Environmental Science and Pollutant Research (In Press). DOI: 10.1007/s11356-017-9634-9.

Gómez-Cuervo, S., Alfonsin, C., Hernandez, J., Feijoo, G., Moreira, M.T., Omil F., 2017. Diffuse methane emissions abatement by organic and inorganic packed biofilters: Assessment of operational and environmental indicators. Journal of Cleaner Production 143, 1191-1202. DOI: 10.1016/j.jclepro.2016.11.185.

Graham, D.W., Chaudhary, J.A., Hanson, R.S., Arnold, R.G., 1993. Factors affecting competition between type I and type II methanotrophs in two-organism, continuous-flow reactors. Microbial Ecology 25(1), 1-17. DOI: 10.1007/BF00182126.

Ho, A., de Roy, K., Thas, O., Neve, J.D., Hoefman, S., Vandamme, P., Heylen, K., Boon, N., 2014. The more, the merrier: Heterotroph richness stimulates methane methanotrophic activity. The ISME Journal 8, 1945-1948. DOI: 10.1038/ismej.2014.74.

Intergovernmental Panel on Climate Change, 2014. Fifth Assessment Report: Climate Change 2014, Synthesis Report. http://www.ipcc.ch/report/ar5/syr/ (accessed 12.08.16).

Kirkpatrick, J., Oakley, B., Fuchsman, C., Srinivasan, S., Staley, J.T., Murray, J.W., 2006. Diversity and distribution of *Planctomycetes* and related bacteria in the suboxic zone of the Black Sea. Applied and Environmental Microbiology 72(4), 3079-3083. DOI: 10.1128/AEM.72.4.3079-3083.2006.

Klindworth, A., Pruesse, E., Schweer, T., Peplies, J., Quast, C., Horn, M., Glöckner, F.O., 2013. Evaluation of general 16S ribosomal RNA gene PCR primers for classical and next-generation sequencing-based diversity studies. Nucleic Acids Research 41(1), e1. doi: 10.1093/nar/gks808.

Lebrero, R., Hernández, L., Pérez, R., Estrada, J.M., Muñoz, R., 2015. Two-liquid phase partitioning biotrickling filters for methane abatement: Exploring the potential of hydrophobic methanotrophs. Journal of Environmental Management 151, 124-131. DOI: 10.1016/j.jenvman.2014.12.016.

Lebrero, R., López, J.C., Lehtinen, I., Pérez, R., Quijano, G., Muñoz, R., 2016. Exploring the potential of fungi for methane abatement: Performance evaluation of a fungal-bacterial biofilter.

Chemosphere 144, 97-106. DOI: 10.1016/j.chemosphere.2015.08.017.

López, J.C., Quijano, G., Souza, T.S., Estrada, J.M, Lebrero, R., Muñoz, R., 2013. Biotechnologies for greenhouse gases (CH_4, N_2O, and CO_2) abatement: State of the art and challenges. Applied Microbiology and Biotechnology 97(6), 2277-2303. DOI: 10.1007/s00253-013-4734-z.

López, J.C., Quijano, G., Pérez, R., Muñoz, R., 2014. Assessing the influence of CH_4 concentration during culture enrichment on the biodegradation kinetics and population structure. Journal of Environmental Management 146, 116-123. DOI: 10.1016/j.jenvman.2014.06.026.

López, J.C., Porca, E., Collins, G., Pérez, R., Rodríguez-Alija, A., Muñoz, R., Quijano, G., 2017. Biogas-based denitrification in a biotrickling filter: Influence of nitrate concentration and hydrogen sulfide. Biotechnology and Bioengineering 114(3), 665-673. DOI: 10.1002/bit.26092.

Ménard, C., Avalos-Ramirez, A., Nikiema, J., Heitz, M., 2012. Effect of trace gases, toluene and chlorobenzene, on methane biofiltration: An experimental study. Chemical Engineering Journal 204-206, 8-15. DOI: 10.1016/j.cej.2012.07.070.

Morgan-Sagastume, F., Sleep, B.E., Allen, D.G., 2001. Effects of biomass growth on gas pressure drop in biofilters. Journal of Environmental Engineering 127(5). DOI: 10.1061/(ASCE)0733-9372(2001)127:5(388).

Oksanen, J., Blanchet, F.G., Kindt, R., Legendre, Minchin, P.R., O'Hara, R.B., Simpson, G.L., Solymos, M., Stevens, H.H., Wagner, H., 2015. Vegan: community ecology package. R package version 2.3-1. http://CRAN.R-project.org/ package=vegan (accessed 01.02.17).

Ondov, B.D., Bergman, N.H., Phillippy, A.M., 2011. Interactive metagenomic visualization in a Web browser. BMC Bioinformatics 12, 385. DOI: 10.1186/1471-2105-12-385.

Oshkin, I.Y., Beck, D.A.C., Lamb, A.E., Tchesnokova, V., Benuska, G., McTaggart, T.L., Kalyuzhnaya, M.G., Dedysh, S.N., Lidstrom M.E., Chistoserdova, L., 2015. Methane-fed microbial microcosms show differential community dynamics and pinpoint taxa involved in communal response. The ISME Journal 9, 1119-1129. DOI:10.1038/ismej.2014.203.

Pawlowska, M., 2014. Biological oxidation as a method for mitigation of LFG emission. In: Pawlowska, M. (ed) Mitigation of landfill gas emissions, 1st edn. CRC Press, Taylor & Francis Group, London, UK, pp 59-101.

Pfluger, A.R., Wu, W.M., Pieja, A.J, Wan, J., Rostkowski, K.H., Criddle, C.S.,

2011. Selection of type I and type II methanotrophic bacteria in a fluidized bed reactor under non-sterile conditions. Bioresource Technology 102, 9919-9926. DOI: 10.1016/j.biortech.2011.08.054.

Pieja, A.J., Rostkowski, K.H., Criddle, C.S., 2011. Distribution and selection of poly-3-hydroxybutyrate production capacity in methanotrophic proteobacteria. Microbial Ecology 62(3), 564-573. DOI: 10.1007/s00248-011-9873-0.

R Core Team, 2014. R: A language and environment for statistical computing. R Foundation for Statistical Computing, Vienna, Austria. http://www.R-project.org/ (accessed 1.02.17).

Rocha-Rios, J., Kraakman, N.J.R., Kleerebezem, R., van Loosdrecht, M.C.M. A capillary bioreactor to increase methane transfer and oxidation through Taylor flow formation and transfer vector addition. Chemical Engineering Journal 217, 91-98. DOI: 10.1016/j.cej.2012.11.065.

Rodríguez-Sánchez, A., Purswani, J., Lotti, T., Maza-Márquez, P., van Loosdrecht, M.C.M, Vahala, R., González-Martínez, A., 2016. Distribution and microbial community structure analysis of a single stage partial nitritation/anammox granular sludge bioreactor operating at low temperature. Environmental Technology 37(18), 2281-2291. DOI: 10.1080/09593330.2016.1147613.

Rojo, N., Muñoz, R., Gallastegui, G., Barona, A., Gurtubay, L., Prenafeta-Boldú, F.X., Elías, A., 2012. Carbon disulfide biofiltration: Influence of the accumulation of biodegradation products on biomass development. Journal of Chemical Technology and Biotechnology 87, 764-771. DOI: 10.1002/jctb.3743.

San-Valero, P., Penya-Roja, J.M., Sempere, F., Gabaldón, C., 2013. Biotrickling filtration of isopropanol under intermittent loading conditions. Bioprocess and Biosystems Engineering 36, 975-984. DOI: 10.1007/s00449-012-0833-y.

Schmieder, R., Edwards, R., 2011. Quality control and preprocessing of metagenomic
datasets. Bioinformatics 27(6), 863-864. DOI: 10.1093/bioinformatics/btr026.

Smith, F.L., Sorial, G.A., Suidan, M.T., Breen, A.W., Biswas, P., Brenner, R.C., 1996. Development of two biomass control strategies for extended, stable operation of highly efficient biofilters with high toluene loadings. Environmental Science and Technology 30(5), 1744-1751. DOI: 10.1021/es950743y.

Solomon, S., Qin, D., Manning, M., Chen, Z., Marquis, M., Averyt, K.B., Tignor, M., Miller, H.L., 2007. Climate change 2007: The physical science

basis. Contribution of working group I to the fourth assessment report of the Intergovernmental Panel on Climate Change. Cambridge University Press, Cambridge, UK and New York, NY, USA.

Veillette, M., Viens, P., Avalos-Ramirez, A., Brzezinski, R., Heitz, M., 2011. Effect of ammonium on microbial population and performance of a biofilter treating air polluted with methane. Chemical Engineering Journal 171, 1114-1123. DOI: 10.1016/j.cej.2011.05.008.

Wang, Q., Garrity, G.M., Tiedje, J.M., Cole, J.R., 2007. Naïve Bayesian classifier for rapid assignment of rRNA sequences into the new bacterial taxonomy. Applied Environmental Microbiology 73(16), 5261-5267. DOI: 10.1128/AEM.00062-07.

Wang, X., Hu, M., Xia, Y., Wen, X., Ding, K., 2012. Pyrosequencing analysis of bacterial diversity in 14 wastewater treatment systems in China. Applied and Environmental Microbiology 78(19), 7042-7047. DOI: 10.1128/AEM.01617-12.

Whittenbury, R., Phillips, K.C., Wilkinson, J.F., 1970. Enrichment, isolation and some properties of methane-utilizing bacteria. Journal of General Microbiology 61, 205-218.

Woertz, J., Van Heiningen, W., Van Eekert, M., Kraakman, N., Kinney, K., Van Groenestijn, J., 2002. Dynamic bioreactor operation: effects of packing material and mite predation on toluene removal from off-gas. Applied Microbiology and Biotechnology 58, 690-694. DOI: 10.1007/s00253-002-0944-5.

Wright, W.F., Schroeder, E.D., Chang, D.P.Y., 2005. Regular transient loading response in a vapour-phase flow-direction-switching biofilter. Journal of Environmental Engineering 131, 1649-1658. DOI: 10.1061/(ASCE)0733-9372(2005)131:12(1649).

Wübker, S.M., Laurenzis, A., Werner, U., Friedrich, C., 1997. Controlled biomass formation and kinetics of toluene degradation in a bioscrubber and in a reactor with a periodically moved trickle-bed. Biotechnology and Bioengineering 55(4), 686-692. DOI: 10.1002/(sici)1097-0290(19970820)55:43.0.co;2-a.

Xing, Z.L, Zhao, T.T, Gao, Y.H., Yang, X., Liu, S., Peng, X.Y., 2017. Methane oxidation in a landfill cover soil reactor: Changing of kinetic parameters and microorganism community structure. Journal of Environmental Science and Health Part A 52(3), 254-264. DOI: 10.1080/10934529.2016.1253394.

Ye, L., Shao, M.F., Zhang, T., Tong, A.H.Y., Lok, S., 2011. Analysis of the bacterial community in a laboratory-scale nitrification reactor and a wastewater treatment plant by 454-

pyrosequencing. Water Research 45, 4390-4398. DOI:10.1016/j.watres.2011.05.028.

Zhang, P., Shen, Y., Guo, J.S., Li, C., Wang, H., Chen, Y.P., Yan, P., Yang, J.X., Fang, F., 2015. Extracellular protein analysis of activated sludge and their functions in wastewater treatment plant by shotgun proteomics. Scientific Reports 5, 12041. DOI: 10.1038/srep12041.

Zhang, T., Shao, M.F., Ye, L., 2012. 454 Pyrosequencing reveals bacterial diversity of activated sludge from 14 sewage treatment plants. The ISME Journal 6, 1137-1147. DOI: 10.1038/ismej.2011.188.

Feast-famine biofilter operation for methane mitigation

*Juan C. López, Laura Merchán, Raquel Lebrero, Raúl Muñoz**

Department of Chemical Engineering and Environmental Technology, University of Valladolid, Dr. Mergelina, s/n, 47011, Valladolid, Spain.

*Corresponding author: mutora@iq.uva.es, Tel. +34 983186424, Fax: +34 983423013.

Supporting Information Section

containing 12 pages, with 8 figures and 3 tables.

Materials and methods

Chemicals and nutrient solution

Table S1. Physical/chemical characteristics of the 3-fold diluted centrate supplemented with SO_4^{2-} used during the present study.

TOC (mg L^{-1})	IC (mg L^{-1})	TN (mg L^{-1})	N-NH_4^+ (mg L^{-1})	N-NO_3^- (mg L^{-1})	N-NO_2^- (mg L^{-1})	P-PO_4^{3-} (mg L^{-1})	S-SO_4^{2-} (mg L^{-1})	pH
16.3 ± 12.3	156.4 ± 27.7	197.4 ± 14.6	181.5 ± 19.8	0.2 ± 0.6	6.0 ± 5.7	15.6 ± 5.0	52.4 ± 2.0	7.8 ± 0.2

Methanotrophic enrichment

The STR was filled up with 7.2 L of Kaldnes K1 Micro rings (Evolution Aqua Ltd., UK) and 6 L of 3-fold diluted centrate inoculated at 10% (*v/v*) with activated sludge. Magnetic agitation and temperature were maintained at 200 rpm and 25 ºC. The STR was operated at a dilution rate of 0.11 d^{-1}. The synthetic CH_4-laden air emission (30.9 ± 1.1 gCH_4 m^{-3}, 4.7 ± 0.2% CH_4 *v/v*) was obtained by mixing a pure CH_4 stream with pre-humidified air (sparged through a 9 L water column) and fed at 420 mL min^{-1} through a 10 µm porous ceramic diffuser located at the bottom of the tank, which resulted in a CH_4 inlet load (IL) of 92.5 ± 3.2 g m^{-3} h^{-1}. The suspended-growth methanotrophic culture enriched was then centrifuged and the biomass pellet resuspended in 450 mL of 3-fold diluted centrate (total suspended solids – TSS – concentration of 0.7 g L^{-1}) for BFs inoculation. In addition, the impregnated Kaldnes K1 Micro rings were used as the BFs packing material.

Calculations

Table S2. Parameters used to evaluate process performance during the operation of the BFs.

Parameter	Equation	Units
Inlet load (IL)	$IL = [CH_4]_{in} \times Q/V$	$g\ m^{-3}\ h^{-1}$
CH_4 removal efficiency (RE)	$RE = ([CH_4]_{in} - [CH_4]_{out}/[CH_4]_{in}) \times 100$	%
CH_4 elimination capacity (EC)	$EC = IL \times RE$	$g\ m^{-3}\ h^{-1}$
CO_2 production rate (PCO_2)	$PCO_2 = ([CO_2]_{out} - [CO_2]_{in}) \times Q/V$	$g\ m^{-3}\ h^{-1}$
Maximum theoretical CO_2 production rate ($PCO_{2\ MAX}$)	$PCO_{2\ MAX} = EC \times \alpha$	$g\ m^{-3}\ h^{-1}$
CH_4 mineralization (R_{CO2})	$R_{CO2} = (PCO_2/PCO_{2\ MAX}) \times 100$	%
CO_2 production yield (Y_{CO2})	$Y_{CO2} = PCO_2/EC$	$gCO_2\ gCH_4^{-1}$
TN/N-NH_4^+/P-PO_4^{3-} removal efficiency (TN/N-NH_4^+/P-PO_4^{3-} RE)	$RE_i = ([i]_{in} - [i]_{out})/[i]_{in} \times 100$	%

Q is the total air flow rate ($m^3\ h^{-1}$); V is the working volume of the BFs (m^3); $[CH_4]_{in}$, $[CH_4]_{out}$, $[CO_2]_{in}$ and $[CO_2]_{out}$ are the CH_4 and CO_2 concentrations at the inlet and outlet of the BFs, respectively ($g\ m^{-3}$); α is the molecular weight ratio M_{CO2}/M_{CH4} (2.75), which represents the maximum amount of CO_2 that can be produced by oxidizing all CH_4 to CO_2 if no biomass is produced. Finally, $[i]_{in}$ and $[i]_{out}$ stand for, respectively, the inlet (diluted centrate) and outlet (leachate) aqueous concentrations ($g\ m^{-3}$) of the target monitored parameter i (TN, N-NH_4^+ or P-PO_4^{3-}).

Results and Discussion

Reactor performance

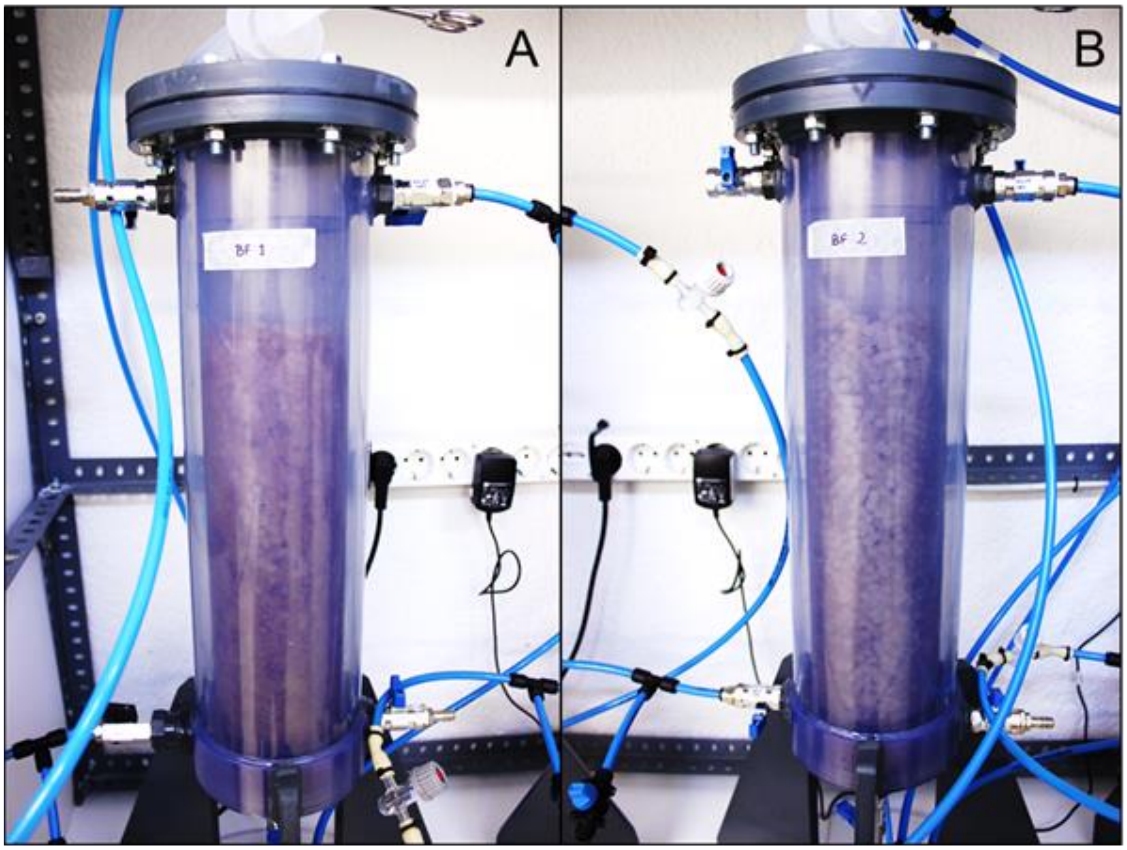

Figure S1. Biomass accumulation in the control unit (A) and in one of the alternate units (B).

Richness, diversity and structure of the active microbial communities

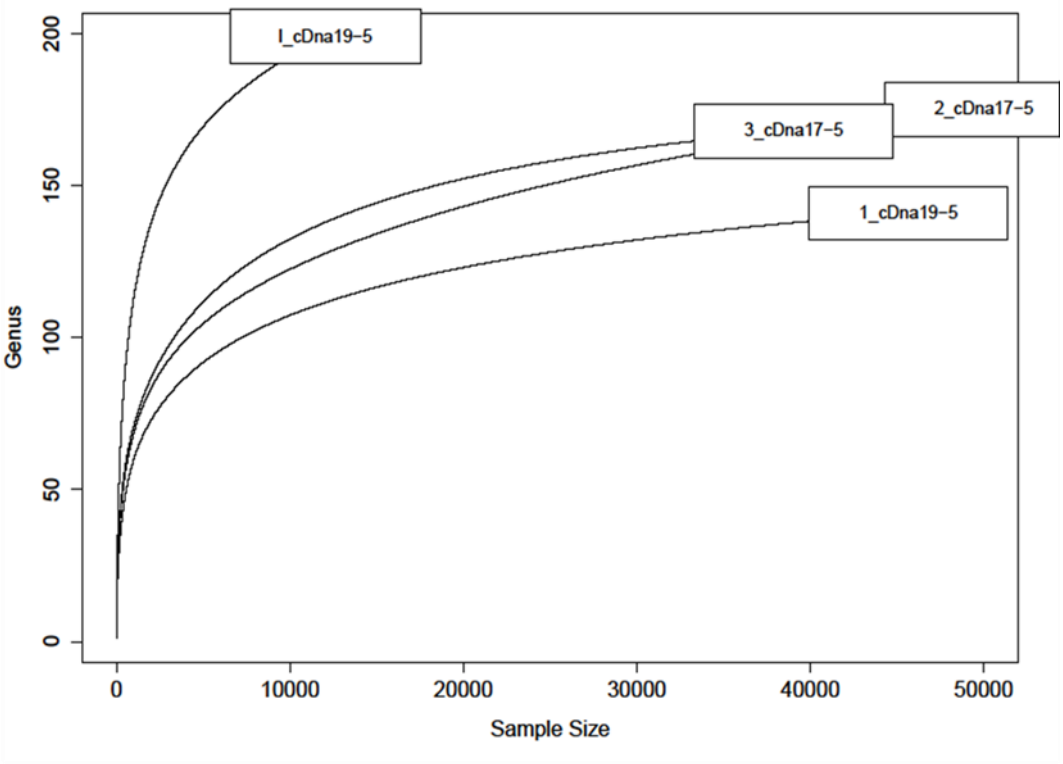

Figure S2. Rarefaction curves for cDNA samples I, 1, 2 and 3.

Table S3. Bacterial diversity in cDNA samples I, 1, 2 and 3.

cDNA sample	Simpson index (adimensional)	Shannon index (adimensional)
I	0.95	3.84
1	0.88	2.77
2	0.85	2.92
3	0.88	3.09

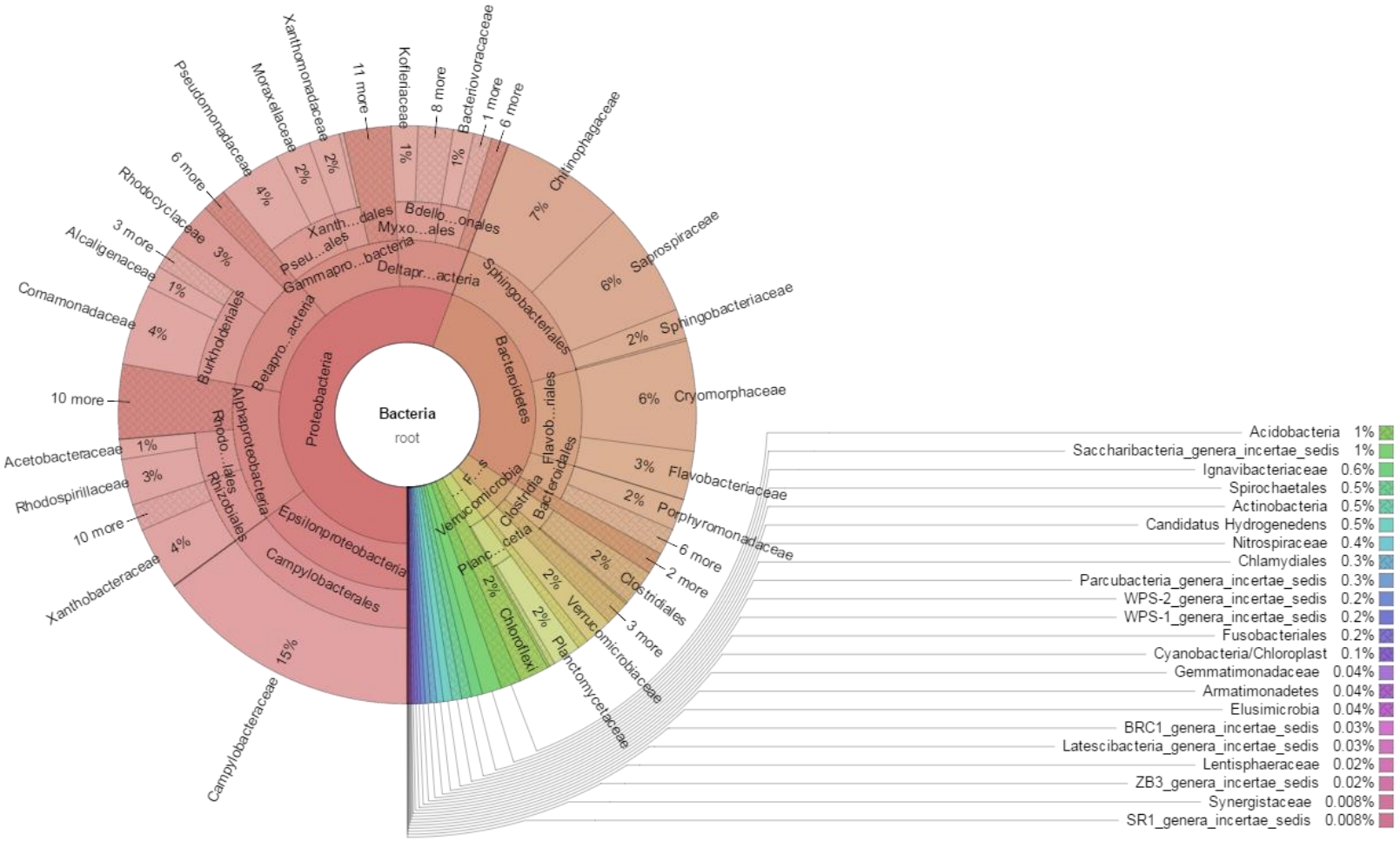

Figure S3. Microbial community structure of sample I displayed using Krona tool. Taxonomy nodes are shown as nested sectors arranged from the top level of the hierarchy at the center and progressing outward until family level was reached.

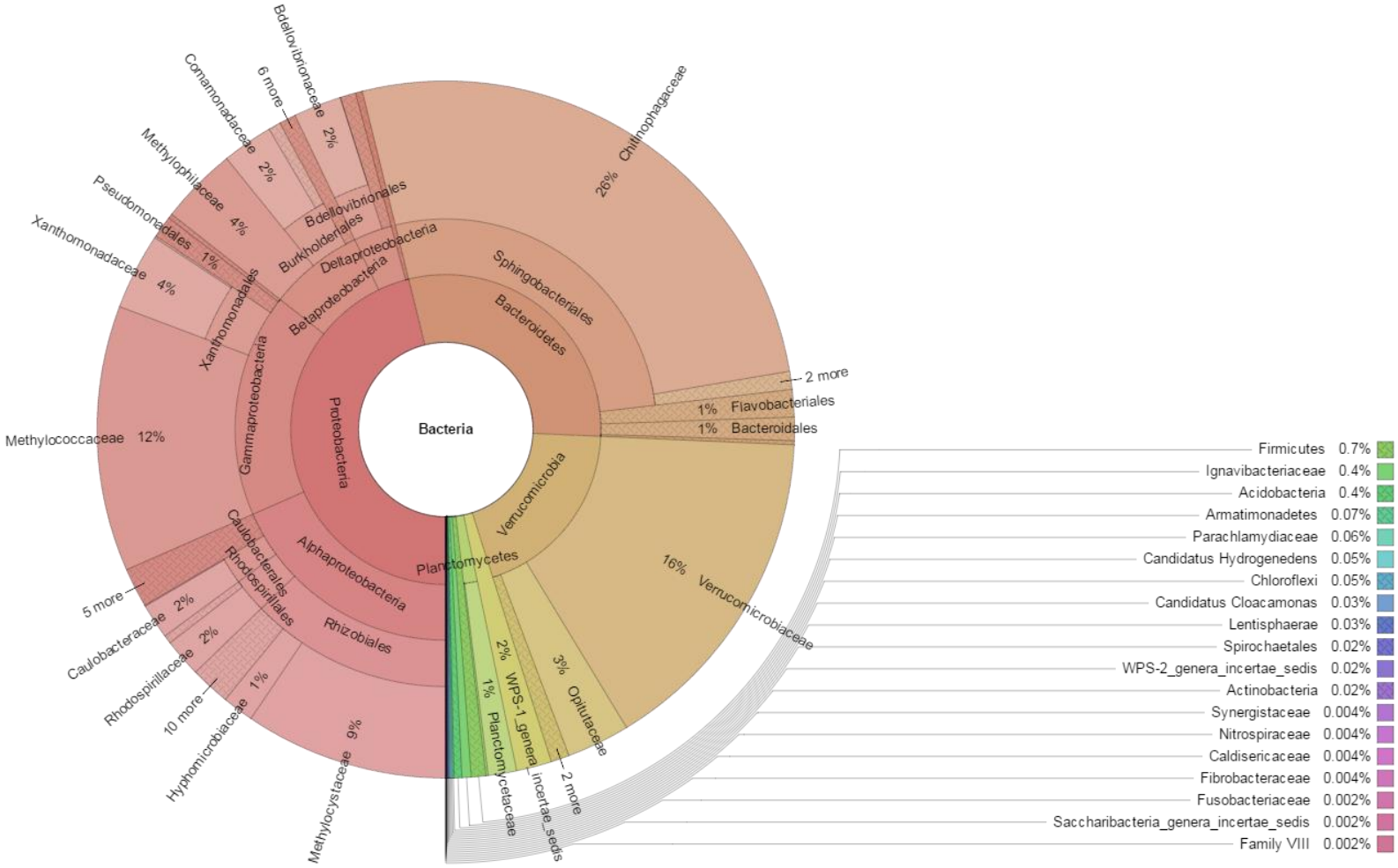

Figure S4. Microbial community structure of sample 1 displayed using Krona tool. Taxonomy nodes are shown as nested sectors arranged from the top level of the hierarchy at the center and progressing outward until family level was reached.

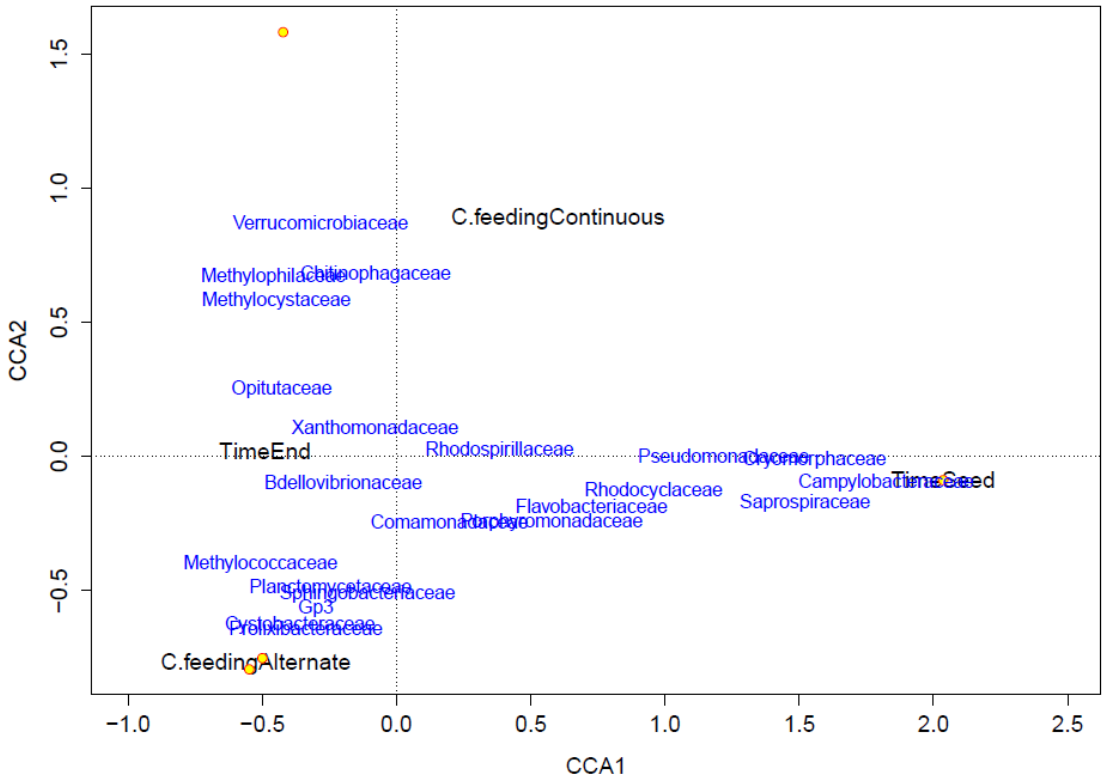

Figure S5. Canonical correspondence analysis (CCA) of Illumina data and variables at a family level in samples I, 1, 2 and 3. Taxa represented occurred at an abundance threshold >0.5 % in at least one sample. Yellow circles represent the different dataset samples.

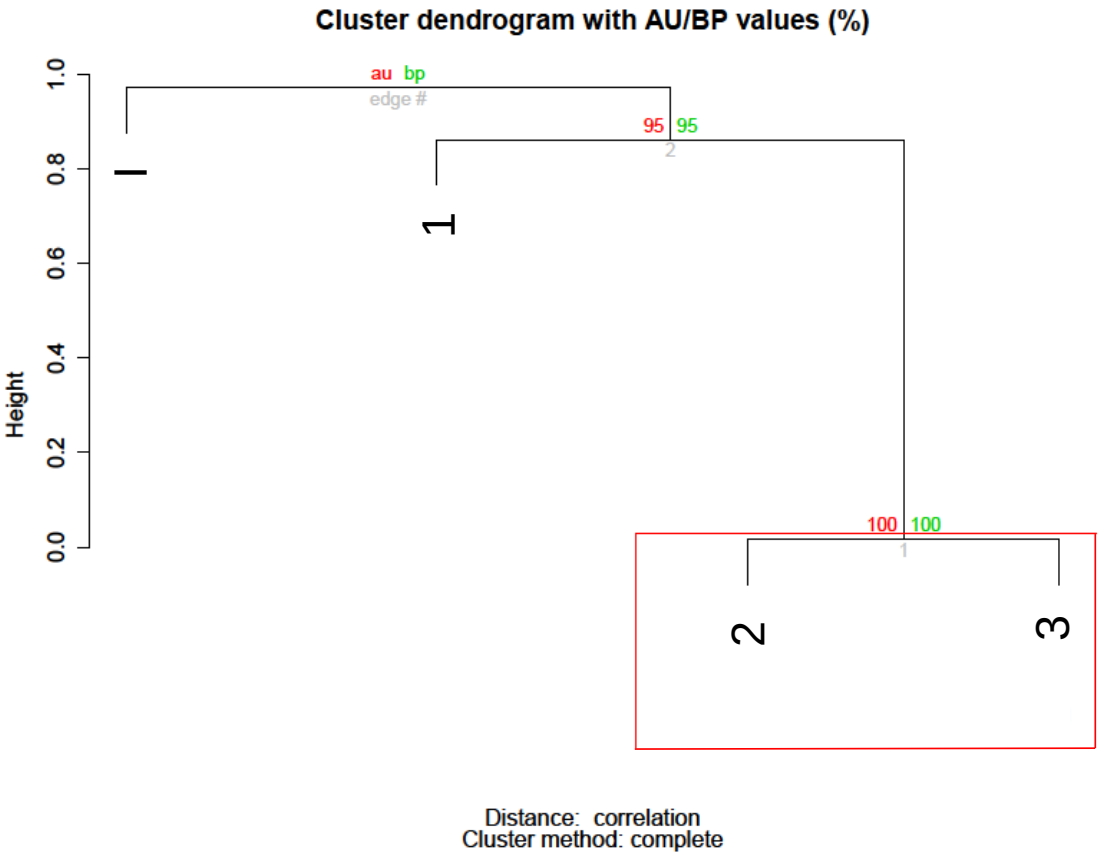

Figure S6. Hierarchical clustering of samples I, 1, 2 and 3. Values at branches are AU *p*-values (left) and BP values (right). Clusters with AU ≥ 95 are indicated by a red rectangle.

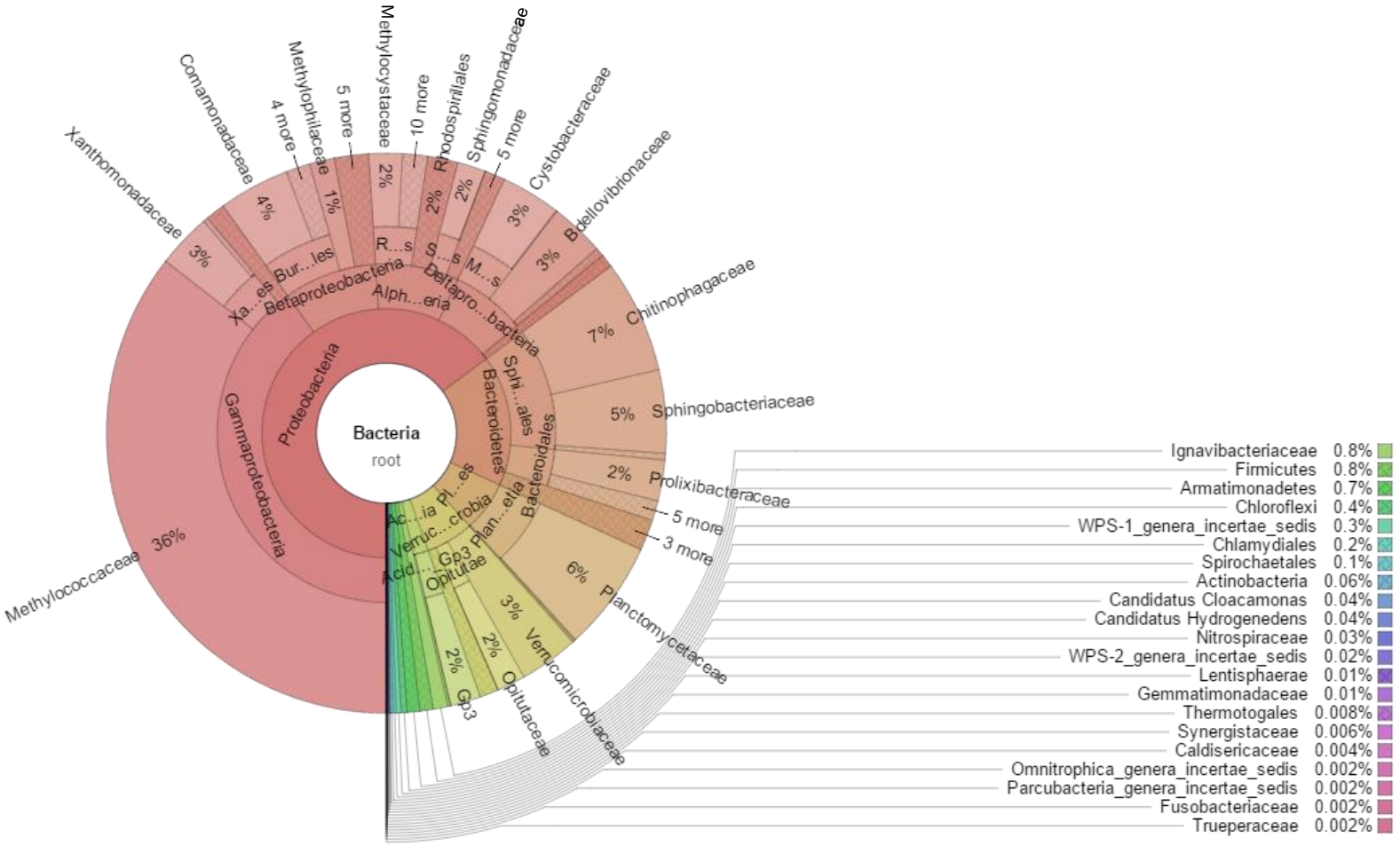

Figure S7. Microbial community structure of sample 2 displayed using Krona tool. Taxonomy nodes are shown as nested sectors arranged from the top level of the hierarchy at the center and progressing outward until family level was reached.

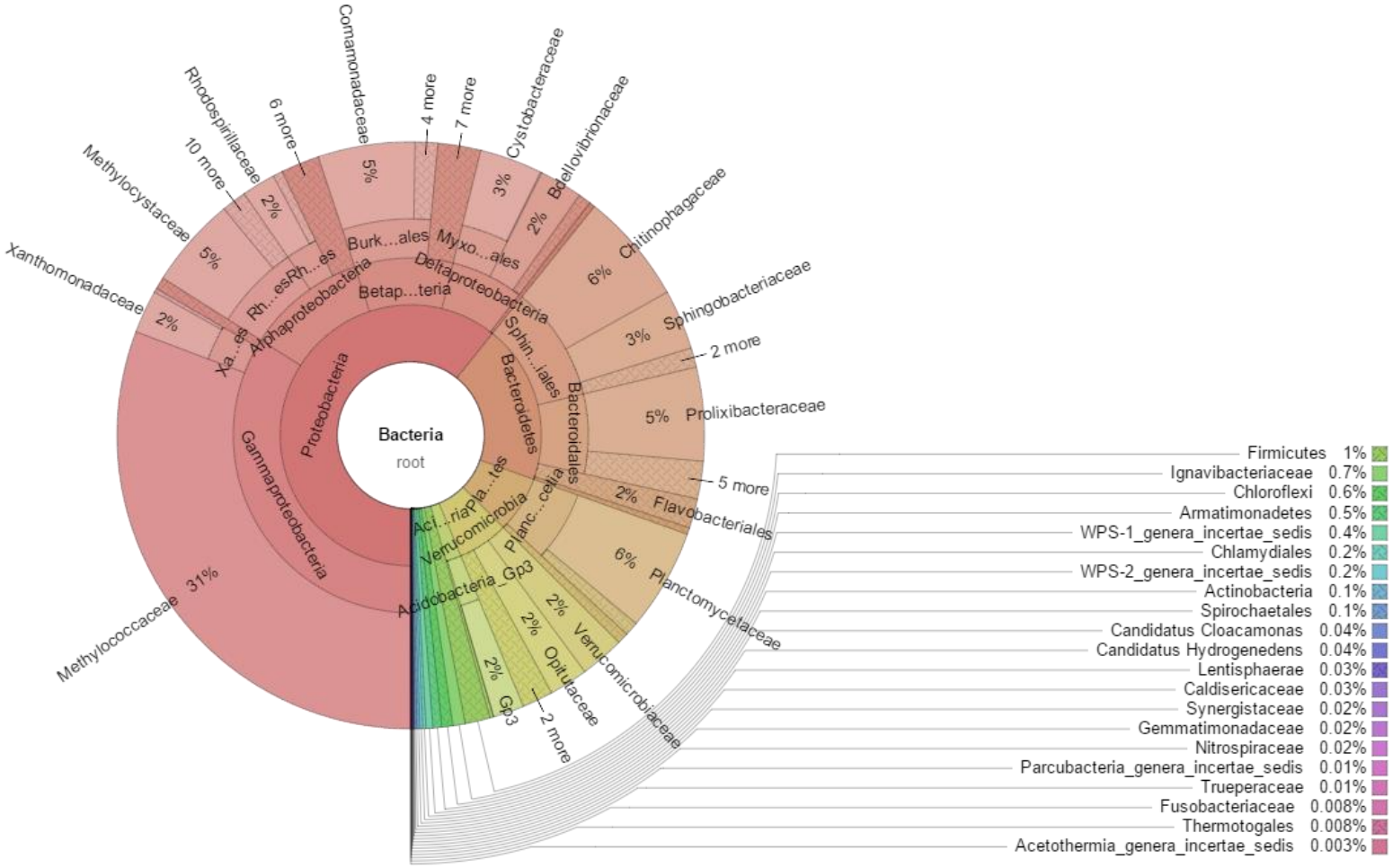

Figure S8. Microbial community structure of sample 3 displayed using Krona tool. Taxonomy nodes are shown as nested sectors arranged from the top level of the hierarchy at the center and progressing outward until family level was reached.

Chapter 5

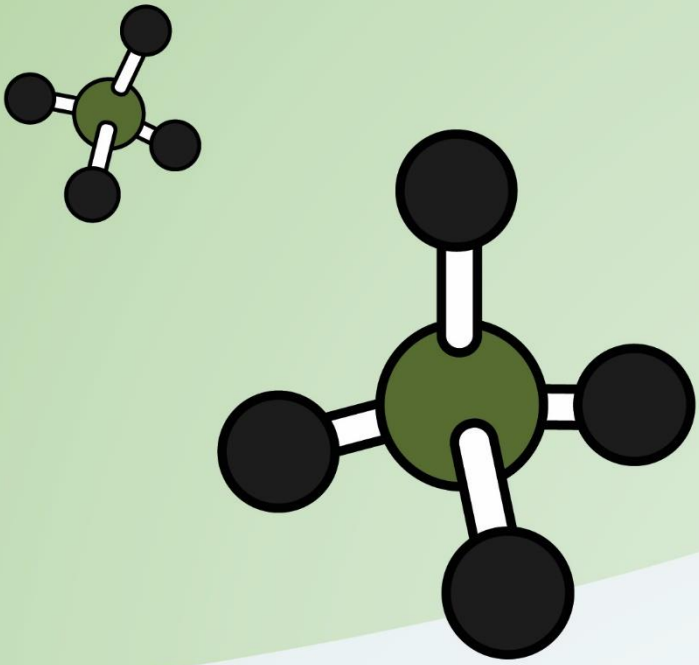

Assessing the influence of CH_4 concentration during culture enrichment on the biodegradation kinetics and population structure

Journal of Environmental Management 146 (2014) 116–123

Contents lists available at ScienceDirect

Journal of Environmental Management

journal homepage: www.elsevier.com/locate/jenvman

Assessing the influence of CH_4 concentration during culture enrichment on the biodegradation kinetics and population structure

Juan C. López, Guillermo Quijano, Rebeca Pérez, Raúl Muñoz*

Department of Chemical Engineering and Environmental Technology, University of Valladolid, Dr. Mergelina, s/n, 47011, Valladolid, Spain

ARTICLE INFO

Article history:
Received 28 February 2014
Received in revised form
25 June 2014
Accepted 26 June 2014
Available online

Keywords:
Biodegradation kinetics
CH_4 concentration
Methanotroph
Microbial population structure
Polyhydroxyalkanoate

ABSTRACT

Methanotrophic communities were enriched in three stirred tank reactors continuously supplied with CH_4-laden air at 20, 2 and 0.2 $gCH_4\ m^{-3}$ in order to evaluate the influence of CH_4 concentration on the biodegradation kinetics, population structure and potential polyhydroxyalkanoate production under sequential nitrogen limitations. The population structure of the enriched cultures, dominated by type I methanotrophs, was influenced by CH_4 concentration. No significant correlation between CH_4 concentration and the maximum specific degradation rate (q_{max}) or the half-saturation constant (K_S) was recorded, microorganisms enriched at 2 $gCH_4\ m^{-3}$ presenting the highest q_{max} and those enriched at 20 and 0.2 $gCH_4\ m^{-3}$ exhibiting the lowest K_S. Maximum polyhydroxybutyrate (PHB) contents of 1.0% and 12.6% (*w*/*w*) were achieved at 20 and 2 g $CH_4\ m^{-3}$, respectively. Polyhydroxyvalerate (PHV) was also detected at PHV:PHB ratios of up to 12:1 and 4:1 in the communities enriched at 20 and 0.2 $gCH_4\ m^{-3}$, respectively.

1. Introduction

Methane (CH_4) contributes to approximately 20% of the worldwide greenhouse gas (GHG) emissions, with an atmospheric concentration increase of 150% from the pre-industrial era to 2011 (Environmental Protection Agency, 2013; Intergovernmental Panel on Climate Change, 2013). CH_4 presents a global warming potential 25 times higher than that of CO_2 (excluding additional harmful effects of water vapor production from CH_4 breakdown) and is mainly emitted from organic waste treatment activities such as landfilling, composting and wastewater treatment (122 million tn CO_2-eq in the EU-15), coal mining (6 million tn CO_2-eq in the EU-15) and livestock farming (120 million tn CO_2-eq in the EU-15) (European Environment Agency, 2013). CH_4 concentration in anthropogenic emissions greatly varies from 0 to 0.2 $gCH_4\ m^{-3}$ in compost piles or livestock farms up to 20–100 $gCH_4\ m^{-3}$ in old landfills (Nikiema et al., 2007).

Based on the urgent need to limit the increase in the global average temperature to a maximum of 2 °C above pre-industrial levels, the EU committed itself under the upgraded Kyoto Protocol to reduce its GHG emissions by 20% in 2020 (compared to 1990) (European Environment Agency, 2013; Intergovernmental Panel on Climate Change, 2013). In this context, apart from the actions oriented to reduce CO_2 emissions from fossil fuel combustion, additional measurements such as an active CH_4 abatement must be considered in order to achieve these target emission cuts. Moreover, the gradual application of the EU landfill Directive 1999/31 will result in emissions with lower CH_4 concentrations, which will significantly restrict the implementation of CH_4 abatement technologies based on energy recovery (applied at CH_4 concentrations higher than ~400 g m^{-3}). Therefore, there is an urgent need to develop cost-efficient and sustainable technologies for the active abatement of CH_4 diluted emissions. Biotechnologies could become, if properly tailored, a platform technology for the abatement of diluted CH_4 emissions based on their proven robustness and cost-effectiveness for the treatment of malodours or industrial VOC emissions (Estrada et al., 2012b; López et al., 2013).

However, despite the fact that methanotroph-based technologies such as biofiltration or biotrickling filtration have been implemented over the past 40 years for the active abatement of CH_4, the performance of such conventional biotechnologies is still limited by the low CH_4 mass transfer rates from the gas phase to the microorganisms and by the insufficient knowledge on the microbiology underlying CH_4 oxidation (López et al., 2013; Yoon et al., 2009). In this regard, microorganisms with high specific oxidation rates (q_{max}) and a high affinity for CH_4 (low half-saturation constant, K_S) are desirable to guarantee an efficient biocatalytic activity during the treatment of diluted CH_4 emissions and to reduce the

* Corresponding author. Tel.: +34 983186424; fax: +34 983423013.
E-mail addresses: mutora@iq.uva.es, mutoraul@gmail.com (R. Muñoz).

http://dx.doi.org/10.1016/j.jenvman.2014.06.026
0301-4797/

start-up period of bioreactors. However, CH_4 biodegradation kinetic studies under non-mass transfer limiting conditions are scarce, especially at the trace level CH_4 concentrations (~mg m^{-3}) often encountered under real case applications (Estrada et al., 2012a; López et al., 2013). On the other hand, the economic sustainability of biological CH_4 oxidation processes, often compromised by the high gas residence time required to overcome mass transfer limitations, can be positively impacted by the co-production of high-added value products such as biopolymers (i.e. poly-3-hydroxybutyrate, PHB) (Zúñiga et al., 2011). Unfortunately, the potential of methanotrophic communities to accumulate polyhydroxyalkanoates during the continuous biodegradation of CH_4 at trace level concentrations has been poorly explored.

This study evaluated the influence of CH_4 concentration during methanotrophic community enrichment on biodegradation kinetic parameters and population structure. Moreover, the influence of CH_4 concentration and the CH_4/biomass ratio on the ability to accumulate PHB under nitrogen limiting scenarios was also assessed.

2. Materials and methods

2.1. Chemicals and mineral salt medium

Methane was purchased from Abelló Linde S.A. (Barcelona, Spain) with a purity of at least 99.5%. Poly-3-hydroxybutyrate, chloroform (>99.5%), phosphotungstic acid solution 10% (*w/v*), uranyl acetate dihydrate (≥98%), propylene oxide (>99%) and benzoic acid (>99.5%) were obtained from Sigma–Aldrich® (Sigma–Aldrich, St. Louis, MO, USA). Osmium tetroxide was obtained from EMS with a purity of at least 99.95% (Hatfield, USA). Lead nitrate and sodium citrate were purchased from Merck (Darmstadt, Germany). The Spurr resin kit TK4 4221D-1 was obtained from TAAB Laboratories Equipment Ltd. (Aldermaston, England). Paraformaldehyde and ethanol (96%) were purchased from AppliChem (Darmstadt, Germany). The rest of reagents and chemicals were purchased from Panreac® (Barcelona, Spain) with a purity of at least 99%.

The mineral salt medium (MSM) used for microbial enrichment and the in-vitro kinetic assays was composed of (in g L^{-1}): $Na_2HPO_4 \cdot 12H_2O$ 6.15, KH_2PO_4 1.52, $MgSO_4 \cdot 7H_2O$ 0.2, $CaCl_2 \cdot 2H_2O$ 0.0503, $NaNO_3$ 1.32 and 10 mL L^{-1} of SL4 trace element solution (containing per liter: EDTA 0.5 g, $FeSO_4 \cdot 7H_2O$ 0.2 g, $ZnSO_4 \cdot 7H_2O$ 0.01 g, $MnCl_2 \cdot 4H_2O$ 0.003 g, H_3BO_3 0.03 g, $CoCl_2$ 0.011 g, $CuCl_2 \cdot 2H_2O$ 0.443 g, $NiCl_2 \cdot 6H_2O$ 0.002 g, $Na_2MoO_4 \cdot 2H_2O$ 0.003 g).

2.2. Inoculum and cultivation conditions

Fresh aerobic activated sludge from Valladolid wastewater treatment plant (Valladolid, Spain), soil from the cover of an abandoned landfill (Almazán, Spain) and sludge from an aerobic lagoon stabilizing the effluents from a full-scale anaerobic digester treating swine manure (Almazán, Spain) were used as inoculum for the enrichment of methanotrophs. Aliquots of the 3 microbial sources were equally mixed (on a volume basis), diluted in MSM in a 1:18 ratio and then incubated at 25 °C and 150 rpm for 1 h in a rotary shaker.

2.3. Experimental set-up and operation mode

Three 500 mL jacketed stirred tank reactors (STRs) (Afora S.A., Spain) initially containing 380 mL of MSM were inoculated with 20 mL of the mixed inoculum above described. The cultivation broth was maintained at 25 °C and magnetically agitated at 250 rpm with a stir bar placed at the bottom of each STR. Inert polyurethane polymers (0.92 g) were introduced in each reactor in order to prevent the formation of biofilm onto the reactor walls, thus avoiding the underestimation of biomass concentration. CH_4 was continuously supplied via aeration (400 mL min^{-1}) at 20 g m^{-3}, 2 g m^{-3} and 0.2 g m^{-3} into reactors 1 (R1), 2 (R2) and 3 (R3), respectively, using 10 μm porous stainless steel diffusers located at the bottom of the reactors. The concentrations of CH_4 were regulated via mass flow controllers (Aalborg™, USA) by mixing an air stream with either pure methane or serial dilutions of CH_4-laden air streams (Fig. 1). The pH of the enrichment broths was maintained at 7.2 ± 0.2 by periodic addition of HCl (0.2 M). Distilled water was added every two days to compensate for water losses by evaporation. Double concentrated MSM without nitrogen was also added to compensate for sampling losses and to provide enough nutrients for microbial growth. The enrichment of potential PHB-accumulating methanotrophs was performed by operating the reactors under 8 sequential periods of N limitation (48–72 h per period) within the entire 310-days experimentation period. $N-NO_3^-$ concentration was restored at 248.8 ± 65.3, 48.1 ± 22.9, 17.2 ± 6.9 mg L^{-1} in R1, R2 and R3, respectively, after each limitation period. At the end of the 8th N limitation cycle, the influence of the CH_4/biomass ratio on microbial PHB accumulation under N limiting conditions was assessed for a period of 18 days by diluting the biomass concentration in R1 and R2 to the levels of R3.

Liquid samples (3 mL) were periodically drawn from the reactors to determine the concentration of biomass via culture absorbance measurements (OD_{650}), dissolved total organic carbon (TOC) and total nitrogen (TN). Additionally, 15 mL liquid samples were drawn on days 95–100 (week 14) and 130–135 (week 19) to determine the CH_4 biodegradation kinetic parameters and periodically monitor the total suspended solid concentration (TSS). Liquid samples of 3 mL were also drawn to quantify the bacterial PHB content and to confirm PHB accumulation by transmission electron microscopy at the end of each 3 days nitrogen limitation period. Liquid samples were also taken on days 28 (week 4), 95 (week 14) and 130 (week 19) to determine the dynamics of microbial population structure by denaturing gradient gel electrophoresis (DGGE). CH_4 and CO_2 gas concentrations were monitored by GC-TCD at the inlet and outlet of the reactors.

2.4. Kinetics of CH_4 biodegradation

The maximum specific CH_4 biodegradation rate q_{max} ($gCH_4\ g^{-1}_{biomass}\ h^{-1}$) and the Monod half-saturation constant K_S (g m^{-3}) under non-limiting N conditions were determined for R1, R2 and R3 cultures on days 95–100 (week 14) and 130–135 (week 19) in order to record the dynamics of CH_4 biodegradation kinetics. These assays were conducted in 120-mL glass bottles containing 20 mL of MSM and inoculated with fresh biomass at an initial concentration of 51.7 ± 14.7 $g_{biomass}\ m^{-3}$, which ensured that the kinetic parameters were obtained under non-limiting mass transfer conditions (according to preliminary tests). The bottles were closed with butyl septa, sealed with aluminum caps and supplied with CH_4 at initial headspace concentrations of 91.5 ± 3.9 g m^{-3}, 17.9 ± 0.8 g m^{-3} and 4.7 ± 0.4 g m^{-3} (corresponding to initial methane aqueous concentrations of 3.1 ± 0.1 g m^{-3}, 0.61 ± 0.1 g m^{-3} and 0.16 ± 0.1 g m^{-3}, respectively). The bottles were incubated at 25 °C and 150 rpm for 25 h. The concentrations of CH_4 and CO_2 in the headspace of the bottles were periodically measured by GC-TCD. The Lineweaver–Burk correlation (Equation (1)) was used to determine the biodegradation kinetic parameters from the initial CH_4 biodegradation rates (Walkiewicz et al., 2012):

$$1/q = K_S/q_{max} \times 1/[CH_4] + 1/q_{max} \quad (1)$$

where q represents the initial CH_4 biodegradation rate (g CH_4 m^{-3}_{liq} h^{-1}) and $[CH_4]$ the methane concentration in the

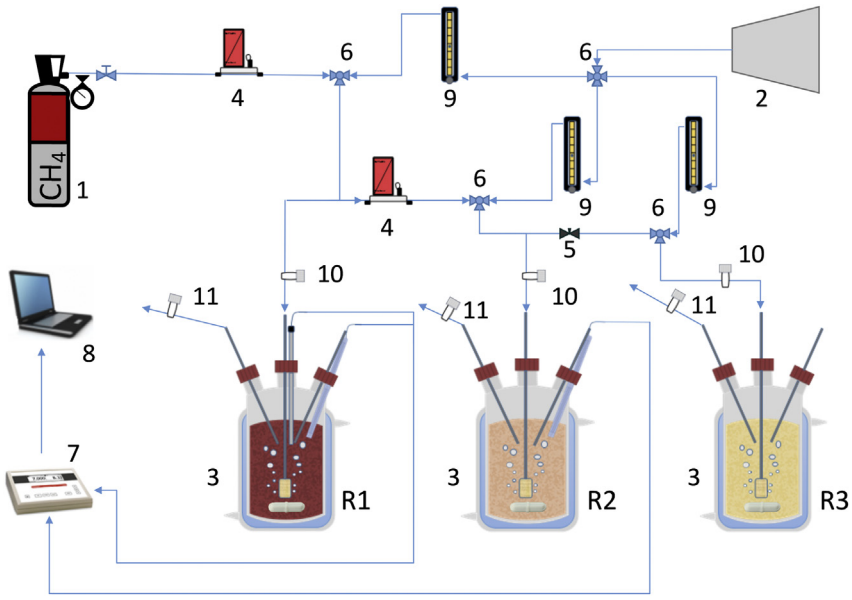

Fig. 1. Schematic representation of the experimental set-up. *1* CH_4 gas cylinder, *2* air compressor, *3* jacketed 500-mL glass reactors, *4* mass flow controllers, *5* needle valve, *6* T-connections, *7* pH data acquisition system, *8* PC data logger, *9* rotameters, *10* inlet sampling points, *11* outlet sampling points.

aqueous phase (g m^{-3}_{liq}) estimated using the dimensionless Henry's law constant at 25 °C and 1 atm (29.4).

2.5. Molecular biology analysis

To evaluate the richness and composition of the microbial community, biomass samples from the inoculum (A) and from R1, R2 and R3 were collected on week 4 (B, C and D, respectively), 14 (E, F and G, respectively) and 19 (H, I and J, respectively) and stored immediately at −20 °C. The procedures of the DNA extraction, PCR amplification, DGGE analysis, sequencing and DNA sequence analysis can be found in the Supplementary Data Annex.

2.6. Electron microscopy analysis

Liquid samples of 1 mL drawn from the STRs at the end of the 3rd limitation period were centrifuged at 4000 rpm and 4 °C for 5 min. Subsequent biomass fixation, dehydration and embedding were carried out according to Bozzola (2007). The samples were finally cutted and contrasted according to Wendlandt et al. (2001). A TEM JEOL JEM-1011 electron microscope (Teknolab, Indonesia) with an ES1000W Erlangshen CCD camera (Gatan, Germany) was used for the analysis.

2.7. Measurement of PHB

The quantitative determination of the cellular PHB content was carried out according to Zúñiga et al. (2011) using chloroform as extraction solvent.

2.8. Analytical procedures

CH_4 and CO_2 gas concentrations were determined in a Bruker 430 GC-TCD (Palo Alto, USA) equipped with a CP-Molsieve 5A (15 m × 0.53 μm × 15 μm) and a CP-PoraBOND Q (25 m × 0.53 μm × 10 μm) columns. The oven, injector and detector temperatures were maintained at 45 °C, 150 °C and 200 °C, respectively. Helium was used as the carrier gas at 13.7 mL min^{-1}. Samples for the determination of TOC/TN concentrations were filtered through 0.22 μm glass fiber filters (Merck Millipore, USA) prior to analysis in a TOC-VCSH analyzer (Shimadzu, Japan) coupled with a chemiluminescense detection TN module (TNM-1) (Shimadzu, Japan). Culture absorbance measurements at 650 nm were performed using a Shimadzu UV-2550 UV/Vis spectrophotometer (Shimadzu, Japan). The determination of TSS concentration was performed according to standard methods (APHA, 2005). Temperature and pH were on-line monitored using a multiparametric analyser C-3020 (Consort, Belgium). PHB concentration was quantified in an Agilent 6890N GC–MS equipped with a DB-WAX column (30 m × 0.250 mm × 0.25 μm) (J&W Scientific®, CA, USA). The injector temperature was set at 250 °C. The oven temperature was initially maintained at 40 °C for 5 min, increased at 10 °C min^{-1} up to 200 °C, then at 5 °C min^{-1} up to 240 °C and finally maintained at 240 °C for 2 min.

3. Results and discussion

3.1. Methane biodegradation performance during culture enrichment

CH_4 biodegradation in the three enrichment STRs was indirectly assessed by CO_2 production and biomass growth rather than by CH_4 consumption based on the higher reliability of CO_2 measurements and the low CH_4 removal rates achieved. Since the reactors were not designed to maximize CH_4 abatement, the removal rates obtained were lower than the average error of the GC-FID method. In this context, a rapid CH_4 oxidation was recorded at the highest CH_4 concentration in R1 from the second day of operation, with an increase in CO_2 production up to 104 g m^{-3} h^{-1} concomitant with a rise in biomass concentration up to 4 g L^{-1} (Fig. 2a, b). However, CH_4 mineralization progressively decreased to average values of 60 gCO_2 m^{-3} h^{-1} from day 40–60 and fluctuated at 42.3 ± 17 g m^{-3} h^{-1} from day 60 onwards. Biomass concentration stabilized at 4 g L^{-1} from days 33–45 and at 6 g L^{-1} from days 75–125 likely due to the accumulation of both metabolites and cell lysis products in the cultivation broth. The complete renewal of MSM in R1 (prior biomass centrifugation) by days 45 and 125 restored TOC concentrations at 110–120 mgC L^{-1} and supported

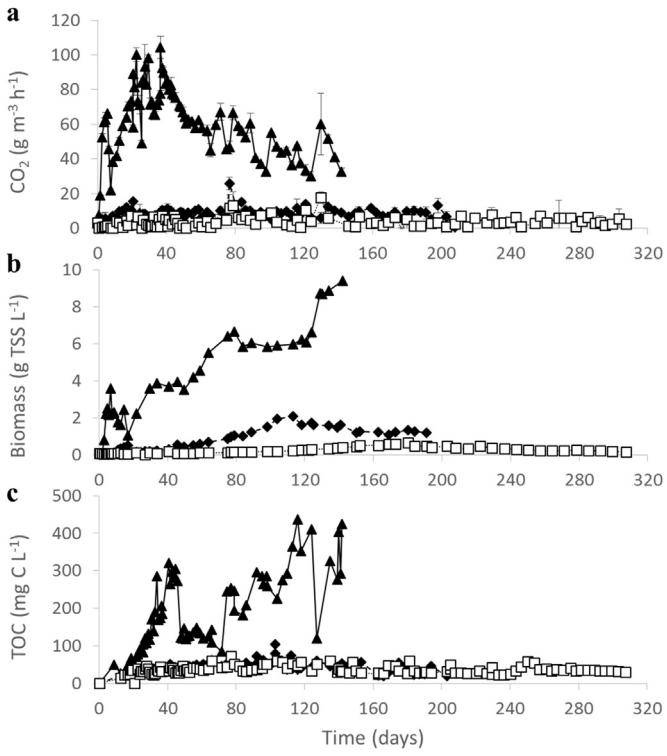

Fig. 2. Time course of CO_2 production rate (**a**), biomass concentration (**b**) and TOC concentration (**c**) during methanotroph enrichment in R1 (▲), R2 (◆) and R3 (▫).

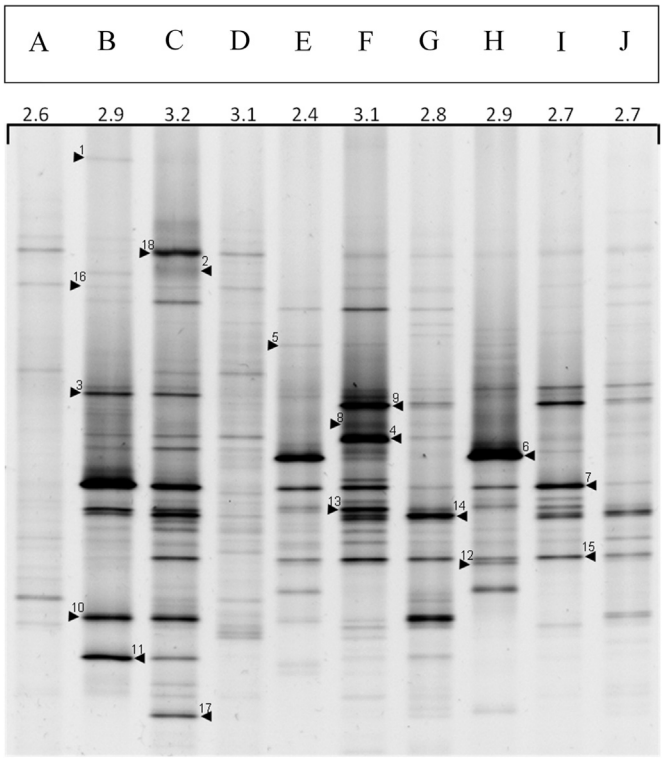

Fig. 3. DGGE profiles of the bacterial communities present in: *A* Inoculum, *B* R1 on week 4, *C* R2 on week 4, *D* R3 on week 4, *E* R1 on week 14, *F* R2 on week 14, *G* R3 on week 14, *H* R1 on week 19, *I* R2 on week 19, *J* R3 on week 19. The name of the samples and their Shannon–Weiner diversity indexes are shown in the upper part of the gel.

further biomass growth (Fig. 2c). The CO_2 production rates in R2 and R3 underwent less variations than those recorded in R1, with average values of 7.9 and 3.7 g m^{-3} h^{-1}, respectively (Fig 2a). These lower CO_2 production rates were attributed to the lower CH_4 concentration gradients and therefore mass transfer rates at 2 and 0.2 g m^{-3}, compared to R1. Biomass growth in R2 and R3 was also significantly lower than that recorded in R1 as a result of the lower CH_4 loading rates (10 and 100 times lower, respectively). Maximum biomass concentrations of 2.1 and 0.7 g L^{-1} were achieved, respectively, in R2 and R3 by days 113 and 180, to finally decrease to 1.2 and 0.2 g L^{-1}, respectively. Likewise, TOC concentrations in both reactors remained constant at ~40 mg L^{-1}, which suggests that the accumulation of metabolites or cell lysis products in R2 and R3 was not significant during the experimentation period (Fig. 2c). The CO_2 production rates recorded in R1 and R2 were similar to those reported by Rocha-Rios et al. (2010, 2009) in STRs at CH_4 loading rates of approximately 65 and 210 g m^{-3} h^{-1} (10 and 80 g CO_2 m^{-3} h^{-1}, respectively).

3.2. Structure of the enriched communities

The Shannon–Wiener diversity index (*H*) ranges typically from 1.5 to 3.5 and accounts for both the number (richness) and the eveness of the species (evaluating and comparing the intensity of the bands), thus allowing to obtain semi-quantitative results from the DGGE analysis (McDonald, 2003). In our particular case, the complex inoculum exhibited the lowest species evenness and richness among the samples analyzed as demonstrated by its low *H* of 2.6. Despite the increase in microbial diversity of the communities at week 4 in R1, R2 and R3 (*H* of 2.9, 3.2 and 3.1, respectively), culture aging mediated a lower biodiversity at week 14 as confirmed by the decrease in *H* values to 2.4, 3.1 and 2.8 in R1, R2 and R3, respectively. Further culture aging resulted in the stabilization in microbial diversity by week 19 in R2 and R3 at *H* of 2.7, and at *H* of 2.9 in R1. It is noteworthy that these *H* values were achieved using CH_4 as the sole C and energy source and were not significantly influenced by CH_4 concentration. In contrast, Estrada et al. (2012a) observed that high toluene concentrations supported lower biodiversity indexes, which was attributed to the high toxicity of the model VOC used in the study.

The analysis of the pair-wise similarity indexes revealed a low correspondence between the inoculum and the cultures in the three STRs, even by week 4 (Fig. 4a). Hence, similarity coefficients of 8%, 18% and 34% were recorded between the seed and the cultures R1, R2 and R3 by week 4, respectively (Fig. 4b). These results confirmed the rapid dynamics of the methanotrophic communities in the STRs and agreed well with the differences observed among the Shannon–Wiener diversity indexes. The highest similarities in the phylogenetic composition of the communities were obtained between the communities on weeks 14 and 19 (88% in R1, 80% in R2 and 75% in R3) (Fig. 4a, b). These empirical findings confirmed the stabilization of the methanotrophic populations from week 14 onward regardless of the CH_4 concentration evaluated. Moreover, the comparison of communities in the STRs by week 19 revealed that cultures enriched at CH_4 concentrations differing in one order of magnitude were more similar (similarities of 51% between R1 and R2, and 66% between R2 and R3) than those enriched at CH_4 concentrations differing in two orders of magnitude (32% between R1 and R3) (Fig. 4b). Thus, these results confirmed the significant influence of CH_4 concentration during culture enrichment on the structure of the microbial populations.

Three different phyla were retrieved according to the RDP classifier tool among the 18 bands sequenced from the DGGE gel (Fig. 3): *Proteobacteria* (15 bands), *Firmicutes* (1 band) and *Actinobacteria* (1 band), while the sequence of the last band remained unclassified. The closest matches for each bacterial sequence from

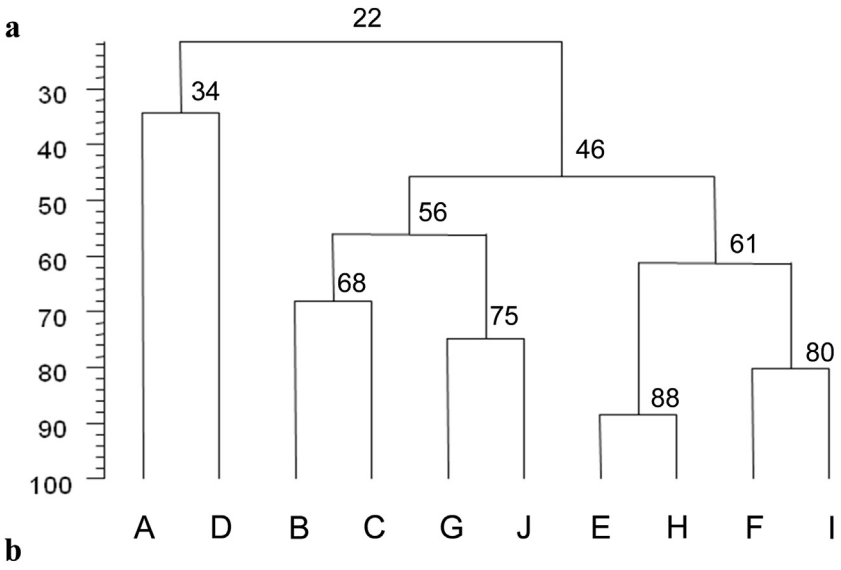

b

Sample	A	B	C	D	E	F	G	H	I	J
A	100	-	-	-	-	-	-	-	-	-
B	8	100	-	-	-	-	-	-	-	-
C	18	67	100	-	-	-	-	-	-	-
D	34	23	37	100	-	-	-	-	-	-
E	1	52	41	31	100	-	-	-	-	-
F	12	60	53	41	66	100	-	-	-	-
G	2	50	63	38	27	46	100	-	-	-
H	9	47	31	36	88	77	21	100	-	-
I	19	61	60	29	54	80	48	51	100	-
J	9	50	65	29	32	59	75	32	66	100

Fig. 4. Bacterial similarity dendrogram (UPGMA clustering) (**a**) and matrix (**b**) with error resampling (500 resampling experiments) for: *A* Inoculum, *B* R1 on week 4, *C* R2 on week 4, *D* R3 on week 4, *E* R1 on week 14, *F* R2 on week 14, *G* R3 on week 14, *H* R1 on week 19, *I* R2 on week 19, *J* R3 on week 19. The names of the samples in the dendrogram are shown in the lower part of the figure.

the NCBI database are provided in the Supplementary Data Annex (Table 1) with indication of the similarity percentages and sources of origin. In addition, the presence and relative abundance of each band within the samples analyzed are also shown in the Supplementary Data Annex (Table 1). Most bands were affiliated to the phylum *Proteobacteria* and more specifically to *Alphaproteobacteria*, *Betaproteobacteria* and *Gammaproteobacteria* classes. Despite CH_4-oxidizing bacteria belonging to type I methanotrophs (*Methylosarcina*, *Methylomicrobium, Methylosoma* and *Methylobacter* genera) were detected in the three STRs along the entire enrichment, type I methanotrophs were more abundant in R1 and R2 (samples B, C, E, F, H and I) and their abundance gradually deteriorated over time. Type II methanotrophs (*Methylocystis* genus) were also present in the three STRs and gradually increased their abundance in R2 and, in a lesser extent, in R3 (samples F, G, I and J). The fact that type II methanotrophs exhibited a lower abundance than type I methanotrophs in the STRs can be attributed to the enrichment of cultures at high Cu^{2+} concentrations. In this context, preliminary quantitative-PCR results revealed the higher expression of particulate methane monooxygenases (pMMO) compared to the type II-specific soluble methane monooxygenases (sMMO), which also supported the predominance of type I methanotrophs along the entire enrichment in the STRs (data not shown). Most methanotrophic genera here described were previously identified in CH_4 abatement bioreactors (Gebert et al., 2008; Veillette et al., 2011), which confirmed their ability to degrade CH_4. Thus, the methylotrophic *Methylobacillus* and *Hyphomicrobium* genera have been detected in sewers and biofilters treating CH_4, respectively (Chistoserdova et al., 2007; Kim et al., 2013). In our particular study, the *Hyphomicrobium* genus (DGGE band 15) was significantly present in almost all samples analyzed, while bacteria from the *Methylobacillus* genus (DGGE band 12) were only found in R1 by week 19 (sample H). Despite members of the *Dokdonella*, *Rhodanobacter*, *Turicibacter* and *Rhodococcus* genera (DGGE fragments 10, 11, 16 and 17, respectively) were also detected by week 4 in the three STRs, these microorganisms gradually disappeared likely due to their incapability to assimilate CH_4, CH_4-derived metabolites or cell lysis products. Bacteria from the *Rhodanobacter* genus were previously detected in a CH_4 abatement bioreactor, but their role in this particular microbial community was not clearly identified (Veillette et al., 2011).

3.3. Determination of kinetic parameters

The highest q_{max} obtained from the Lineweaver–Burk linearization ($4.8 \times 10^{-4} \pm 8.1 \times 10^{-5}$ $gCH_4\ g_{biomass}^{-1}\ h^{-1}$) was recorded at week 14 in the communities enriched in R2, which was attributed to the high biodiversity encountered both for type I and II methanotrophic bacteria. No significant differences were observed between the communities of R1 and R3 in terms of q_{max} at week 14, with values of $2.7 \times 10^{-4} \pm 5.6 \times 10^{-5}$ and $1.6 \times 10^{-4} \pm 1.8 \times 10^{-5}$ $gCH_4\ g_{biomass}^{-1}\ h^{-1}$, respectively (Fig. 5a). The q_{max} values determined at week 14 in the three microbial communities were higher than those previously reported in the literature, which typically ranged from 4.2×10^{-5} to 1.3×10^{-4} $gCH_4\ g_{biomass}^{-1}\ h^{-1}$ (Bender and Conrad, 1992; Gebert et al., 2003). These findings can be explained by the fact that biomass concentration was optimized in the biodegradation assays in order

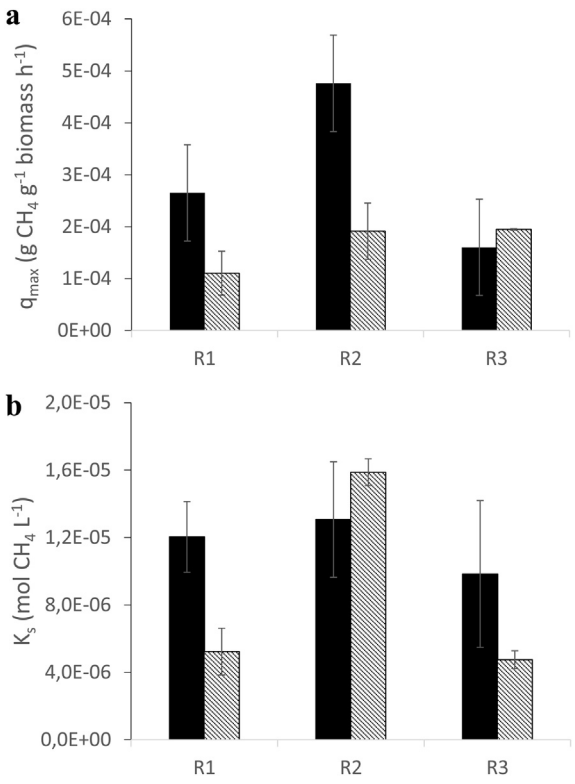

Fig. 5. Influence of CH_4 concentration during enrichment on the CH_4 biodegradation kinetic parameters q_{max} (**a**) and K_S (**b**) at week 14 (black bar) and 19 (scratched bar).

to avoid CH_4 mass transfer limiting conditions, resulting in more realistic kinetic parameters. On the contrary, most kinetic studies reported for methanotrophs were carried out at high biomass concentration, which did not ensure the absence of mass transport limitations and, therefore, the validity of the kinetic parameters obtained. At week 19, the communities of R1 and R2 exhibited lower q_{max} compared to week 14 ($1.1 \times 10^{-4} \pm 3.1 \times 10^{-5}$ and $1.9 \times 10^{-4} \pm 5.4 \times 10^{-5}$ gCH_4 $g_{biomass}^{-1}$ h^{-1}, respectively), while q_{max} in the community of R3 remained similar. These findings suggested that culture aging negatively affected the specific CH_4 biodegradation rate of the microbial communities exposed to the two highest CH_4 concentrations likely due to the presence of a higher inert biomass fraction.

On the other hand, no significant differences in the K_S of the microbial communities enriched in the three STRs were recorded at week 14, exhibiting values of $1.2 \times 10^{-5} \pm 1.7 \times 10^{-6}$ M (Fig. 5b). K_S values at week 19 significantly decreased in the communities enriched in R1 and R3 ($5.2 \times 10^{-6} \pm 1.4 \times 10^{-6}$ M and $4.8 \times 10^{-6} \pm 5.3 \times 10^{-7}$ M, respectively) and remained constant in R2 ($1.6 \times 10^{-5} \pm 8 \times 10^{-7}$ M). The results here obtained indicated that long-term culture exposure to CH_4 would promote the enrichment of high affinity (low K_S) microorganisms, although no significant influence of CH_4 concentration on K_S was observed. This empirical finding was in agreement with the fact that type I (which exhibit the highest affinities for CH_4) rather than type II methanotrophs were dominant in both R1 and R3. Whalen et al. (1990) reported K_S values for type I methanotroph-like cultures isolated from landfill cover soils as low as 2.5×10^{-6} M under gas CH_4 concentrations of 1–1.7 g m^{-3}, which are comparable to those recorded at week 19 in R1 and R3. In contrast, K_S values of $6.8 \times 10^{-5} - 4.7 \times 10^{-4}$ M are typically reported in literature for type II methanotrophs (Delhoménie et al., 2009; Hornibrook et al., 2009).

3.4. PHB accumulation

PHB was present as refractive inclusions or granules inside the methanotrophic cells, which were identified in the enriched cultures by their intracytoplasmatic membranes (Fig. 6). The transmission electron micrographs confirmed the microbiological feasibility of coupling CH_4 abatement with the production of an added value product such as PHB, which could significantly contribute to improve the economic viability of the process. Polyhydroxyalkanoate accumulation in methanotrophs can be induced under excess of C source and limitation in the availability of nutrients such as N, P or Mg (Asenjo and Suk, 1986), N limitation being the best scenario for PHB accumulation according to Wendlandt et al. (2001). Hence, the enrichment of methane-oxidizing bacteria capable of accumulating PHB was performed by operating the reactors under 8 sequential periods of N limitation. To the best of our knowledge, this is the first systematic study assessing the influence of different CH_4 concentrations and CH_4/biomass ratios on PHB accumulation by methanotrophic consortia.

PHB cell contents of 0.3–0.5% (*w/w*), 2.9–9.7% (*w/w*) and 0.1–0.8% (*w/w*) were recorded following the N limitation periods in R1, R2 and R3, respectively (Table 1). Despite sequential N limitations were expected to induce an increasing PHB accumulation, the biopolymer content was low and neither correlated with CH_4 concentration nor with the time course of the enrichment. Similar results were obtained by Pieja et al. (2012) in batch reactors subjected to sequential N limitations, although sequential CH_4 and N limitations indeed promoted PHB accumulation up to 24% (*w/w*). These results, compared to our particular study, were likely due to the use of the PHB-producer *Methylocystis parvus OBBP* and the use of C and N feast-famine

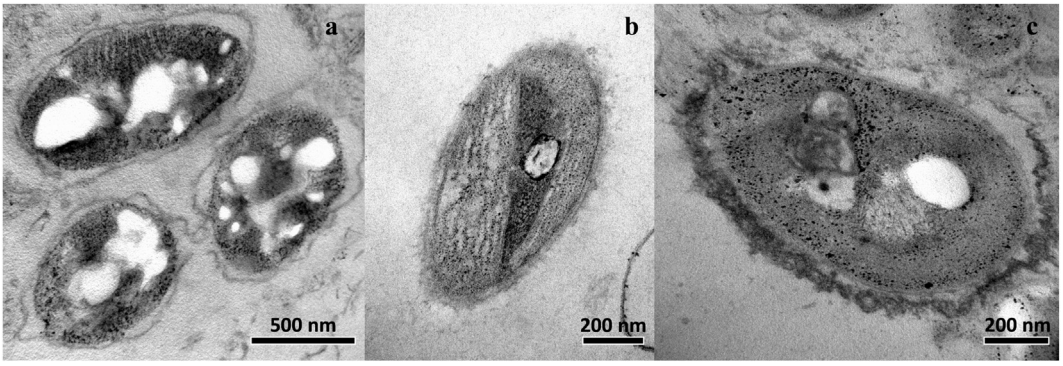

Fig. 6. Transmission electron micrographs of methanotrophic cells containing PHB enriched in R1 (**a**), R2 (**b**) and R3 (**c**) (60 000 ×, 120 000 × and 100 000 × magnification, respectively).

Table 1
Polyhydroxyalkanoate content in the biomass enriched in the three STRs following N limitation.

Cycle	R1		R2		R3	
	%PHB[a]	PHV:PHB	%PHB	PHV:PHB	%PHB	PHV:PHB
1	nd	nd	nd	nd	0.8 ± 0.0	3:1
2	nd	nd	3.2 ± 0.2	1:2	0.8 ± 0.0	2:1
3	nd	nd	3.1 ± 0.1	1:2	0.6 ± 0.0	2:1
4	nd	nd	9.7 ± 0.2	1:4	0.5 ± 0.1	3:1
5	nd	nd	7.5 ± 0.0	1:4	0.4 ± 0.0	4:1
6	0.3 ± 0.1	11:1	2.9 ± 0.1	1:2	0.5 ± 0.0	3:1
7	0.5 ± 0.1	10:1	4.3 ± 0.1	1:2	0.1 ± 0.0	3:1
8	0.3 ± 0.0	12:1	5.5 ± 0.2	1:3	0.5 ± 0.0	2:1
8 (3 days)	1.0 ± 0.1	3:1	12.6 ± 0.9	1:6	0.5 ± 0.0	3:1
8 (6 days)	0.6 ± 0.0	7:1	6.2 ± 0.1	1:7	0.4 ± 0.0	3:1
8 (10 days)	0.7 ± 0.0	6:1	6.4 ± 0.1	1:5	0.5 ± 0.0	4:1
8 (18 days)	0.6 ± 0.0	6:1	5.5 ± 0.3	1:5	1 ± 0.0	1:1

nd: not determined.
[a] %PHB = (gPHB/gTSS) × 100.

strategies. Methanotroph cultivation at higher CH_4/biomass ratios following the 8th N limitation episode initially resulted in the highest PHB cell contents in both R1 and R2 (1% and 12.6%, respectively), likely due to the higher bioavailability of the C source.

The differences in the PHB cell content of the communities enriched in the reactors at the different CH_4 concentrations can be explained by the different structure of these methanotrophic communities revealed by DGGE analysis (Fig. 3; Supplementary Data Annex). The key role of the type of methanotrophs on the ability to accumulate PHB was recently highlighted by Pieja et al. (2011), who suggested that only type II methanotrophs exhibited the ability to accumulate PHB under N limiting conditions. In our particular case, the highest abundance of type II methanotrophs (*Methylocystis* genus) was found in R2, which also corresponded to the community with the highest PHB contents.

GC–MS analyses revealed also the accumulation of poly-3-hydroxyvalerate (PHV) in the cultures enriched (Table 1). The highest PHV:PHB ratios were found in R1 (up to 12:1) and R3 (up to 4:1), which corresponded to the communities with the lowest PHB contents. The low PHB cell contents detected in both reactors could be attributed to the preferential microbial accumulation of PHV. In this regard, Zúñiga et al. (2013) reported maximum PHV:PHB ratios of 7:11 in a STR fed with CH_4 and citrate as carbon sources and highlighted that the co-production of polyhydroxyalkanoates such as PHV together with PHB can improve the mechanical properties and biodegradability of the composite biopolymers. In our particular study, the different PHV:PHB ratios obtained could be attributed to the use of consortia and CH_4 instead of pure cultures and CH_4/cosubstrates, as reported by Zúñiga et al. (2013).

4. Conclusions

The analysis of the pair-wise similarity indexes clearly showed that CH_4 concentration during culture enrichment determined the structure of the microbial populations, which exhibited rapid dynamics and high species evenness and richness. In addition, kinetic assays revealed high specific biodegradation capacities and affinities for CH_4, correlated to the dominance of type I/II methanotrophs rather than to CH_4 concentration. On the other hand, the use of sequential N limitations under continuous CH_4-laden air flow did not promote a high PHB accumulation in the cultures likely due to the low abundance of type II methanotrophs. Interestingly, the communities with lower PHB contents exhibited higher PHV contents. These findings brought new insights on the development of specific inocula not only to reduce the start-up period of bioreactors devoted to CH_4 abatement, but also to co-produce high-added value products. Although further experiments on optimizing the conditions for PHB/PHV production are still necessary, the industrial use of these high-added value products will certainly promote the application of biological processes for GHG emissions abatement.

Acknowledgments

This research was supported by the Spanish Ministry of Economy and Competitiveness (JCI-2011-11009 and BES-2013-063922 contracts; CTQ2012-34949 project). The contributions of Manuel Avella Romero and Teresa Martín Herrero (University of Valladolid) in the transmission electronic microscopy analyses are also gratefully acknowledged.

Appendix A. Supplementary data

Supplementary data related to this article can be found online at http://dx.doi.org/10.1016/j.jenvman.2014.06.026.

Nomenclature

STR	stirred tank reactor
VOC	volatile organic compound
PHB	poly-3-hydroxybutyrate
PHV	poly-3-hydroxyvalerate
TSS	total suspended solids (g L^{-1})
TOC	total organic carbon (mg L^{-1})
H	Shannon–Wiener diversity index (dimensionless)
K_S	half-saturation constant (M)
q_{max}	maximum specific biodegradation rate ($gCH_4\ g^{-1}_{biomass}\ h^{-1}$)

References

APHA, 2005. Standard Methods for the Examination of Water and Wastewater, twentyfirst ed. American Public Health Association, Whasington, D.C.
Asenjo, J.A., Suk, J., 1986. Microbial conversion of methane into poly-beta-hydroxybutyrate (PHB) – growth and intracellular product accumulation in a type-II methanotroph. J. Ferment. Technol. 64, 271–278.
Bender, M., Conrad, R., 1992. Kinetics of CH_4 oxidation in oxic soils exposed to ambient air or high CH_4 mixing ratios. FEMS Microbiol. Ecol. 101, 261–270.
Bozzola, J.J., 2007. Conventional specimen preparation techniques for transmission electron microscopy of cultured cells. In: Kuo, J. (Ed.), Electron Microscopy, Methods in Molecular Biology, vol. 369. Humana Press, Springer, pp. 1–18. http://dx.doi.org/10.1007/978-1-59745-294-6_1.
Chistoserdova, L., Lapidus, A., Han, C., Goodwin, L., Saunders, L., Brettin, T., Tapia, R., Gilna, P., Lucas, S., Richardson, P.M., Lidstrom, M.E., 2007. Genome of *Methylobacillus flagellatus*, molecular basis for obligate methylotrophy, and polyphyletic origin of methylotrophy. J. Bacteriol. 189, 4020–4027. http://dx.doi.org/10.1128/JB.00045-07.
Delhoménie, M.C., Nikiema, J., Bibeau, L., Heitz, M., 2009. A new method to determine the microbial kinetic parameters in biological air filters. Chem. Eng. Sci. 63, 4126–4136. http://dx.doi.org/10.1016/j.ces.2008.05.020.
Environmental Protection Agency, April 2013. Inventory of US Greenhouse Gas Emissions and Sinks: 1990–2011. EPA 430-R-13–001. http://epa.gov/climatechange/ghgemissions/usinventoryreport.html (accessed 21.01.14).
Estrada, J.M., Rodríguez, E., Quijano, G., Muñoz, R., 2012a. Influence of gaseous VOC concentration on the biodiversity and biodegradation performance of microbial communities. Bioproc. Biosyst. Eng. 35, 1477–1488. http://dx.doi.org/10.1007/s00449-012-0737-x.
Estrada, J.M., Kraakman, N.J.R., Lebrero, R., Muñoz, R., 2012b. A sensitivity analysis of process design parameters, commodity prices and robustness on the economics of odour abatement technologies. Biotechnol. Adv. 30, 1354–1363. http://dx.doi.org/10.1016/j.biotechadv.2012.02.010.
European Environment Agency, 2013. Annual European Union Greenhouse Gas Inventory 1990–2011 and Inventory Report 2013. http://www.eea.europa.eu/publications/european-union-greenhouse-gas-inventory-2013 (accessed 15.12.13).
Gebert, J., Gröngröft, A., Miehlich, G., 2003. Kinetics of microbial landfill methane oxidation in biofilters. Waste Manag. 23, 609–619. http://dx.doi.org/10.1016/S0956-053X(03)00105-3.
Gebert, J., Stralis-Pavese, N., Alawi, M., Bodrossy, L., 2008. Analysis of methanotrophic communities in landfill biofilters using diagnostic microarray. Environ. Microbiol. 10, 1175–1188. http://dx.doi.org/10.1111/j.1462-2920.2007.01534.x.

Hornibrook, E.R.C., Bowes, H.L., Culbert, A., Gallego-Sala, A.V., 2009. Methanotrophy potential versus methane supply by pore water diffusion in peatlands. Biogeosciences 6, 1491–1504.
Intergovernmental Panel on Climate Change, 2013. Fifth Assessment Report: Climate Change 2013, the Physical Science Basis. http://www.climatechange2013.org (accessed 21.01.14).
Kim, T.G., Jeong, S.Y., Cho, K.S., 2013. Functional rigidity of a methane biofilter during the temporal microbial succession. Appl. Microbiol. Biotechnol. 98, 3275–3286. http://dx.doi.org/10.1007/s00253-013-5371-2.
López, J.C., Quijano, G., Souza, T.S.O., Estrada, J.M., Lebrero, R., Muñoz, R., 2013. Biotechnologies for greenhouse gases (CH_4, N_2O and CO_2) abatement: state of the art and challenges. Appl. Microbiol. Biotechnol. 97, 2277–2303. http://dx.doi.org/10.1007/s00253-013-4734-z.
McDonald, G., 2003. Biogeography: space, time and life. Wiley, New York, p. 409.
Nikiema, J., Brzezinski, R., Heitz, M., 2007. Elimination of methane generated from landfills by biofiltration: a review. Rev. Environ. Sci. Biotechnol. 6, 261–284. http://dx.doi.org/10.1007/s11157-006-9114-z.
Pieja, A.J., Rostkowski, K.H., Criddle, C.S., 2011. Distribution and selection of poly-3-hydroxybutyrate production capacity in methanotrophic proteobacteria. Microb. Ecol. 62, 564–573. http://dx.doi.org/10.1007/s00248-011-9873-0.
Pieja, A.J., Sundstrom, E.R., Criddle, C.S., 2012. Cyclic, alternating methane and nitrogen limitation increases PHB production in a methanotrophic community. Bioresour. Technol. 107, 385–392. http://dx.doi.org/10.1016/j.biortech.2011.12.044.
Rocha-Rios, J., Bordel, S., Hernández, S., Revah, S., 2009. Methane degradation in two-phase partition bioreactors. Chem. Eng. J. 152, 289–292. http://dx.doi.org/10.1016/j.cej.2009.04.028.
Rocha-Rios, J., Muñoz, R., Revah, S., 2010. Effect of silicone oil fraction and stirring rate on methane degradation in a stirred tank reactor. J. Chem. Technol. Biotechnol. 85, 314–319. http://dx.doi.org/10.1002/jctb.2339.
Veillette, M., Viens, P., Avalos, A., Brzezinski, R., Heitz, M., 2011. Effect of ammonium concentration on microbial population and performance of a biofilter treating air polluted with methane. Chem. Eng. J. 171, 1114–1123. http://dx.doi.org/10.1016/j.cej.2011.05.008.
Walkiewicz, A., Bulak, P., Brzezinska, M., Wlodarczyk, T., Polakowski, C., 2012. Kinetics of methane oxidation in selected mineral soils. Int. Agrophys. 26, 401–406. http://dx.doi.org/10.2478/v10247-012-0056-0.
Wendlandt, K.D., Jechorek, M., Helm, J., Stottmeister, U., 2001. Producing poly-3-hydroxybutyrate with a high molecular mass from methane. J. Biotechnol. 86, 127–133. http://dx.doi.org/10.1016/S0168-1656(00)00408-9.
Whalen, S.C., Reeburgh, W.S., Sandbeck, K.A., 1990. Rapid methane oxidation in a landfill cover soil. Appl. Environ. Microbiol. 56, 3405–3411.
Yoon, S., Carey, J.N., Semrau, J.D., 2009. Feasibility of atmospheric methane removal using methanotrophic biotrickling filters. Appl. Microbiol. Biotechnol. 83, 949–956. http://dx.doi.org/10.1007/s00253-009-1977-9.
Zúñiga, C., Morales, M., Le Borgne, S., Revah, S., 2011. Production of polyhydroxybutyrate (PHB) by *Methylobacterium organophilum* isolated from a methanotrophic consortium in a two-phase partition bioreactor. J. Hazard. Mater. 190, 876–882. http://dx.doi.org/10.1016/j.jhazmat.2011.04.011.
Zúñiga, C., Morales, M., Revah, S., 2013. Polyhydroxyalkanoates accumulation by *Methylobacterium organophilum* CZ-2 during methane degradation using citrate or propionate as cosubstrates. Bioresour. Technol. 129, 686–689. http://dx.doi.org/10.1016/j.biortech.2012.11.120.

Assessing the influence of CH_4 concentration during culture enrichment on the biodegradation kinetics and population structure

*Juan C. López, Guillermo Quijano, Rebeca Pérez, Raúl Muñoz**

Department of Chemical Engineering and Environmental Technology, University of Valladolid, Dr. Mergelina, s/n, 47011, Valladolid, Spain. Tel. +34 983186424, Fax: 983423013.

*Corresponding author: mutora@iq.uva.es

Supporting Information Section

containing 6 pages, with 1 table.

DNA isolation, 16S rRNA gene amplification and DGGE analysis

Genomic DNA was extracted using the protocol described in the Fast® DNA Spin Kit for Soil handbook (MP Biomedicals, LLC), adjusting the time of binding of DNA to the silica matrix to 1 h. The V6-V8 regions of the bacterial 16S rRNA genes were amplified by Polymerase Chain Reaction (PCR) using the universal bacterial primers 968-F-GC and 1401-R (Sigma- Aldrich, St. Louis, MO, USA) (Nübel et al., 1996). The PCR mixture (50 µL) contained 1 µL of each primer (10 ng μL^{-1} each primer), 25 µL of BIOMIX ready-to-use 2× reaction mix (Bioline, UK), PCR reaction buffer and deoxynucleotide triphosphates (dNTPs), 2 µL of the extracted DNA and Milli-Q water up to the final volume. PCR was performed in a iCycler Thermal Cycler (Bio-Rad Laboratories, Hercules, CA) with the following thermo-cycling program for bacterial amplification: 2 min of pre-denaturation at 95ºC, 35 cycles of denaturation at 95ºC for 30 s, annealing at 56ºC for 45 s, and elongation at 72ºC for 1 min, with a final elongation at 72ºC for 5 min.

DGGE analysis of the amplicons was performed on 8% (*w/v*) polyacrylamide gels with an urea/formamide denaturing gradient of 45-65% (Roest et al., 2005). Electrophoresis was performed with a D-Code Universal Mutation Detection System (Bio-Rad Laboratories, Hercules, CA) in 0.5× Tris-acetate-EDTA (TAE) buffer at 60ºC and 85 V for 16 h. The gels were stained with GelRed Nucleic Acid Gel (1:10000 dilution) (Biotium Inc, Hayward, CA) for 1 h.

Sequencing and DNA sequence analysis

Individual bands were excised from the DGGE gel with a sterile blade, resuspended in 50 µL of ultrapure water, and maintained at 60ºC for 1 h to allow DNA extraction from the gel. A volume of 5 µL of the supernatant was used for reamplification with the original primer sets. Before sequencing, PCR products were purified using the GenElute PCR DNA Purification Kit (Sigma- Aldrich, St. Louis, MO, USA). The taxonomic position of the sequenced DGGE bands was obtained using the RDP classifier tool (50% confidence

level) (Wang et al., 2007). The closest matches to each band were obtained using the Standard Nucleotide BLAST search tool at the NCBI (National Centre for Biotechnology Information) (McGinnis and Madden, 2004). The absence of chimeras in the sequences was assessed using the DECIPHER search tool (Wright et al., 2012) before depositing them in GenBank Data Library under accession numbers KF957448 – KF957465. The DGGE patterns obtained were compared using the GelCompar IITM software (Applied Maths BVBA, Sint-Martens-Latem, Belgium). The gels were normalized by using internal standards within the DGGE gels. After image normalization, bands were defined for each sample using the bands search algorithm within the program. The software carried out a density profile analysis for each lane, detected the bands and calculated their relative contribution to the total band intensity in the lane, thus allowing the estimation of the relative abundances. Similarity indexes within the bacterial populations were calculated from the densitometric curves of the scanned DGGE profiles by using the Pearson product-moment correlation coefficient (Häne et al., 1993), and were subsequently used to depict the dendrogram by using UPGMA clustering with error resampling (500 resampling experiments). Peak heights in the densitometric curves were also used to determine the diversity indexes based on the Shannon-Wiener diversity index, calculated as follows (Equation 1):

$$H = -\sum \left[P_i \ln(P_i) \right] \quad (1)$$

where P_i is the importance probability of the bands in a lane ($P_i = n_i/n$, n_i is the height of an individual peak and n is the sum of all peak heights in the densitometric curves).

Table 1 SI. RDP classification of the bacterial DGGE bands sequences and corresponding matches (Standard Nucleotide BLAST) using the NCBI database with indication of the similarity percentages and sources of origin. The relative abundance of each band in the samples was ranked by x, xx or xxx

Taxonomic placement (50% confidence level)	Band n°	A	B	C	D	E	F	G	H	I	J	Closest relatives in Blast Name (accession number)	Similarity (%)	Source of origin
Phylum *Proteobacteria*														
Class *Gammaproteobacteria*	1		x	x								*Methylomicrobium agile* (EU144026)	93	Culture collection
Order *Methylococcales*														
Family *Methylococcaceae*	2		x	xx	x		x			x		*Methylomicrobium agile* (EU144026)	97	Culture collection
												Methylobacter sp.(AJ868427)	96	Soil exposed to low methane mixing ratios
	3		xxx	xxx		xx	xx		xxx	xx		*Methylomicrobium agile* (EU144026)	96	Culture collection
	4		xx	xx	xx		xxx	xx			x	*Methylobacter* sp.(AY007295)	99	Freshwater lake sediments
												Methylosarcina lacus (NR_042712)	99	Culture collection
												Methylomonas sp. (FR79895)	97	Wastewater treatment plant, wetland, biofilter and slurry pit
Genus *Methylosarcina*	5			x		xx	xx		xx		x	Uncultured bacterium (AB722248)	98	Freshwater iron-rich microbial mat at circumneutral pH
												Methylosarcina quisquiliarum (NR_025040)	96	Landfill soil
	6					xxx	xx		xxx			Uncultured bacterium (AB722248)	98	Freshwater iron-rich microbial mat at circumneutral pH
Genus *Methylomicrobium*	7		xxx	xxx		xxx	xxx	xx	xxx	xxx	xx	*Methylomicrobium agile* (EU144026)	99	Culture collection
												Methylomicrobium album (EU144025)	99	Culture collection
Genus *Methylobacter*	8			xx			xxx	x	xxx	xx	x	*Methylobacter* sp. (AY007295)	97	Freshwater lake sediments
Genus *Methylosoma*	9		xx				xxx	xx		xxx	xx	Uncultured bacterium (AB240311)	94	PCR-derived sequence from a rhizosphere biofilm of a reed bed reactor in laboratory-scale
Order *Xanthomonadales*														
Family *Xanthomondaceae*														
Genus *Dokdonella*	10		xxx	xxx	xx	x	x	xxx			xx	Uncultured bacterium (FJ660601)	99	Activated sludge from a full-scale wastewater treatment plant
												Dokdonella sp.(NR_044554)	99	Islander and composted potting soils
												Dokdonella fugitiva (NR_042397)	98	Potting soil
Genus *Rhodanobacter*	11		xxx	xxx		x	x	xx		x		Uncultured bacterium (FM213061)	99	Biotrickling filter removing H_2S from wastewater treatment sludge
												Uncultured *Rhodanobacter* sp. (HM447919)	97	Agricultural soil
Class *Betaproteobacteria*														
Order *Methylophilales*														
Family *Methylophilaceae*														
Genus *Methylobacillus*	12								xx			*Methylobacillus* sp. (JX099508)	93	Activated sludge from a wastewater treatment plant
Class *Alphaproteobacteria*														
Order *Rhizobiales*														
Family *Methylocystaceae*														
Genus *Methylocystis*	13	x	xxx	xxx		xx	xxx	xxx	xx	xxx	xx	*Methylocystis parvus* (AF150805)	96	Lake sediments
	14		xxx	xxx	xx	xx	xxx	xxx	x	xxx		*Methylocystis* sp. (AJ868423)	99	Soil exposed to low methane mixing ratios
												Uncultured bacterium (AB504613)	99	Down-flow hanging sponge reactor inoculated with activated sludge coming from a wastewater treatment plant.
												Methylocystis echinoides (NR_025544)	98	Sludge from a sewage treatment plant

Family *Hyphomicrobiaceae*														
Genus *Hyphomicrobium*	15		x	xxx		xx	xxx	xxx	xx	xxx	xx	Uncultured *Hyphomicrobium* sp. (JF515535)	100	Agricultural soil
												Uncultured bacterium (AY328641)	99	Drinking water from a distribution system simulator (DSS)
												Uncultured *Hyphomicrobium* sp. (JX504970)	98	Soil from both natural wetlands and an anthropogenic wetland of a paddy field
Phylum *Firmicutes*														
Class *Erysipelotrichia*														
Order *Erysipelotrichales*														
Family *Erysipelotrichaceae*														
Genus *Turicibacter*	16	x	x	x	xx		xx	x		x	x	Uncultured bacterium (KC551602)	94	Activated sludge from wastewater treatment plants
Phylum *Actinobacteria*														
Class *Actinobacteria*														
Subclass *Actinobacteridae*														
Order *Actinomycetales*														
Suborder *Corynebacterineae*														
Family *Nocardiaceae*														
Genus *Rhodococcus*	17			xxx				x	xx		x	*Rhodococcus yunnanensis* (KC493986)	99	Soil sample from a coastal wetland
												Rhodococcus sp. (JQ928360)	99	Domestic drinking water
Unclassified Bacteria	18	xx		xxx	xx		xx	x	x	x	x	Uncultured *Acidobacteria* bacterium (JN802215)	99	Biofilm attached to electrode materials in microbial fuel cell
												Uncultured *Acidobacterium* (AF368181)	97	Sludge from laboratory-scale sequencing batch reactors (SBR) fed with synthetic wastewater

References

Häne, B.G., Jäger, K., Drexler, H.G., 1993. The Pearson product-moment correlation coefficient is better suited for identification of DNA fingerprint profiles than band matching algorithms. Electrophoresis 14, 967-972. doi: 10.1002/elps.11501401154.

McGinnis, S., Madden, T.L., 2004. BLAST: at the core of a powerful and diverse set of sequence analysis tools. Nucleic Acids Res. 32, W20-W25. doi: 10.1093/nar/gkh435.

Nübel, U., Engelen, B., Felske, A., Snaidr, J., Wieshuber, A., Amann, R.I., Ludwig, W., Backhaus, H., 1996. Sequence heterogeneities of genes encoding 16S rRNAs in *Paenibacillus polymyxa* detected by temperatue gradient gel electrophoresis. J. Bacteriol. 178, 5636-5643.

Roest, K., Heilig, H.G., Smidt, H., de Vos, W.M., Stams, A.J.M., Akkermans, A.D.L., 2005. Community analysis of a full-scale anaerobic bioreactor treating paper mill wastewater. Syst. Appl. Microbiol. 28, 175-185. doi: 10.1016/j.syapm.2004.10.006.

Wang, Q., Garrity, G.M., Tiedje, J.M., Cole, J.R., 2007. Naive Bayesian classifier for rapid assignment of rRNA sequences into the new bacterial taxonomy. Appl. Environ. Microb. 73, 5261-5267. doi:10.1128/AEM.00062-07.

Wright, E.S., Yilmaz, L.S., Noguera, D.R., 2012. DECIPHER, a search-based approach to chimera identification for 16S rRNA sequences. Appl. Environ. Microb. 78, 717-725. doi: 10.1128/AEM.06516-11.

Chapter 6

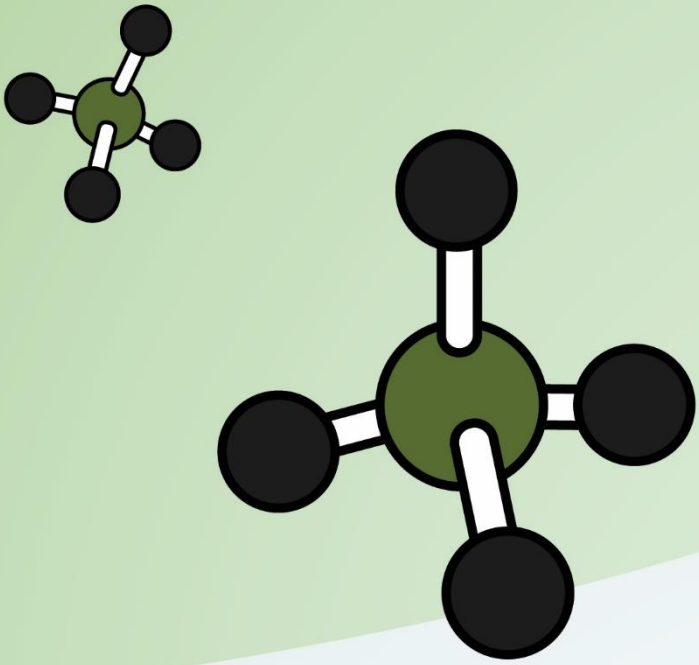

Biogas-based polyhydroxyalkanoates production by *Methylocystis hirsuta*: a step further in anaerobic digestion biorefineries

Biogas-based polyhydroxyalkanoates production by *Methylocystis hirsuta*: a step further in anaerobic digestion biorefineries

*Juan C. López, Esther Arnáiz, Laura Merchán, Raquel Lebrero, Raúl Muñoz,**

Department of Chemical Engineering and Environmental Technology, School of Industrial Engineerings, University of Valladolid, C/Dr. Mergelina s/n, 47011 Valladolid, Spain.

*Corresponding author: mutora@iq.uva.es, Tel. +34 983186424, Fax: +34 983423013.

Abstract

The potential of biogas (with and without H_2S) and volatile fatty acids (VFAs) to support microbial growth and accumulation of polyhydroxyalkanoates (PHAs) in type II methanotrophs was evaluated batchwise under aerobic conditions. *Methylocystis hirsuta* was able to grow on biogas (70 % CH_4, 29.5 % CO_2, 0.5 % H_2S) and accumulate PHA up to 45 ± 1 % (wt %) under N-limited conditions. The presence of CO_2 and H_2S did not significantly influence the growth and PHA synthesis in *M. hirsuta* compared to control tests provided with pure CH_4 at similar concentrations. Likewise, the addition of VFAs to the cultivation broth at initial concentrations of 100–200 mg L^{-1} did not hamper the growth of this strain on biogas. Indeed, the addition of 10 % extra carbon in the form of individual VFAs resulted in an increase in the maximum PHA yield and final PHA content up to 0.45–0.63 gPHA gSubstrate^{-1} and 48–54 % (wt %), respectively, at the expense of a higher energy demand. Valeric acid supplementation supported the highest 3-hydroxyvalerate content (13.5 %) within the biocomposite. In this context, this study demonstrated for the first time that 3-hydroxyvalerate synthesis by *M. hirsuta* did not depend on CH_4 assimilation.

Keywords: Biorefinery, methane, methanotroph, polyhydroxybutyrate, polyhydroxyvalerate, volatile fatty acid.

1 Introduction

Methane (CH_4), which accounts for 10-16% of the global warming impact worldwide, represents nowadays the second most important greenhouse gas. In nature, CH_4 is mainly emitted from the anaerobic decomposition of organic matter in wetlands and oceans. However, more than 60% of CH_4 emissions worldwide are anthropogenic [1-3]. Waste and wastewater treatment plants (WWTPs) represent one of the most significant emission sources of CH_4 (20000 ktons CO_2-eq in 2014 in the EU-28), which is often released in the form of a biogas typically composed of 50–70% CH_4, 30–50% CO_2 and 0–0.5% H_2S (*v/v*) [4,5]. Despite biogas constitutes a renewable energy source for heat and electricity generation, the high investment costs needed for on-site energy recovery or the high costs associated to biomethane production (1.08 € Nm^{-3} in the EU market compared to 0.30–0.67 € Nm^{-3} for natural gas) promote biogas flaring or venting to the atmosphere in low-medium size facilities [6,7]. In addition, the huge reserves of shale gas worldwide, along with its affordable extraction costs, do not forecast a scenario of increased natural gas prices (where biogas could advantageously compete). In this context, the development of cost-effective technologies for the bioconversion of biogas into high-added value products could eventually mitigate biogas emissions from waste/wastewater treatment facilities along with the implementation of anaerobic digestion as a platform for organic pollution control.

Polyhydroxyalkanoates (PHAs), such as poly-3-hydroxybutyrate (PHB), poly-3-hydroxyvalerate (PHV) and their copolymer (PHBV), are polyesters biologically produced under unbalanced nutrient conditions (e.g. N limitation). PHAs have the potential to substitute conventional plastics such as polyethylene or polypropylene due to their biocompatibility, biodegradability and their versatile thermal and mechanical properties. The market price of PHAs ranges from 4 to 20 € kg_{PHA}^{-1}, which greatly depends on the monomer composition of the biocomposite, the carbon source, the microbial strain used and the product purity [8]. Despite its rapid decrease in the past 5 years, the market price of PHAs is still higher than that of fossil-based polyesters due to the high costs of biopolymer downstreaming and carbon source acquisition, the later accounting for 30–40% of the final PHA price [7,8]. In this regard, CH_4 has recently emerged as a low-cost and environmentally friendly feedstock for PHA production [9,10]. To the best of the authors' knowledge, the studies reported to date on methanotrophic PHA production have been mainly restricted

to the use of pure CH_4 or natural gas as substrate [11-13]. Controversy still exists in literature about the technical and microbiological feasibility of biogas (containing the toxic and acid gases CO_2 and H_2S) as a feedstock for PHA production [11,14]. Moreover, the direct addition to the methanotrophic cultivation broth of volatile fatty acids (VFAs), which are readily available during anaerobic digestion, could increase PHA yields and tailor the composition of the biocomposite during biogas bioconversion. However, the few studies reported to date restrict the use of VFAs to their corresponding salts (i.e. sodium valerate, sodium propionate or sodium 3-hydroxybutyrate), which overcome the pH-associated effects of VFAs but hinder their applicability within this biorefinery concept. In this context, neither the potential of biogas nor the influence of VFA supplementation on PHA accumulation by methanotrophs have been yet systematically addressed [15-18]. A successful bioconversion of biogas into VFA-tailored biopolymers would represent the cornerstone of a new generation of biogas biorefineries supporting a low-cost and environmentally friendly conversion of residual organic matter into multiple high-added value products.

This study aimed at evaluating the feasibility of biogas as a feedstock to support the growth of the type II methanotroph *Methylocystis hirsuta* coupled to the synthesis of PHAs. Additionally, the potential of acetic, butyric, propionic and valeric acids to support *M. hirsuta* growth and modify the composition of the biogas-based PHA biocomposite was here evaluated for the first time.

2 Materials and methods

2.1 Strain, chemicals and culture conditions

The methanotrophic strain *Methylocystis hirsuta* was acquired from DSMZ culture collection (DSM No. 18500, Leibniz Institut, Germany). This type II methanotroph was selected based on its ability to produce PHB through the serine pathway [12]. Synthetic biogas (70 % CH_4, 29.5 % CO_2, 0.5 % H_2S), CH_4 (≥ 99.5 %), He (≥ 99.5 %), O_2 (≥ 99.5 %) and CO_2 (≥ 99.9 %) were purchased from Abelló Linde S.A. (Barcelona, Spain). Poly[(R)-3-hydroxybutyric acid-*co*-(R)-3-hydroxyvaleric acid] (molar ratio 88/12, ≥ 99.99 %), valeric acid (≥ 99 %) and butyric acid (≥ 99 %) were obtained from Sigma-Aldrich® (Sigma-Aldrich, St. Louis, USA). Acetic acid (≥ 99 %) was purchased from Cofarcas S.A. (Burgos, Spain). Additional reagents and chemicals were purchased from Panreac® (Barcelona, Spain) with a purity of at least 99 %.

Balanced growth cultures were cultivated in Whittenbury nitrate mineral salt (NMS) medium (pH of 6.8) [19]. NMS medium supplemented with agar at 1.5 % (*w/v*) was used to test culture purity along the experiment. In contrast, unbalanced growth cultures devoted to accumulate PHAs were incubated in a nitrate-free Whittenbury mineral salt medium (NFMS).

2.2 Experimental procedures

Inocula

M. hirsuta inocula were prepared in 125-mL serum bottles capped with butyl-rubber stoppers and crimp-sealed under a CH_4:O_2 headspace (35:65 % *v/v*) and sterile conditions (Figure 1). The serum bottles contained 50 mL of NMS inoculated at 10 % (*v/v*) and were incubated in an orbital shaker at 250 rpm and 25 ºC for 7 days, which entailed five CH_4:O_2 headspace renewals. The final optical density of the cultures at 600 nm (OD_{600}) was 4.0 ± 0.4 (total suspended solid concentration – TSS – of 1690 ± 169 mg L^{-1}). Unless otherwise specified, this inoculum was used for Test Series 1 – 4.

Test Series 1: Influence of biogas on M. hirsuta *growth*

The ability of *M. hirsuta* to grow on biogas (with and without H_2S) was assessed in triplicate in 2.15-L serum bottles capped with butyl-rubber stoppers and aluminium crimp seals under three different O_2-supplemented headspace atmospheres (*v/v*): H_2S-free biogas (CH_4:O_2:CO_2:He at 31.5:55.0:13.27:0.23 %), biogas (CH_4:O_2:CO_2:H_2S at 31.5:55.0:13.27:0.23 %) and control

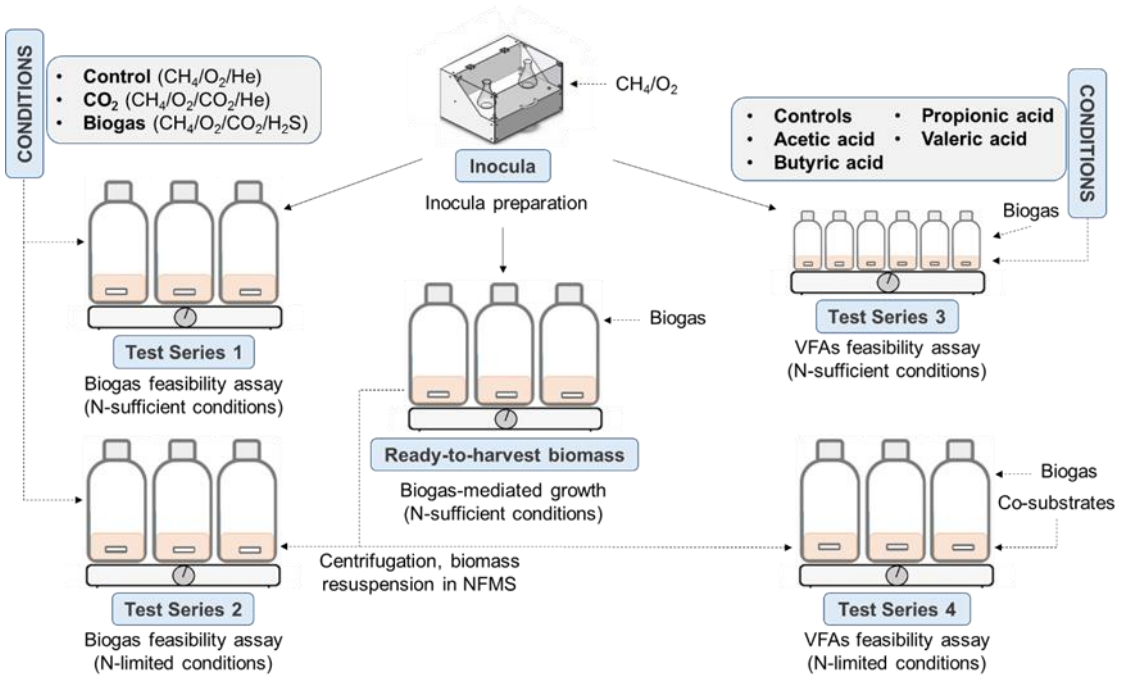

Figure 1. Test series overview.

(CH_4:O_2:He at 31.5:55.0:13.5 %). The headspace mixtures were prepared in 25 L-Tedlar bags (Sigma-Aldrich®, St. Louis, USA) using the appropriate volumes of each gas component from the cylinders and further pumped into the corresponding bottles in order to completely flush the air atmosphere out. The cultures, which contained 400 mL of NMS inoculated at 3 % (*v/v*) (initial OD_{600} of 0.13 ± 0.01, corresponding to 55 ± 2 mgTSS L^{-1}), were magnetically stirred at 300 rpm (Multipoint 15 Variomag, Thermo Fisher Scientific, Bartlesville, USA) and 25.0 ± 0.5 ºC in a temperature-controlled room. Abiotic controls for the three headspace mixtures were also prepared as above described to rule out any potential CH_4 removal due to adsorption or photolysis.

Test Series 2: Influence of biogas on PHA synthesis by M. hirsuta

M. hirsuta was initially grown as above described in 2.15-L serum bottles containing 400 mL of NMS inoculated at 3 % (*v/v*) under a CH_4:O_2:CO_2:H_2S atmosphere (31.5:55.0:13.27:0.23 %) for 9–12 days (to completely deplete CH_4 from the headspace). The methanotrophic biomass was harvested by centrifugation (10000 rpm, 8 min) and resuspended in NFMS. Then, the ability of biogas-grown *M. hirsuta* to accumulate PHAs was assessed in triplicate in 2.15-L serum bottles capped with butyl-rubber stoppers and aluminium crimp seals under three different O_2-supplemented headspace atmospheres (*v/v*): H_2S-free biogas (CH_4:O_2:CO_2:He at 31.5:55.0:13.27:0.23 %), biogas (CH_4:O_2:CO_2:H_2S at 31.5:55.0:13.27:0.23 %) and control (CH_4:O_2:He at 31.5:55.0:13.5 %). The bottles were incubated under magnetic agitation at 300 rpm and 25.0 ± 0.5 ºC in a temperature-controlled room.

Test Series 3: Influence of the type and concentration of VFA on biogas-based M. hirsuta *growth*

M. hirsuta was grown in VFA-supplemented 125 mL serum bottles capped with butyl-rubber stoppers and crimp-sealed under sterile conditions and a biogas headspace (CH_4:O_2:CO_2:H_2S at 31.5:55.0:13.27:0.23 %). The bottles, which initially contained 50 mL of NMS inoculated at 4 % (*v/v*) (initial OD_{600} of 0.15 ± 0.01, corresponding to 65 ± 2 mgTSS L^{-1}), were incubated at 300 rpm and 25.1 ± 0.3 ºC in a temperature-controlled room. The influence of the concentration of acetic, butyric, propionic and valeric acid (named C1–C5, where C1 represented the lowest and C5 the highest VFA concentration) on *M. hirsuta* growth was evaluated in duplicate in separate batch assays. The initial concentrations of acetic acid were 92 ± 10, 197 ± 5, 243 ± 2, 324 ± 5 and

482 ± 4 mg L^{-1}, of butyric acid 68 ± 1, 139 ± 3, 182 ± 7, 273 ± 2 and 345 ± 3 mg L^{-1}, of propionic acid 64 ± 2, 123 ± 2, 214 ± 26, 258 ± 0 and 320 ± 3 mg L^{-1} and of valeric acid 57 ± 5, 114 ± 1, 177 ± 3, 238 ± 4 and 292 ± 0 mg L^{-1}. These concentrations represented 16, 31, 47, 63 and 78 % of the C initially supplied as CH_4. Abiotic controls under a CH_4:O_2:CO_2:H_2S atmosphere (31.5:55.0:13.27:0.23 %) and an initial C2 concentration for each VFA were prepared to rule out any potential CH_4 or VFA removal due to adsorption or photolysis. Individual biogas-deprived controls at an initial C2 concentration for each VFA were included in this batch assay to evaluate the ability of the strain to remove the VFA in the absence of biogas. Cosubstrate-deprived controls under a CH_4:O_2:CO_2:H_2S atmosphere (31.5:55.0:13.27:0.23 %) were also conducted.

Test Series 4: Influence of the type of VFA on biogas-based PHA synthesis by M. hirsuta

M. hirsuta was initially grown as above described in 2.15-L serum bottles containing 400 mL of NMS inoculated at 3 % (*v/v*) under a CH_4:O_2:CO_2:H_2S atmosphere (31.5:55.0:13.27:0.23 %) for 9–12 days (to completely deplete CH_4 from the headspace). The methanotrophic biomass was again harvested by centrifugation (10000 rpm, 8 min) and resuspended in NFMS supplemented with either acetic, butyric, propionic and valeric acids at concentrations of 181 ± 16, 123 ± 2, 139 ± 1 and 130 ± 6 mg L^{-1}, respectively (corresponding to 10 % of the C initially supplied as CH_4). The bottles were finally crimp-sealed, filled with a fresh CH_4:O_2:CO_2:H_2S atmosphere (31.5:55.0:13.27:0.23 %) and incubated at 300 rpm and 25.0 ± 0.5 ºC. Abiotic controls under a CH_4:O_2:CO_2:H_2S atmosphere (31.5:55.0:13.27:0.23 %) and/or an initial C2 concentration for each VFA were prepared to rule out any potential CH_4 or VFA removal due to adsorption or photolysis. Individual biogas-deprived controls at an initial C2 concentration for each VFA were included in this batch assay to evaluate the ability of the strain to produce PHAs in the presence of VFA without biogas. Cosubstrate-deprived controls under a CH_4:O_2:CO_2:H_2S atmosphere (31.5:55.0:13.27:0.23 %) were also carried out to assess the influence of VFAs on the content and composition of the PHA synthesized.

The headspace concentration of CH_4, CO_2, O_2 and H_2S was periodically measured by GC-TCD in all test series. Liquid samples (3 mL) were periodically drawn to monitor the concentration of VFAs, PHAs, TSS and OD_{600} in all test series. Liquid samples (1 mL) were also randomly withdrawn to measure the

SO_4^{2-} concentration in the liquid phase by HPLC-IC in Test Series 1 and 2. The pH of the cultivation broth was measured at the beginning and at the end of each test series. Cultivation broth samples (100 µL) were systematically drawn from all test series to test strain purity in agar plates incubated under CH_4:O_2 atmosphere (35:65 % *v/v*) in 2 L-Tedlar bags.

2.3 Analytical methods

CH_4, O_2, CO_2 and H_2S gas concentrations were determined according to López et al. in a Bruker 430 GC-TCD (Bruker, Palo Alto, USA) equipped with a CP-Molsieve 5A (15 m × 0.53 mm × 15 mm) and a CP-PoraBOND Q (25 m × 0.53 mm × 10 mm) columns [20]. The determination of OD_{600} and TSS concentration was performed as described elsewhere [21]. SO_4^{2-} concentration in the liquid phase was determined by HPLC-IC according to López et al. [20]. Cultivation broth samples of 1 mL were filtered (0.22 µm) and acidified with 20 µL H_2SO_4 (96-97 % (*w/v*)) prior to VFAs analysis in an Agilent 7820A GC-FID (Agilent Technologies, Santa Clara, USA) equipped with a G4513A autosampler and a Chromosorb WAW packed column (2 m × 1/8" × 2.1 mm SS) (10 % SP 1000, 1 % H_3PO_4, WAW 100/120) (Teknokroma, Barcelona, Spain). The injector, oven and detector temperatures were maintained at 375, 130 and 350 °C, respectively. N_2 was used as the carrier gas at 45 mL min^{-1}.

Cultivation broth samples of 1.5 mL were centrifuged for 5 min at 13000 rpm and further processed according to López et al. [21]. The PHAs extracted from the samples were measured in a 7820A GC coupled with a 5977E MSD (Agilent Technologies, Santa Clara, USA) and equipped with a DB-wax column (30 m × 250 µm × 0.25 µm). The detector and injector temperatures were maintained at 250 ºC. The oven temperature was initially maintained at 40 ºC for 5 min, increased at 10 ºC min^{-1} up to 200 ºC and maintained at this temperature for 2 min. Finally, the oven temperature was increased up to 240 ºC at a rate of 5º C min^{-1}. The PHA content (wt %, w_{PHA}/w_{TSS}) of the samples, and the HB and HV fractions of the PHAs (mol %) were refered to the initial biomass concentration of the sample. The time course of the PHA yield (Y_{PHA}), based on the consumption of CH_4 or CH_4 and VFAs (and therefore expressed as gPHA gCH_4^{-1} or gPHA $gSubstrate^{-1}$, respectively), was estimated by dividing the mass of PHA produced by the mass of the substrate consumed at each sampling interval. The stoichiometry, kinetics and carbon distribution calculations were described in the Supporting Information section.

2.4 Statistical analyses

Arithmetic mean values and standard deviations were calculated for the replicate bottle cultures. The statistical data analysis was performed using OriginPro 8.5 (OriginLab Corporation, USA). The occurrence of significant differences within the data sets was analysed by a one-way analysis of variance (ANOVA) and a Tukey test. A Levene test was also applied to study homocedasticity. Differences were considered significant at $P \leq 0.05$.

3. Results and discussion

3.1 Biogas-based growth and PHA synthesis by *M. hirsuta*

Abiotic controls showed neither a significant CH_4/O_2 consumption nor CO_2 production along Test Series 1 and 2 (Figure S1, S2). On the other hand, the presence of CO_2 and H_2S (biogas with/without H_2S) did not result in significant differences either on *M. hirsuta* growth or CH_4/O_2 consumption compared to the cultures provided exclusively with CH_4 under N-sufficient conditions in Test Series 1 (Figure 2A, B, C; Figure S2A). Thus, CH_4 at 204 ± 3 g m^{-3} was completely depleted within 12 days of cultivation, which entailed the concomitant consumption of 78 % of the O_2 initially supplied, regardless of the headspace composition. Despite the fact that the presence of CO_2 could theoretically increase biomass productivity in methanotrophic cultures, similar net CO_2 and TSS productions of 279 ± 5 g m^{-3} and 619 ± 16 mg L^{-1}, respectively, were recorded regardless of the cultivation headspace (Figure 2, Figure S3A) [14]. In this context, the fraction of electrons used for energy generation (f_e) and cell assimilation (f_s) (estimated according to Rostkowski et al. [22], Supporting Information), the specific growth rates (μ) and the biomass yields (Y_X) were 0.48 ± 0.03, 0.52 ± 0.03, 0.30 ± 0.03 d^{-1} and 0.58 ± 0.03 gTSS gCH_4^{-1} under the three headspace compositions evaluated (Table S1). These values, which are strain-dependent and greatly influenced by the cultivation conditions, were identical to those previously reported for *M. parvus* OBBP when nitrate was used as nitrogen source [22]. These findings reinforced the hypothesis that neither CO_2 nor H_2S negatively affect the metabolism of type II species despite the decrease in the initial pH down to 6.12 ± 0.04. Surprisingly, H_2S rapidly disappeared from the headspace without resulting in an increase in SO_4^{2-} concentration in the culture broth, which suggested that it was completely solubilisized into the liquid phase (data not shown). In addition, no culture contamination by heterotrophic bacteria was found during the culture streak plating performed in Test Series 1 (and

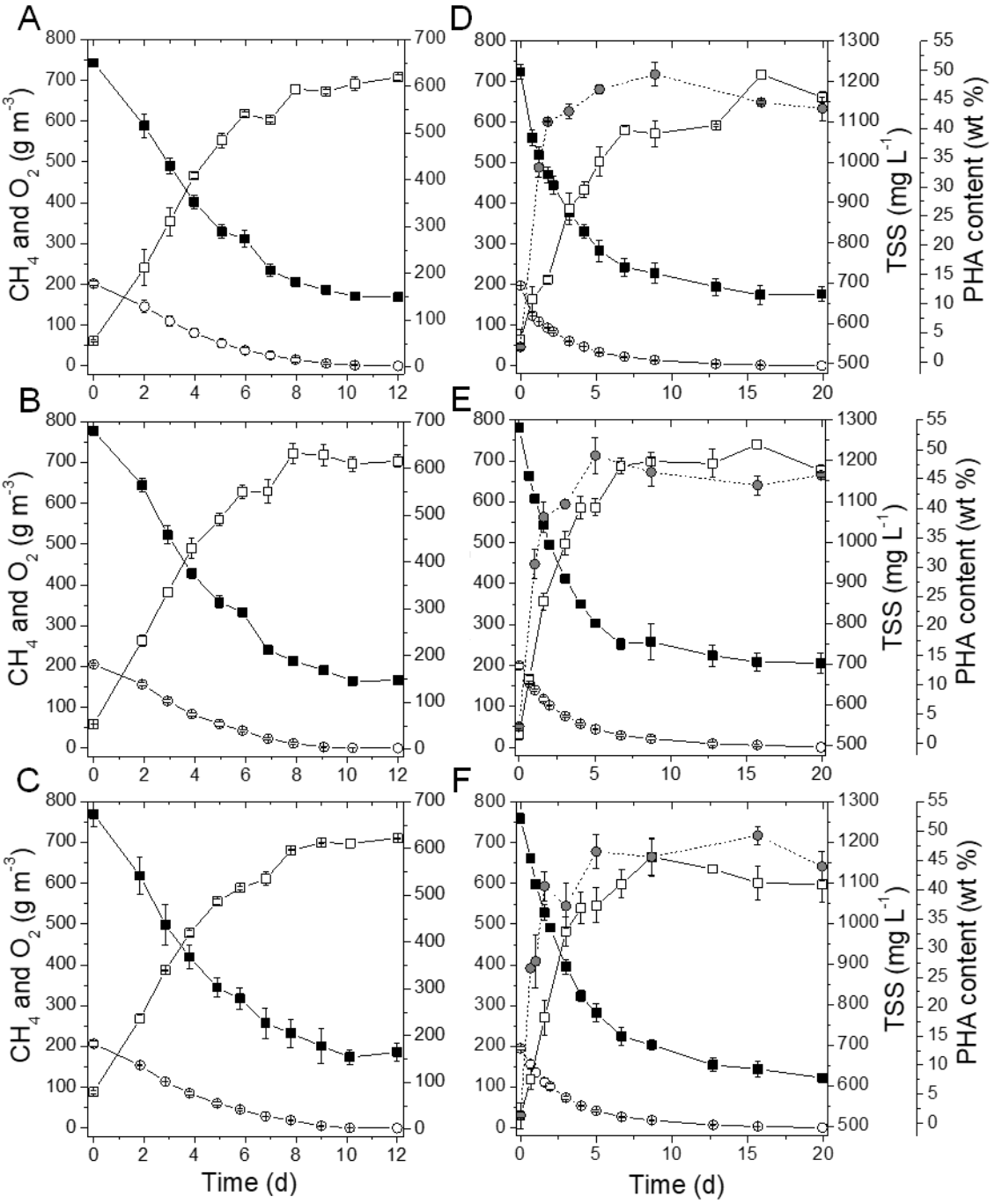

Figure 2. Time course of CH_4 (○), O_2 (■), TSS (□) and PHA (●) concentrations during the growth phase of Test Series 1 (A–C) and during the accumulation phase of test series 2 (D-F) using CH_4 (A, D), H_2S-free biogas (B, E) and biogas (C, F) as carbon and energy source. PHA content was not represented during the growth phase since contents below 1 % were found regardless of the headspace composition.

along Test Series 2, 3 and 4) (Figure S4).

Likewise, similar patterns of CH_4/O_2 consumption and biomass/PHA synthesis were observed during *M. hirsuta* cultivation in NFMS regardless of the headspace composition (Figure 2D, E, F, S3B). In this regard, the substrate partitioning parameter f_s increased up to 0.69 ± 0.02 compared to the previous

growth phase as a result of the electron deviation to PHB accumulation, regardless of the headspace composition (Table S2). Accordingly, a 2-fold decrease in μ (0.14 ± 0.01 d^{-1}) was observed during the accumulation phase likely mediated by extra energy requirements derived from PHB synthesis and by the metabolic unbalances caused by the lack of N in the culture medium (Table S2). More than 80 % of the final content of PHA (identified as PHB) accumulated during the first 48–72 h of cultivation. The PHA content remained constant at 45 ± 1 % (corresponding to a maximum Y_{PHA} = 0.44 ± 0.03 gPHB gCH_4^{-1}) from day 5 onwards for the three headspace conditions evaluated, which confirmed the potential of biogas (with and without H_2S) as a feedstock for biopolymer production (Figure 2D, E, F). The contents and yields of PHB here obtained were in agreement with previous findings on PHA production by *Methylocystis* species (PHA contents of 28–51 % and yields of 0.38–0.55 gPHB gCH_4^{-1}) [9,12-18,23,24]. At this point it should be stressed that the carbon mass balances carried out for Test Series 1 and 2 entailed an error < 10 %, which validated both the analytical and instrumental methods used in the current study (Tables S1, S2).

3.2 Effect of VFAs concentration on biogas-based *M. hirsuta* growth

Cosubstrate-deprived controls consumed CH_4 within the first 48–72 h, exhibiting similar CH_4 consumption rates to those obtained for acetic and propionic-supplemented cultures at C1 (Figure 3A, B; Figure S5). Acetic and propionic acids exhibited the largest inhibition on CH_4 consumption and *M. hirsuta* growth, C2 representing the highest concentration tolerated by this methanotrophic strain (Figure 3A, B; Table S3). In fact, negligible CH_4 and VFA degradations were observed at acetic and propionic acid concentrations higher than C3 (Figure 3A, B; Figure S6A, B). It must be also highlighted that the higher the concentration of acetic and propionic acids consumed by the strain, the higher the final TSS concentration reached (Table S3). Unlike type I methanotrophs, type II methanotrophs can grow at low pHs (4–7) and possess a complete tricarboxylic acid cycle pathway, including the α-ketoglutarate dehydrogenase enzyme that enables growth on organic acids [10,25]. However, the tolerance of type II methanotrophs to acetic acid seems to be species-dependent. For instance, repression of the transcription of the methane monooxygenase enzyme at acetate concentrations as low as 30 mg L^{-1} has been reported for *Methylocella* spp., while *Methylocystis* spp. and

Methylocella silvestris BL2 can grow at acetate concentrations of 210–360 mg L^{-1} [25-27]. In our particular study, *M. hirsuta* tolerated and was able to grow below ~200 mg acetic acid L^{-1} and at lower pHs (4.21) than previous studies (Figure S6A; Table S3). On the other hand, propionic acid induced a more severe inhibition on CH_4 consumption in *M. hirsuta,* with a ~3-fold reduction in the volumetric CH_4 removal rates at ~125 mg L^{-1} (compared to the test conducted at 200 mg acetic acid L^{-1}) despite the higher pH values here encountered (5.13) (Figure 3B, Figure S6B; Table S3). Similarly, Wieczorek et al. [28] reported the occurrence of a simultaneous biodegradation of CH_4 and propionate at ~180 mg L^{-1} and pH 4.8–5.1 in *Methylocystis* sp. cultures. Previous studies observed toxic effects of both acetate and propionate in *Methylocystis* species (pK_a values of 4.8 and 4.9, respectively) at pH < 4.8, where the protonated forms of these acids may alter the membrane potentials and uncouple ATP synthesis [28,29]. These findings are in agreement with the observed inability of our strain to grow at C3–C5 concentrations of acetic and propionic acids, and confirmed the hypothesis of a combined detrimental

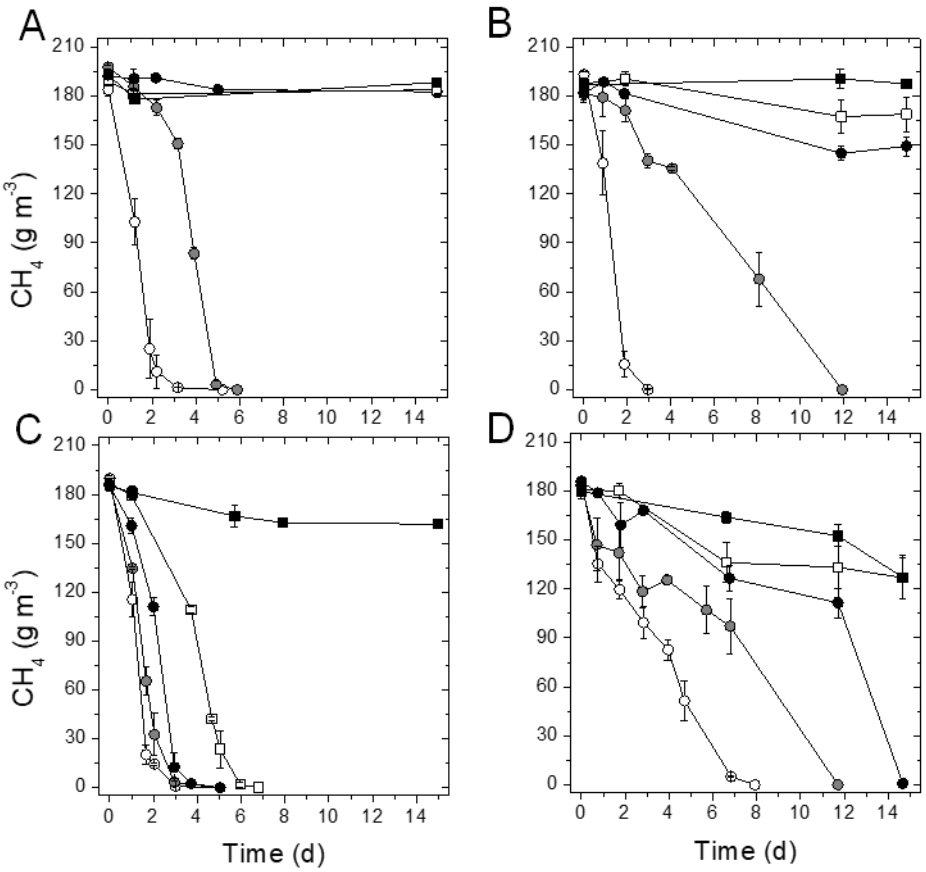

Figure 3. Time course of CH_4 concentration in the presence of A) acetic, B) propionic, C) butyric and D) valeric acids at C1 (○), C2 (◍), C3 (●), C4 (□) and C5 (■) concentrations (Test Series 3).

effect of pH and VFA on *M. hirsuta* growth.

On the contrary, the presence of butyric and valeric acids resulted in a lower detrimental effect on the ability of *M. hirsuta* to degrade CH_4, which can be attributed to the higher pHs induced by these VFAs in the cultivation medium (4.52 > pH < 5.78) (Figure 3C, D; Figure S6C, D; Table S3). Similar volumetric CH_4 consumption rates to those in cosubstrate-deprived controls were found in butyric-supplemented cultures at C1, though 2.7 times lower rates were obtained in the valeric-supplemented cultivations at the lowest concentration here tested (Figure 3C, D; Figure S5). Hence, *M. hirsuta* tolerated up to 273 ± 2 mg butyric acid L^{-1} (C4) and 177 ± 3 mg valeric acid L^{-1} (C3). In this context, the higher final TSS concentrations were recorded at increasing VFA concentrations consumed (Table S3). The maximum concentrations of butyric and valeric acids here tolerated by *M. hirsuta* were in the range of VFA concentrations previously tested in CH_4-based PHA production studies under controlled pH conditions (100–120 mg butyrate L^{-1} and 100–400 mg valerate L^{-1}) [15-17].

Finally, biogas-deprived controls cultivated at C2 concentration for each VFA demonstrated the ability of *M. hirsuta* to grow on acetic, propionic, butyric and valeric acids under nutrient-sufficient conditions (Figure S7). Surprisingly, the VFA consumption rates were slightly lower compared to those obtained when biogas was also supplied, which could be due to a higher activity of the C-1 driven electron transport chain enhanced by the oxidation of CH_4 (Figure S6). To the best of the authors' knowledge, this is the first work reporting the growth of a type II methanotroph on butyrate, valerate and propionate as the sole carbon and energy source.

3.3 Evaluation of the tailored PHA production via integration of biogas and VFAs biodegradation

C2 concentration was thus selected for the integration of both biogas and VFAs biodegradation towards a tailored PHA synthesis during Test Series 4. No significant CH_4 or VFA degradation was recorded in the abiotic controls, which ruled out any potential removal of these compounds due to adsorption or photolysis (Figures S8, S9). The supplementation of the cultivation broth with acetic, butyric and propionic acids in the absence of biogas under N limitation did not enhance PHA accumulation, the maximum PHA content being 2.8 % (> 91 % mol 3HB fraction) (Table 1). Surprisingly, the highest content of PHAs among the control tests without biogas was

Table 1. Final content and composition of the PHA synthesized by *M. hirsuta* during the biodegradation of biogas and/or VFAs under N limitation (Test Series 4).

Culture condition	PHA		
	PHA content (% w_{PHA}/w_{TSS})	3HB fraction (mol %)	3HV fraction (mol %)
Biogas	43.1 ± 1.8	100	0
Acetic acid	2.4 ± 0.4	98	2
Propionic acid	1.1 ± 0.7	91	9
Butyric acid	1.8 ± 0.9	99	1
Valeric acid	9.0 ± 1.7	17	83
Biogas + Acetic acid	52.3 ± 0.7	100	0
Biogas + Propionic acid	47.9 ± 0.7	98	2
Biogas + Butyric acid	52.2 ± 2.1	100	0
Biogas + Valeric acid	53.8 ± 0.8	75	25

obtained with valeric acid (up to 9.0 ± 1.7 % PHA), which entailed a high 3HV fraction of 83 mol %. These results suggested that the synthesis of PHV in *M. hirsuta* was not strictly linked to the assimilation of CH_4. In contrast, Myung et al. [16] found that *Methylocystis parvus* OBBP was not able to accumulate PHAs using valerate as the sole carbon and energy source, which highlights the higher metabolic versatility of *M. hirsuta*. It must be noticed that no biomass formation was observed during *M. hirsuta* cultivation on VFAs as the sole carbon source during the accumulation phase, where the carbon belonging to VFAs was mainly deviated towards the production of CO_2 (Table S4). The use of biogas as the sole substrate during the accumulation phase supported similar maximum Y_{PHA} and PHA contents to those found during Test Series 2 (0.41 ± 0.02 gPHA $gSubstrate^{-1}$ and 43 ± 2 %, respectively), with 3HB as the main monomer within the biocomposite (Table 1, Table S4). The addition of propionic, acetic or butyric acid as co-substrates during biogas biodegradation by *M. hirsuta* enhanced PHA accumulation, which increased from 43.1 ± 1.8 % up to 47.9 ± 0.7, 52.3 ± 0.7 and 52.2 ± 2.1 %, respectively. This represented a 10–20 % increase in PHA accumulation over the basal content obtained only with biogas and matched the increase in the maximum Y_{PHA} (by 10–30 %) achieved (Table S4). To the best of the authors' knowledge, there are no previous studies evaluating the supplementation of acetate as co-substrate during CH_4-based PHA accumulation by

methanotrophic bacteria, which could presumably act as direct precursor for the synthesis of 3-hydroxybutyryl-CoA and thus, of 3HB units (Figure 4). The final PHA content here reported for the simultaneous cultivation of *M. hirsuta* in propionic and biogas were higher than those found by Myung et al. using pure CH_4 and propionate at 100 mg L^{-1} (32 ± 4 %) [16]. Surprisingly, the 3HV fraction obtained by these authors with *M. parvus* OBBP (25 mol %) significantly differed from the one obtained in *M. hirsuta* in the present study (2 mol %), which suggests that propionic acid bioconversion in methanotrophic bacteria is species-dependent [16]. The PHA contents and HB:HV ratios here obtained were comparable to those obtained in *M. parvus* OBBP when butyrate was supplemented together with CH_4 (55 ± 3 %, 100:0 ratio) [17]. In our particular study, the highest PHA content was found when valeric acid was used as co-substrate during biogas-based *M. hirsuta* cultivation, which resulted in a final PHA content of 53.8 ± 0.8 % (corresponding to a maximum Y_{PHA} = 0.63 ± 0.05 gPHA $gSubstrate^{-1}$) and a 3HB:3HV ratio of 75:25 (Table 1, Table S4). Maximum PHA contents of 54 ± 4 %, with 3HB:3HV ratios of 75:25 and Y_{PHA} of 0.67 gPHA $gSubstrate^{-1}$ have been reported in *Methylocystis* species when valerate was added together with CH_4 [15,17,18]. Likewise, previous studies have consistently demonstrated that fatty acids assimilation by methanotrophic bacteria is an energy intensive process, which increases f_e when co-substrates such as valerate are supplemented [16,30]. In this regard,

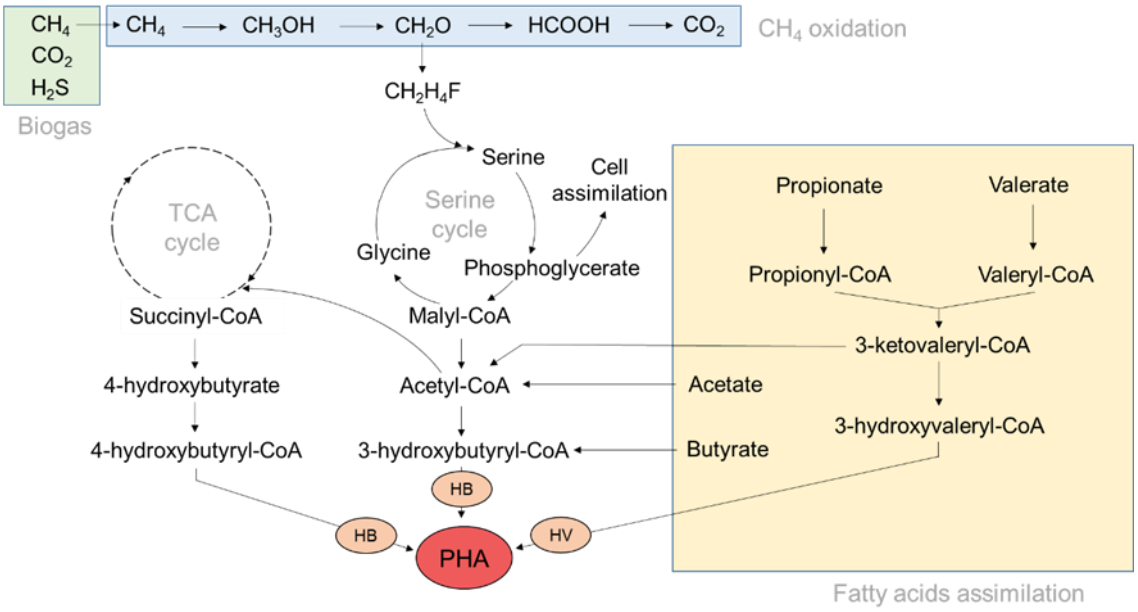

Figure 4. Tentative PHA production pathway for type II methanotrophs using both biogas and VFAs as carbon sources. Dotted arrows indicate the existence of intermediates not mentioned for clarity purposes. The pathways proposed are based on previous CH_4-driven PHA accumulation studies [15,17].

Bahr et al. demonstrated that the lower the carbon oxidation-reduction state (CORS) of a pollutant, the higher the energy requirements (and therefore the oxygen demands) during the cultivation of a methanotrophic bacterial consortium [31]. In our particular study, a gradual increase in f_e was observed as the CORS of the VFA decreased. Thus, f_e increased from 0.52 ± 0.02 under acetic acid (CORS = 0) cultivation to 0.94 ± 0.05 under valeric acid (CORS = -6) co-addition, the later likely explaining the reduced biomass growth observed (Table S4). These f_e values were higher than those previously obtained during PHA accumulation under valerate co-supplementation, which could be attributed to the lower pHs here encountered [15,16].

4 Conclusions

Biogas (with and without H_2S) supported a similar growth and PHA accumulation (under nitrogen limitation) to pure CH_4 in *M. hirsuta* cultures, which confirmed for the first time the feasibility of biogas-based biorefineries devoted to the production of these high-added value product. *M. hirsuta* was able to use acetic, butyric, propionic and valeric acids as the sole carbon and energy source. This study also demonstrated the potential of the individual supplementation of these VFAs to modify the composition of the biocomposite, valeric acid supporting up to 25 % HV fraction within the whole biopolymer. Further research is still needed to elucidate the effects of the multiple supplementation of VFAs on biogas-based *M. hirsuta* growth and PHA synthesis.

Acknowledgments

This research was supported by the Spanish Ministry of Economy and Competitiveness, the European Union through the FEDER Funding Program (CTM2015-70442-R and RED NOVEDAR projects and BES-2013-063922 contract) and the Regional Government of Castilla y León (UIC71). J. Prieto and E. Marcos are gratefully acknowledged for their practical assistance during PHA extractions and VFA analyses, respectively.

References

[1] Intergovernmental Panel on Climate Change, Fifth assessment report: Climate change 2014, Synthesis Report. https://www.ipcc.ch/report/ar5/syr/, 2014 (accessed 12.03.17).

[2] Environmental Protection Agency, Inventory of US greenhouse gas emissions and sinks: 1990-2014. http://epa.gov/climatechange/ghgemissions/usinventoryreport.html, 2016 (accessed 12.03.17).

[3] J.C. López, G. Quijano, T.S.O Souza, J.M. Estrada, R. Lebrero, R.

Muñoz, Biotechnologies for greenhouse gases (CH_4, N_2O, and CO_2) abatement: State of the art and challenges, Appl. Microbiol. Biotechnol. 97(6) (2013) 2277–2303; DOI 10.1007/s00253-013-4734-z.

[4] European Environment Agency, Annual European Union Greenhouse Gas Inventory 1990 - 2014 and Inventory Report 2016. http://www.eea.europa.eu//publications/european-union-greenhouse-gas-inventory-2016, 2016 (accessed 12.03.17).

[5] G. Gupta, K.N. Bhardwaj, C. Choudhary, P. Chandna, K.K. Jain, A. Kaur, S. Kumar, B. Shrivastava, S. Ninawe, A. Singh, R.C. Kuhad, Biofuels: The environment-friendly energy carriers, in: A. Singh, R.C. Kuhad (Eds.) Biotechnology for Environmental Management and Resource Recovery, Springer India: New Delhi, India, 2013, pp. 125–148.

[6] J. Vestman, S. Liljemark, M. Svensson, Cost benmarking of the production and distribution of biomethane/CNG in Sweden. http://www.sgc.se/ckfinder/userfiles/files/SGC296_v2.pdf, 2014 (accessed 15.03.17).

[7] Eurostat Statistics Explained, Natural gas price statistics. http://ec.europa.eu/eurostat/statistics-explained/index.php/Natural_gas_price_statistics, 2016 (accessed 15.03.17).

[8] E. Bugnicourt, P. Cinelli, A. Lazzeri, V. Alvarez, The main characteristics, properties, improvements, and market data of polyhydroxyalkanoates, in: V.K. Thakur, M.K. Thakur (Eds.), Handbook of sustainable polymers: Processing and applications, first ed., Pan Stanford Publishing Pte. Ltd., Boca Ratón, 2016, pp. 899–928.

[9] K.H. Rostkowski, C.S. Criddle, M.D. Lepech, Cradle-to-gate life cycle assessment for a cradle-to-cradle cycle: biogas-to-bioplastic (and back), Environ. Sci. Technol. 46 (18) (2012) 9822–9829; DOI 10.1021/es204541w.

[10] P.J. Strong, S. Xie, W.P. Clarke, Methane as a resource: Can the methanotrophs add value?, Environ. Sci. Technol. 49 (7) (2015) 4001–4018; DOI 10.1021/es504242n.

[11] D. van der Ha, L. Nachtergaele, F.M. Kerckhof, D. Rameiyanti, P. Bossier, W. Verstraete, N. Boon, Conversion of biogas to bioproducts by algae and methane oxidizing bacteria, Environ. Sci. Technol. 46 (2012) 13425–13431; DOI 10.1021/es303929s.

[12] F. Rahnama, E. Vasheghani-Farahania, F. Yazdian, S.A. Shojaosadati, PHB production by *Methylocystis hirsuta* from natural gas in

a bubble column and a vertical loop bioreactor, Biochem. Eng. J. 65 (2012) 51–56; DOI 10.1016/j.bej.2012.03.014.

[13] J. Myung, Microbial enrichment enabling stable production of poly(3-hydroxybutyrate) using pipeline natural gas, in: Recovery of resources and energy using methane-utilizing bacteria: synthesis and regeneration of biodegradable, tailorable bioplastics and production of nitrous oxide, Ph.D. Dissertation, Stanford University, California, U.S., 2016.

[14] O.P. Karthikeyan, K. Chidambarampadmavathy, S. Cirés, K. Heimann, Review of sustainable methane mitigation and biopolymer production, Crit. Rev. Env. Sci. Tec. 45 (15) (2015) 1579–1610; DOI 10.1080/10643389.2014.966422.

[15] J. Myung, W.M. Galega, J.D. van Nostrand, T. Yuan, J. Zhou, C.S. Criddle, Long-term cultivation of a stable *Methylocystis*-dominated methanotrophic enrichment enabling tailored production of poly(3-hydroxybutyrate-*co*-3-hydroxyvalerate), Biores. Technol. 198 (2016) 811–818; DOI 10.1016/j.biortech.2015.09.094.

[16] J. Myung, J.C.A. Flanagan, R.M. Waymouth, C.S. Criddle, Methane or methanol-oxidation dependent synthesis of poly(3-hydroxybutyrate-*co*-3-hydroxyvalerate) by obligate type II methanotrophs, Process Biochem. 51(5) (2016) 561–567; DOI 10.1016/j.procbio.2016.02.005.

[17] J. Myung, J.C.A. Flanagan, R.M. Waymouth, C.S. Criddle, Expanding the range of polyhydroxyalkanoates synthesized by methanotrophic bacteria through the utilization of omega-hydroxyalkanoate co-substrates, AMB Expr. 7 (2017) 118; DOI 10.1186/s13568-017-0417-y.

[18] A.J. Cal, W.D. Sikkema, M.I. Ponce, D. Franqui-Villanueva, T.J. Riiff, W.J. Orts, A.J. Pieja, C.C. Lee, Methanotrophic production of polyhydroxybutyrate-*co*-hydroxyvalerate with high hydroxyvalerate content, Int. J. Biol. Macromol. 87 (2016) 302–307; DOI 10.1016/j.ijbiomac.2016.02.056.

[19] R. Whittenbury, K.C. Phillips, J.F. Wilkinson, Enrichment, isolation, and some properties of methane-utilizing bacteria, J. Gen. Microbiol. 61 (1970) 205–218.

[20] J.C. López, E. Porca, G. Collins, R. Pérez, A. Rodríguez-Alija, R. Muñoz, G. Quijano, Biogas-based denitrification in a biotrickling-filter: Influence of nitrate concentration and hydrogen sulfide, Biotechnol. Bioeng. 114(3) (2017) 665–673; DOI 10.1002/bit.26092.

[21] J.C. López, G. Quijano, R. Pérez, R. Muñoz, Assessing the influence of CH_4 concentration during culture

enrichment on the biodegradation kinetics and population structure, J. Environ. Manage. 146 (2014) 116–123; DOI 10.1016/j.jenvman.2014.06.026.

[22] K.H. Rostkowski, A.R. Pfluger, C.S. Criddle, Stiochiometry and kinetics of the PHB-producing type II methanotrophs *Methylosinus trichosporium* OB3b and *Methylocystis parvus* OBBP, Biores. Technol. 132 (2013) 71–77; DOI 10.1016/j.biortech.2012.12.129.

[23] J. Helm, K.D. Wendlandt, G. Rogge, U. Kappelmeyer, Characterizing a stable methane-utilizing mixed culture used in the synthesis of a high-quality biopolymer in an open system, J. Appl. Microbiol. 101 (2006) 387–395.

[24] A.J. Pieja, K.H. Rostkowski, C.S. Criddle, Distribution and selection of poly-3-hydroxybutyrate production capacity in methanotrophic proteobacteria, Microb. Ecol. 62 (2011) 564–573; DOI 10.1007/s00248-011-9873-0.

[25] S.N. Dedysh, C. Knief, P.F. Dunfield, *Methylocella* species are facultatively methanotrophic, J. Bacteriol. 187(13) (2005) 4665–4670; DOI 10.1128/JB.187.13.4665–4670.2005.

[26] M.T. Rahman, A. Crombie, H. Moussard, Y. Chen, J.C. Murrell, Acetate repression of methane oxidation by supplemental *Methylocella silvestris* in a peat soil microcosm, Appl. Environ. Microb. 77(12) (2011) 4234–4236; DOI 10.1128/AEM.02902-10.

[27] S.E. Belova, M. Baani, N.E. Suzina, P.L.E. Bodelier, W. Liesack, S.N. Dedysh, Acetate utilization as a survival strategy of peat-inhabiting *Methylocystis* spp., Environ. Microbiol. Rep. 3(1) (2011) 36–46; DOI 10.1111/j.1758-2229.2010.00180.x.

[28] A.S. Wieczorek, H.L. Drake, S. Kolb, Organic acids and ethanol inhibit the oxidation of methane by mire methanotrophs, FEMS Microbiol. Ecol. 77 (2011) 28–39; DOI 10.1111/j.1574-6941.2011.01080.x.

[29] J.B. Russel, Another explanation for the toxicity of fermentation acids at low pH: anion accumulation vs. uncoupling, J. Bacteriol. 73 (1992) 363–370.

[30] V.N. Shishkina, Y.A. Trotsenko, Multiple enzymic lesions in obligate methanotrophic bacteria, FEMS Microbiol. Lett. 13 (1982) 237–242.

[31] M. Bahr, A.J.M. Stams, F. De la Rosa, P.A. García-Encina, R. Muñoz, Assessing the influence of the carbon oxidation-reduction state on organic pollutant biodegradation in algal-bacterial photobioreactors, Appl. Microbiol. Biot. 90 (2011) 1527–1536; DOI 10.1007/s00253-011-3204-8.

Biogas-based polyhydroxyalkanoates production by *Methylocystis hirsuta*: a step further in anaerobic digestion biorefineries

*Juan C. López, Esther Arnáiz, Laura Merchán, Raquel Lebrero, Raúl Muñoz**

Department of Chemical Engineering and Environmental Technology, School of Industrial Engineerings, University of Valladolid, C/Dr. Mergelina s/n, 47011 Valladolid, Spain.

*Corresponding author: mutora@iq.uva.es, Tel. +34 983186424, Fax: +34 983423013.

Supporting Information Section

containing 13 pages, with 9 figures and 4 tables.

Materials and methods

Stoichiometry, kinetics and carbon distribution

The stoichiometry of methanotrophic growth under both nutrient-sufficient and nutrient-limited conditions has been previously described elsewhere [1,2]. According to Rostkowski et al., methanotrophic cell synthesis involves the use of a fraction of electrons (f_e) from CH_4 to reduce O_2 to H_2O (with a concomitant production of energy), while the remaining fraction (f_s) is derived to cell synthesis [1]. Thus, CH_4 metabolism requires O_2 as i) the terminal electron acceptor to produce energy (Eq. 1), and ii) a reactant during the first step of methane monooxygenase attack on CH_4 within the electron donor reaction (Eq. 2).

$$f_e\ (1/4\ [O_2 + 4H^+ + 4e^- \rightarrow 2H_2O]) \quad \text{(Eq. 1)}$$

$$1/4\ [CH_4 + O_2 \rightarrow CO_2 + 4H^+ + 4e^-] \quad \text{(Eq. 2)}$$

The nature of the micro- and macronutrients greatly influences the stoichiometry of the cell synthesis half reaction, which can be expressed by Eq. (3) when nitrate is the sole nitrogen source and biomass is represented by the empirical formula $C_5H_7O_2N$ [3].

$$f_s\ (1/28\ [5CO_2 + NO_3^- + 29H^+ + 28e^- \rightarrow C_5H_7O_2N + 11H_2O]) \quad \text{(Eq. 3)}$$

Thus, the overall stoichiometric reaction for the microbial biodegradation of CH_4 (Eq. 4) using nitrate as the nitrogen source can be obtained by suming up Eq. (1), (2) and (3):

$$1/4\ CH_4 + (1/4 + f_e/4)O_2 + (f_s/28)NO_3^- + (29/28f_s + f_e - 1)H^+ \rightarrow (1/4 - 5f_s/28)CO_2 + (f_e/2 + 11f_s/28)H_2O + (f_s/28)C_5H_7O_2N \quad \text{(Eq. 4)}$$

Therefore, the number of moles of O_2 consumed per mole of CH_4 oxidized is $1 + f_e$, where $f_e + f_s = 1$. On the other hand, the biomass yield (Y_X, gTSS gCH_4^{-1}) depends also on the nitrogen source employed and can be then calculated as $113f_s/28$:4. In addition, the specific growth rate due to biomass synthesis (μ, d^{-1}) can be calculated using Eq. (5) under no mass transfer limitation [3]:

$$\mu = (1/X_a \times dX_a/dt) \quad \text{(Eq. 5)}$$

where X_a is the concentration of active biomass (gTSS L^{-1}) and t the reaction time (d^{-1}).

During PHA accumulation, the overall stoichiometry can be also expressed in terms of PHA (with an empirical formula of $C_4H_6O_2$), which formation does not require nitrogen (Eq. 6) [1,2]:

$$1/4\ CH_4 + (1/4 + f_e/4)O_2 \rightarrow (1/4 - 2f_s/9)CO_2 + (f_e/2 + f_s/3)H_2O + (f_s/18)C_4H_6O_2 \quad \text{(Eq. 6)}$$

Results and Discussion

Biogas-based growth and PHA synthesis by *M. hirsuta*

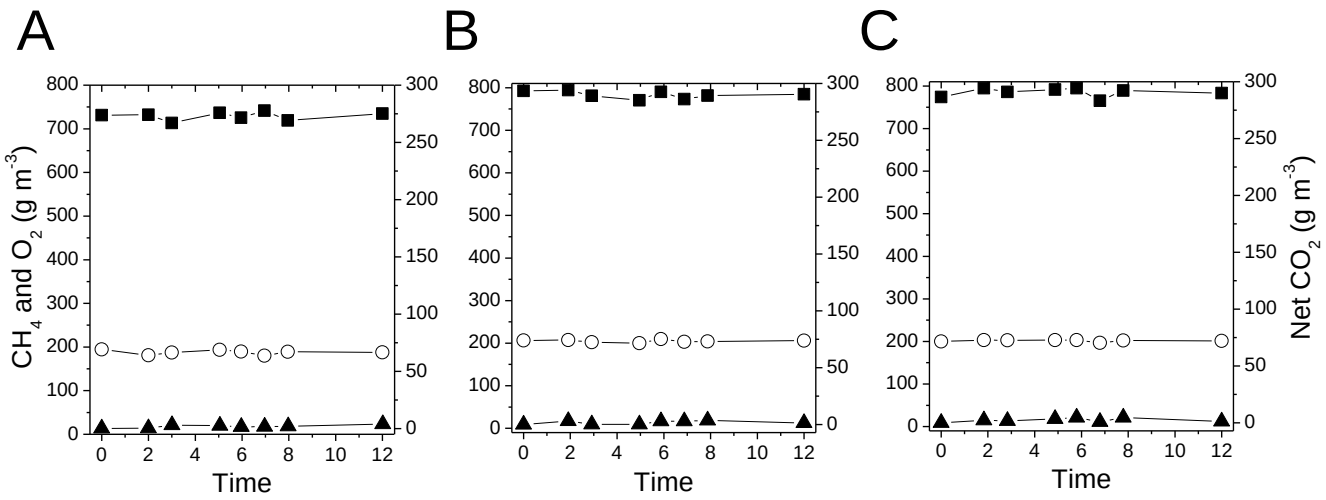

Figure S1. Time course of the CH_4 (○), O_2 (■) and net CO_2 (▲) concentration in the abiotic controls during the growth phase in Test Series 1 using CH_4 (A), H_2S-free biogas (B) and biogas (C) as headspace conditions. Net CO_2 concentration was calculated by subtracting the actual CO_2 concentration to the initial concentration in the bottles containing H_2S-free biogas and biogas.

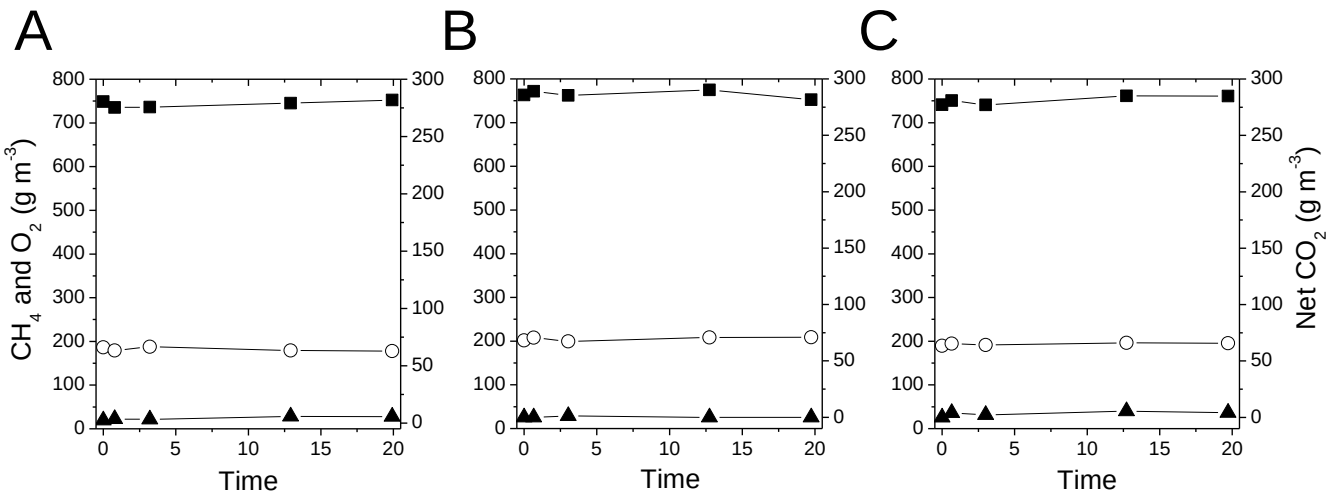

Figure S2. Time course of the CH_4 (○), O_2 (■) and net CO_2 (▲) concentration in the abiotic controls during the accumulation phase in Test Series 2 using CH_4 (A), H_2S-free biogas (B) and biogas (C) as headspace conditions. Net CO_2 concentration was calculated by subtracting the actual CO_2 concentration to the initial concentration in the bottles containing H_2S-free biogas and biogas.

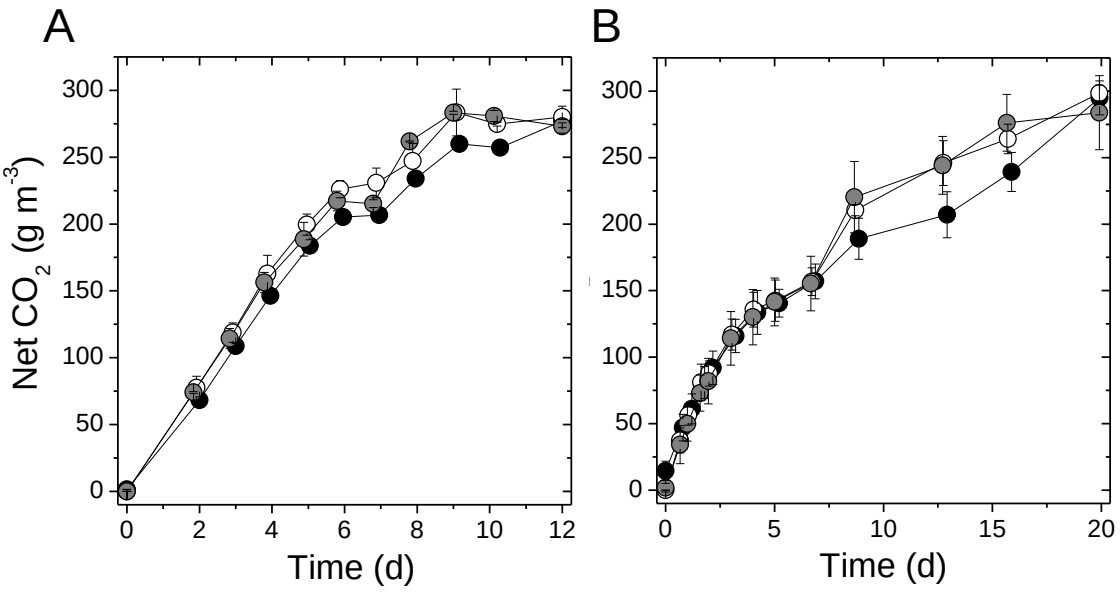

Figure S3. Time course of the net CO_2 concentration during the growth phase in Test Series 1 (A) and during the accumulation phase in Test Series 2 (B) using CH_4 (●), H_2S-free biogas (○) and biogas (◍) as a carbon and energy source. Net CO_2 concentration was calculated by subtracting the actual CO_2 concentration to the initial concentration in the bottles containing H_2S-free biogas and biogas.

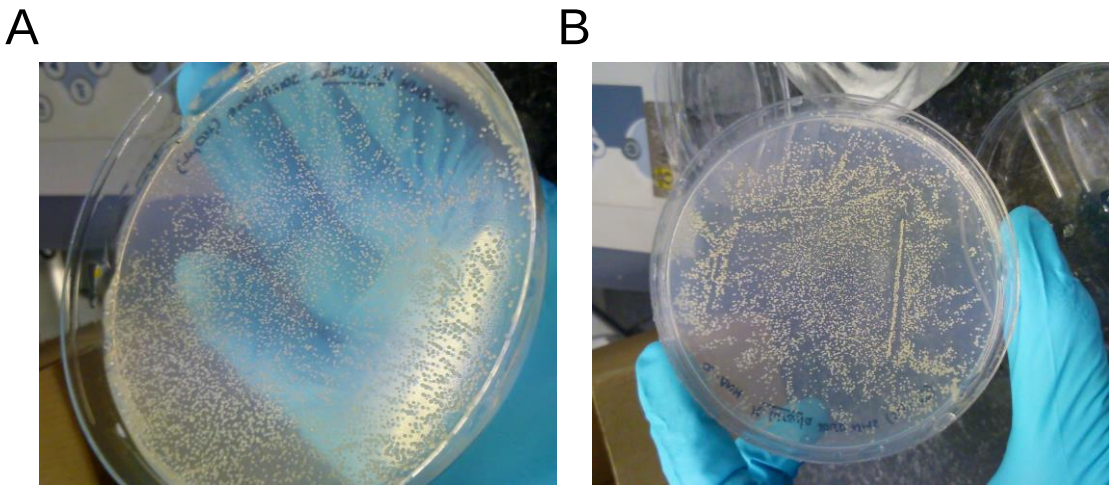

Figure S4. Solid cultures of *M. hirsuta* from culture samples at the end of Test Series 1 (A) and 4 (B).

Table S1. Substrate partitioning parameters (f_e, f_s), cellular yield (Y_X), specific growth rate (μ) and carbon distribution during the growth phase of *M. hirsuta* under the three different headspace compositions (Test Series 1).

Test serie	f_e	f_s	Y_X (gTSS gCH_4^{-1})	μ (d^{-1})	Carbon balances (C-mmol)			
					CH_4	CO_2	Biomass	Balance error (%)
Control	0.47 ± 0.01	0.53 ± 0.01	0.60 ± 0.01	0.31 ± 0.05	27.1 ± 0.3	14.6 ± 0.1	11.0 ± 0.1	5.6
H_2S-free biogas	0.51 ± 0.04	0.49 ± 0.04	0.55 ± 0.05	0.31 ± 0.02	27.3 ± 0.3	14.9 ± 0.4	10.9 ± 0.2	5.6
Biogas	0.47 ± 0.01	0.53 ± 0.01	0.60 ± 0.01	0.29 ± 0.01	27.6 ± 0.1	15.0 ± 0.1	10.9 ± 0.1	6.3

Table S2. Substrate partitioning parameters (f_e, f_s), PHA yield (Y_{PHA}), specific growth rate (μ) and carbon distribution during the accumulation phase of *M. hirsuta* under the three different headspace compositions (Test Series 2).

Test serie	f_e	f_s	Maximum Y_{PHA} (gPHA gCH_4^{-1})	μ (d^{-1})	Carbon balances (C-mmol)				
					CH_4	CO_2	Biomass	PHA	Balance error (%)
Control	0.30 ± 0.02	0.70 ± 0.02	0.46 ± 0.02	0.13 ± 0.00	26.9 ± 0.2	14.6 ± 0.1	6.3 ± 0.2	5.6 ± 0.1	1.5
H_2S-free biogas	0.33 ± 0.02	0.67 ± 0.02	0.44 ± 0.02	0.14 ± 0.00	26.6 ± 0.7	14.7 ± 0.3	6.5 ± 0.3	5.9 ± 0.7	1.6
Biogas	0.32 ± 0.03	0.68 ± 0.03	0.42 ± 0.04	0.14 ± 0.01	26.8 ± 0.4	13.2 ± 0.1	6.0 ± 0.1	5.8 ± 0.4	6.7

Effect of VFAs concentration on biogas-based *M. hirsuta* growth

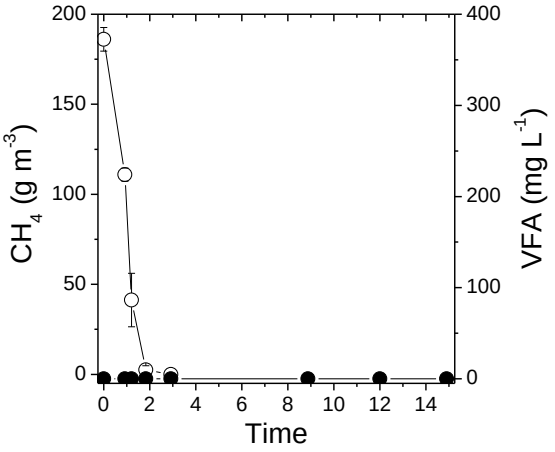

Figure S5. Time course of CH_4 (○) and VFA concentration (●) in cosubstrate-deprived controls during Test Series 3.

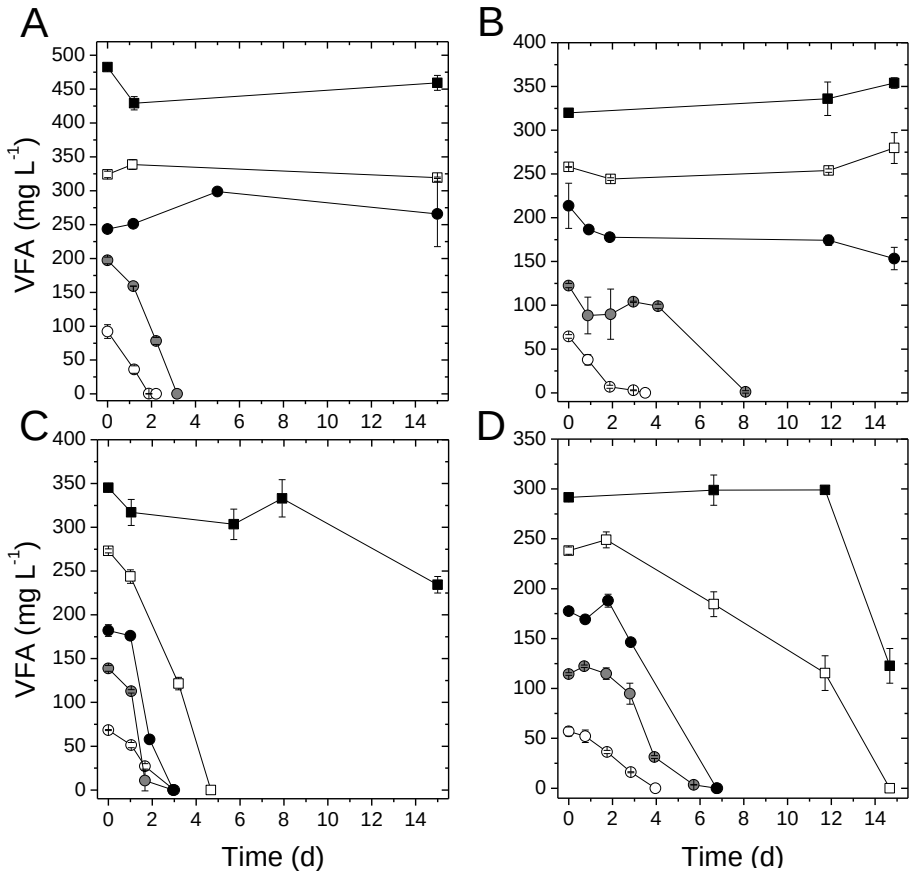

Figure S6. Time course of the concentrations of A) acetic, B) propionic, C) butyric and D) valeric acids at C1 (○), C2 (◍), C3 (●), C4 (□) and C5 (■) cultivations (Test Series 3).

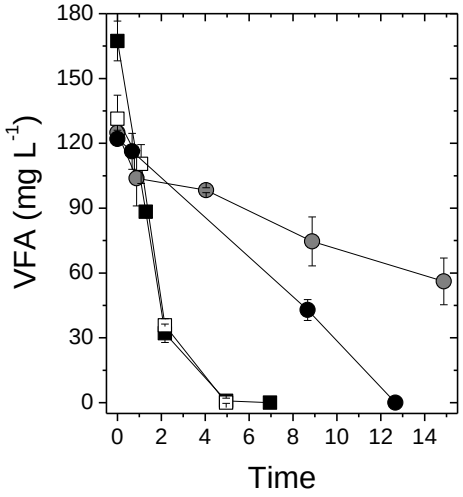

Figure S7. Time course of the concentrations of acetic (■), propionic (◍), butyric (□) and valeric (●) acids at C2 concentration in biogas-deprived controls (Test Series 3).

Table S3. Initial and final pH and final TSS concentration during Test Series 3.

Condition	VFA concentration	Initial pH	Final pH	Maximum TSS concentration (mg L^{-1})
Biogas	-	6.12 ± 0.02	6.09 ± 0.04	222 ± 5
Acetic acid	C2	4.92 ± 0.03	6.92 ± 0.02	93 ± 2
Propionic acid	C2	5.84 ± 0.05	6.34 ± 0.04	106 ± 10
Butyric acid	C2	5.67 ± 0.01	6.66 ± 0.01	108 ± 1
Valeric acid	C2	6.18 ± 0.04	6.62 ± 0.01	94 ± 2
Biogas + Acetic acid	C1	5.30 ± 0.05	6.85 ± 0.17	242 ± 9
	C2	4.21 ± 0.04	6.31 ± 0.32	284 ± 5
	C3	3.75 ± 0.08	4.73 ± 0.04	83 ± 7
	C4	3.53 ± 0.02	4.43 ± 0.01	73 ± 0
	C5	3.38 ± 0.04	4.28 ± 0.01	63 ± 2
Biogas + Propionic acid	C1	5.68 ± 0.10	6.08 ± 0.07	271 ± 7
	C2	5.13 ± 0.04	6.00 ± 0.01	294 ± 8
	C3	4.43 ± 0.04	5.47 ± 0.03	86 ± 0
	C4	4.05 ± 0.01	5.03 ± 0.01	84 ± 3
	C5	3.80 ± 0.00	4.82 ± 0.05	85 ± 8
Biogas + Butyric acid	C1	5.56 ± 0.06	6.31 ± 0.07	281 ± 5
	C2	4.96 ± 0.02	6.27 ± 0.24	310 ± 7
	C3	4.76 ± 0.00	6.17 ± 0.08	335 ± 4
	C4	4.52 ± 0.07	6.12 ± 0.03	357 ± 7
	C5	3.79 ± 0.03	4.96 ± 0.02	73 ± 7
Biogas + Valeric acid	C1	5.78 ± 0.02	6.48 ± 0.15	277 ± 7
	C2	5.47 ± 0.05	6.25 ± 0.08	301 ± 3
	C3	5.02 ± 0.10	6.09 ± 0.01	310 ± 6
	C4	4.57 ± 0.01	6.08 ± 0.05	138 ± 5
	C5	4.08 ± 0.03	6.00 ± 0.04	123 ± 15

Evaluation of the tailored PHA production via integration of biogas and VFAs biodegradation

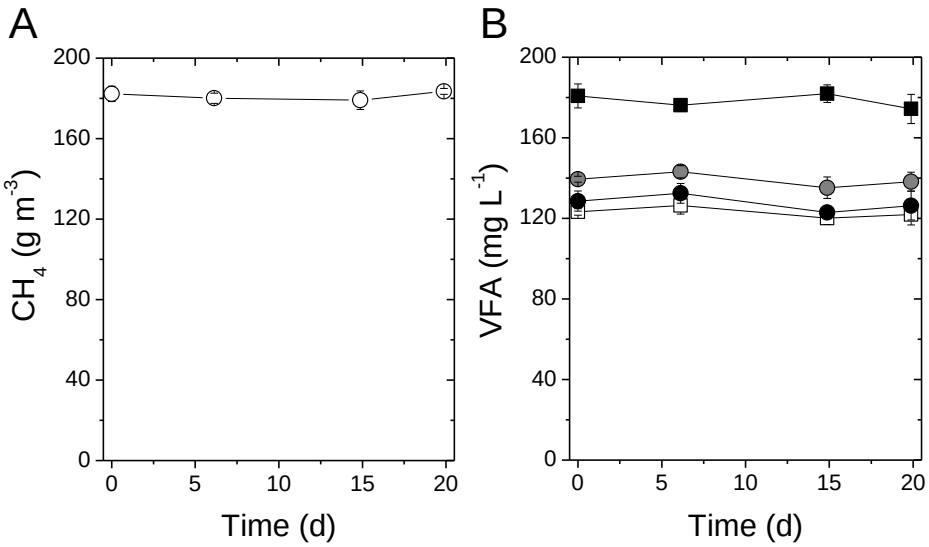

Figure S8. Time course of the concentrations of A) CH_4 and B) acetic (■), propionic (●), butyric (□) and valeric (●) acids in the abiotic cosubstrate-deprived controls and biogas-deprived controls, respectively (Test Series 4).

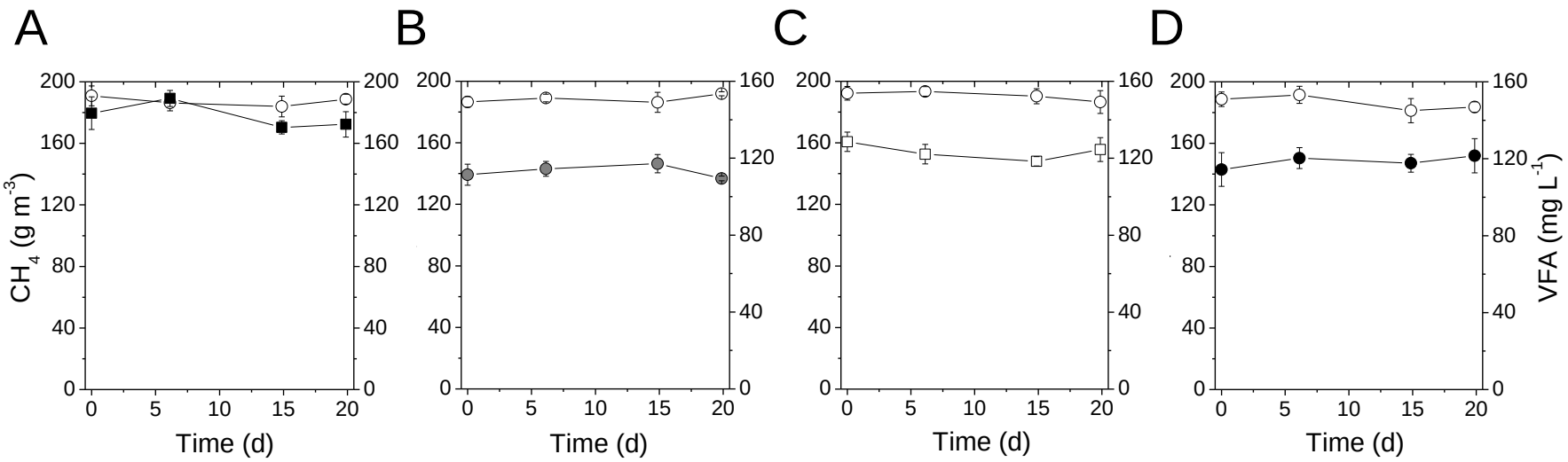

Figure S9. Time course of the concentrations of CH_4 (○), acetic (■), propionic (●), butyric (□) and valeric (●) acids in the abiotic controls supplemented with both biogas and VFA at C2 concentration for A) acetic, B) propionic, C) butyric and D) valeric acid (Test Series 4).

Table S4. Substrate partitioning parameters (f_e, f_s), PHA yield (Y_{PHA}) and carbon distribution during the accumulation phase of *M. hirsuta* in Test Series 4.

Test serie	f_e	f_s	Maximum Y_{PHA} (gPHA $gSubstrate^{-1}$)	Carbon balances (C-mmol)					
				CH_4	VFA	CO_2	Biomass	PHA	Balance error (%)
Biogas	0.34 ± 0.05	0.66 ± 0.05	0.41 ± 0.02	26.1 ± 0.5	-	14. ± 0.3	5.8 ± 0.5	4.8 ± 0.3	4.1
Acetic acid	nd[a]	nd	< 0.1	-	2.4 ± 0.1	2.3 ± 0.0	-	0.0 ± 0.0	4.3
Propionic acid	nd	nd	< 0.1	-	1.8 ± 0.1	1.7 ± 0.1	-	-	6.2
Butyric acid	nd	nd	< 0.1	-	2.3 ± 0.1	2.3 ± 0.1	-	0.0 ± 0.0	1.8
Valeric acid	nd	nd	0.1	-	2.2 ± 0.2	2.1 ± 0.1	-	0.1 ± 0.0	1.4
Biogas + Acetic acid	0.52 ± 0.02	0.48 ± 0.02	0.50 ± 0.04	27.0 ± 0.9	2.3 ± 0.0	17.7 ± 0.7	5.4 ± 0.0	6.2 ± 0.0	3.4
Biogas + Propionic acid	0.59 ± 0.03	0.41 ± 0.03	0.45 ± 0.03	27.0 ± 0.2	2.3 ± 0.0	17.7 ± 0.4	5.0 ± 0.2	4.8 ± 0.1	6.2
Biogas + Butyric acid	0.83 ± 0.03	0.17 ± 0.03	0.54 ± 0.02	25.8 ± 0.1	2.3 ± 0.0	16.6 ± 0.2	5.4 ± 0.0	6.0 ± 0.0	0.3
Biogas + Valeric acid	0.94 ± 0.05	0.06 ± 0.05	0.63 ± 0.05	25.9 ± 0.6	2.6 ± 0.1	18.8 ± 0.4	3.3 ± 0.0	4.1 ± 0.	8.3

[a]nd: not determined

References

[1] K.H. Rostkowski, A.R. Pfluger, C.S. Criddle, Stiochiometry and kinetics of the PHB-producing type II methanotrophs *Methylosinus trichosporium* OB3b and *Methylocystis parvus* OBBP, Biores. Technol. 132 (2013) 71–77; DOI 10.1016/j.biortech.2012.12.129.

[2] J. Myung, J.C.A. Flanagan, R.M. Waymouth, C.S. Criddle, Methane or methanol-oxidation dependent synthesis of poly(3-hydroxybutyrate-*co*-3-hydroxyvalerate) by obligate type II methanotrophs, Process Biochem. 51(5) (2016) 561–567; DOI 10.1016/j.procbio.2016.02.005.

[3] B.E. Rittmann, P.L. McCarty, P.L., Environmental Biotechnology: Principles and Applications, first ed., McGraw-Hill, Boston, U.S., 2001.

Chapter 7

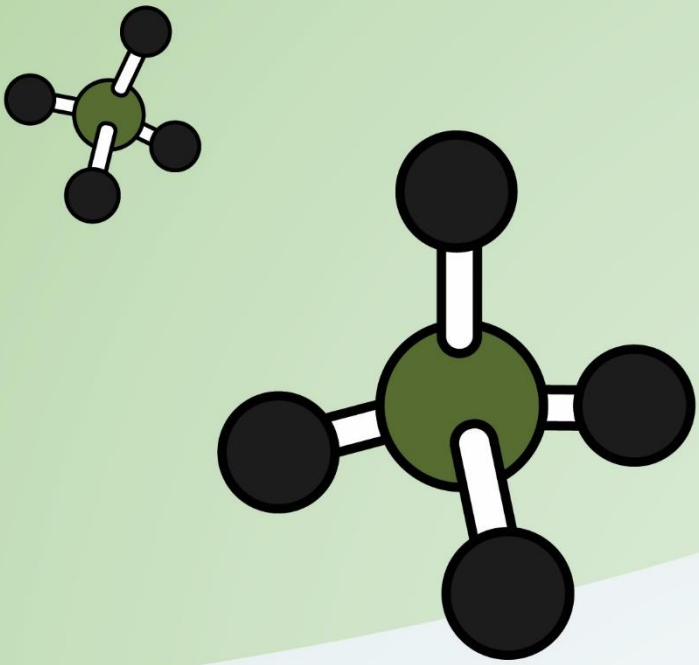

Biogas-based denitrification in a biotrickling filter: Influence of nitrate concentration and hydrogen sulfide

ARTICLE

BIOTECHNOLOGY and BIOENGINEERING

Biogas-Based Denitrification in a Biotrickling Filter: Influence of Nitrate Concentration and Hydrogen Sulfide

Juan C. López,[1,2] Estefanía Porca,[2] Gavin Collins,[2] Rebeca Pérez,[1] Alberto Rodríguez-Alija,[1] Raúl Muñoz,[1] Guillermo Quijano[1,3]

[1]Department of Chemical Engineering and Environmental Technology, University of Valladolid, Dr. Mergelina, s/n, Valladolid 47011, Spain; telephone: +34-975129404; fax: +34-975129401; e-mail: gquijano@iq.uva.es

[2]Microbial Communities Laboratory, School of Natural Sciences and Ryan Institute, National University of Ireland Galway, University Road, Galway H91 TK33, Ireland

[3]Laboratory for Research on Advanced Processes for Wastewater Treatment – Engineering Institute, Juriquilla Academic Unit, National Autonomous University of Mexico (UNAM), Blvd. Juriquilla 3001, Querétaro 76230, Mexico

ABSTRACT: The feasibility of NO_3^- removal by the synergistic action of a prevailing denitrifying anoxic methane oxidising (DAMO), and nitrate-reducing and sulfide-oxidising bacterial (NR-SOB) consortium, using CH_4 and H_2S from biogas as electron donors in a biotrickling filter was investigated. The influence of NO_3^- concentration on N_2O production during this process was also evaluated. The results showed that NO_3^- was removed at rates up to 2.8 g $m_{reactor}^{-3}$ h^{-1} using CH_4 as electron donor. N_2O production rates correlated with NO_3^- concentration in the liquid phase, with a 10-fold increase in N_2O production as NO_3^- concentration increased from 50 to 200 g m^{-3}. The use of H_2S as co-electron donor resulted in a 13-fold increase in NO_3^- removal rates (~18 gNO_3^- m^{-3} h^{-1}) and complete denitrification under steady-state conditions, which was supported by higher abundances of *narG*, *nirK*, and *nosZ* denitrifying genes. Although the relative abundance of the DAMO population in the consortium was reduced from 60% to 13% after H_2S addition, CH_4 removals were not compromised and H_2S removal efficiencies of 100% were achieved. This study confirmed (i) the feasibility of co-oxidising CH_4 and H_2S with denitrification, as well as (ii) the critical need to control NO_3^- concentration to minimize N_2O production by anoxic denitrifiers.

Biotechnol. Bioeng. 2017;114: 665–673.

KEYWORDS: anoxic hydrogen sulfide oxidation; biotrickling filter; denitrifying anoxic methane oxidation; denitrification; nitrate removal; nitrous oxide production

Conflict of interest: The authors confirm they have no conflict of interest to declare.
Correspondence to: G. Quijano
Contract grant sponsor: Spanish Ministry of Economy and Competitiveness
Contract grant numbers: BES-2013-063922; CTQ2012-34949
Contract grant sponsor: European Research Council Starting Grant
Contract grant number: 3C-BIOTECH 261330
Received 7 June 2016; Revision received 14 August 2016; Accepted 29 August 2016
Accepted manuscript online 29 August 2016;
Article first published online 26 September 2016 in Wiley Online Library (http://onlinelibrary.wiley.com/doi/10.1002/bit.26092/abstract).
DOI 10.1002/bit.26092

Introduction

The atmospheric concentration of methane (CH_4) has increased by 150% in the period between the pre-industrial era and 2011, and it now contributes 10–16% of global greenhouse gas (GHG) emissions, with a warming potential 28 times higher than CO_2 (EPA, 2015; IPCC, 2014). Significant hot-spots for CH_4 generation include intensive livestock farms and waste management facilities, such as landfills or wastewater treatment plants (WWTPs). In fact, WWTPs generate up to 13,000 m^3 CH_4 d^{-1} in Europe (De Mes et al., 2003; IPCC, 2014; Russell, 2006) and CH_4 emissions from WWTPs were estimated to be ~11 million tn CO_2-eq in the EU-15 in 2013, although these values can reach up to 10 times higher in tropical countries, such as Brazil (EEA, 2014; Lobato et al., 2012).

Notwithstanding the proven potential of CH_4 as a biofuel for the production of both electricity and heat through co-generation, the CH_4 concentrations found in many emission hot-spots, such as old landfills or livestock farms, are usually not sufficient for energy generation purposes (<30% v/v) (Haubrichs and Widmann, 2006; McCarty et al., 2014). On the other hand, the conversion of biogas produced in anaerobic digesters at WWTPs is also still constrained—in this case by prohibitive costs, as well as the presence of undesirable compounds (e.g., H_2S). It has been estimated that less than 1% of the WWTPs in the United States utilize the biogas produced to generate energy, and biogas is instead typically burned in flares or even vented to the atmosphere without any treatment (McCarty et al., 2014; Noyola et al., 2006; Van Lier, 2008). In this regard, CH_4 flaring does not constitute an environmentally friendly practice since it supports low combustion efficiencies and usually requires a fuel support (Muñoz et al., 2013). Thus, there is an urgent need to develop cost-efficient and environmentally friendly processes and (bio) technologies for emissions abatement (López et al., 2013).

Previous studies demonstrated CH_4 can be used as electron donor under anoxic conditions for nitrogen (both NO_3^- and NO_2^-)

removal in a process known as denitrifying anoxic methane oxidation (DAMO), which can circumvent the requirement at WWTPs for expensive electron donors, such as methanol or acetate, to lower the operational costs and carbon footprint of the denitrification process (Raghoebarsing et al., 2006; Thalasso et al., 1997). To date, however, the implementation of DAMO in bioreactors with potential for full-scale applications is not widespread (especially for NO_3^- rather than for NO_2^- reduction) and reported NO_3^- removal rates indicate the process may not be economically viable (Cai et al., 2015; Kampman et al., 2014; Shi et al., 2013). Little attention has been given to the relationship between the concentration of the nitrogen source for prevailing DAMO enrichments and the production of N_2O within the process, which itself is an important intermediate GHG. Moreover, the few DAMO studies so far reported were restricted to CH_4 as the sole carbon and energy source (Ding et al., 2014; Hatamoto et al., 2014). Thus, it is relevant to elucidate the influence of biogas contaminants, such as H_2S, and the presence of other microbial communities, on the performance of DAMO applications (Shen et al., 2012). To the best of our knowledge, no previous studies have reported on the simultaneous, interdependent removal of CH_4, H_2S, and NO_3^-.

The aim of this study was to evaluate the feasibility of simultaneous CH_4 and NO_3^- removal by DAMO in a biotrickling filter under anoxic conditions, with a special focus on the influence of NO_3^- concentrations. The influence of H_2S on the efficiency and the microbial ecology of the DAMO process was also investigated.

Materials and Methods

Feeding Media and Gases

Synthetic biogas (70% CH_4, 29.5% CO_2, 0.5% H_2S), CH_4 ($\geq$99.5%) and CO_2 ($\geq$99.9%) were purchased from Abelló Linde S.A. (Barcelona, Spain). Additional reagents and chemicals were purchased from Panreac® (Barcelona, Spain) with a purity of at least 99%. Mineral salt medium (MSM; final pH, 7.0) used for enrichments and operating the biotrickling filter comprised (g L^{-1}): $Na_2HPO_4 \cdot 12H_2O$ 2.44, KH_2PO_4 1.52, $NaHCO_3$ 1.05, $MgSO_4 \cdot 7H_2O$ 0.02 and $CaCl_2 \cdot 2H_2O$ 0.038, along with 10 mL SL4 trace element solution (g L^{-1}: EDTA 0.5, $FeSO_4 \cdot 7H_2O$ 0.2, $ZnSO_4 \cdot 7H_2O$ 0.01, $MnCl_2 \cdot 4H_2O$ 0.003, H_3BO_3 0.03, $CoCl_2$ 0.011, $CuCl_2 \cdot 2H_2O$ 0.162, $NiCl_2 \cdot 6H_2O$ 0.002, $Na_2MoO_4 \cdot 2H_2O$ 0.003) per litre of medium. A $NaNO_3$ stock solution up to 31.8 g L^{-1} was prepared to supplement the MSM with NO_3^- as electron acceptor and *N* source for microbial growth. The MSM and $NaNO_3^-$ solutions were flushed with He for 15 min to eliminate dissolved O_2.

Inoculum and Enrichment Conditions

An inoculum was prepared by mixing together equal volumes of fresh secondary activated sludge from Valladolid WWTP (Valladolid, Spain) and anoxic sludge from a denitrifying fixed-film bioreactor from the University of Valladolid (Valladolid, Spain).

Batch cultures to enrich microorganisms capable of CH_4 degradation under anoxic denitrifying conditions were set in 1.25-L glass bottles each containing 175.2 mL MSM, 4.8 mL of a $NaNO_3$ stock solution (initial concentration in the enrichment of $\sim$150 gNO_3^- m^{-3}) and 20 mL of the mixed inoculum. The bottles were closed with butyl septa and plastic caps, and the headspace was flushed with He for 15 min to eliminate O_2. CH_4 was then supplied at an initial headspace concentration of 318 ± 25 g m^{-3} and the bottles were incubated in an orbital shaker (MaxQ 4000, Thermo Scientific, Marietta, OH) at 25°C and 180 rpm. The concentrations of CH_4, CO_2 and N_2 in the headspace were periodically measured by GC-TCD. NO_3^- and NO_2^- concentrations in the liquid phase were also periodically monitored by HPLC-IC. The enrichment period lasted 45 days, corresponding to five cycles of CH_4/NO_3^- addition. Then, the enriched biomass was centrifuged and resuspended in 200 mL fresh MSM for subsequent inoculation of the biotrickling filter (BTF).

Biotrickling Filter Set-Up and Operation Mode

A laboratory-scale BTF, which comprised a cylindrical PVC column (height, 0.45 m; inner diameter, 0.08 m), was packed with Kaldnes K1 rings (Evolution Aqua Ltd., Wigan, UK) to a working volume of 1 L. The packing material was characterized by a ring diameter of 1 cm, a density (as received) of 0.17 g mL^{-1}, a void fraction of 83% and a water-holding capacity (volume basis) of 11% (Lebrero et al., 2012). Gas and liquid streams were operated in counter-current flow mode. The MSM (1.0 ± 0.1 L) was continuously recycled at a rate of 0.01 m^3 h^{-1} from an external 1.2-L holding tank, which was magnetically stirred at 150 rpm (Agimatic-S, Selecta, Barcelona, Spain) (Fig. 1). NO_3^- was supplied from the $NaNO_3$ stock solution to the holding tank by means of a 120-U peristaltic pump (Watson Marlow, Wilmington, MA). Accordingly, a 120-U peristaltic pump was also used to purge the system and maintain the working volume of the STR. The pH of the recirculating MSM was maintained at 6.9 ± 0.1 by periodic addition of 5 M NaOH. The BTF was operated at 25.8 ± 1.3°C in a temperature-controlled room. Double-concentrated MSM was also added periodically to compensate for sampling losses and to provide sufficient nutrients for microbial growth. The BTF was operated under abiotic conditions for 7 days to rule out any potential CH_4 removal due to adsorption or photolysis. Finally, 200 mL enriched inoculum were introduced to the holding tank up to a final volume of 1 L. Biomass attachment on the packing material was observed after 24 h.

Synthetic biogas without H_2S (70% CH_4, 30% CO_2), obtained by mixing pure CH_4 and CO_2 streams using mass flow controllers (Aalborg™), was fed to the BTF at 0.001 m^3 h^{-1} in experimental Stage 1 (day 0–114). This resulted in an empty bed residence time (EBRT) of 1 h and a methane inlet load (IL_{CH4}) of 495 ± 12 g m^{-3} h^{-1}. To evaluate the influence of NO_3^- concentration on CH_4 removal and N_2O production, different NO_3^- stock solution dosing rates (*F*) were tested, which required process operation at liquid dilution rates ($D = F/V$) ranging from 0.03 to 0.16 d^{-1}. Thus, the NO_3^- concentration of the recycling medium was progressively increased as follows: 35 ± 3 g m^{-3} (day 0–5), 99 ± 16 g m^{-3} (day 6–18), 171 ± 21 g m^{-3} (day 19–31), 211 ± 15 g m^{-3} (day 32–54). Then, the concentration was decreased stepwise to 166 ± 18 g m^{-3} (day 55–72), 87 ± 17 g m^{-3} (day 73–83) and, finally, to 48 ± 11 g m^{-3} (day 84–114) (Fig. 2a). Nitrate consumption rates (rNO_3^-) were estimated by mass balance calculations in the STR,

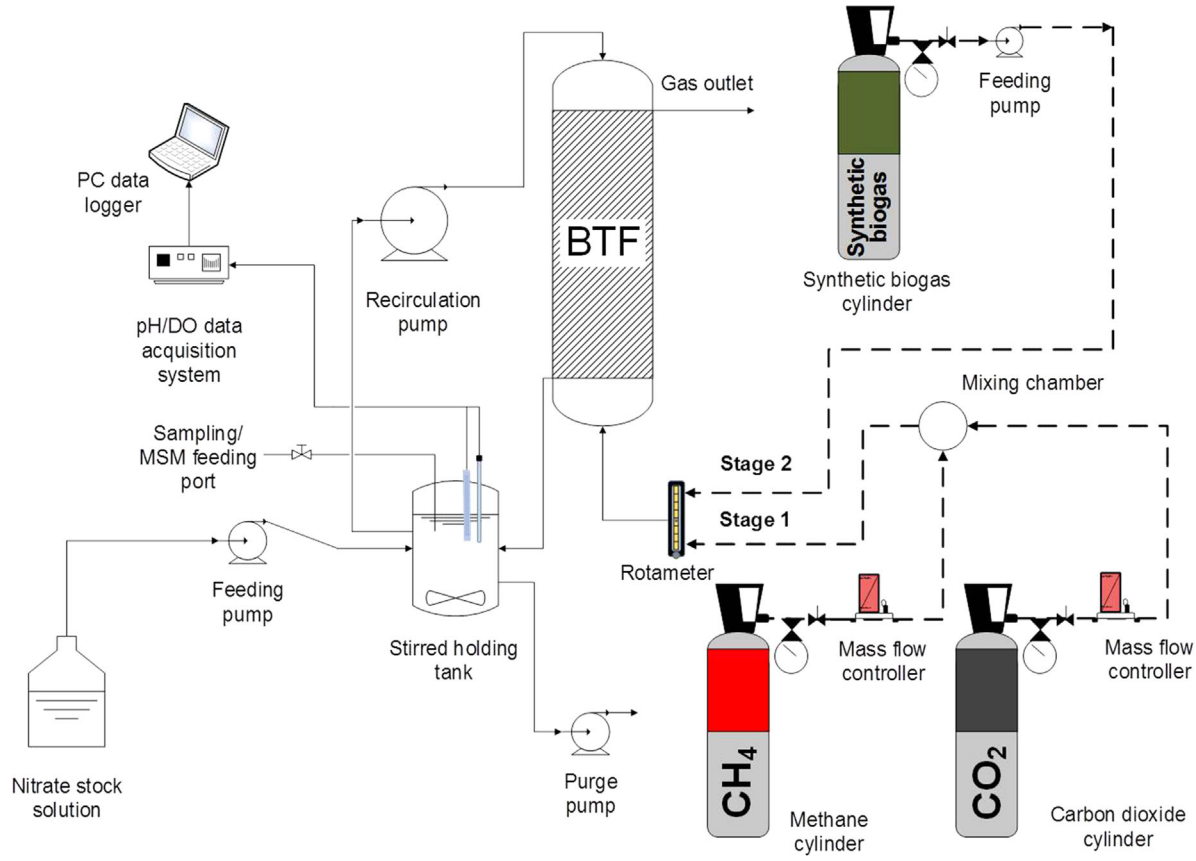

Figure 1. Schematic of the experimental set-up. Dashed lines indicate the different gas streams used during operational Stages 1 and 2.

considering inlets from the NO_3^- stock solution and outlets through the purge.

The influence of H_2S on overall BTF performance was assessed during Stage 2 (day 115–180) by feeding a synthetic biogas mixture composed of 29.5% CO_2, 70% CH_4, and 0.5% H_2S. This biogas mixture was also supplied with an L/S peristaltic pump (Watson Marlow) from filled-up 25 L-Tedlar bags (Sigma–Aldrich®, St. Louis, MO) at 0.001 $m^3 h^{-1}$, resulting in an EBRT of 1 h, an IL_{CH4} of 477 ± 20 g $m^{-3} h^{-1}$ and an IL_{H2S} of 7.9 ± 0.5 g $m^{-3} h^{-1}$. During Stage 2, the D ranged from 0.03 to 0.07 d^{-1} and was increased to 0.12 d^{-1} to avoid inhibition by SO_4^{2-} accumulation from day 156 onwards.

Gas samples were taken periodically from the sampling ports located at the inlet and outlet of the BTF to monitor the CH_4, O_2, CO_2, H_2S, N_2, and N_2O concentrations by GC-TCD and ECD. Liquid samples (10 mL) were also periodically drawn from the holding tank to determine the concentration of NO_3^-, NO_2^- and SO_4^{2-}.

Analytical Procedures and Biomass Sampling

CH_4, H_2S, O_2, N_2, and CO_2 gas concentrations were determined in a Bruker 430 GC-TCD (Palo Alto) equipped with a CP-Molsieve 5A (15 m × 0.53 μm × 15 μm) and a CP-PoraBOND Q (25 m × 0.53 μm × 10 μm) columns. The oven, injector and detector temperatures were maintained at 45°C, 150°C, and 200°C, respectively. Helium was used as the carrier gas at 13.7 mL min^{-1} (López et al., 2014). N_2O gas concentrations were analysed by GC-ECD according to Frutos et al. (2014). NO_3^- and SO_4^{2-} concentrations in the liquid phase were determined by HPLC-IC according to Muñoz et al. (2013). NO_2^- concentration measurements in the liquid phase followed the 4,500-NO_2^- B standard method (APHA, 2005) using a Shimadzu UV-2550 UV/Vis spectrophotometer (Shimadzu, Japan). Dissolved oxygen (DO), temperature and pH were monitored on-line using calibrated probes connected to a multiparametric analyser C-3020 (Consort, Belgium).

Biomass samples from the mixed inoculum prior to enrichment (sample A), and from the BTF at days 114 (sample B) and 180 (sample C), were collected and stored immediately at −20°C for further analysis.

Fluorescence In Situ Hybridization (FISH)

The procedures for FISH analyses are described in the Supporting Information (SI). The following probes were used: EUB338 I-II-FITC (for most bacteria); ARCH915-Rhodamin (for most archaea); DBACT1027-Rhodamin and DBACT193-Rhodamin (for DAMO bacteria belonging to the NC10 phylum); and DARCH872-Fam (for DAMO archaea belonging to ANME-2d) (Raghoebarsing et al., 2006).

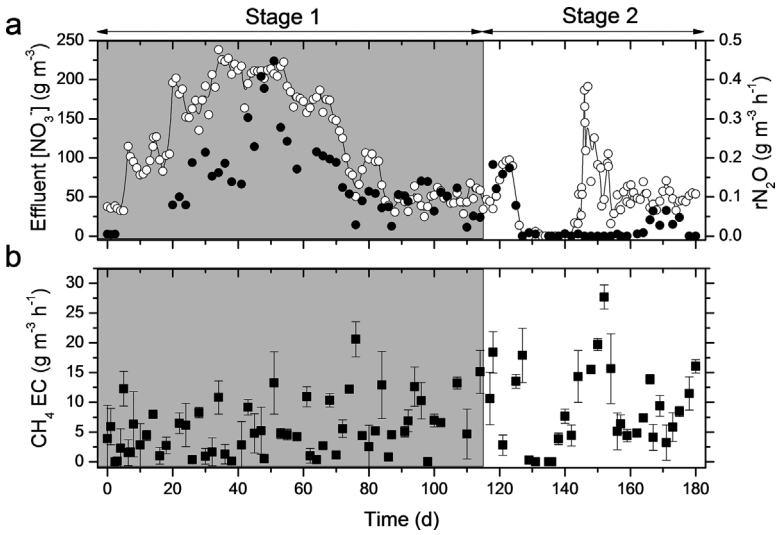

Figure 2. Time course of (**a**) NO_3^- concentration (○) and N_2O production rate (●), and (**b**) CH_4 elimination capacities in the BTF.

Genomic DNA Extraction and Purification

Genomic DNA was extracted from the samples using a Maxwell®-16 bench-top instrument and the Maxwell®-16 Tissue DNA Purification kit (Promega, Madison, WI) according to the manufacturer's instructions. DNA was purified according to the protocol provided in the Wizard® DNA Clean-Up System kit (Promega, Madison, WI) and concentrations were determined using a Qubit® Fluorometer (Invitrogen, Carlsbad, CA). The procedures for end-point PCR amplification of the target genes in this study are described in the Supporting Information (SI).

Clone Library and Sequencing of Denitrifying Genes

The PCR products of the genes encoding for the NO_3^-, NO_2^-, and N_2O reductases (*narG*, *nirK*, and *nosZ*, respectively) from the denitrification pathway were excised from agarose gels, purified using the Wizard® SV Gel and PCR Clean-Up System kit (Promega, Madison, WI), and further used to transform competent *Escherichia coli* TOP10 cells (Invitrogen, Carlsbad, CA) using the TOPO® TA Cloning® Kit for Sequencing (Invitrogen) according to the manufacturer's instructions. Insert-positive clones were selected and transferred to sterile 1.5-mL tubes containing Luria-Bertani (LB) medium supplemented with 50 μg kanamycin mL^{-1} and glycerol (20% v/v), which were stored at −80°C. The clones were sequenced (Biosource, Tramore, Ireland) using the M13F primer (5′-GTAAAACGACGGCCAG-3′) (Huey and Hall, 1989). Sequences were analysed using the BioEdit software to ensure the correct assemblage of the insert, and were then compared to the closest matches using the BLASTn search tool at the NCBI.

Quantitative PCR Analysis

Plasmid DNA was extracted from clones using a mini-prep kit (Isolate Plasmid Mini Kit, Bioline, UK) according to the manufacturer's instructions, and concentrations were determined using a Qubit® Fluorometer (Invitrogen). Serial dilutions of the plasmids were prepared containing 10^8–10^1 genes μL^{-1} to generate a standard curve for each target gene used as biomarker. Quantitative PCR (qPCR) mixtures (20 μL) for bacterial and archaeal 16S rRNA genes comprised 10 μL LightCycler® 480 Probes Master (Roche, Basel, Switzerland), 1 μL of each of the forward and reverse (10 μM) primers, 1 μL specific Taqman probe (10 μM), 2 μL PCR H_2O and 5 μL 10-fold dilution of the respective DNA template. Similarly, *narG*, *nirK*, and *nosZ* qPCR mixtures (20 μL) comprised 10 μL of LightCycler® 480 SYBR Green I Master (Roche, Basel, Switzerland), 1 μL of each primer (10 μM), 3 μL PCR H_2O and 5 μL 10-fold DNA dilutions. Thermal cycling conditions and primers used in qPCR assays are summarized in the SI section (SI Table SI). Assays were done in a NanoLight Cycler (Roche, Basel, Switzerland) and included duplicates for the standard curves, the samples and the non-template control (NTC). Automatic analysis settings were selected to determine the threshold cycle (C_t) values and the baselines settings. PCR efficiency was calculated for the standard curve of each gene using the formula $E = (10^{-1/\text{slope}}) - 1$, where the slope was obtained from the linear regression of C_t values against the logarithm of the copy numbers. The qPCR amplification efficiencies ranged between 90 and 110%, with R^2 values >0.94. The specificity of the qPCR reactions was confirmed by melting curve analysis (55–95°C), agarose gel electrophoresis and further Sanger sequencing analysis.

Statistical Analyses

The values reported for the gas phase concentrations at the inlet and outlet of the BTF are the mean of triplicate measurements. Error bars represent standard deviations. A Student's *t*-test (two-tailed) was used to calculate the *P*-level between the independent samples under analysis and confirm the significant differences among them, considering a 95% confidence level.

Results

Long-Term Bioreactor Performance

Upon inoculation, nitrate consumption rates (rNO_3^-) in the range of 0.1–2.8 g m^{-3} h^{-1} were observed throughout Stage 1, regardless of the NO_3^- concentration evaluated (Figs. 2a and 3). The N_2 production rate (rN_2) and the CH_4 elimination capacity (CH_4 EC) in the BTF along this period fluctuated from 0.03 to 1.1 g m^{-3} h^{-1} and from 0.05 to 20.6 g m^{-3} h^{-1}, respectively (Figs. 2, and S1). The N_2O production rate (rN_2O) was negligible during the first 4 days but progressively increased along with NO_3^- dosing concentrations. Thus, rN_2O values of 0.09 ± 0.01, 0.17 ± 0.03, and 0.41 ± 0.04 g m^{-3} h^{-1} were observed at NO_3^- concentrations of 113 ± 23, 172 ± 21, and 212 ± 15 g m^{-3}, respectively (Fig. 2a). Thereafter, N_2O production slowed to 0.21 and 0.09 g m^{-3} h^{-1} as the NO_3^- concentration was decreased to ~170 and to 50–90 g m^{-3}, respectively (Fig. 2a). A linear correlation with an R^2 of 0.70 was found between the NO_3^- concentration and the N_2O production rates in the BTF (Fig. S2). Finally, no accumulation of NO_2^- was observed during Stage 1 (Fig. S3).

The addition of H_2S did not cause any significant change in NO_3^- concentration, rNO_3^-, CH_4 EC, rN_2, or rN_2O from days 114–129 (Figs. 2, 3, and S1). During this period, the average N-NO_3^-/S-H_2S ratio applied onto the system was 0.3 mol mol^{-1} and the H_2S elimination capacity (H_2S EC) was 4.9 ± 0.9 g m^{-3} h^{-1}, which corresponded to a removal efficiency (RE) of 67.8 ± 15.6% (Fig. 4). The rNO_3^- increased by day 133 up to 5.1 g m^{-3} h^{-1}, which was twice the average rate recorded in the previous 5 days, thus leading to nitrogen-limiting conditions until day 142 (Figs. 2a and 3). Both the CH_4 EC and rN_2O decreased to 0 g m^{-3} h^{-1} during this period (Fig. 2). The H_2S EC rapidly increased to ~8 g m^{-3} h^{-1} by day 131 (RE = 100%), which was concomitant with increased SO_4^{2-} in the liquid broth to 1,521 g m^{-3} by day 142 (Fig. 4). The occurrence of elemental sulfur (S^0) deposition in the packing material was also visually observed during this period of operation.

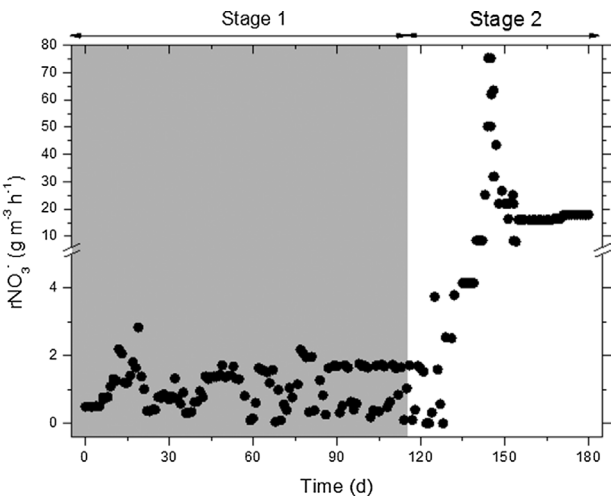

Figure 3. Time course of the NO_3^- removal rates during BTF operation.

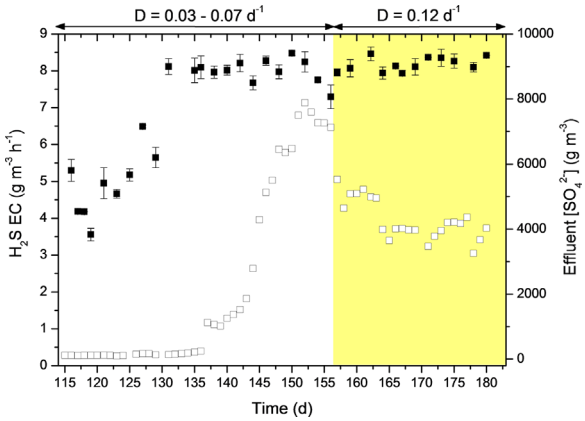

Figure 4. Time course of H_2S elimination capacities (■) and SO_4^{2-} concentration (□) during Stage 2 of BTF operation.

As a result of the increase in the inlet nitrate load from day 143 onwards, the rNO_3^- had increased to 75.2 g m^{-3} h^{-1} by day 145, but it gradually stabilized at 17.8 ± 0.03 g m^{-3} h^{-1} by day 171 (Fig. 3). Average NO_3^- concentrations of 65 ± 40 g m^{-3} were maintained in the liquid recycling medium from day 143 onwards (Fig. 2a). The CH_4 EC had gradually increased from 0 to 27.7 g m^{-3} h^{-1} by day 152 and then remained at 7.7 ± 4.0 g m^{-3} h^{-1} from day 156, while the rN_2 increased to 1.5 g m^{-3} h^{-1} by day 157 to finally stabilize at 0.5 ± 0.1 g m^{-3} h^{-1} from day 159 (Figs. 2b and S1). In contrast, the rN_2O was 0.04 ± 0.02 g m^{-3} h^{-1} from day 166 toward day 175 (Fig. 2a). The use of a dilution rate of 0.12 d^{-1} from day 156 led to steadily decreasing SO_4^{2-} concentrations, while the RE of H_2S remained at 100% (Fig. 4) at an average N/S ratio of 1.3 mol mol^{-1}. Indeed, the S^0 accumulations previously observed in the packing bed under nitrogen-limiting conditions gradually disappeared after day 143.

Dynamics of DAMO Bacteria and Archaea

DAMO bacteria and archaea were detected by FISH analysis in all samples tested (Fig. 5). In the inoculum (sample A), DAMO bacteria belonging to the NC10 phylum accounted for only 5% of the microbial population, while DAMO archaea from the ANME-2d group represented 12.5% (81% of the total archaeal population). In sample B, retrieved at the end of Stage 1, the NC10 bacteria and ANME-2d accounted for up to almost 60% of the total population (37.1% and 22.5%, respectively). However, in the sample drawn from the BTF at the end of Stage 2 (sample C), both of the DAMO groups were less abundant—the NC10 bacteria and ANME-2d represented 11.5 and 1.7% of the cells, respectively. At the conclusion of Stage 2, ANME-2d still represented ~65% of all archaea, but NC10 organisms accounted for only 15% of all bacteria in the system.

Quantification of 16S rRNA and Denitrification Genes (*narG, nirK, nosZ*)

A temporal increase in the concentration of bacterial 16S rRNA genes, which ranged from $2.0 \times 10^5 \pm 3.7 \times 10^4$ to $6.0 \times 10^5 \pm 5.6$

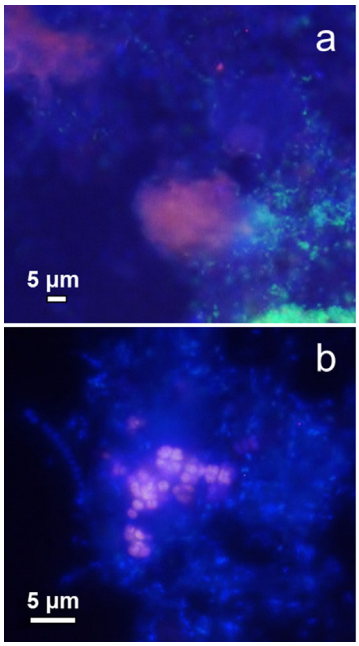

Sample	NC10 bacteria content (%)
A	5
B	37.1
C	11.5

Sample	ANME-2d archaea content (%)
A	12.5
B	22.5
C	1.7

Figure 5. FISH micrographs of the (**a**) bacterial and (**b**) archaeal biomass from the BTF by the conclusion of Stage 1. NC10 bacteria appear pink due to triple hybridisation with the DBACT1027 and DBACT193 probes (orange), the EUB338 I-II probes (green), and DAPI (cyan) (**a**); while ANME-2d archaea appear pink due to triple hybridisation with the DARCH872 (green) and ARCH915 (orange) probes, and DAPI (cyan) (**b**). The abundances of group-specific targets relative to the total biomass in samples A, B, and C are also shown (right).

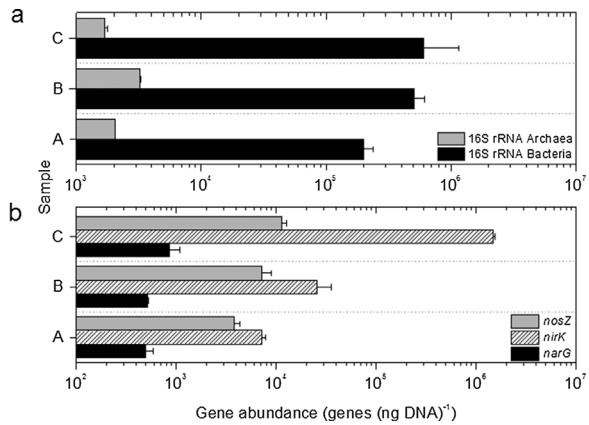

Figure 6. Gene abundances of (**a**) 16S rRNA Bacteria and Archaea and (**b**) *narG*, *nirK*, and *nosZ* in samples A, B, and C.

$\times 10^5$ genes ng^{-1} DNA, was observed (Fig. 6a). The abundance of archaeal 16S rRNA genes increased slightly from sample A ($2.0 \times 10^3 \pm 1.2 \times 10^1$ genes ng^{-1} DNA) to sample B ($3.2 \times 10^3 \pm 4.8 \times 10^1$ genes ng^{-1} DNA), but was lower in sample C ($1.7 \times 10^3 \pm 8.3 \times 10^1$ genes ng^{-1} DNA). The concentration of denitrification genes was significantly higher in samples B and C compared to sample A (Fig. 6b). In this sense, the *narG* concentration almost doubled from $5.0 \times 10^2 \pm 8.6 \times 10^1$ genes ng^{-1} DNA in the inoculum to $8.6 \times 10^2 \pm 2.3 \times 10^2$ genes ng^{-1} DNA by the conclusion of Stage 2. An exponential increase was found in the concentration of *nirK* genes, from $7.2 \times 10^3 \pm 7.4 \times 10^2$ genes ng^{-1} DNA in sample A to $2.6 \times 10^4 \pm 9.7 \times 10^3$ genes ng^{-1} DNA in sample B, and finally by two further orders of magnitude to $1.5 \times 10^6 \pm 8.7 \times 10^4$ genes ng^{-1} DNA in sample C. Similarly, the *nosZ* abundance increased from $3.8 \times 10^3 \pm 4.7 \times 10^2$ genes ng^{-1} DNA in sample A to $1.2 \times 10^4 \pm 1.2 \times 10^3$ genes ng^{-1} DNA in sample C (Fig. 6b), indicating the enrichment of denitrifying genes over the trial.

Discussion

A Novel DAMO Configuration for Biogas-Based Denitrification

The recently discovered DAMO process has scarcely been studied under continuous bioreactor conditions. Nonetheless, at WWTPs where biogas is not used for energy or power generation, DAMO provides a significant potential opportunity for nutrient removal using CH_4 as electron donor for NO_3^-/NO_2^- reduction. However, CH_4 and NO_3^- removal rates thus far reported in the literature are not sufficiently high to support DAMO applications at WWTPs, mostly due to the low mass transfer of CH_4 from the gas to liquid phase where microorganisms are present, and also to the low growth rates of DAMO archaea and bacteria (Ding et al., 2014). Recent studies suggested the supply of additional nitrogen sources (NO_2^- or NH_4^+) in membrane biofilm reactors, as an alternative to systems fed only with NO_3^-, to achieve higher NO_3^- removals by co-ocurring DAMO and anammox processes. However, the implementation of this innovation as a practical technology still suffers from the extended time required for the full formation of combined DAMO and anammox biofilms (>400 days) (Cai et al., 2015; Shi et al., 2013).

In this context, the bioreactor configuration presented here demonstrates the capability of a BTF to support the growth and activity of DAMO microorganisms, and the feasibility of using both CH_4 and H_2S as electron co-donors by a mixed microbial community to achieve higher rates of nitrogen removal. The maximum NO_3^- removal rates achieved under CH_4 feeding during Stage 1 (2.8 g NO_3^- m^{-3} h^{-1}) were 2–10 times higher than those reported in literature for sequencing batch, and stirred tank, reactors at higher EBRTs (2.8–21.7 h) (Table I). In addition, the NO_3^- removals obtained here under steady-state conditions, and maximum activity (induced by the co-supply of CH_4 and H_2S), rank among the highest values reported in literature (17.8 and 75.2 g m^{-3} h^{-1}, respectively) (Table I). The differences in NO_3^- removal rates between Stages 1 and 2 can be attributed not only to the simultaneous use of NO_3^- by two different microbial bioreactions (see Eq. 1–3) (Fernández et al., 2014; Raghoebarsing et al., 2006), but also to the higher solubility of H_2S in the liquid phase compared to CH_4. In this regard, the dimensionless Henry's law constants ($H = C_L/C_G$) for CH_4 (0.03) and H_2S (2.48) differ by almost two orders of magnitude (at 25°C, 1 atm), which resulted in higher bioavailability of H_2S and, accordingly, to proportionately more use of H_2S than CH_4 as electron donor for denitrification during Stage 2 (Sander, 2014). This would explain the absence of

Table I. Comparison of the most significant DAMO processes with nitrate as *N* source and electron acceptor for denitrification reported to date.

Reference	Process	Configuration (working volume)	Gas feeding composition	Gas EBRT (h)	NO_3^- concentration/Additional *N* sources ($g\,m^{-3}$)	CH_4-EC/rNO_3^- ($g\,m^{-3}\,h^{-1}$)	Time and composition of the enriched community
Islas-Lima et al. (2004)	DAMO	Batch cultures (0.135 L), agitation not specified	95% CH_4, 5% CO_2	—	34.7	1/4	6 months; composition not determined
Raghoebarsing et al. (2006)	DAMO	SBR (1.65 L), 350–500 rpm	95% CH_4, 5% CO_2	2.75	$<62/NO_2^-$ (276)	0.21/1.41	16 months, 10% DAMO archaea and 80% DAMO bacteria
Ettwig et al. (2008)	DAMO	SRT (13 L), 200 rpm	95% CH_4, 5% CO_2	21.67	$186/NO_2^-$ (46)	n.d. (excesively low)/0.32	19 months, 10% DAMO archaea and 80% DAMO bacteria (inoculum from Raghoebarsing et al., 2006)
Hu et al. (2009)	DAMO	SBR (1.6 L), 200 rpm	90% CH_4, 5% CO_2, 5% N_2	n.d.	465–1165	1/5.05	10.7 months, 40% DAMO archaea and 30% DAMO bacteria
Hu et al. (2011)	DAMO	SBR (1.6 L), 200 rpm	90% CH_4, 5% CO_2, 5% N_2	n.d.	233	0.01/0.1	3.5 months, 30% DAMO bacteria and 45% DAMO archaea (inoculum from Hu et al., 2009)
Haroon et al. (2013)	DAMO + Anammox	STR (4.6 L), 200 rpm	90% CH_4, 5% CO_2, 5% N_2	n.d.	310–620/NH_4^+ (90–180)	0.15/2.84	11.7 months, 78% DAMO archaea, 3% anammox bacteria (inoculum from Hu et al., 2009)
Shi et al. (2013)	DAMO + Anammox	MBfR (0.45 L)	90% CH_4, 5% CO_2, 5% N_2	n.d.	885–2657/NH_4^+ (257–386)	1.98/7.92	24 months, 20–30% DAMO bacteria, 20–30% DAMO archaea and 20–30% anammox bacteria
Ding et al. (2014)	DAMO + Anammox	SBR (2 L), agitation not specified	95% CH_4, 5% CO_2	n.d.	50–850/NH_4^+ (50–850)	1.33/12.5	4.5 months, 29% DAMO archaea, 12% DAMO bacteria and 21% anammox bacteria
Hatamoto et al. (2014)	DAMO	CSTR (0.27 L), agitation no specified	100% CH_4	4.2	31	1.13/10.33	9 months, 37% DAMO bacteria and possible presence of DAMO archaea
Hu et al. (2015)	DAMO + Anammox	SBR (1.6 L), 200 rpm	90% CH_4, 5% CO_2, 5% N_2	n.d.	465	0.18/2.95	11.7 months, 70% DAMO archaea and 26% anammox bacteria (inoculum from Hu et al., 2009)
Cai et al. (2015)	DAMO + Anammox	MBfR (0.45 L)	90% CH_4, 5% CO_2, 5% N_2	n.d.	2657–6643	nd/35–126.2	15 months, 50% DAMO archaea, 20% DAMO bacteria and 20% anammox bacteria (inoculum from Shi et al., 2013)
This study	DAMO/DAMO + anoxic H_2S oxidation	BTF (1 L)	70% CH_4, 30% CO_2/70% CH_4, 29.5% CO_2, 0.5% H_2S	1	50–200	7/1.5–80	3.8 months, 37% DAMO bacteria and 23% DAMO archaea/6 months, 11.5% DAMO bacteria and 2% DAMO archaea accompanied by NR-SOB

n.d., not determined; SBR, sequencing batch reactor; STR, stirred tank reactor; MBfR, membrane biofilm reactor; CSTR, continuous stirred tank reactor; BTF, biotrikling filter.

CH_4 biodegradation and the rapid increase of NO_3^- removal during the nitrogen-limiting period.

$$8NO_3^- + 5CH_4 + 8H^+ \rightarrow 14H_2O + 4N_2 + 5CO_2 \quad (1)$$

$$2NO_3^- + 5H_2S \rightarrow 5S^0 + N_2 + 4H_2 + 2OH^- (\text{complete } H_2S \text{ oxidation}) \quad (2)$$

$$8NO_3^- + 5H_2S \rightarrow 5SO_4^{2-} + 4N_2 + 4H_2O + 2H^+ (\text{partial } H_2S \text{ oxidation}) \quad (3)$$

To the best of our knowledge, this is the first work elucidating the role of NO_3^- concentration on N_2O production from anoxic denitrifying bioreactors and identifying operating conditions that support minimizing N_2O emissions. The findings are relevant for process implementation since N_2O presents a global warming potential 300 times higher than CO_2 (IPCC, 2014). The emission factors recorded during Stage 1 (0.097–0.49 $gN\text{-}N_2O\,g^{-1}\,N_{load}$) were comparable or even higher to those previously reported for WWTPs, and were mainly attributed to conventional anoxic denitrifiers, since DAMO microorganisms do not have the capacity to produce this GHG (Ettwig et al., 2010; Gustavsson and la Cour Jansen, 2011). On the other hand, N_2O emissions in Stage 2 were far below the IPCC emission factors due to complete denitrification supported by H_2S (Gustavsson and la Cour Jansen, 2011; IPCC, 2014; Kampschreur et al., 2009). The results indicate the sustainability of co-oxidising CH_4 and H_2S under anoxic conditions in this type of system. Nonetheless, more information on the biological mechanisms controlling N_2O consumption and production by DAMO and the accompanying denitrifiers, respectively, is still required to enable optimization with respect to the GHG footprint of the process.

Dynamics of the DAMO Population Before and After the Supply of Hydrogen Sulfide

A co-culture, of which up to 60% comprised DAMO populations (40% bacteria, 20% archaea), was enriched in the BTF for 114 days with NO_3^- as the sole electron acceptor. This is one of the shortest enrichment times so far reported for DAMO populations (Table I). The successful enrichment obtained here was attributed to the high CH_4 mass transfer performance achieved in the BTF compared to previous experimental set-ups. In addition, the type of biofilm grown in the packing bed of the BTF likely favored a better interaction between DAMO bacteria and archaea compared to suspended systems. Recent metagenomics studies of DAMO communities, which described bacteria (*Candidatus* "*Methylomirabilis oxyfera*," from NC10 phylum) and archaea (*Candidatus* "*Methanoperedens nitroreducens*" from lineage ANME-2d), revealed that both microorganisms possess an incomplete denitrification pathway, with *M. nitroreducens* being necessary to catalyse the conversion of NO_3^- to NO_2^-, which is the preferred substrate of *M. oxyfera* (Ettwig et al., 2010; Haroon et al., 2013). In our particular study, NO_2^- accumulation was not observed, which suggests that NO_3^- reduction was limited by the activity of DAMO archaea (Cai et al., 2015; Hu et al., 2009). Recent studies also demonstrated the capability of aerobic methanotrophs to reduce nitrate under hypoxia (e.g., gas phase concentrations $<2\%$ O_2) (Kits et al., 2015; Liu et al., 2014). In this regard, the detection of aerobic methanotrophs in our consortium, based on PCR-amplification of the *pmoA* gene, also indicates the presence of micro-aerobic niches, which likely supported an increase in the CH_4 EC to the levels attained by this bacterial group (Fig. S4).

On the other hand, the fact that H_2S addition did not compromise CH_4 biodegradation except under nitrogen-limiting conditions suggests that this biogas pollutant generated a shift in the population toward nitrate-reducing and sulfide-oxidising bacteria (NR-SOB) (Fig. S4), rather than a toxic effect toward the DAMO population, as initially hypothesized (Pan et al., 2013; Shen et al., 2012). Thus, if a NR-SOB enrichment supported by H_2S addition occured, bacterial abundance in the biofilm should be similar or even higher after the H_2S addition, whereas archaeal abundance would be lower. Results of qPCR assays targeting 16S rRNA genes support this hypothesis. Moreover, more denitrifying genes were present in the consortium at the end of the Stage 2, than in the prevailing DAMO consortium (Stage 1), further indicating the bigger impact of H_2S than CH_4 on biomarker concentrations, especially for *nirK* and *nosZ*. In fact, the abundance of denitrifying genes reported here was higher than in studies reporting on nitrate-rich wastewater treatment in bioreactors fed with acetate as the carbon and energy source (Herbert et al., 2014; Miao et al., 2015). Previous studies showed that increasing *nirK*/*narG* and *nosZ*/*narG* ratios correlate with higher denitrification rates and lower N_2O emissions (Herbert et al., 2014; Warneke et al., 2011). Here, the *nosZ*/*narG* ratio remained roughly stable, whereas the *nirK*/*narG* and the *nosZ*/*narG* ratios steadily increased, thus leading to the observed 13-fold increase in NO_3^- removal and 10-fold decrease in N_2O production by the consortium of DAMO/NR-SOB/conventional-denitrifiers, respectively.

Finally, it was observed that SO_4^{2-} accumulation must be avoided since the denitrification performance of the NR-SOB was compromised at SO_4^{2-} concentrations $>8{,}000\ g\ m^{-3}$. Ramirez et al. (2009) reported SO_4^{2-} inhibition in NR-SOB enrichments at concentrations of 10,000–12,000 $g\ m^{-3}$, which was in the range of the maximum values here reported. In this regard, recent studies demonstrated the potential to control SO_4^{2-} concentrations in NR-SOB systems by applying low N/S ratios (i.e., N-limiting conditions), and thus favoring the metabolism of these microorganisms toward S^0 production (Fernández et al., 2013, 2014), as was observed during the N-limiting period of Stage 2 (days 127–142, Fig. 2a).

This research was supported by the Spanish Ministry of Economy and Competitiveness (BES-2013-063922 contract; CTQ2012-34949 project), and a European Research Council Starting Grant (3C-BIOTECH; no. 261330) to GC. C. Mongil is gratefully acknowledged for the practical assistance in the HPLC-IC analyses. The contribution of C. Smith, A. Lisik, A. Duff, and E. Tatti (National University of Ireland Galway) to qPCR analysis is also gratefully acknowledged.

References

APHA, AWWA, WEF. 2005. Standard methods for the examination of water and wastewater, 21st edition. Washington: Amer Water Works Assn.

Cai C, Hu S, Guo J, Shi Y, Xie G-J, Yuan Z. 2015. Nitrate reduction by denitrifying anaerobic methane oxidizing microorganisms can reach a practically useful rate. Water Res 87:211–217.

De Mes TZD, Stams AJM, Reith JH, Zeeman G. 2003. Methane production by anaerobic digestion of wastewater and solid wastes. In: Reith JH, Wijffels RH, Barten H, editors. Biomethane and biohydrogen: Status and perspectives of biological methane and hydrogen production. The Netherlands: Dutch Biological Hydrogen Foundation. p 58–102.

Ding ZW, Ding J, Fu L, Zhang F, Zeng RJ. 2014. Simultaneous enrichment of denitrifying methanotrophs and anammox bacteria. Appl Microbiol Biot 98:10211–10221.

European Environment Agency. 2014. Annual European Union greenhouse gas inventory 1990–2012 and inventory report 2014. http://www.eea.europa.eu/publications/european-union-greenhouse-gas-inventory-2014 Accessed 8 November 2015.

Environmental Protection Agency. 2015. Inventory of US greenhouse gas emissions and sinks: 1990–2013 (April 2015), EPA 430-R-15-004. http://www3.epa.gov/climatechange/ghgemissions/usinventoryreport.html Accessed 8 November 2015.

Ettwig KF, Shima S, van de Pas-Schoonen KT, Kahnt J, Medema MH, Op den Camp HJ, Jetten MS, Strous M. 2008. Denitrifying bacteria anaerobically oxidize methane in the absence of Archaea. Environ Microbiol 10:3164–3173.

Ettwig KF, Butler MK, Le Paslier D, Pelletier E, Mangenot S, Kuypers MMM, Schreiber F, Dutilh BE, Zedelius J, de Beer D, Gloerich J, Wessels HJCT, van Alen T, Luesken F, Wu ML, van de Pas-Schoonen KT, Op den Camp HJM, Janssen-Megens EM, Francoijs KJ, Stunnenberg H, Weissenbach J, Jetten MSM, Strous M. 2010. Nitrite-driven anaerobic methane oxidation by oxygenic bacteria. Nature 464:543–548.

Fernández M, Ramírez M, Pérez RM, Gómez JM, Cantero D. 2013. Hydrogen sulphide removal from biogas by an anoxic biotrickling filter packed with Pall rings. Chem Eng J 225:456–463.

Fernández M, Ramírez M, Gómez JM, Cantero D. 2014. Biogas biodesulfurization in an anoxic biotrickling filter packed with open-pore polyurethane foam. J Hazard Mater 264:529–535.

Frutos OD, Arvelo IA, Pérez R, Quijano G, Muñoz R. 2014. Continuous nitrous oxide abatement in a novel denitrifying off-gas bioscrubber. Appl Microbiol Biot 99:3695–3706.

Gustavsson DJ, la Cour Jansen J. 2011. Dynamics of nitrogen oxides emission from a full-scale sludge liquor treatment plant with nitritation. Water Sci Technol 63:2838–2845.

Haroon MF, Hu S, Shi Y, Imelfort M, Keller J, Hugenholtz P, Yuan Z, Tyson GW. 2013. Anaerobic oxidation of methane coupled to nitrate reduction in a novel archaeal lineage. Nature 500:567–570.

Hatamoto M, Kimura M, Sato T, Koizumi M, Takahashi M, Kawakami S, Araki N, Yamaguchi T. 2014. Enrichment of denitrifying methane-oxidizing microorganisms using up-flow continuous reactors and batch cultures. PLoS ONE 9:e115823.

Haubrichs R, Widmann R. 2006. Evaluation of aerated biofilter systems for microbial methane oxidation of poor landfill gas. Waste Manage 26:408–416.

Herbert RBJ, Winbjörk H, Hellman M, Hallin S. 2014. Nitrogen removal and spatial distribution of denitrifier and anammox communities in a bioreactor for mine drainage treatment. Water Res 66:350–360.

Hu S, Zeng RJ, Burow LC, Lant P, Keller J, Yuan Z. 2009. Enrichment of denitrifying anaerobic methane oxidizing microorganisms. Environ Microbiol Rep 1: 377–384.

Hu S, Zeng RJ, Keller J, Lant PA, Yuan Z. 2011. Effect of nitrate and nitrite on the selection of microorganisms in the denitrifying anaerobic methane oxidation process. Environ Microbiol Rep 3:315–319.

Hu S, Zeng RJ, Haroon MF, Keller J, Lant PA, Tyson GW, Yuan Z. 2015. A laboratory investigation of interactions between denitrifying anaerobic methane oxidation (DAMO) and anammox processes in anoxic environments. Sci Rep 5:8706.

Huey B, Hall J. 1989. Hypervariable DNA fingerprinting in *Escherichia coli*: Minisatellite probe from bacteriophage M13. J Bacteriol 171:2528–2532.

Intergovernmental Panel on Climate Change. 2014. Fifth assessment report: Climate change 2014, Synthesis Report. https://www.ipcc.ch/report/ar5/syr/ Accessed 8 November 2015.

Islas-Lima S, Thalasso F, Gómez-Hernandez J. 2004. Evidence of anoxic methane oxidation coupled to denitrification. Water Res 38:13–16.

Kampman C, Temmink H, Hendrickx TLG, Zeeman G, Buisman CJN. 2014. Enrichment of denitrifying methanotrophic bacteria from municipal wastewater sludge in a membrane bioreactor at 20°C. J Hazard Mater 274:428–435.

Kampschreur MJ, Temmink H, Kleerebezem R, Jetten MSM, van Loosdrecht MCM. 2009. Nitrous oxide emission during wastewater treatment. Water Res 43:4093–4103.

Kits KD, Klotz MG, Stein LY. 2015. Methane oxidation coupled to nitrate reduction under hypoxia by the Gammaproteobacterium *Methylomonas denitrificans*, sp. nov. type strain FJG1. Environ Microbiol 17:3219–3232.

Lebrero R, Rodríguez E, Pérez R, García-Encina PA, Muñoz R. 2012. Abatement of odorant compounds in one- and two-phase biotrickling filters under steady and transient conditions. Appl Microbiol Biot 97:4627–4638.

Liu J, Sun F, Wang L, Ju X, Wu W, Chen Y. 2014. Molecular characterization of a microbial consortium involved in methane oxidation coupled to denitrification under micro-aerobic conditions. Microb Biotechnol 7:64–76.

López JC, Quijano G, Pérez R, Muñoz R. 2014. Assessing the influence of CH_4 concentration during culture enrichment on the biodegradation kinetics and the population structure. J Environ Manage 146:116–123.

López JC, Quijano G, Souza TSO, Estrada JM, Lebrero R, Muñoz R. 2013. Biotechnologies for greenhouse gases (CH_4, N_2O and CO_2) abatement: State of the art and challenges. Appl Microbiol Biotechnol 97:2277–2303.

Lobato LCS, Chernicharo CAL, Souza CL. 2012. Estimates of methane loss and energy recovery potential in anaerobic reactors treating domestic wastewater. Water Sci Technol 66:2745–2753.

McCarty PL, Bae J, Kim J. 2014. Domestic wastewater treatment as a net energy producer—can this be achieved?. Environ Sci Technol 45:7100–7106.

Miao Y, Liao R, Zhang X-X, Liu B, Li Y, Wu B, Li A. 2015. Metagenomic insights into salinity effect on diversity and abundance of denitrifying bacteria and genes in an expanded granular sludge bed reactor treating high-nitrate wastewater. Chem Eng J 277:116–123.

Muñoz R, Souza TSO, Glittmann L, Pérez R, Quijano G. 2013. Biological anoxic treatment of O2-free VOC emissions from the petrochemical industry: A proof of concept study. J Hazard Mater 260:442–450.

Noyola A, Morgan-Sagastume JM, López-Hernández JE. 2006. Treatment of biogas produced in anaerobic reactors for domestic wastewater: Odor control and energy/resource recovery. Rev Environ Sci Biotechnol 5:93–114.

Pan Y, Ye L, Yuan Z. 2013. Effect of H_2S on N_2O reduction and accumulation during denitrification by methanol utilizing denitrifiers. Environ Sci Technol 47:8408–8415.

Raghoebarsing AA, Pol A, van de Pas-Schoonen KT, Smolders AJ, Ettwig KF, Rijpstra WI, Schouten S, Damste JS, Op den Camp HJ, Jetten MSM, Strous M. 2006. A microbial consortium couples anaerobic methane oxidation to denitrification. Nature 440:918–921.

Ramirez M, Fernández M, Cáceres MS, Pérez RM, Gómez JM, Cantero D. 2009. Biotrickling filters for H_2S, MM, DMS and DMDS removal by *Thiobacillus Thioparus* and *Acidithiobacillus Thiooxidans*. Proceedings of the 3rd International Congress on Biotechniques for Air Pollution Control, Delft, The Netherlands, p. 137–150.

Russell DL. 2006. Practical wastewater treatment, 1st edition. Hoboken, New Jersey: Wiley.

Sander R. 2014. Compilation of Henry's law constants, version 3.99. Atmos Chem Phys Discuss 14:29615–30521.

Shen LD, He ZF, Zhu Q, Chen DQ, Lou LP, Xu XY, Zheng P, Hu BL. 2012. Microbiology, ecology, and application of the nitrite-dependent anaerobic methane oxidation process. Front Microbiol 3:269.

Shi Y, Hu S, Lou J, Lu P, Keller J, Yuan Z. 2013. Nitrogen removal from wastewater by coupling anammox and methane-dependent denitrification in a membrane biofilm reactor. Environ Sci Technol 47:11577–11583.

Thalasso F, Vallecillo A, García-Encina PA, Fdz-Polanco F. 1997. The use of methane as a sole carbon source for wastewater denitrification. Water Res 31:55–60.

Van Lier JB. 2008. High-rate anaerobic wastewater treatment: Diversifying from end-of-the-pipe treatment to resource-oriented conversion techniques. Water Sci Technol 57:1137–1148.

Warneke S, Schipper LA, Matiasek MG, Scow KM, Cameron S, Bruesewitz DA, McDonald IR. 2011. Nitrate removal, communities of denitrifiers and adverse effects in different carbon substrates for use in denitrification beds. Water Res 45:5463–5475.

Supporting Information

Additional supporting information may be found in the online version of this article at the publisher's web-site.

Biogas-based denitrification in a biotrickling filter: Influence of nitrate concentration and hydrogen sulfide

Juan C. López,[a,b] Estefanía Porca,[b] Gavin Collins,[b] Rebeca Pérez,[a] Alberto Rodríguez-Alija,[a] Raúl Muñoz,[a] Guillermo Quijano,[a,c]*

[a]Department of Chemical Engineering and Environmental Technology, University of Valladolid, Dr. Mergelina, s/n, 47011, Valladolid, Spain.

[b]Microbial Communities Laboratory, School of Natural Sciences and Ryan Institute, National University of Ireland Galway, University Road, Galway, H91 TK33, Ireland.

[c]Agrarian Engineering School, University of Valladolid – Soria Campus, C/Universidad s/n, 42004 Soria, Spain.

*Corresponding author: gquijano@iq.uva.es, Tel. +34 975129404, Fax: +34 975129401.

Supporting Information Section

containing 9 pages, with 4 figures and 1 table.

Materials and methods

Fluorescence *in situ* hybridization (FISH)

Biomass samples (250 uL) were fixed in 4% (*w/v*) paraformaldehyde for 3 h and then washed three times with phosphate-buffered saline (PBS). Aliquots of 10 µL of biofilm samples were deposited on the wells of gelatin-coated, acid-washed, glass microscope slides and dehydrated by passing through a 50%, 80% and 96% (*v/v*) ethanol series. Hybridisation with 30% formamide (*v/v*) and the oligonucleotide probes was at 46ºC for 2 h. After hybridization, and once the slides were washed and dried, the specimens were counter-stained for 5 min at room temperature with the DNA stain DAPI to quantify the total number of cells. For quantitative FISH analysis, 15 images were randomly acquired from inside each well on the slides using a Leica DM4000B microscope (Leica Microsystems, Wetzlar, Germany). The relative biovolumes of total archaea, total bacteria, DAMO bacteria and DAMO archaea from the total DAPI-stained biomass were calculated using DAIME software and split into individual colour channels before image segmentation (Daims et al. 2006).

End-point PCR of Bacterial 16S rRNA, Archaeal 16S rRNA, *narG*, *nirK*, *nosZ*, *pmoA* and *soxB* genes

Purified DNA from the samples was used to amplify the target Bacterial 16S rRNA, Archaeal 16S rRNA*, narG, nirK, nosZ*, *pmoA* and *soxB* genes by end-point PCR. The PCR mixture (25 µL) contained 0.5 □L of each primer (10 □M), 5 µL of 5× ready-to-use MyTaq reaction buffer (Bioline, UK), 0.5 µL of MyTaq DNA Polymerase, 1 µL purified DNA and PCR H_2O up to a final volume of 25 µL. PCR was performed in a Super Cycler Trinity (Kyratec, Australia) following thermo-cycling programs for Bacterial and Archaeal 16S rRNA according to Yu et al. (2005). End-point PCR amplifications of *narG*, *nirK,* and *nosZ* genes were performed according to Philippot et al. (2002), Braker et al. (2000), and Henry et al. (2006), respectively. Additionally, the detection of the genes *pmoA* (encodes

for the particulate methane monooxygenase; present in aerobic methane-oxidizing bacteria) and *soxB* (encodes for the thiosulfate-oxidising Sox enzyme complex; present in hydrogen sulfide-oxidizing bacteria) in the purified samples was assessed according to previous studies (Holmes et al. 1995; Thomas et al. 2014). The success of each amplification reaction was determined by electrophoresis in a 2% (*w/v*) agarose gel in 5× TAE buffer.

Real-time PCR analysis

Table SI. Primers and thermocycling conditions used during qPCR analysis

Target gene	Primer and sequence (5' – 3')	Amplicon size (bp)	qPCR thermocycling program	Reference
Bacterial 16S rRNA[a]	BAC338F: ACTCCTACGGGAGGCAG BAC805R:GACTACCAGG GTATCTAATCC	468	94°C for 10 min; 45 cycles of: 94ºC for 10 s, 60ºC for 30 s (acquisition step) (±5ºC/s ramp)	Yu et al. (2005)
Archaeal 16S rRNA[a]	ARC787F: ATTAGATACCCSBGTAGTCC ARC1059R: GCCATGCACCWCCTCT	273	94°C for 10 min; 45 cycles of: 94ºC for 10 s, 60ºC for 30 s (acquisition step) (±5ºC/s ramp)	Yu et al. (2005)
narG	narG 1960F: TAYGTSGGCCARGARAA narG 2659R: TTYTCRTACCABGTBGC	699	95°C for 10 min; 40 cycles of: 95ºC for 45 s, 66ºC for 45 s, 72ºC for 78 s, 80ºC for 18 s (acquisition step); 72°C for 5 min	This study
nirK	nirK 1F: GG(A/C)ATGGT(G/T)CC(C/G)TGGCA nirK 5R: GCCTCGATCAG(A/G)TT(A/G)TGG	514	95°C for 5 min; 45 cycles of: 95ºC for 30 s, 68ºC for 40 s, 72ºC for 30 s, 83ºC for 15 s (acquisition step)	This study
nosZ	nosz F: CGYTGTTCMTCGACAGCCG nosz 1R: CAKRTGCAKSGCRTGGCAGAA	699	95ºC for 15 min; 6 cycles of: 95ºC for 30 s, 67ºC for 30 s (-1ºC/cycle), 72ºC for 30 s, 85ºC for 15 s (acquisition data step); 40 cycles of: 95ºC for 30 s, 60ºC for 30 s, 72ºC for 30 s	This study

[a]TaqMan probes were set according to Yu et al. (2005).

Results

Long-term reactor performance

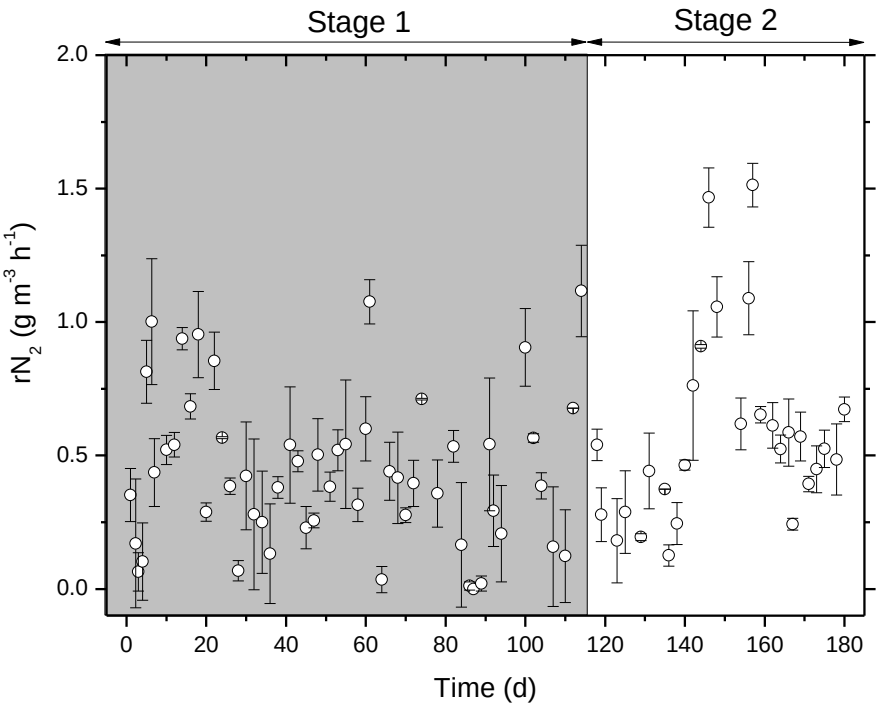

Figure S1. Time course of the N_2 production rates during BTF operation.

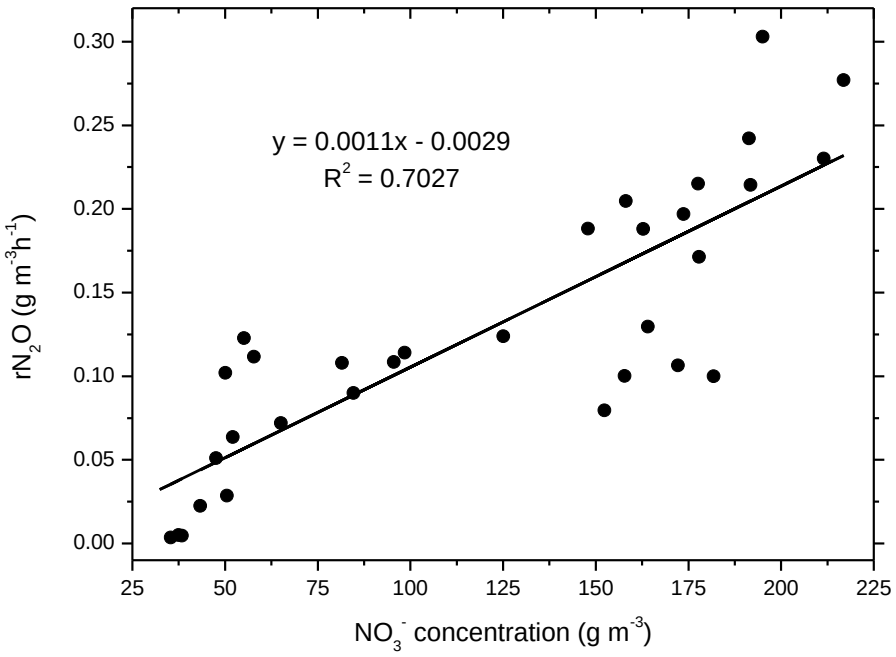

Figure S2. Influence of nitrate concentration on nitrous oxide production rate during Stage 1 of BTF operation.

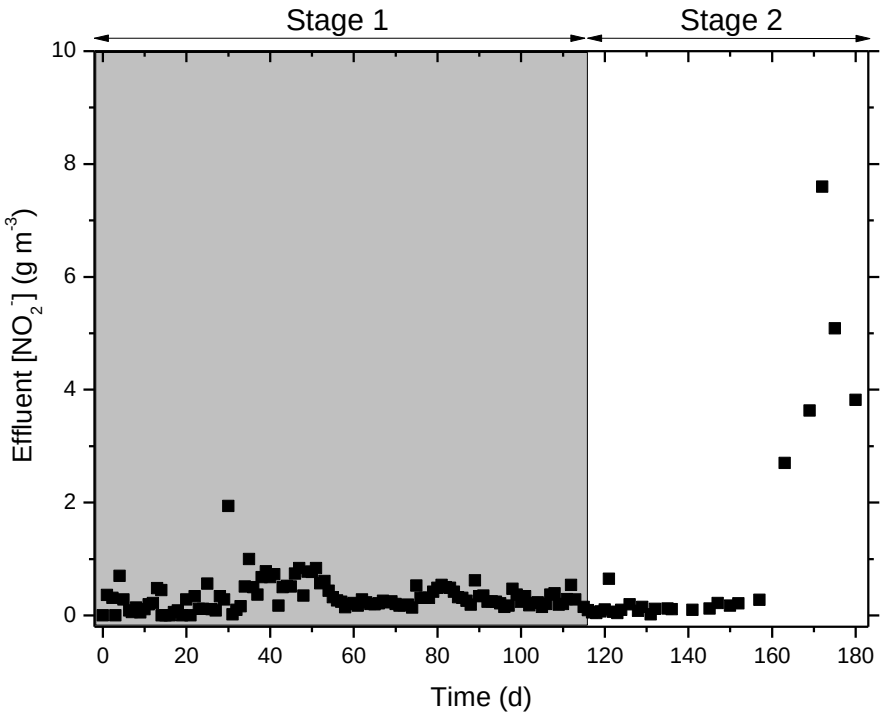

Figure S3. Time course of NO_2^- concentration during BTF operation.

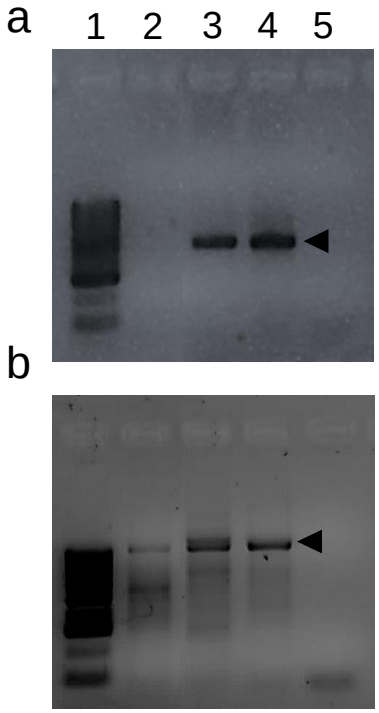

Figure S4. DNA fragments on gel electrophoresis of a) *pmoA* (510 bp) and b) *soxB* (1020 bp) in the samples under study (lane 1, HypperLadder™ 50bp; lane 2, sample A; lane 3, sample B; lane 4, sample C; lane 5, negative template control (NTC)). The arrows indicate the migration place of both fragments.

References

Braker G, Zhou J, Wu L, Devol AH, Tiedje JM. 2000. Nitrite reductase genes (*nirK* and *nirS*) as functional markers to investigate diversity of denitrifying bacteria in pacific northwest marine sediment communities. Appl Environ Microb 66:2096-2104.

Daims H, Lücker S, Wagner M. 2006. Daime, a novel image analysis program for microbial ecology and biofilm research. Environ Microbiol 8:200-213.

Henry S, Bru D, Stres B, Hallet S, Phillipot L. 2006. Quantitative detection of the *nosZ* gene, encoding nitrous oxide reductase, and comparison of the abundances of 16S rRNA, *narG*, *nirK*, and *nosZ* Genes in Soils. Appl Environ Microb 72:5181-5189.

Holmes AJ, Costello A, Lidstrom ME, Murrell JC. 1995. Evidence that particulate methane monooxygenase and ammonia monooxygenase may be evolutionarily related. FEMS Microbiol Lett 132:203-208.

Philippot L, Piutti S, Martin-Laurent F, Hallet S, Germon JC. 2002. Molecular analysis of the nitrate-reducing community from unplanted and maize-planted soils. Appl Environ Microb 68:6121-6128.

Thomas F, Giblin AE, Cardon ZG, Sievert SM. 2014. Rhizosphere heterogeneity shapes abundance and activity of sulfur-oxidizing bacteria in vegetated salt marsh sediments. Front Microbiol 5:309.

Yu Y, Lee C, Kim J, Hwang S. 2005. Group-specific primer and probe sets to detect methanogenic communities using quantitative real-time polymerase chain reaction. Biotechnol Bioeng 89:670-679.

Chapter 8

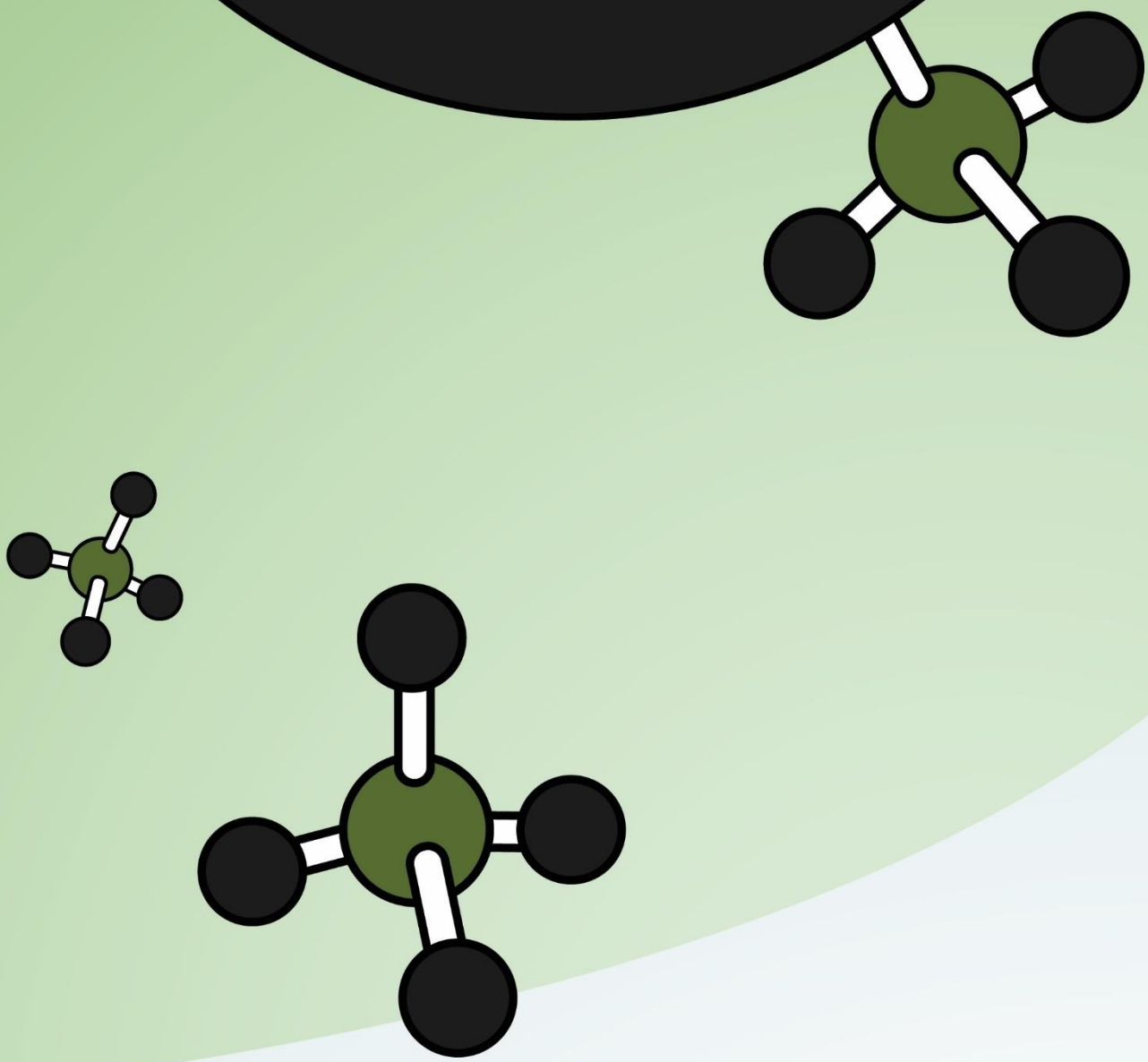

Conclusions and future work

Conclusions and future work

Methanotroph-based biofilters are one of the most applied CH_4 abatement technologies worldwide at lab- and field-scale for the treatment of CH_4 emissions. This fact has been attributed to their cost-effectiveness, the extensive knowledge in design and operation available and the recent advances in packing material techonology achieved in the past years. Nonetheless, the limited abatement performance at the typical EBRTs for VOC/odour biofiltration, due to the mass transfer limitations resulting from the low aqueous solubility of CH_4, often hinders its implementation at industrial scale. In **Chapter 3**, the ability of *Graphium* sp. to biodegrade CH_4 through co-metabolism when methanol is present as a source of reductive power was demonstrated for the first time, which is of key relevance to elucidate the potential and role of fungi during CH_4 abatement. The synergistic action of fungi and bacteria in a compost biofilter supported steady and high CH_4 removals at significantly lower EBRTs than those reported in literature, which might boost the implementation of fungal biofilters at full-scale.

In order to overcome the limitations imposed by biomass overgrowth during CH_4 biofiltration, the potential of feast-famine strategies in alternate units to reduce the biomass accumulated per volume unit of biofilter was comparatively and systematically evaluated in **Chapter 4**. Compared to a standard biofilter, feast-famine strategies triggered the CH_4 abatement performance of the alternate biofilters in the early stages of operation, while allowing significantly lower pressure drops under long-term operation as a result of the lower biomass concentrations supported by the feast-famine feeding. These findings suggested the adequacy of this biomass control strategy to increase the lifespan of the packed bed and reduce operating costs compared to standard CH_4 biofiltration, while supporting higher CH_4 removals compared to continuous biofiltration. Moreover, the methanotrophic communities subjected to the feast-famine cycles were

robust and exhibited a very rapid recovery even after 5 days of starvation (with and without air). This study is of key relevance to support the full-scale implementation of these strategies, and confirmed the robustness of microbial communities to process shutdowns typically ocurring during weekends or holiday periods and operational failures.

The applicability of biotechnologies is often challenged by the claimed lack of efficient biological activity – possibly attributed to the use of microorganisms with undesirable kinetic characteristics – and by their long start-up periods. **Chapter 5** demonstrated the key role of CH_4 concentration during the enrichment of methanotrophic communities to guarantee efficient biodegradation kinetics (in terms of K_S and q_{max}) and an adequate population structure. This study also showed the feasibility of synthesizing bioproducts such as PHAs during CH_4 abatement under nitrogen limiting conditions in non-acclimated cultures.

Chapter 6 represented a successful proof of concept study of the feasibility of biogas, with and without H_2S, to grow methanotrophic bacteria and intracellularly accumulate PHAs under nitrogen-limited conditions. Biogas-based biorefineries might boost the application of anaerobic digestion as an organic waste stabilization technology via PHA production, which would also decrease the cost of these biopolymers (since substrate acquisition typically accounts for 30-40% of the PHAs production costs). In addition, the co-integration of volatile fatty acids and biogas in terms of methanotrophic growth and production of tailor-made PHAs within this biorefinery concept not only increased the PHA content in type II methanotrophs such as *Methylocystis hirsuta*, but also modified PHAs composition, which ultimately enhanced their physical/chemical properties and market value.

The potential of biotechnologies to create additional value out of CH_4 mitigation was also demonstrated by coupling biogas abatement with dissimilatory N removal, via the so-

called denitrifying anaerobic methane oxidation process. However, the implementation of DAMO at full-scale is up to date hindered by the poor gas-liquid mass transfer of CH_4 (which extends the enrichment periods of DAMO communities and lowers its biodegradation rates), and the inefficient biomass retention in the bioreactor configurations tested. In **Chapter 7**, a biotrickling filter configuration was implemented for the first time to overcome the aforementioned issues and enrich a DAMO community within 4.5 months, which is one of the shortest enrichment periods so far reported in literature. When H_2S was present in the biogas, nitrate removals were significantly enhanced and a nitrate-reducing and sulphide-oxidizing bacterial community was co-enriched together with the pre-existing DAMO bacteria and archaea. To the best of our knowledge, this is the first work reporting the use of CH_4 and H_2S as electron donors for denitrification in biotrickling filters, and one of the highest nitrogen removals supported by DAMO ever reported.

In spite of the fact that biotechnologies have the potential to effectively abate CH_4 under different bioreactor configurations and operational strategies, their cost-effective and robust operation still requires significant research efforts. Similarly, the use of the so-called '-omics' techniques would entail a better understanding of the microbiology underlying CH_4 oxidation and the role of each specific partner in the process. Moreover, despite the promising results here obtained on the creation of added value out of CH_4 degradation using biogas a raw material, further optimization at lab-scale is still required to implement this biorefinery concept at full-scale. Based on the results here obtained, future lines of research in the field of CH_4 abatement biotechnologies should be focused on:

i. The implementation of fungal-bacterial communities and feast-famine strategies at pilot scale to confirm their potential for carbon footprint reduction, and energy and costs savings.

ii. The performance evaluation of a fungal biofilter under intermittent methanol irrigation. In this regard, the application of '-omics' techniques might be of key relevance to fully elucidate the metabolic pathways underlying CH_4 biodegradation in fungal strains such as *Graphium* sp.

iii. The exploration of new microbiological and technological approaches to address issues such as CH_4 mass transfer limitation and biomass overgrowth typically found in conventional CH_4 abatement biotechnologies. Future research should focus on the use of hydrophobic methanotrophs and rotating drum biofilters, or on the design of capillary-based monoliths.

iv. The study of the CH_4 biodegradation kinetics and the population structure of methanotrophic communities during enrichment under different environmental parameters or macro-/micronutrient concentrations. This would allow identifying the key conditions to optimize not only CH_4 biodegradation, but also the synthesis of bioproducts such as PHAs under continuous operation. The characterization of these enrichments with advanced molecular biology techniques such as next-generation sequencing (e.g. Illumina MiSeq platform) would be also crucial to fully understand the microbial ecology of methanotrophs.

v. The elucidation of the effect of supplementation of multiple VFAs on biogas-based PHA production by type II methanotrophs might provide new insights on the production of tailor-made biopolymers with enhanced physical/chemical properties and a higher market value. The potential of anaerobic digestion with a partial organic matter hydrolysis coupled to a methanotrophic bioreactor should be further evaluated in order to develop a new generation of biogas-based biorefinery.

vi. The application of '-omics' techniques and systems biology to fully understand the synergistic action of DAMO and NR-SOB communities during biogas-based denitrification. Despite the promising results here obtained, further research should be focused on identifying alternative microbial partners in DAMO and

innovative high-mass transfer bioreactor configurations in order to scale up this novel N removal technology.

Chapter 9

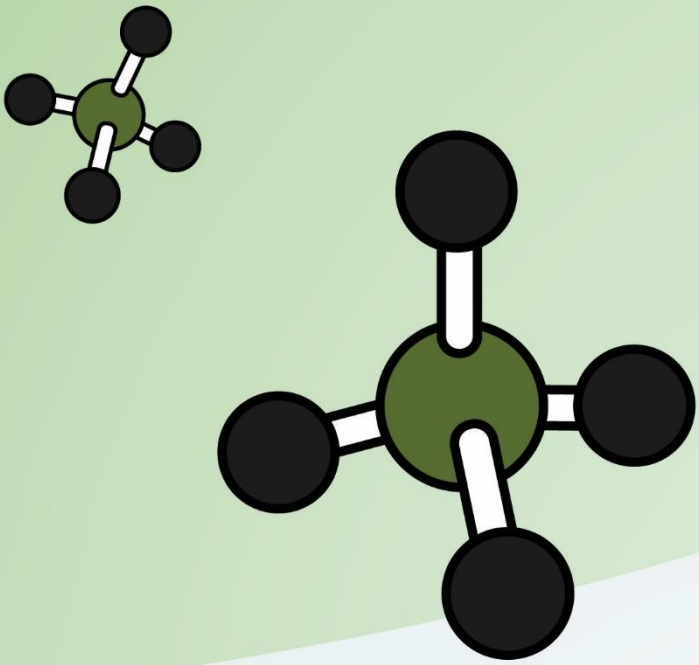

Acknowledgements

Acknowledgements

Muchos de nosotros (yo el primero) decimos una media de 20 veces al día gracias, y olvidamos no sólo la importancia que tiene el estar realmente agradecido por algo sino también lo difícil que puede llegar a ser expresar tanta gratitud en tan poco espacio. Han sido 5 duros y, a la vez, gratificantes años de trabajo en los que sin vosotros no habría sido capaz de llegar a donde estoy hoy. Indivualmente, me gustaría con todo el cariño agradecerle:

A Raúl su dedicación las 24 horas durante los 7 días de la semana, la exigencia por el trabajo bien hecho, por escucharme y aconsejarme en cada propuesta y, por supuesto, por su bendita paciencia conmigo. Y digo bendita porque sé que en más de una ocasión te saqué de tus casillas. Gracias por haberme dado esta oportunidad hace años sin apenas conocerme y por la confianza depositada en mí durante este tiempo en el laboratorio. Sin duda, te debo en gran parte la seguridad y las ganas de seguir trabajando en ciencia que hace años seguramente no tenía.

A Raquel y Guillermo, por su cosupervisión y consejos durante estos años. Hicisteis fácil lo difícil y conseguisteis darle más valor, si cabe, a cada uno de los trabajos realizados.

Al grupo de investigación de Gases y Microalgas por todo lo vivido, por estar siempre dispuestos a ayudar en el trabajo y ser capaces de compaginarlo con unas risas. Específicamente a Dimas y David, por la diversión asegurada pese a que me convirtáis frecuentemente en diana de bromas. Zu Ilker, für seine beständige Fröhlichkeit, seine komische Witze und sein groβes Vertrauen im Labor. A Rebe, por todo lo que me ha enseñado en el área de Biología Molecular. A las chicas de algas, así como a Esther A., Sonia y Elisa, por estar siempre dispuestas a colaborar con una sonrisa de oreja a oreja. A Sara – sin duda la mamá de la gran familia metanótrofa – por sonreir siempre y quitarle

hierro al asunto. Sabes que eso prima por encima de cualquier problema. A Osvaldo, por todo lo que me enseñó en ingeniería y lo fácil que hizo el trabajar con él. A los estudiantes de carrera que he supervisado, Alberto, Ahn y Laura, por el apoyo tan valioso que me han dado en laboratorio y por incentivar mi motivación a enseñaros lo (poco) que sabía. A los nuevos miembros de la familia metanótrofa, Yadira y Víctor, por el buen rollo y sumarse con tanta entrega al maravilloso mundo del hirsutismo (¡y que dure, eh! ☺). A Fabi, por desvivirse por ayudarme en todo sin apenas conocerme; aquí tendrás un amigo para siempre. A antiguos compañeros como Jose, Cynthia, Silvia, Edinéia o Mariana, por la huella que dejasteis y lo mucho que aprendí con vosotros.

A Judit, Alberto y las marichochos de Marta S. y Marta F., por estar ahí para lo bueno y para lo no tan bueno. No tengo palabras para agradeceros el apoyo que me habéis dado, sobretodo en los momentos de bajón y por la razón que fuese. Espero que esto sea el inicio de algo muy bueno, sabéis que siempre estaré ahí para lo que necesitéis. Al resto de compañeros y técnicos del Departamento de Ingeniería Química y Tecnología de Medio Ambiente, por haber hecho de él prácticamente mi segundo hogar durante este tiempo. Espero que lo momentos vividos dentro de él, más agradables o amargos, sirvan para aprender y superarnos tanto en lo personal como en lo profesional.

To Gavin Collins for accepting me in the Microbial Communities Lab at NUIG University and giving me the opportunity to go deeper into my molecular biology skills. To all lab mates there, Este, Anna, Sarah, Kityee, Enrico, Agatha and Aoife, for both the great fun and all they teached me.

A mi familia por apoyarme en todas las decisiones tomadas y aguantarme algún que otro desplante los fines de semana por “tener que ir a ver a las bacterias”. En especial a mi madre, por las innumerables llamadas de ánimo, las preocupaciones innecesarias y, sobretodo, ser paciente en mis peores momentos. A mi padre, porque pase lo que pase, siempre se preocupa de hacerme saber que me quiere. A mi hermano, por

recordarme constantemente que “soy un tío grande” (a uno siempre le gusta escucharlo, lo sea o no) que ha de trabajar en la vida de lo que a uno le gusta, luchando con uñas y dientes por alcanzar una meta.

Zu meinen Mitschülern aus dem Deutschunterricht, für die gemeinsame Zeit in meinem dritten Haus, la Escuela de Idiomas. Ich bedanke mich bei euch nicht nur für die guten Momente, sondern auch für alles, was wir zusammen gelernt haben.

A mis amig@s por hacer de cada plan un atajo de risas y la evasión perfecta del trabajo. Especialmente a mis zamoranas María, MariaH y Cris, por seguir dándome razones de peso para visitar la ciudad natal. A mis maris Álvaro, Manu, Rodri, Sam, David, Dani y Rober, por saber liarme para cualquier plan y hacer que me divierta como nadie (aunque a veces eso conlleve algún que otro despropósito). A mis valencianos Carlos, María, Rubén y Miguel, por estar ahí y hacer de las Fallas el punto de encuentro anual para el ahogo de penas (glup, glup!). A mis biotecnólogas favoritas Irene, Gore, Bea y Cris, por esos ya 10 años a piñón, por las quedadas hasta las tantas, por haber hecho de la biotecnología una pequeña familia – que lo que una la ciencia no lo separe ya nadie.

A todas aquellas personas que me dejo en el tintero mientras escribo estas líneas y que han contribuido, en mayor o menor medida, a que este trabajo saliese adelante.

Gracias. Thank you. Danke schön.

“*Es casi imposible corresponder a todas las personas que nos ayudan a lo largo de la vida. Quizá sea más sencillo rendirse ante el milagroso alcance de la generosidad humana y seguir diciendo gracias, eterna y sinceramente, mientras nos alcance la voz.*”

Elisabeth Gilbert

Chapter 10

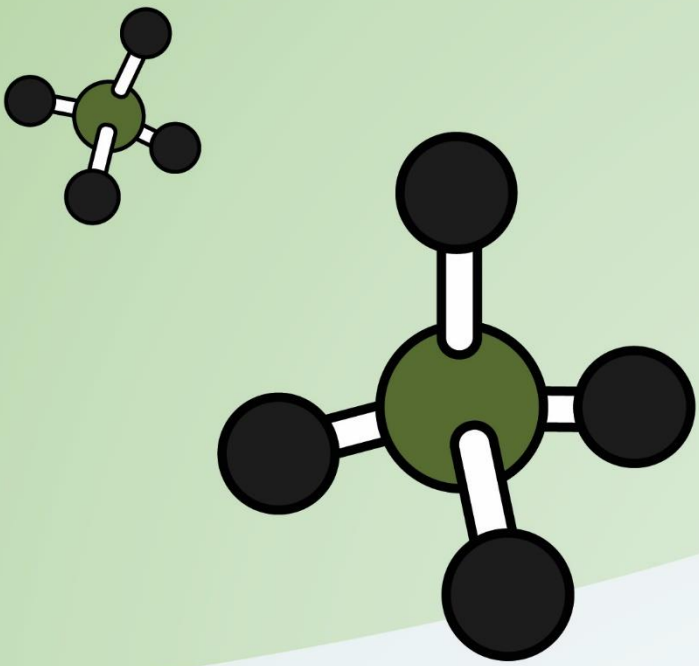

About the author

Biography

Juan Carlos López Neila (Zamora, 1989) started his Biotechnology studies in 2007 at the University of León. He collaborated with research centers such as Inbiotec (León) and IU-IAD (Valencia) between 2009 and 2011. Juan Carlos finished his studies in July 2012 and immediately joined the VOC & Microalgae Research Group headed by Associate Professor Raúl Muñoz in the Environmental Technology Research Group (Department of Chemical Engineering and Environmental Technology – University of Valladolid). After one year and a half carrying out research within a project funded by the Spanish Ministry of Science and Innovation, Juan Carlos was awarded in January 2014 with a FPI Grant by the aforementioned institution.

His PhD studies were initially focused on improving CH_4 abatement performance in biotechnologies and exploring the microbiology underlying CH_4 biodegradation, within the recently started research line on biotechnologies for greenhouse gases abatement. Afterwards, the experimental work of Juan Carlos moved towards the creation of added value out of CH_4 mitigation using biogas as a readily available and low-cost substrate for biopolymer production and on-site pollution control. This research was framed within the recent research line on biogas bioconversion to commodities and high added-value products. During his PhD thesis, the candidate carried out a four-month research stay at the Department of Microbiology of the National University of Ireland Galway (NUI Galway) (2014, Galway, Ireland) under the supervision of Associate Professor Gavin Collins.

Publications in international journals

i. López, J.C., Quijano, G., Souza, T.S.O., Estrada, J.M., Lebrero, R., Muñoz R., 2013. Biotechnologies for greenhouse gases (CH_4, N_2O, and CO_2) abatement: state-of-the-art and challenges. Applied Microbiology and Biotechnology 97(6), 2277-2303. DOI: 10.1007/s00253-013-4734-z.

ii. López, J.C., Quijano, G., Pérez, R., Muñoz, R., 2014. Assessing the influence of CH_4 concentration during culture enrichment on the biodegradation kinetics and population structure. Journal of Environmental Management 146, 116-123. DOI: 10.1016/j.jenvman.2014.06.026.

iii. Ordaz, A., López, J.C., Figueroa-González, I., Muñoz, R., Quijano, G., 2014. Assessment of methane biodegradation kinetics in two-phase partitioning bioreactors by pulse respirometry. Water Research 67, 47-54. DOI: 10.1016/j.watres.2014.08.054.

iv. Lebrero, R., López, J.C., Lehtinen, I., Pérez, R., Quijano, G., Muñoz, R., 2016. Exploring the potential of fungi for methane abatement: Performance evaluation of a fungal-bacterial biofilter. Chemosphere 144, 97-106. DOI: 10.1016/j.chemosphere.2015.08.017.

v. López, J.C., Porca, E., Collins, G., Pérez, R., Rodríguez-Alija, A., Muñoz, R., Quijano, G., 2017. Biogas-based denitrification in a biotrickling filter: Influence of nitrate concentration and hydrogen sulfide. Biotechnology and Bioengineering 114(3), 665-673. DOI: 10.1002/bit.26092.

vi. López, J.C., Merchán, L., Lebrero, R., Muñoz, R., 2017. Feast-famine biofilter operation for methane mitigation. Journal of Cleaner Production (accepted).

vii. López, J.C., Arnáiz, E., Merchán, L., Lebrero, R., Muñoz, R., 2017. Biogas-based polyhydroxyalkanoates production by *Methylocystis hirsuta*: a step further in anaerobic digestion biorefineries. Chemical Engineering Journal (submitted for publication).

viii. García-Pérez, T., López, J.C., Passos, F., Lebrero, R., Revah, S., Muñoz, R., 2017. Simultaneous methane abatement and PHB production by *Methylocystis hirsuta* in a novel gas-recycling bubble column bioreactor. Chemical Engineering Journal (submitted for publication).

ix. Cantera, S., López, J.C., Rodríguez, Y., Lebrero, R., Muñoz, R., García-Encina, P. A., 2017. Technologies for the bioconversion of methane into more valuable products. Current Opinion in Biotecnology (submitted for publication).

x. López, J.C., Porca, E., Muñoz, R., Clifford, E., Quijano, G., Collins, G., 2017. Influence of ammonium on the methane oxidation kinetics and microbial community structure of methanotrophic consortia (In preparation).

xi. Rodríguez, E., López, J.C., Prieto, P., Merchán, L., García-Encina, P., Lebrero, R., Muñoz, R., 2017. Assessing microbial robustness in continuous vs. feast-famine bioreactors treating methane via quantitative analysis of transcribed methane monooxygenase (In preparation).

xii. Rodríguez, E., López, J.C., Prieto, P., Merchán, L., García-Encina, P., Lebrero, R., Muñoz, R., 2017. Transcriptional response (methane monooxygenase.based) of methanotrophs to fluctuating methane loads in continuous vs. feast-famine bioreactors (In preparation).

Book chapters

i. Cantera, S., Frutos, O.D., López, J.C., Lebrero, R., Muñoz, R. Technologies for the bio-conversion of GHGs into high added value products: Current state and future prospects. In *Carbon Footprint and the Industrial Life Cycle, From Urban Planning to Recycling*; Álvarez-Fernández, R.; Zubelzu, S.; Martínez R., Eds.; Springer International Publishing, 2017; pp. 359–388; DOI 10.1007/978-3-319-54984-2.

ii. López, J.C., Rodríguez, Y., Pérez, V., Lebrero, R., Muñoz, R. CH_4-based polyhydroxyalkanoate production: a step further towards a sustainable bioeconomy. In *Biotechnological Applications of Biopolymers: Polyhydroxyalkanoates*; Kalia, V.C., Ed.; Springer Nature, 2018 (In Preparation).

Contributions to conferences

i. Calabuig, L., Seguí, L., López, J.C., Fito, P. Propiedades antioxidantes de los azúcares de caña no refinados. VII Congreso Ciencia y Tecnología de los Alimentos, 12-14 June 2013, Córdoba, Spain (Poster Presentation).

ii. López, J.C., Quijano, G., Pérez, R., Muñoz, R. Effect of pollutant concentration during isolation on the CH_4 biodegradation kinetics, population structure and PHB production. NOSE 2014: 4th International Conference on Environmental Odour Monitoring & Control, 14-17 September 2014, Venice, Italy (Oral Presentation).

iii. López, J.C., Porca, E., Collins, G., Pérez, R., Rodríguez-Alija, A., Muñoz, R., Quijano, G. Exploring the impact of hydrogen sulphide on denitrifying anoxic methane oxidizing (DAMO) communities. 10th ISEB Conference, 1-3 June 2016, Barcelona, Spain (Poster Presentation).

iv. López, J.C., Lebrero, R., Lehtinen, I., Pérez, R., Quijano, G., Muñoz, R. Evaluation of the fungal-bacterial synergism in methane abatement biotechnologies. 10th ISEB Conference, 1-3 June 2016, Barcelona, Spain (Oral Presentation).

v. López, J.C., Muñoz, R., Quijano, G. The role of nitrogen availability on methane abatement biotechnologies. 1st International Conference on Bioenergy and Climate Change - Towards a Sustainable Development, 6-7 June 2016, Soria, Spain (Oral Presentation).

vi. López, J.C., Merchán, L., Lebrero, R., Muñoz, R. Feast-famine strategies as a low-cost and robust alternative for CH_4 biofiltration. Biotechniques 2017, 19-21 July 2017, A Coruña, Spain (Oral Presentation).

vii. Rodríguez, E., López, J.C., Merchán, L., Prieto, P., García-Encina, P., Lebrero, R., Muñoz, R. Evaluating microbial robustness in continuous vs. feast-famine bioreactors via methane-oxidizing activity by qPCR. Biotechniques 2017, 19-21 July 2017, A Coruña, Spain (Oral Presentation).

viii. López, J.C., Arnáiz, E., Merchán, L., Lebrero, R., Muñoz, R. Biogas and volatile fatty acids-driven polyhydroxyalkanoates production by *Methylocystis hirsuta*. 7th IWA Conference on Odours and Air Emissions, 25-27 September 2017, Warsaw, Poland (Oral Presentation).

Research stays abroad

i. Department of Microbiology, National University of Ireland Galway (Galway, Ireland) January 2015 – May 2015. Supervisor: Professor Gavin Collins. Scope: i) New insights on the response of methane-oxidizing bacteria to ammonium, and

ii) HiSeq Illumina sequencing and qPCR assays of bacterial/arqueal communities performing anaerobic nitrate-driven methane oxidation.

Committees and Reviewer Experience

i. ***Reviewer for*** Journal of Environmental Sciences since 2017.

ii. ***Member of the organizing committee*** of the NOVEDAR technical seminar: Characterization and Management of Odours and Greenhouse Gases in WWTPs, 5 October 2015 (Valladolid, Spain).

Awards

i. Special prize for the best Master Thesis in the Program of Processes and Systems Engineering, October 2013 (Valladolid, Spain).

ii. Special prize for the 3rd best PhD oral presentation, entitled 'Evaluation of the fungal-bacterial synergism in methane abatement biotechnologies' at 10th ISEB Conference, June 2016 (Barcelona, Spain).

Co-supervision

i. ***Research project:*** Ahn Tuan Nguyen (March 2016 – July 2016) 'Feast-famine strategies during CH_4 abatement: A proof of concept study', University of Valladolid (Spain).

ii. ***Final year project:*** Laura Merchán Catalina (September 2015 – April 2016) 'Evaluación de estrategias de alimentación/hambruna como alternativa robusta en la biofiltración de metano', University of Valladolid (Spain).

Teaching

i. Master in Environmental Engineering (2015-2016). Assistant lecturer on laboratory practices. University of Valladolid (Spain). 2 ECTS.

Attended short-courses and seminars

i. 'Kinetic characterization of bioprocesses by respirometry'. November 2013, Department of Chemical Engineering and Environmental Technology (Valladolid, Spain). Lecturer: Professor Alberto Ordáz Cortés. Duration: 15 hours.

ii. 'Culture of microalgae'. November 2014, Department of Chemical Engineering and Environmental Technology (Valladolid, Spain). Lecturer: Professor Gabriel Acién Fernández. Duration: 10 hours.

iii. 'Microbiology and microbial ecology of biofilms in environmental biotechnology'. September 2015, Department of Chemical Engineering and Environmental Technology (Valladolid, Spain). Lecturer: Professor Gavin Collins. Duration: 12 hours.

iv. 'NOVEDAR technical seminar: Characterization and management of odours and greenhouse gases in WWTPs'. October 2015, Department of Chemical Engineering and Environmental Technology (Valladolid, Spain). Duration: 8 hours.

v. 'Vegetal biotechnology: Vegetal cellular cultures as biorefineries for the production of high-added value products'. December 2015, Department of Chemical Engineering and Environmental Technology (Valladolid, Spain). Lecturer: Professor María Ángeles Pedreño. Duration: 12 hours.

vi. ‘Basic computational skills for genomic analysis: taxonomic analyses in R’. August 2016, Foundation for the Promotion of Health and Biomedical Research of Valencia Region (Valencia, Spain). Lecturers: Dr. Giuseppe D'Auria and MSc David Pérez Villarroya. Duration: 24 hours.

vii. ‘Microalgae biotechnology’. May 2017, Department of Chemical Engineering and Environmental Technology (Valladolid, Spain). Lecturer: Professor Marcia Morales Ibarria. Duration: 10 hours.

Participation in Research & Development Projects

i. Development of a new generation of compact, low-cost, high-performance Bioreactors for odour abatement in wastewater treatment plants. Spanish Ministry of Science and Innovation (2009-2012). PI. Dr. Raúl Muñoz.

ii. Advanced biological processes for the abatement of the greenhouse gases CH_4 and N_2O: targeting the direct gas-cell mass transport and process microbiology. Ministry of Economy, Industry and Competitiveness (2013-2016). PI. Dr. Raúl Muñoz.

iii. Biogas purification for injection in natural gas grid using symbiotic algal-bacterial processes. PI. Dr. Raúl Muñoz. Regional Government of Castilla y León (2015-2017). PI. Dr. Raúl Muñoz.

iv. Biogas Bioconversion to commodities and high-added value products: Exploring new strategies for biogas valorization. Ministry of Economy, Industry and Competitiveness (2016-2019). PI. Dr. Raúl Muñoz and Dr. Raquel Lebrero Fernández.